Control of gene expression and cell cycle by modulation of nuclear pore complexes

Vasilisa Pozharskaia

Université de Strasbourg

UNIVERSITÉ DE STRASBOURG

École doctorale Sciences de la vie et de la santé | ED 414
Université de Strasbourg

ÉCOLE DOCTORALE 414 – Sciences de la vie et de la santé

Institut de Génétique et de Biologie Moléculaire et Cellulaire

CNRS UMR 7104 – INSERM U 964

THÈSE

présentée par :

Vasilisa POZHARSKAIA

soutenue le : **16 décembre 2022**

Pour obtenir le grade de :
Docteur de l'université de Strasbourg

Discipline/ Spécialité : Aspects moléculaires et cellulaires de la biologie

Contrôle de l'expression génétique et du cycle cellulaire par modulation des complexes des pores nucléaires

THÈSE dirigée par :

M MENDOZA Manuel, PhD	Directeur de Recherche DR2, Université de Strasbourg

RAPPORTEURS :

M ALDEA Martí, PhD	Directeur de Recherche, Institut de Biologie Moleculaire de Barcelone
M PALANCADE Benoit, PhD	Directeur de Recherche DR2, Institut Jacques Monod

AUTRES MEMBRES DU JURY :

Mme EWALD Jennifer, PhD	Directrice de Recherche, Université de Tübingen
Mme SUMARA Izabela, PhD	Directrice de Recherche DR1, IGBMC

For what it’s worth

Acknowledgements

I was told to write acknowledgements first, so here it is.

I start writing on the 2nd of August right after coming back from yet another trip to Switzerland, where I put together several people of different backgrounds together to reach the cave in the ever-diminishing in volumes Rhone glacier. Since it will likely melt down completely by the time I finish with the writing and hopefully defend my thesis, I can say that it used to be located near the village Obergoms in Swiss Alps, and that the journey there and back took much longer than the actual visit to the cave, filled with blue light and with walls of ice with trapped air bubbles organized in unequally spaced layers. I can definitely say that I enjoyed the 10-hour trip at the very least the same as the 15 minutes of cave examination. And I firmly believe that this is because I had the nicest people by my side. Same goes for the thesis journey, and I want to express my great adoration for the people who, by being active participants and helping me on the way, have reached this point together with me.

I would like to first and foremost thank the people who agreed to read, evaluate and discuss my manuscript and join me during my defense - alphabetically based on the surnames - Martí Aldea, Jennifer Ewald, Benoit Palancade, Izabela Sumara. Thank you.

To Merce, Celia and Bogdan, for collaborating with me on the project and contributing the most to bringing me here.

I want to say “thank you”s to certain people, in case they ever look through this thesis, even though I rather doubt that.

To my lovely lab mates, current and those who already moved on in their scientific or life journey, I want to express my gratitude for all the things that I learned from them and for all the time that we spent together in the rooms and hallways, in the canteen and outside, in restaurants and bars, on the bikes and on the way to the tram stop, in celebrations and despair, in happiness and in sorrow, in sickness and in health. To Monica, Celine, Ines, Laurine, Faezeh, Audrey, Max and Sandrine.

To our enthusiastic and collaborative friendly yeast lab with Gilles, Basile, Theo, Sophie, Audrey and others with whom I did not interact that much.

To the facilities of IGBMC and people who work there for making this research possible. I would like to specifically thank Erwan, Bertrand and Elvire, the members of microscopy dream team.

To the community of the guardians who are always at the entrance or nearby, with whom I interacted a lot, leaving and arriving far from the ordinary human working hours. Thank you for being there for us.

To fellow PhD students of the Institute, who, by being “external” to the lab, had the unique ability of switching my mindset to a different point of view. Dimitra, Gregoire, Archit, Salvatore, Юра, Оля, Лиля, Юля.

To my numerous friends from school and university with whom I keep contact and who largely contribute to keeping me sane. Димка, Настя, Катя, Алена, Аня, Гаража, Паркер, Красовочек.

To my mother and grandmother, for leading your life independently from my own.

To my best friend Данила Дмитриевич, for always finding a way to make a joke wherever possible and whatever it takes, and for supporting my spirit immensely throughout my PhD.

To my beloved husband Мишка, who was right next to me spiritually, though physically far away most of the time. I love how things that I love doing can be done in your company, and how you make them even more enjoyable. I cannot imagine making it through up until now without you. I also thank you for trying to help me write this thesis, even though mostly by morning messages motivating me to wake up. I want to specifically mention that florentiner cookie that you sent me by mail from Zurich so that I can both write the thesis and drink tea with you over Skype.

To my PI Manuel Mendoza for the deepest and most encouraging discussions, and for shaping the research presented in this thesis.

Table of contents

Summary

Introduction

Nuclear pore complexes (NPCs) are multiprotein assemblies that form channels through the nuclear envelope connecting the nuclear and cytoplasmic compartments. NPCs mediate protein and RNA transport between the nucleus and cytoplasm. In addition, NPCs are also directly involved in the regulation of gene expression. Many genes associate with NPCs upon activation, and these interactions regulate the synthesis and nuclear export of corresponding mRNAs. Although the structure of NPCs is largely conserved across organisms and cell types, subtle changes in NPC composition can lead to changes in gene expression, for example during embryonic stem cell differentiation.

Our laboratory has previously demonstrated that in budding yeast, changes in acetylation of NPC components (nucleoporins) lead to shifts in gene expression in a cell type-specific manner. Budding yeast divides asymmetrically, producing mother and daughter cells that differ in size, gene expression programs, and cell cycle dynamics. NPCs are acetylated in mother cells but deacetylated in daughter cells. Deacetylation of daughter nuclear pores is ensured by daughter nuclear periphery localized deacetylase Hos3. In newborn daughter cells, the deacetylation of NPCs promotes their interaction with a cyclin gene (*CLN2,* a homologue of cyclin E in mammalian cells), which inhibits its expression. This inhibition results in a delay of the G1/S transition in daughter cells compared to mother cells.

The goal of my PhD studies was to understand the molecular mechanisms linking NPC acetylation to the regulation of gene expression and cell cycle progression in budding yeast. NPCs are acetylated in mammalian cells, but the function of these modifications is unknown. Our study reveals a novel mechanism for gene regulation that could be conserved in animal cells.

Results

In our paper we find that the acetyltransferase that counteracts Hos3 at the periphery is Esa1, a component of conserved acetyltransferase complex NuA4. Gene expression of most genes is affected to some extent by Esa1 inactivation, and we find that one way Esa1 opposes Hos3 is through activating transcription of G1/S genes, and specifically that of the *CLN2* gene. In this respect, Esa1 activity can be partially compensated by Gcn5 acetyltransferase, a component of another conserved chromatin

modifying complex SAGA. Together these two enzymes, which target histones H4 and H3 respectively, are responsible for nearly all RNA polymerase II-dependent transcription in budding yeast. In the context of G1/S transition, inactivation of both Esa1 and Gcn5 leads to a complete block of cells in G1. In contrast, Esa1 deficient cells are largely delayed, and this is reflected in decreased or compromised expression of several candidate genes checked by RT-qPCR.

We find that both Esa1 and Gcn5 acetylate a formerly identified Hos3 substrate Nup60. In agreement with our hypothesis that Nup60 could be the target of both Hos3 and Esa1 in G1/S control, the *nup60K467N* allele partially rescued the defect of *esa1-ts* cells. It also rescued Cln2 protein levels, which peak at the G1/S transition. However, we could not find any difference in *CLN2* transcript levels. In search for a link between RNA transcription and protein levels, we sought to examine the mRNA export.

In asynchronous culture budding yeast daughter cells export transcriptions In order to monitor *CLN2* mRNA export by microscopy imaging, we used the *CLN2-PP7* yeast strain that has engineered loops able to bind a viral capsid protein derivative fused to GFP. Our imaging results support the data from RT-qPCR on *CLN2,* showing that in the daughter cells, Nup60K467N does not promote transcription of *CLN2* in *esa1-ts* cells, but apparently promotes mRNA export*,* since more cytoplasmic foci are visible in these cells. A mild decrease in peripheral localization of the nascent mRNA foci is observed in *esa1-ts* and rescued in *esa1-ts nup60KN* cells, which may reflect the link between gene locus positioning being affected in *esa1-ts* cells and mRNA export efficiency.

To strengthen our claim and to see how special is the case of Nup60, we performed polyA RNA FISH that allows us the detection of mRNA export defects. Esa1 deficient cells started accumulating polyA RNA after several hours of temperature inactivation, and *nup60K467N* mutation rescued this defect. Hos3-NLS is an artificially engineered form of Hos3 that is constitutively localized to the nuclear periphery of all cells; overexpression of Hos3-NLS is toxic and the cells present an mRNA export defect; however, overexpression of mRNA export factors Mex67 and Mtr2 rescues this phenotype. Collectively this data argues that deacetylation of the NPCs decreases export.

In the search for a way to connect NPC acetylation with the mRNA export, we turned to the TREX-2 complex. TREX-2 associates with the basket nucleoporin Nup1 and interacts with multiple transcription and export regulators such as mediator and

Mex67:Mtr2 dimer. Consistently, we found a positive correlation between the NPC acetylation state and Sac3 enrichment at the periphery. To test its functional significance in G1/S, when the daughter pores are deacetylated, we artificially anchored Sac3 to the nuclear periphery, which lead to an overall increase in Sac3 peripheral localization. Under such conditions, Sac3 promoted G1/S transition in *esa1-ts* daughter cells. Our data suggest that Esa1-dependent acetylation of Nup60 promotes the association of Sac3 with the nuclear periphery and this promotes cell cycle progression, likely by modulation of mRNA export and/or transcription.

Additionally, we evaluated the role of nuclear pore acetylation in the expression of genes that are not expressed in the G1/S transition. We chose to focus on the *GAL* locus, which is known to be associated with the nuclear periphery once it is active. By monitoring the expression of the fluorescent reporter sfGFP integrated into the *GAL* locus under the control of the *GAL1* promoter, we showed that acetylation of the NPC promotes sfGFP expression. Interestingly, we found that *HOS3* deletion leads to a faster protein appearance than *nup60KN* acetyl mimic mutation, which indicates that there are likely other targets of Hos3 at the nuclear periphery that modulate *GAL* gene expression. We also find that daughter cells are delayed in expression in the wild type, and this mother-daughter difference is lost in nuclear pore deacetylation mutants. Our evidence speaks in favor of Sac3 being important in GAL1 promoter activation, since forcing Sac3 to the periphery leads to advanced sfGFP expression in the daughter cells.

Conclusion

We present the data arguing that the cell cycle entry in budding yeast is promoted by the activity of the Esa1/NuA4 acetyltransferase complex and that another complex Gcn5/SAGA can partially compensate for its absence. Both SAGA and NuA4 are known regulators of transcription, supposedly driving chromatin decompaction by histone acetylation (H3 and H4, respectively). We show that Esa1 has an additional role and that it acetylates Nup60 to promote the association of Sac3/TREX-2 with the NPC and thus facilitate mRNA export and/or transcription. The mechanism of acetylation-dependent regulation of mRNA export is likely universal, as we show global mRNA export defects in acetylation mutants. Additionally, we directly show the role of acetylated Nup60 in *CLN2* mRNA export and the role of Sac3/TREX-2 acetylation-dependent association with the nuclear pore in G1/S transition and the expression of a nutrient-responsive gene *GAL1*.

However, there is still much that we do not know about the role of the NPC. Our work opens many questions that are to be answered in future research. What is the role of Nup60 acetylation in the structure of the NPC? What other components of the complex may be acetylated in order to control its function? In the case of the *GAL* locus, is mRNA export promoted by Nup60 acetylation? Is the export of some specific classes of the mRNAs affected by the NPC deacetylation? Finally, is the mechanism we describe conserved in metazoans? These and other questions remain to be addressed in the future.

Résumé

Introduction

Les complexes de pores nucléaires (NPC) sont des assemblages multiprotéiques qui forment des canaux à travers l'enveloppe nucléaire reliant ainsi les compartiments nucléaire et cytoplasmique. Les NPC assurent le transport des protéines et des ARN entre le noyau et le cytoplasme. En outre, les NPCs sont aussi directement impliqués dans la régulation de l'expression des gènes. De nombreux gènes s'associent aux NPC lors de leur activation, et ces interactions régulent la synthèse et l'exportation nucléaire des ARNm correspondants. Bien que la structure des NPCs soit globalement conservée à travers les organismes et les types cellulaires, des variations subtiles dans la composition des NPCs peuvent conduire à des changements dans l'expression de certains gènes, par exemple pendant la différenciation des cellules embryonnaires souches.

Notre laboratoire a précédemment démontré que, chez la levure *S.cerevisiae*, les changements d'acétylation des composants des NPCs (nucléoporines) entraînent des modifications de l'expression génétique d'une manière spécifique au type cellulaire. *S.cerevisiae* se divise de manière asymétrique, produisant des cellules mères et filles qui diffèrent par leur taille, leur programme d'expression génique et leur dynamique de cycle cellulaire. Les NPCs sont acétylés chez les cellules mères mais désacétylés chez les cellules filles. La désacétylation des pores nucléaires chez les cellules filles est assurée par la désacétylase Hos3, localisée à la périphérie nucléoplasmique des cellules filles. Chez les cellules filles nouveau-nées, la désacétylation des NPCs favorise leur interaction avec un gène de cycline (*CLN2*, un homologue de la cycline E dans les cellules de mammifères), inhibant ainsi son expression. Cette inhibition se traduit par un retard de la transition G1/S chez les cellules filles par rapport aux cellules mères.

L'objectif de mes études doctorales était de comprendre les mécanismes moléculaires reliant l'acétylation des NPCs à la régulation de l'expression des gènes et de la progression du cycle cellulaire chez la levure. Les NPCs sont acétylés chez les mammifères, mais la fonction de ces modifications reste vague. Notre étude révèle un nouveau mécanisme de régulation des gènes qui pourrait être conservé dans les cellules animales.

Résultats

Dans notre étude, nous trouvons que l'acétyltransférase qui contrecarre Hos3 à la périphérie nucléoplasmique est Esa1, un composant du complexe acétyltransférase NuA4. L'expression de la plupart des gènes est affectée dans une certaine mesure par l'inactivation d'Esa1, et nous constatons que l'une des façons dont Esa1 s'oppose à Hos3 est en activant la transcription des gènes G1/S, et spécifiquement celle du gène *CLN2*. À cet égard, l'activité d'Esa1 peut être partiellement compensée par l'acétyltransférase Gcn5, un composant d'un autre complexe de modification de la chromatine, SAGA. Ensemble, ces deux enzymes, qui ciblent respectivement les histones H4 et H3, sont responsables de la transcription de la plupart des gènes transcrits par l'ARN polymérase II chez la levure. Dans le contexte de la transition G1/S, l'inactivation d'Esa1 et de Gcn5 conduit à un blocage complet des cellules en G1, tandis que les cellules déficientes en Esa1 sont largement retardées, ce qui se traduit par une expression diminuée ou nulle de plusieurs gènes candidats vérifiés par RT-qPCR.

Nous constatons que Esa1 et Gcn5 acétylent tous deux un substrat de Hos3 précédemment identifié: Nup60. En accord avec notre hypothèse selon laquelle Nup60 pourrait être la cible à la fois de Hos3 et d'Esa1 dans le contrôle de la transition G1/S, l'allèle *nup60K467N* a partiellement corrigé le défaut des cellules *esa1-ts* et a également rétabli les niveaux de protéine Cln2, qui atteignent un pic à la transition G1/S. Cependant, nous n'avons trouvé aucune différence dans les niveaux de transcription de *CLN2*. À la recherche d'un lien entre la transcription de l'ARN et les niveaux de protéines, nous avons alors cherché à examiner l'exportation de l'ARNm.

Afin de surveiller l'exportation de l'ARNm de *CLN2* par microscopie, nous avons utilisé une souche *CLN2-PP7* dont l'ARN à été modifié afin de contenir des boucles capables de lier un dérivé d'une protéine de capside virale fusionné à la GFP. Nos résultats d'imagerie confirment les données issues de la RT-qPCR sur CLN2, montrant que chez les cellules filles, Nup60K467N ne favorise pas la transcription de *CLN2* dans les cellules *esa1-ts,* mais favorise apparemment l'exportation de l'ARNm, puisque davantage de signaux cytoplasmiques sont visibles dans ces cellules. Une légère diminution de la localisation périphérique des foyers d'ARNm naissants est observée dans les cellules *esa1-ts* et corrigée dans les cellules *esa1-ts nup60KN*, ce qui peut refléter le lien entre le positionnement du locus du gène qui est affecté dans les cellules *esa1-ts* et l'efficacité de l'exportation de l'ARNm.

Pour renforcer ces affirmations et évaluer dans quelles mesures le cas de Nup60 est particulier, nous avons réalisé une FISH de l'ARN polyA, permettant de détecter les défauts d'exportation de l'ARNm. Les cellules déficientes en Esa1 ont commencé à accumuler de l'ARN polyA après plusieurs heures d'inactivation par la température, et ce défaut a été corrigé par *nup60K467N*. Hos3-NLS est une forme artificielle de Hos3 qui est constitutivement localisée à la périphérie nucléaire de toutes les cellules ; la surexpression de Hos3-NLS est toxique et les cellules présentent un défaut d'exportation d'ARNm ; cependant, la surexpression des facteurs d'exportation d'ARNm Mex67 et Mtr2 résout ce phénotype. Collectivement, ces données soutiennent que la désacétylation des NPCs diminue l'exportation de l'ARNm.

Dans la recherche d'un moyen de relier l'acétylation des NPC à l'exportation de l'ARNm, nous nous sommes tournés vers le complexe TREX-2. TREX-2 s'associe à la nucléoporine Nup1 du côté nucléoplasmique du NPC et interagit avec de nombreux régulateurs de transcription et d'exportation tels que Médiateur et le dimère Mex67:Mtr2. Nous avons ainsi trouvé une corrélation positive entre l'état d'acétylation du NPC et l'enrichissement de Sac3 à la périphérie nucléoplasmique. Afin de tester la signification fonctionnelle de ces résultats en G1/S (lorsque les NPC des cellules filles sont désacétylés), nous avons artificiellement ancré Sac3 à la périphérie nucléoplasmique, conduisant à une augmentation globale de la localisation périphérique de Sac3. Dans ces conditions, Sac3 a favorisé la transition G1/S dans les cellules filles *esa1-ts*. Nos données suggèrent que l'acétylation de Nup60 par Esa1 favorise l'association de Sac3 avec la périphérie nucléaire, promouvant ainsi la progression dans le cycle cellulaire probablement par la modulation de l'exportation de l'ARNm ou/et de la transcription.

De plus, nous avons évalué le rôle de l'acétylation du pore nucléaire dans l'expression de gènes qui ne sont pas exprimés lors de la transition G1/S. Nous avons choisi de nous concentrer sur le locus *GAL*, qui est connu pour être associé à la périphérie nucléaire une fois qu'il est actif. En contrôlant l'expression du gène rapporteur sfGFP intégré au locus *GAL* sous le contrôle du promoteur *GAL1*, nous avons montré que l'acétylation du NPC favorise son expression. Étonnamment, nous avons constaté que la délétion de *HOS3* conduit à une apparition plus rapide de la protéine que la mutation acétylée de *nup60KN*, ce qui indique qu'il existe probablement d'autres cibles de Hos3 à la périphérie nucléaire qui modulent l'expression des gènes *GAL*. En outre, l'expression chez les cellules filles est retardée dans la souche sauvage, et cette différence mère-fille est perdue chez les mutants ayant leurs NPCs désacétylés. Nos preuves plaident en faveur

de l'importance de Sac3 dans l'activation du promoteur *GAL1*, puisque le fait de forcer Sac3 à la périphérie entraîne une expression avancée de la sfGFP dans les cellules filles.

Conclusion

Nous présentons les données soutenant que l'entrée dans le cycle cellulaire chez la levure est favorisée par l'activité du complexe acétyltransférase Esa1/NuA4 et qu'un autre complexe Gcn5/SAGA peut partiellement compenser en son absence. SAGA et NuA4 sont tous deux des régulateurs connus de la transcription, censés conduire à la décompaction de la chromatine par acétylation des histones (H3 et H4, respectivement). Nous montrons que Esa1 possède un rôle supplémentaire et qu'il acétyle Nup60 pour favoriser l'association de Sac3/TREX-2 avec le NPC et ainsi faciliter l'exportation et/ou la transcription de l'ARNm. Le mécanisme de régulation de l'exportation d'ARNm dépendant de l'acétylation est probablement universel, car nous montrons des défauts globaux d'exportation d'ARNm chez les mutants d'acétylation. En outre, nous montrons le rôle de l'acétylation de Nup60 dans l'exportation de l'ARNm de *CLN2* et le rôle de l'association Sac3/TREX-2 avec le pore nucléaire dans la transition G1/S et l'expression du gène *GAL1*.

Cependant, il reste de nombreuses incertitudes sur le rôle du NPC. Notre travail pose de multiples questions auxquelles des recherches futures devront répondre. Quel est le rôle de l'acétylation de Nup60 dans la structure de la NPC ? Quels autres composants du complexe peuvent être acétylés afin de contrôler sa fonction ? Dans le cas du locus *GAL*, l'exportation de l'ARNm est-elle favorisée par l'acétylation de Nup60 ? L'exportation de certaines classes spécifiques d'ARNm est-elle affectée par la désacétylation du NPC ? Enfin, le mécanisme que nous décrivons est-il conservé chez les métazoaires ? Ces questions, ainsi que d'autres, restent à être abordées dans le futur.

List of abbreviations

acetyl-CoA - acetyl coenzyme A

APC - anaphase-promoting complex

ATP - adenosine triphosphate

CBC - capping binding complex

CTD - C-terminal domain

Cdk - cyclin-dependent kinase

ChIP - chromatin immunoprecipitation

cryo-EM - cryogenic electron microscopy

CTD - C-terminal domain

DNA - deoxyribonucleic acid

DSB - double strand break

DUB module - deubiquitinating module

ER - endoplasmic reticulum

ERC - extrachromosomal rDNA circle

ESCRT - endosomal sorting protein required for transport

FACT complex - “facilitates chromatin transcription” complex

GDP - guanosine diphosphate

GNAT - Gcn5-related N-acetyltransferase

GTP - guanosine triphosphate

HAT - histone acetyltransferase

HDAC - histone deacetylase

HML - HoMothallism Left

HMR - HoMothallism Right

INM - inner nuclear membrane

KARMA - kinetic analysis of incorporation rates in macromolecular assemblies

KAT - lysine acetyltransferase

KDAC - lysine deacetylase

MAR - meiotic autonomous region

MBF - Mlu1-binding factor

MCB - MluI cell cycle box

mRNA - messenger RNA

mRNP - messenger ribonucleoprotein particle

mRNP - mRNA-protein complex

MYST family - MOZ-Tbf/Sas3-Sas2-Tip60 family

NAD - nicotinamide adenine dinucleotide

NAM - nicotinamide

NAT - N-terminal acetyltransferase

NDAC - N-terminal deacetylase

NE - nuclear envelope

NER - nucleotide excision repair

NLS - nuclear localization signal

NMD - nonsense-mediated decay

NPC - nuclear pore complex

NTR - nuclear transport receptor

nup - nucleoporin

ONM - outer nuclear membrane

ORC - origin recognition complex

ORF - open reading frame

PDC - pyruvate dehydrogenase complex

PIC - preinitiation complex

RBP - RNA-binding protein

rDNA - ribosomal DNA

RIP-qPCR - RNA immunoprecipitation and consecutive qPCR

RLS - replicative life span

RNA - ribonucleic acid

rSAM - radical S-adenosylmethionine

RTS - RNA transport signal

SAGA - Spt-Ada-Gcn5-acetyltransferase

SAS - something about silencing

SBF - SCB-binding factor

SCB - Swi4/Swi6-regulated cell cycle box

SCF box - Skp1–Cullin–F box

SDS - sodium dodecyl sulphate

SeRP - selective ribosome profiling

SG - stress granule

SINC - storage of improperly assembled nuclear pore complexes compartment

SIR complex - silent information regulator complex

SLIK complex - SAGA-like complex

SPB - spindle pole body

SPEED microscopy - single-point edge-excitation subdiffraction microscopy

SWI/SNF - Switch/Sucrose Non-Fermentable

TBP - TATA-binding protein

TEM - transmission electron microscopy

TF - transcription factor

TFIID - transcription factor II D

TOR - target of rapamycin

TPR - tetratrico peptide repeat

TREX-2 complex - transcription and export complex 2

tRNA - transfer RNA

TSA - trichostatin A

TSS - transcription start site

UTR - untranslated region

WT - wild type

1. Introduction

Protein-encoding gene expression in eukaryotes is an intricate process that always starts at the level of gene loci promoter and enhancer regions being bound by a specific set of transcriptional activators and/or repressors, together called transcription factors (TFs). If the gene is not constitutively active, gene activation may require changes in transcription factor binding coupled with local binding of transcriptional co-activators and chromatin remodelers. A complex known as Mediator binds to the TFs and promotes the formation of a pre-initiation complex with RNA polymerase II, and eventually, the mRNA synthesis can be initiated. The resulting mRNA undergoes several processing events, including mRNA 5'-capping, removal of introns and 3'-polyadenylation. One of the fundamental factors correlated with gene expression at the level of mRNA synthesis is the reversible post-translational acetylation of histones, the proteins that form the beads around which the DNA is coiled. The enzymes regulating the acetylation state of histones can often acetylate other targets in the cell and in this way affect gene expression through multiple pathways.

The processes described above happen in the context of highly compacted chromatin in the nucleus, a cellular compartment separated from the rest of the cellular content (cytoplasm) by the nuclear envelope, a double-layered membrane connected with the endoplasmic reticulum. The inside of the nucleus, called the nucleoplasm, contains the information of all proteins and RNAs encoded in the genome in the form of DNA, as well as certain proteins and RNAs. The mRNAs found in the nucleus are usually the ones that have not been fully processed and/or have not yet been exported to the cytoplasm, where mature mRNAs are being translated into proteins currently required to support cell homeostasis and cell cycle progression. In order to be transported from the nucleus to the cytoplasm (exported), the mRNA needs to bind specific RNA-binding proteins (RBPs), which associate co-transcriptionally and in coordination with the mRNA maturation process. Some of these RBPs are important for mRNA quality control and for the selective export of mature mRNAs.

Large molecules such as the mRNA-protein complexes (mRNP) are transported through the pores in the nuclear envelope formed by multisubunit complexes called the nuclear pore complexes (NPCs). These structures are the biggest protein complexes in living cells. Some of their components contain highly disordered regions with patches of specific amino acid sequences thought to be interacting with the nuclear transport receptors - a unique class of proteins that bind to other molecules and facilitate their

passage through the NPC. The functions of the NPCs are not limited to transport as they have been implicated in genome organization, gene expression regulation, and aging. The complexity of the NPC and the possible connections between its functions are making it a complex object for studies. A complete knowledge of the specific roles of individual proteins comprising the NPC (collectively called nucleoporins or nups) and the multiple ways cells use to regulate its diverse functions is still lacking.

During my PhD, I investigated the role of non-histone protein acetylation in gene expression in budding yeast. I found that post-translational acetylation of one of the nuclear pore components (budding yeast homologue of mammalian Nup153, Nup60) is important for gene expression, specifically for the mRNA export of *CLN2*, encoding one of the key components of cell cycle entry machinery in yeasts. I also show that differential acetylation of mother and daughter budding yeast cells in mitosis leads to distinct interaction with mRNA export factors, which is partially responsible for delayed cell cycle entry in daughter cells.

Keeping this in mind, I will first introduce the molecular players of the study such as the nuclear pore complex and the cellular enzymes regulating protein acetylation. I then finish the introduction by giving an overview of the regulation of gene expression and the cell cycle entry regulation network, with a particular focus on the role of NPC and protein acetylation.

2. Nuclear pore complex (NPC)

2.1. First description

The porous structure of the nucleus was first described in the middle of the 20th century when examination of *Xenopus laevis* oocytes revealed the presence of two layers in the nuclear "membrane". At the moment it was predicted that the inner layer largely determines the selective permeability of the nuclear envelope, same as its "elastic properties and remarkable strength", while the outside porous layer exerts a supporting function. The inner layer did not present any structural features and seemed continuous, which was at the time interpreted as possibly misleading, partially due to limited resolution (Callan & Tomlin, 1950). We can now say that the outside layer actually contained two lipid bilayer membranes of the nuclear envelope with embedded nuclear pore complexes (or NPCs), while the inner layer likely represented nuclear lamina, reviewed in (X. Wong et al., 2022).

2.2. The nuclear envelope of budding yeasts

The nuclear envelope (NE) is a membrane-based structure that physically separates the chromatin and other nuclear proteins and RNAs from the cytoplasm. It consists of two lipid bilayers which are different in terms of the proteins associated with them and consistently called the outer and the inner nuclear membranes (ONM and INM). In fact both of them are continuous with the endoplasmic reticulum (ER), and the ER lumen is the continuation of the space between the ONM and INM. (Meseroll & Cohen-Fix, 2016)

The nuclear lamina in multicellular organisms is the layer of intermediate filaments underlying the INM. It is functionally important for maintaining the nuclear shape in response to mechanical stress and for the organization of the genome within the nucleus. (Gruenbaum & Foisner, 2015) Budding yeasts do not have such a structure, but some metazoan proteins associated with lamina are functionally homologous to budding yeast proteins embedded in the INM (Grund et al., 2008; Mekhail et al., 2008).

The NE of certain fungi including budding yeasts is different in some aspects from that of multicellular organisms. It remains intact during the whole cell cycle including the time of mitosis which happens in a "closed" scenario (Arnone et al., 2013). It expands symmetrically during interphase and elongates in the anaphase of mitosis. The yeast NE is only safely breached in order to mix the genetic material during mating and

to incorporate big structures in itself, such as the spindle pole bodies (SPB) which are the yeast centrosome equivalents, and the nuclear pore complexes (or the NPCs) (Jaspersen & Ghosh, 2012; Rothballer & Kutay, 2013).

2.3. The NPC: general information, structure and function

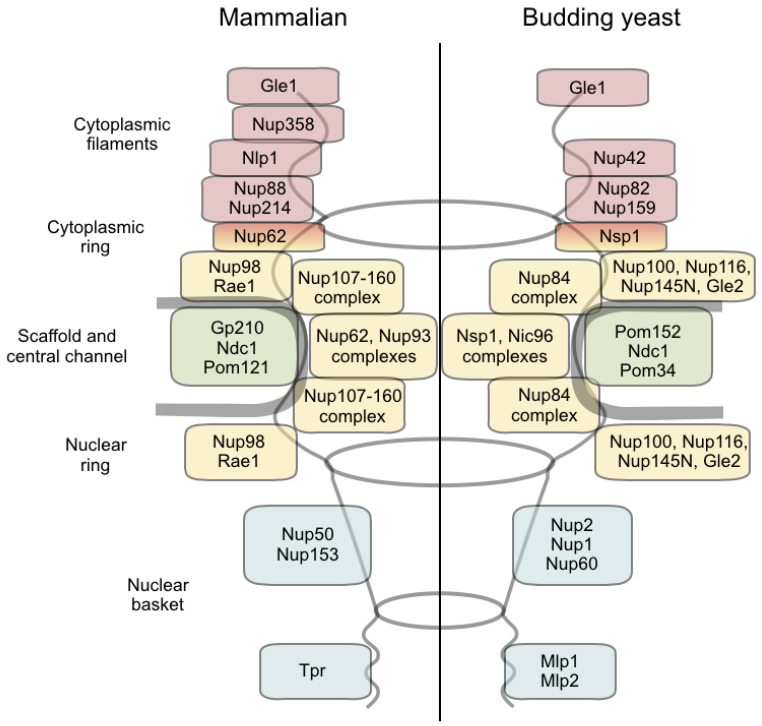

Figure 1 The nuclear pore complex *Adapted from (Lange and Corbett 2013). Mammalian nucleoporins and nucleoporin complexes are on the left, and budding yeast homologues are on the right.*

The NPC is the largest protein complex in the living cell that forms a channel embedded in the nuclear envelope, across both INM and ONM, and extends beyond both of their planes (Knockenhauer & Schwartz, 2016; Raices & D'Angelo, 2022). The primary function of the NPC is to ensure the transport of molecules between the nuclear interior (called nucleoplasm) and the cytoplasm. Small uncharged molecules (<100 Da) can diffuse through the phospholipid bilayers, whereas others have to move through the channels formed in the NE by the nuclear pore. The maximum size for passive movement determined in the experiments with gold nanoparticles in mammalian cells was between 6 and 10 nm, which approximately corresponds to 40 kDa globular protein (Huo et al., 2014). Bigger proteins and RNAs are transported actively and selectively, with the help of specialized adaptor proteins. However, recent studies propose that there is no sharp

distinction between passive and facilitated diffusion mechanisms based on the size of the protein (Timney et al., 2016).

Another group of NPC functions is connected with its components located in the nucleoplasm, which form a structure named “nuclear basket” for its shape. The nuclear basket components serve as a hub for many other proteins, which act in genome organization, regulation of gene expression, and mRNA quality control and export.

The budding yeast NPC is an ~50 MDa complex with 8-fold symmetry and a diameter of ~120 nm composed of approximately 30 subunits each present in multiple copies that form subcomplexes, schematically presented in Figure 1 (Rout & Wente, 1994). Each haploid nucleus has ~80-140 NPCs depending on the cell cycle stage. The number of NPCs per nucleus gradually increases in the cell cycle, with the highest NPC surface density being observed in the S phase. The distribution of the NPCs is not totally random: they are usually spaced apart by at least 120 nm, not clashing with each other; they form clusters of ~0.5-1 micrometer across; late anaphase and mitotic cells have a zone with increased NPC density adjacent to the SPB. (Winey et al., 1997) However, the zone in the direct vicinity of the SPB is devoid of NPCs, which has been associated with centromere tethering at SPB in *S. pombe* (Varberg et al., 2022). In recent years our understanding of NPC structure has largely improved thanks to the coordinated efforts in cryo-EM-based reconstructions of native nuclear pore structure, reviewed in (Hampoelz et al., 2019) and elegant fluorescent microscopy studies (Rajoo et al., 2017).

The metazoan NPCs are approximately twice heavier as their yeast counterparts, but the overall structure is strikingly similar. Many nucleoporins of multicellular organisms are orthologous to yeast nucleoporins, and the mechanisms of protein and mRNA transport are largely conserved. In the following sections, I will discuss the NPC functional units and their corresponding nucleoporin components with a focus on budding yeast NPC, unless stated otherwise.

The global principles of protein and mRNA transport through the nuclear pores are similar - both need to be associated with molecules called the nuclear transport receptors (or the NTRs) in order to pass through the NPC. However, the energy used for these two processes comes from distinct pools. Protein transport depends on the protein network that creates a gradient of Ran protein (in its GTP or GDP-bound forms) between the nucleus and the cytoplasm (Stewart, 2007). Another factor contributing to directional transport is the affinity of the nucleoporins along the channel, which was shown to increase for a model importin Kap95 from the cytoplasmic filaments towards the nuclear basket (Pyhtila & Rexach, 2003).

In the case of the mRNA export, the energy is provided by ATP hydrolysis catalyzed by Dbp5 at the cytoplasmic side of the NPC. It results in the removal of the mRNA export factors and mRNA release. (Hodge et al., 2011) Interestingly, ATP is as well required for mRNA "wandering" in the nucleus observed in mammalian cells (Vargas et al., 2005). Interestingly, the Ran cycle has also been implicated in the de novo NPC assembly (Ryan et al., 2003).

Approximately ⅓ of all nucleoporins contain a series of phenylalanine-glycine-rich repeats (GLFG, XFXFG, XXGF, where X is any amino acid) and are collectively denoted FG nups (C. Li et al., 2016). Most FG nups contain 10-30 repeats spaced by polar or more hydrophobic patches of 3-15 amino acids, the composition affecting their *in vitro* structures and properties (Yamada et al., 2010). These repetitive sequences tend to localize nearby in the protein and belong to unstructured regions. Many FG nups are the components of the central channel, and their FG-repeat-containing domains create a meshwork within the NPC channel that is thought to serve as a selective sieve for protein cargos. Recently nucleoporins containing GLFG repeats have been implicated in the stabilization of scaffold interactions within the NPC critical for the late stages of its assembly (Onischenko et al., 2017). To estimate the functional importance of individual FG-repeats in diverse NPC-related processes, a collection of FG-deletion strains has been constructed. (Adams et al., 2015) The commonly accepted role for the FG-repeats is to form transient hydrophobic interactions with the NTR in complex with the cargo, which is thought to ensure selective transport of species (Bayliss et al., 2000), however, there is still debate over the model that would build a satisfactory connection between the physical properties of the FG-nups and the selectivity of the NPC central channel (Frey & Görlich, 2007; Kapinos et al., 2014; Lim et al., 2007; Peters, 2005; Rout et al., 2000; Yamada et al., 2010).

Overall the structure of the nuclear pore complex can be subdivided into three distinct domains: cytoplasmic filaments, the central pore, and the nuclear basket.

2.3.1. Cytoplasmic filaments

The cytoplasmic filaments of the NPC extend by about 30 nm to the cytoplasm and decorate the entrance to the pore. Together with some FG domains of the central pore nucleoporins (e.g. Nup116), they form a dome-shaped "exclusion zone" devoid of ribosomes and other components, revealed by TEM. It includes the dense region, likely corresponding to the cytoplasmic filaments, and strikingly a low-density region extending to the cytoplasm, reaching 90 nm from the NPC central plane. (Fiserova et al., 2014) In

budding yeasts, the cytoplasmic filaments include Gle1, Nup42, and P complex nucleoporins - Nup82, Nup159, and Nsp1, which serve together as the mRNA export platform (Oeffinger & Zenklusen, 2012). The importance of the cytoplasmic part of the NPC is underscored by a number of mutations associated with different developmental diseases found in hsGle1A/B proteins homologous to budding yeast Gle1 (Kaneb et al., 2015; Nousiainen et al., 2008).

2.3.2. Central pore

The NPC central pore is embedded in the NE that forms a local fusion between the INM and ONM to accommodate the complex. The structure of the central pore can be imagined as three concentric rings: the layer directly interacting with the curved membrane at the site where INM and ONM meet, the scaffold layer, providing the stability of the complex, and the barrier layer that forms the innermost part of the pore and ensures the selectivity of the transport. The central pore components are organized symmetrically relative to the NE plane, hence termed symmetric nucleoporins, as opposed to the asymmetric ones that belong to the basket or the cytoplasmic filaments.

The membrane layer is formed by only three transmembrane nucleoporins Ndc1, Pom152, and Pom34. They are important for the correct NPC assembly including the formation of properly sized and functional pores, and for the incorporation of nucleoporins into other layers (Lau et al., 2004; Madrid et al., 2006)

The scaffold layer combines most of the least dynamic exchanging nucleoporins of the NPC. It functions to ensure the stability of the complex and to anchor the other parts of the complex.

The barrier layer consists of Gle2, Nsp1, Nup49, Nup57, Nup100, Nup116, Nup145N. All of them, except for Gle2, are FG-nups. Gle2 promotes mRNA export at elevated temperatures (Izawa et al., 2004) and supports the export of one of the pre-ribosomal subunits (Occhipinti et al., 2013). The others ensure efficient and selective transport of nuclear transport receptor-cargo complexes for both proteins and mRNA and support the permeability barrier for other species (Wente & Rout, 2010). For example, the GLFG domains of Nup116 (and likely those of Nup57) move together with the protein cargo between the cytoplasmic exclusion zone and the nucleoplasmic exclusion zone, “shuttling” within the NPC. (Fiserova et al., 2014) With regard to mRNA transport, the GLFG domains of Nup49 and Nup57 become important for polyA RNA trafficking in the absence of nuclear basket Nup1 and Nup2 GLFG domains, likely due to lower Mex67 recruitment and/or transport through the pore in mutant cells. (Terry & Wente, 2007).

2.3.3. Nuclear basket

The "nuclear basket" is a structure reminiscent of a real basket, with eight protein filaments that emanate from the nucleoplasmic side of the NPC and form a smaller ring with their distal ends, 60-80 nm from the NE edge. The nuclear basket components are Nup1, Nup2, Nup60, Mlp1, and Mlp2, scheme of the basket proteins and their relative attachment and interactions are drawn in Figure 2; however, not all of them are necessarily present in the NPC at once. The nuclear basket has several known functions such as serving as a hub for DNA repair, transcription, mRNA quality control, processing, and export, in addition to disassembly of the imported protein cargo - NTR complexes. These functions imply the role of genome organization and require interaction with diverse mRNA export factors, chromatin modification and remodeling complexes, and regulatory protein complexes such as proteasomes. The structural characterization of the nuclear basket has been complicated by its dynamic nature - *in vivo* exchange rates are comparable to those of the NTRs (Hakhverdyan et al., 2021) - and by its connection to the NE which makes it impossible to be isolated in a lipid-free environment. Esc1 is a non-NPC component protein important for proper nuclear basket assembly and function (A. Lewis et al., 2007).

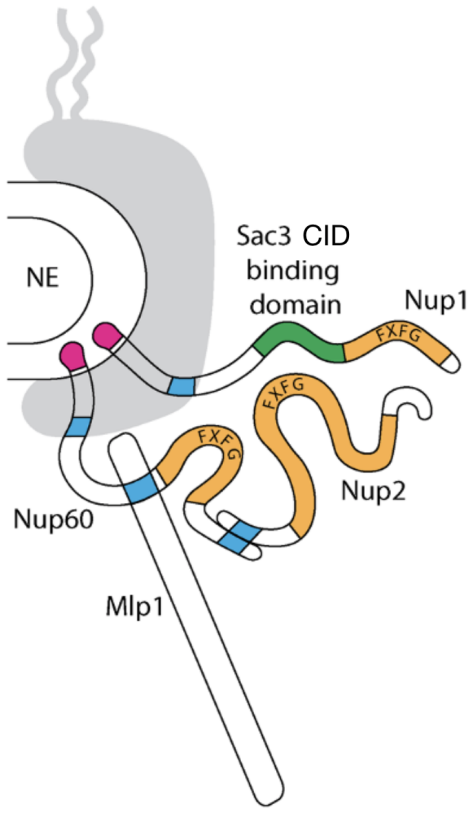

Figure 2 The nuclear pore basket *Based on (Cibulka et al. 2022; Mészáros et al. 2015; Jani et al. 2014). Nup60, Nup2, Nup1, and Mlp1 basket nucleoporins are schematically drawn next to the gray central pore of the NPC. Domains involved in protein-protein interaction are in blue, amphipathic helices of Nup1 and Nup60 are in magenta, FXFG domains are in amber, and green is the Sac3 CID interacting domain within Nup1.*

2.3.3.1. Mlp1/2

Myosin-like proteins Mlp1 and Mlp2, the yeast orthologs of human Tpr, are the heaviest proteins of the basket reaching ~200 kDa with a predicted long filamentous coiled-coil rich N-terminus and a C-terminus with undefined structure. These nucleoporins are excluded from the perinucleolar NPCs but at the same time can be found in proximity to the NE in the inter-NPC regions and in the nuclear interior. Mlp fibers interact with the Y complex of the central pore (Allegretti et al., 2020; S. J. Kim et al., 2018) and require Nup60 to be properly incorporated into the NPC (Niepel et al., 2013). Mlps are unique in several aspects: they are the least dynamically exchanging basket nucleoporins (Hakhverdyan et al., 2021), the last ones to incorporate in the newly assembling NPC (Onischenko et al., 2020), and the only non-FG basket nucleoporins (Adams et al., 2015).

Overexpression of Mlp1 causes nuclear accumulation of polyadenylated RNA (polyA RNA) indicative of mRNA export defect (Strambio-de-Castillia et al., 1999). This may imply that the dynamic association of Mlps with the NPC is important for mRNA export and that a high concentration of Mlp shifts the equilibrium towards its more stable association with the nuclear basket. Alternatively, the excess amounts of Mlps could interact with the mRNA in the nucleoplasm and hinder it from reaching the nuclear gate. Mlp1 and Mlp2 physically interact with a wide variety of NTRs and mRNA export factors, including Sac3, Mex67, and Yra1 (Niepel et al., 2013).

Apart from playing a role in mRNA export, Mlp proteins, and their metazoan homologues have been implicated in most processes connected with nuclear basket function: they support genome integrity (Niepel et al., 2005; Palancade et al., 2007), take part in mRNA quality control pathways and gene regulation (Galy et al., 2004; Vinciguerra et al., 2005), contribute to mRNA export (Green et al., 2003) and genome organization (Hediger et al., 2002).

Mlp1 and Mlp2 are not fully equivalent - for example, even though both of them can be a part of the nuclear basket, Mlp2 is yet another nucleoporin in addition to Ndc1 that functions in concert with the SPB proteins, contributing to SPB biogenesis (Niepel et al., 2005).

2.3.3.2. Nup2

Nup2 is an ortholog of metazoan Nup50. Nup2 binding to the NPC depends on interaction with Nup60 mediated by a Nup60 binding motif (Mészáros et al., 2015).

Interestingly, this motif largely overlaps with the region identified as the Meiotic Autonomous Region (MAR), which is necessary and sufficient for progression through meiosis and spore viability (Chu et al., 2017). Nup2 directly interacts with chromatin-modifying complexes and with histone H2A.Z (Dilworth et al., 2005), which brings forward the possible connection between Nup2 and transcriptional memory. While some genes are constitutively expressed, others are only activated under certain rare conditions. Such genes once activated and repressed again, may stay in a so-called "primed" state. This means that they will reactivate much faster if conditions require gene activation again. Histone variant H2A.Z is incorporated into the recently repressed promoters of *INO1* and *GAL1* inducible genes and contributes to both fast reactivation and retention of the gene loci next to the periphery (D. G. Brickner et al., 2007). However, at least in the case of *INO1*, Nup2 plays a role in the initial interaction of the nuclear pore with the activated gene that is before H2A.Z incorporation, while it is Nup100 that interacts with the repressed locus. (D. G. Brickner et al., 2019; Light et al., 2010)

2.3.3.3. Nup1

Nup1 is the partial homologue of mammalian Nup153 important both for mRNA export via binding of TREX-2 (TRanscription and EXport 2) complex (Jani et al., 2014; Schlaich & Hurt, 1995) and for disassembly of the imported NTR-cargo complexes (Gilchrist et al., 2002). Nup1 association with the NPC is proposed to be mediated by Nup170 (Kenna et al., 1996) and/or by its N-terminal amphipathic helix domain capable of interacting with (and bending) the membrane (Mészáros et al., 2015), however, the exact structural aspects of Nup1 anchoring to the pore are not clear.

Nup1-TREX-2 interaction is important for the *GAL1-10* locus relocation to the nuclear periphery upon activation and for efficient mRNA export, which is thought to promote *GAL1/GAL10* expression. One of the mechanisms proposed to explain the benefits of NPC targeting of the gene locus is the desumoylation of the transcriptional repressors by an NPC-bound Ulp1 peptidase. (Texari et al. 2013).

2.3.3.4. Nup60

Nup60, one of the key molecules discussed in this thesis, is a partial ortholog of human Nup153. It can directly interact with Mlp and with Nup2, as well as with the membrane through an amphipathic helix (Cibulka et al., 2022). Its recruitment to the NPC depends on a known α-helical region (Mészáros et al., 2015). Nup60 is an FG-nup, and Nup60 K467 residue recently linked to the NPC remodeling, gene expression and

gating, and protein transport modulation (Kumar et al., 2018; Meinema et al., 2022) is located within the FG-repeat region (Adams et al., 2015). Together with the Mlps Nup60 is required to attract and stabilize the deubiquitinating enzyme Ulp1 (Zhao et al., 2004).

Nup60 and its modifications affecting the NPC structure have been linked with DNA damage repair and telomere maintenance (Niño et al., 2016; Zhao et al., 2004), sensing cellular stress (Folz et al., 2019), chromatin organization (Galy et al., 2000) and mRNA export (Fischer et al., 2002) and transport of localized transcripts (Powrie et al., 2011).

One of the ways to regulate the Nup60 function is via Nup60 monoubiquitylation at the interaction site with the NPC Y-complex. Non-ubiquitinate mutant Nup60K(105-175)R is more dynamically associated with the NPC and demonstrates a concomitantly increased exchange rate of Nup60 interaction partner Nup2, while monoubiquitinated Nup60 is bound by Nup84 of the Y complex. Interestingly, the deletion of *NUP84* does not lead to a complete mislocalization of Nup60 (Niño et al., 2016) indicating that different modes of Nup60 binding may coexist in the cells.

Interesting roles for Nup60 and Nup2 have been recently identified in meiosis. Nup60 is recruited to meiosis I prophase chromosomes and promotes this cell cycle stage and genome integrity. However, Nup2 (or just its MAR segment) binding to Nup60 is required for the proper function of this mechanism, since otherwise Nup60 activity is inhibited via its own C-terminus. (Komachi & Burgess, 2022) A recent study claims that NPC remodeling with Nup60 detachment required for the process described above depends on Polo kinase that phosphorylates Nup60 at its Y-complex binding site. Furthermore, the binding of Nup60 to the NPC in meiosis is mediated by the amphipathic helix-membrane interaction essential for further nuclear basket formation. (King et al., 2022)

2.3.4. Stoichiometry

Despite individual nucleoporins being highly conserved from yeasts to higher eukaryotes, the overall structure of the NPC presents certain differences along the evolutionary tree. In particular, unlike the human NPC for which most of the scaffold nucleoporins are present in the maximal number of 32 units per complex, the same number for *S. cerevisiae* was determined to be 16, except for Nic96 (24 units per complex), Pom152, Nup42 and Gle1 (8 units per complex). (Rajoo et al., 2017) Another study utilizing another microscopy-based approach, however, gave slightly different

results, pointing towards the same 16 copies of nucleoporins per NPC for most NPC components, but attributing a distinct number of copies for others compared to the Rajoo *et al*. study, including Nup1, Nup60, Nup159 (8 copies per NPC), and Nic96 (16 copies per NPC) (Mi et al., 2015). Rajoo *et al*. failed to get consistent results for Mlp1 and Mlp2, likely due to the fact that these nucleoporins are excluded from the nucleolar region (Galy et al., 2004) which was critical for the method of quantification that was used. On the contrary, Mi *et al.* managed to define Mlp1 and Mlp2 to be present in the numbers of 16 and 14-16 copies per NPC accordingly, thanks to the use of SPEED (single-point edge-excitation subdiffraction) microscopy which allowed for individual NPC observation experiments thus focusing on the NPCs that possess Mlp1/2. SPEED microscopy makes use of inclined illumination that results in the point spread function, the essential microscopy parameter defining the resolution, of lower dimensions; the NPCs that were quantified by this method belonged to NPC-poor areas of the NE (Mi et al., 2015), which on one hand allowed to properly quantify single NPC, but on the other - lead to a biased selection of NPCs. This study additionally demonstrated that altering certain nucleoporin levels leads to marked changes in the NPC stoichiometry leaving them functional, which revealed the plasticity of the complex. (Rajoo et al., 2017)

The authors of the latest work aiming to improve the knowledge of the native NPC structure used gentle NPC isolation by subfractionation or affinity capture followed by mass spectrometry. The two isolation methods gave quite consistent results for most major nups: most were found present in 16 copies per NPC, with 32 copies of Nic96, Nup57, and Nup49 and 48 copies of Nsp1; cytoplasmic ring components Gle1 and Nup42 present in the number of 8 copies per NPC. Less consistent between isolation methods were the results for nuclear basket components, ranging between 4-8 copies per NPC for Mlps, 8-16 copies per NPC for Nup1, and 8-24 copies per NPC for Nup60. (Kim et al. 2018) The discrepancy in the nuclear basket composition may reflect both its variable stability dependent on the isolation method and the variable composition of the native NPCs.

2.4. NPC biogenesis

In order to perform its functions, the NPC has to be correctly assembled and maintained in a functional state. The budding yeast NPC requires coordinated synthesis of ~30 different proteins in defined stoichiometric quantities; it may be specifically challenging because of the large number of subunits with intrinsically disordered domains that are prone to aggregation. This is followed by the nucleation of the pre-NPC next to

the INM and piercing a hole in the NE with simultaneous integration of the pre-NPC. In case something goes wrong on the way, the defective pre-NPC should be detected and the integration process stopped, if not - the later incorporating nucleoporins such as the cytoplasmic filaments and the nuclear basket components are integrated. The speed of new NPC generation in budding yeasts is quite slow since the NPCs in organisms with closed mitosis never leave the NE, and their numbers are growing gradually. Once created, the NPC undergoes continuous remodeling - some nucleoporins are constantly exchanging with the nuclear pool and some are stably integrated. The core components do not exchange within one cell cycle and may last days.

2.4.1. Nucleoporin synthesis

Early steps of NPC biogenesis involve interactions between certain mature NPC subunits and mRNAs encoding their interacting partners engaged in translation. This mechanism favors the co-translational assembly of NPC subcomplexes and co-translational establishment of interactions between distinct subcomplexes as revealed by SeRP (selective ribosome profiling) and RIP-qPCR (RNA immunoprecipitation and consecutive qPCR) (Lautier et al., 2021; Seidel et al., 2022). Additionally, *NUP1* and *NUP2* mRNAs were shown to co-translationally interact with largely assembled NPCs embedded in the nuclear envelope thus serving the correct integration of emerging proteins in the nuclear basket (Lautier et al., 2021). Such hierarchical NPC assembly organization is thought to be beneficial as it allows more time for assembly intermediates to ensure efficient subcomplex formation and avoid protein misfolding. Furthermore, it may contribute to supporting stoichiometry ratios between individual nucleoporins.

The kinetics of NPC biogenesis can be generally described by saying that the first subcomplexes to assemble are symmetrical core nucleoporins followed by asymmetrical ones and finalized by the association of Mlp1/2 subunits as demonstrated in (Onischenko et al., 2020) by metabolic labeling-based approach. Interestingly, this method (termed KARMA) led to the identification of 4 rapidly exchanging slow-maturing nucleoporins, namely Nsp1, Seh1, Nup188, and Nup133. The authors speculate that two out of four, Nsp1 (S. J. Kim et al., 2018) and Seh1 (Dokudovskaya et al., 2011) are known to engage in alternative complexes and their large maturation pools could represent the strategy to avoid competition for protein availability. Strikingly, exactly the same nucleoporins are shown to be associating with partner nucleoporins in a co-translational manner, namely full-length Nsp1 co-translationally binds nascent Nup57

and, in the same way, Seh1 binds Nup85 (Seidel et al., 2022), which could be yet another reason why the protein pools are increased.

The fact that Mlp1/2 incorporation happens at the stage of fully assembled NPC is in agreement with the observation that certain pores are devoid of Mlp1/2 (Galy et al., 2004). Intriguingly, Mlp1 assembly with the NPC has been shown to depend on transcription by Pol II and mRNA processing (Bensidoun et al., 2022).

2.4.2. NPC integration in the NE

Mitosis in multicellular organisms is associated with the profound NPC remodeling and regulated dissolution of the nuclear envelope, which is rebuilt with concomitant incorporation of NPCs in telophase, reviewed in (Otsuka & Ellenberg, 2018). In interphase, however, the newly forming pores have to be incorporated into the continuous NE. Budding yeast divide by closed mitosis, which means that the NE is never undergoing remodeling to the same extent. The fact that both budding yeast and interphase cells of metazoans have to solve the problem of integrating a huge newly formed protein complex in the double membrane, similar mechanisms are thought to be applied in these distant branches of eukaryotes.

The correct integration of the NPC depends on the NE dynamics - the most complicated part of the large structure integration to the NE may be how to make a hole in it and not let the nucleoplasm and the cytoplasm intermix. Studies in a cell-free system - the nuclei assembled in *Xenopus* egg extracts - point towards a stepwise mechanism of the NPC integration that requires the fusion of NE membranes. This is thought to be happening in the sites where the INM and ONM come closer to each other as observed by TEM (D'Angelo et al., 2006). The hypothesis is confirmed in a later electron microscopy study that examined the post-anaphase mammalian cells in the time course. The authors conclude that interphase integration of the NPC to the NE occurs from the nucleoplasmic side and that indeed the process is stepwise. The dome-shaped evaginations of the INM were created that gradually increased in depth and diameter. At this stage, the central pore components including hsNup107 (mammalian homologue of yeast Nup84) and several others were found associated with the curved INM. The cytoplasmic filaments are only incorporated at a later stage of maturation, likely after the membrane fusion step. Interestingly, the 8-fold rotational symmetry of the pre-NPC can be observed from the earliest stages of integration. (Otsuka et al., 2016)

The membrane fusion is thought to be facilitated by transmembrane nucleoporins and certain reticulons - ER membrane proteins able to bend the membrane

(Dawson et al., 2009; Madrid et al., 2006). In particular, deletion mutants for Apq12, the integral NE and ER protein, accumulate NPCs that are associated with the INM but not the ONM. (Scarcelli et al., 2007) Together with two other proteins, Brl1 and Brr6, Apq12 is thought to serve as a sensor coupling the NE piercing with the maturation of NPC components to be inserted (Dultz et al., 2022; Hodge et al., 2010; Kralt et al., 2022). Apq12 may serve as a link between NPC integration and the local lipid composition which is another important factor for membrane fusion (W. Zhang et al., 2021; Zhukovsky et al., 2019).

2.4.3. Dynamic and stable associations of nucleoporins with the NE

While some nucleoporins seem to be stably associated with the NPC, others are dynamically exchanging with soluble pools. In mammalian cells, several other nucleoporins such as nuclear basket components Nup50 and Nup153 and central pore components Nup98 and Rae1/Gle2 were shown to associate dynamically with the NPC, whereas others, specifically scaffold nucleoporins, interact in a stable manner. (Griffis et al., 2002; Lindsay et al., 2002; Pritchard et al., 1999; Rabut et al., 2004)

One example of the budding yeast dynamically associating nucleoporin is Nup2, the component of the nuclear basket. Upon heterokaryon formation, Nup2-GFP relocalized from the GFP-fluorescent nucleus to the non-labeled one, unlike any other of the nucleoporins tested (Nup49, Nup60, Nsp1). Nup60 binding to the nuclear basket depends on Nup60 and on the Ran gradient, one of the major determinants of nuclear protein import. Nup2 in *nup60* deficient cells is distributed throughout the nucleoplasm; interestingly, under the conditions of metabolic poisoning leading to Ran-GTP depletion, Nup2 regains the ability to associate with the nuclear periphery. This could be explained by the suggested existence of an alternative Nup2 docking site at the cytoplasmic face of the nuclear pore since in the same study Nup2 was found associated with both nucleoplasmic and cytoplasmic faces of the NPC in wild-type cells and with the cytoplasmic face in *nup60* deficient cells by immunoelectron microscopy of purified nuclei. (Dilworth et al., 2001)

The dynamic exchange of NPC components with their soluble fractions *in vivo* has been assessed in a proteomic study using radioisotope labeling and tightly regulated expression of tagged nucleoporins (Hakhverdyan et al., 2021). The fastest exchanging nups belong to the nuclear basket (Nup1, Nup2, and Nup60) and, interestingly, Ndc1, the transmembrane nucleoporin which associates with the SPB upon its insertion to the NE (Rüthnick et al., 2017). Slightly slower exchange rates are demonstrated by the several

central pore nups and Gle1 of the cytoplasmic nups. The scaffold of the NPC contains the slowest exchanging nucleoporins, joined by the major nucleoporins that create the selectivity barrier for protein transport, Nsp1-Nup49-Nup57. Interestingly, no correlation between the exchange rates and turnover rates was found. (Hakhverdyan et al., 2021)

2.5. NPC quality control and inheritance

Correct assembly of the functional NPC is supervised by the ESCRT-III/Vps4 dependent mechanisms. ESCRT is a protein family whose name stands for the endosomal sorting complexes required for transport. The components of ESCRT can topologically bend membranes and perform scission of the resulting vesicles (which is specifically the role of ESCRT-III). Vps4 is one of the proteins recycling the ESCRT components from the vesicle back to the cytoplasm. (Schmidt & Teis, 2012) The clearance of the improperly assembled NPCs is performed by ubiquitination-dependent proteasome degradation of the storage of improperly assembled nuclear pore complexes compartment (SINC) contents. SINC is specifically retained in the mother cells. The early NPC intermediates interact with the INM protein Heh2, which in turn may be bound by the Snf7 component of ESCRT-III. The authors of the study referenced below favor the hypothesis that in case the NPC is not timely formed then comes the next step in the NPC quality control which is the Vps4-dependent formation of an intralumenal vesicle and further cytoplasmic degradation of the malformed NPCs, but direct evidence is so far missing. (Webster et al., 2014) Later study points toward Heh2 as the sensor of the NPC assembly state (Borah et al., 2021).

Nucleoporins in budding yeast daughter cells are inherited in the mitosis from the mother cells. This is happening in the course of nuclear extension and fission in anaphase and telophase when the nucleus partially enters the bud through the bud neck as it elongates and divides into two nuclei. At the same time, the NPC delivery from the mother to the daughter is an active process, and the NPCs entering the daughter segment of the dividing nucleus have to cross the selectively permeable septin-mediated diffusion barrier at the level of the bud neck (Makio et al., 2013). For example, the NPCs lacking the Nsp1 subcomplex (Nsp1, Nup57, Nup82) were passing the barrier significantly worse than the wild-type counterparts. (Makio et al., 2013) Interestingly, another paper published closely in the time indicated that the newly synthesized pool of Nsp1 is important for daughter viability and NPC inheritance (Colombi et al., 2013).

Importantly, this barrier ensures the retention of non-centromeric plasmids in the mother cell, and later work supported this model and demonstrated that such plasmids are

retained in the mother cells together with the NPCs to which they are anchored in a mechanism dependent on SAGA and TREX-2 complexes. In aged mother cells this largely contributes to increased NPC numbers, likely due to the formation of an NPC cap - a structure in the nuclear envelope densely packed with NPCs associated with the non-centromeric plasmids increasingly accumulating with cell age. (Denoth-Lippuner et al., 2014; Shcheprova et al., 2008) The non-centromeric plasmids in these studies serve as a model of naturally occurring extrachromosomal DNA circles. The most widely known example of such circles in budding yeast is extrachromosomal ribosomal DNA circles of ERCs. As mother cells age, they accumulate spontaneously excised ERCs which are autonomously replicating sequences encoding 5S and 35S ribosomal RNA. Increasing numbers of ERCs contribute to the gradual loss of homeostasis and entry to senescence due to excessive rDNA transcription (Morlot et al., 2019).

Under starvation or TORC1 pharmacological inhibition, the NPCs are selectively degraded with the participation of the cell autophagy machinery. One of the studies describing this phenomenon reported that the degradation was enhanced in mutants that cause NPC clustering. However, the physiological relevance of this pathway is yet to be described. (C.-W. Lee et al., 2020; Tomioka et al., 2020)

2.6. NPC regulation in the cell cycle

As will be discussed in later chapters, cell cycle progression is associated with changes in gene expression. They may be caused by modulation of nucleo-cytoplasmic protein transport, mRNA nuclear export, or chromatin structure, processes that are in whole or in part dependent on the NPC. The NPC structure is therefore likely subject to regulation in a cell cycle-dependent manner.

One known example of an NPC-dependent cell cycle regulation mechanism is the mitosis-specific inhibitory interaction between Nup53 and Kap121 importin. In G1 and S phases Nup53 interacts with Nup170 and cannot bind Kap121, while in mitosis possibly due to Cdk-dependent phosphorylation, Nup53-Nup170 interaction is lost and the Kap121 binding domain (KBD) of Nup53 is revealed. KBD competes with the cargo of Kap121 for the NLS-binding site and thus likely destroys Kap121-cargo complexes preventing the cargo from being imported. Cells with compromised function of Kap121 are delayed in mitosis. One of the known Kap121 cargos is Cdh1, an activator of the Anaphase-promoting complex which is required for exit from mitosis. (Lusk et al., 2007; Makhnevych et al., 2003; Marelli et al., 1998).

Another example of cell cycle-dependent modification of the NPC is the deacetylation of multiple nups by Hos3, as will be discussed later.

3. Protein acetylation and its role in the regulation of gene expression

Post-translational modifications are changes in the covalent bond composition of protein synthesized by the translation machinery, therefore expanding the information encoded in the mRNA. Such changes may include proteolytic cleavage and modification of side chains or N-/C-terminus. Side chain modifications are getting more attention with an increased number of ways to study them in a high-throughput manner. The functional consequences of protein side chain modifications are diverse and include changes in enzymatic activity, localization, ability to interact with its partners, and stability. Some examples of such modifications are phosphorylation, methylation, ubiquitination, and acylation. One of the many acyl groups that may be found decorating eukaryotic proteins is acetyl, the second smallest of the homologous series of acyl substituents. (Mann & Jensen, 2003; Marino et al., 2015)

There are two types of protein acetylation. The first one, Nα-terminal acetylation, performed co- and/or posttranslationally by N-terminal acetyltransferases (NATs) in the majority of eukaryotic proteins and currently considered irreversible since so far, no enzyme has been discovered that catalyzes N-terminal deacetylation (N-terminal deacetylase or NDAC) (Ree et al., 2018). The second one, post-translational acetylation of lysine ε-amino groups, is less frequent, but possibly more important, providing means for flexible regulation of protein function. It is achieved by the activity of lysine acetyltransferases (KATs) and reversed by lysine deacetylases (KDACs). NATs and KATs require acetyl-CoA as a source of acetyl groups for their activity (Figure 3). Both types of acetylation have been shown to play a role in protein function (Glozak et al., 2005; Polevoda & Sherman, 2000), however in this thesis, I focus on the reversible Nε lysine acetylation.

One consequence of lysine acetylation, positive charge neutralization, is thought to serve two global goals: on one hand, it may hinder electrostatic interactions (for example between the acetylated protein and DNA) and on the other hand, it may promote interaction with certain proteins (such as bromodomain-containing proteins belonging to transcription machinery that interact with acetylated histones (Hassan et al., 2007)).

A recent study comparing global acetylation and phosphorylation between *Drosophila melanogaster* and *Homo sapiens* demonstrates that lysines targeted by acetylation are more evolutionary conserved than serines and threonines targeted by

phosphorylation, and also that acetylated lysines are more conserved than non-acetylates ones. This suggests that the portion of lysine acetylation sites under selective pressure is higher than that for serine/threonine phosphorylation. Gene Ontology terms analysis of the identified conserved acetylation sites suggested that this post-translational modification is important for such cellular processes as protein translation, protein folding, DNA packaging, and mitochondrial metabolism (Weinert et al., 2011).

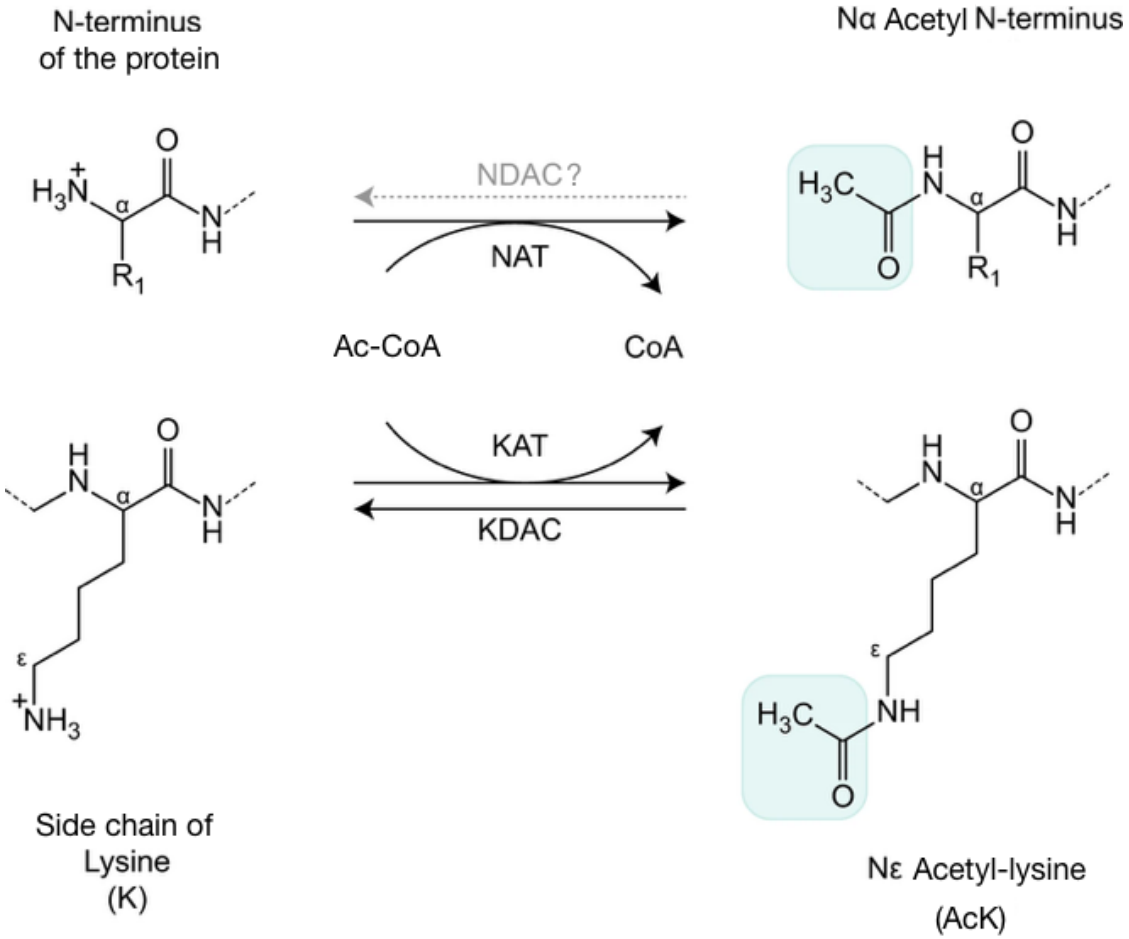

Figure 3 N-terminal and N-ε acetylation *Adapted from (Ree, Varland, and Arnesen 2018) Acetylation of protein N-terminus (top) and lysine N-ε amino group (bottom). Both processes require Ac-CoA, both processes are in principle reversible, although NDAC has not yet been discovered.*

3.1. Histone acetylation

The First evidence that histones are acetylated came in 1963 (Phillips, 1963), while by that time protein acetylation was already known for ovalbumin, cytochrome C, α-melanocyte-stimulating hormone, and tobacco-mosaic-virus protein (Harris, 1959; Narita & Ishii, 1962; Ramachandran & Narita, 1958; Titani et al., 1962).

At the time, histones were thought to inhibit DNA-dependent RNA synthesis in differentiated cells of higher animals and plants. This idea was first proposed in 1951 (Stedman & Stedman, 1951) and later was supported by data from biochemical studies in which, for instance, RNA synthesis was decreased upon the addition of isolated histones to isolated calf thymus nuclei. In a complementary experiment, trypsinization of isolated calf nuclei, preferentially digesting histones because of their high lysine/arginine content, led to enhanced RNA synthesis (Allfrey et al., 1963). However, the idea that histones are inhibitory for RNA synthesis did not give an explanation of how to increase RNA production without histone removal. The revolutionary discovery that minor and likely reversible changes in histone chemistry composition that do not impact their amino acid composition, such as acetylation, may promote RNA synthesis, came from the study in which chemically acetylated histones had significantly lower (or completely lacked) the inhibitory effect on RNA synthesis in calf thymus nuclei, relative to non-acetylated histone control (Allfrey et al., 1964). Further studies revealed that certain transcriptionally active chromatin regions present elevated levels of core histone acetylation (Hebbes et al., 1988; Sealy & Chalkley, 1978) strengthening the idea that histone acetylation does facilitate RNA polymerase function.

It was also known for a long time that newly synthesized histones H3 and H4 are readily acetylated after their synthesis and that these modifications are removed following the assembly of nucleosomes (Jackson et al., 1976). However, it was not until 1995 that the first eukaryotic acetyltransferases started to be identified. Budding yeast Hat1 acetyltransferase activity was discovered in a screen looking for mutants associated with reduced acetylation of histone H4 tail peptide (Kleff et al., 1995). The same year another enzyme harboring acetyltransferase activity *in vitro* was identified in crude macronuclear extracts of *Tetrahymena thermophilus* in a gel-based activity assay for which target core histones were co-polymerized in the SDS gel (Brownell & Allis, 1995). Once the corresponding gene was cloned, its protein sequence turned out to exhibit high homology with yeast Gcn5 protein(Brownell et al., 1996) which was already known to function as a transcriptional adaptor required for transcriptional activation, thus strongly supporting the connection between histone acetylation and transcriptional activation (Georgakopoulos & Thireos, 1992). Further studies confirmed the correlation between the ability of Gcn5 to acetylate histones and to promote transcription (Kuo et al., 1998; L. Wang et al., 1998).

A study on the dynamics of targeted histone acetylation or deacetylation has shown that untargeted HAT (histone acetyltransferases) and HDAC (histone deacetylases) activities are highly dynamic and restore the basal level of acetylation within minutes

after chromatin state modulator is no longer bound to a specific locus. Specifically, targeted VP16-mediated histone H3 hyperacetylation was removed within ~1.5 minutes, while targeted Ume6-mediated hypoacetylation of histones H3 and H4 was recovered within 5-8 minutes at the same promoter. Interestingly, the same study revealed that TATA-binding protein disappears from the promoter immediately after the dissociation of the targeted VP16 activator, before the reversal of histone acetylation, which stresses the need for the activator to be present at the promoter for TBP binding to otherwise hyperacetylated chromatin. (Katan-Khaykovich & Struhl, 2002)

One of the early attempts to decipher the causal relationship between the transcription and histone acetylation showed that histone acetylation at the promoter regions genomewide depends neither on RNA Pol II nor on TAF1, TFIID component, supporting the hypothesis that likely histone acetylation precedes transcription and is not its direct consequence (Durant & Pugh, 2006). This study has recently been contested with regard to results concerning RNA Pol II by a follow-up publication, using pharmacological inhibition of mRNA synthesis instead of the genetic inhibition by the use of the *rpb1-1* allele as in the original research. The conclusion was that RNA Pol II promotes both the recruitment and activity of KATs towards chromatin, essentially shapes the histone acetylation landscape, and contributes to a feed-forward loop facilitating further transcription (Martin et al., 2021). Even though the use of phenanthroline by Martin et al. was reported to affect major signaling pathways that cause changes in certain transcription factors and KAT/KDAC promoter occupancies as mentioned in a critical response by (Zencir et al., 2022), the conclusion that a large proportion of histone acetylation depends on ongoing transcription is supported in other studies (Z. Wang et al., 2022). The arguments of the critical response are addressed in the rebuttal letter, showing that the KAT occupancies are changed only for a minor part of genes and that even if the KAT is not lost from the promoter region, acetylation is decreased. This stands in agreement with their original claim that association of KAT does not automatically mean acetylation, and that KATs are regulated at promoters post-recruitment. (Martin & Howe, 2022)

The functional significance of different histone amino acids including lysines has been evaluated in a number of studies, which revealed several important regions for histone function and cell viability, including the N-terminal tails for histones H3, H4, and H2B - one of the most heavily modified parts of the histones (Dai et al., 2008; Jiang et al., 2017). The tails themselves or modifications within must play an essential role in cells, since N-terminal deletions of both histone H3 and H4 tails are lethal and that the

tails are known to be important for nucleosome assembly (Ling et al., 1996; B. A. Morgan et al., 1991). Interestingly, in the case of H2A, it is the C-terminal but not the N-terminal tail that is more sensitive to amino acid changes (Jiang et al., 2017). However, the precise role of acetylation of individual lysines within histone tails remains unclear (Dai et al., 2008; Jiang et al., 2017).

3.2. Non-histone acetylation that impacts gene expression

In addition to well-established evidence of histone acetylation in gene expression regulation, a significant amount of evidence points to acetylation regulating gene expression in histone-independent ways. Acetylation targets are found among transcription factors and enzymes, and recently the nuclear pore complex function has been shown to depend on the acetylation of its components. The comparisons of acetylation levels in different cellular compartments revealed low levels of acetylation stoichiometry for most proteins, the highest being observed in nuclear ones - transcription factors and components of acetyltransferase and deacetylase complexes (Weinert et al., 2014), which makes their acetylation likely functionally important.

3.2.1. Transcription factor acetylation

Acetylation of transcription factors, similar to that of histones, is thought to mostly change their DNA binding and interactions with other proteins. (Bannister & Miska, 2000) Multiple transcription factors of multicellular organisms are known to be regulated by acetylation, the list including p53, pRb, GATA1, some general transcription factors, and many others. (Polevoda & Sherman, 2002)

It seems that a bit less is known about budding yeast transcription factor acetylation. One of the few examples is Ifh1 which regulates the transcription of ribosomal proteins. It is acetylated on several lysines within the N-terminus by SAGA and deacetylated by sirtuins. Its acetylation is decreased upon rapamycin-induced inhibition of TOR which is accompanied by a decrease in ribosomal protein gene expression. The analysis of the Ifh1 acetyl-mimic mutant and the mutant, mimicking constitutive deacetylation, showed that acetylation is inhibitory for its function. Acetylation of Ifh1 is proposed to limit the otherwise robust initial increase in transcription of ribosomal proteins that follows a switch to a more preferable carbon source. (Downey et al., 2013)

Another example is Swi4, the component of the SBF transcription factor playing a role in cell cycle entry. Acetylation of Swi4 regulates the stability of SBF by

modulating Swi4-Swi6 interaction. Swi4 is the yeast homologue of E2F, which is regulated by acetylation in multicellular organisms (Martínez-Balbás et al., 2000). Swi4 acetylation may be directly regulated by the deacetylase Rpd3. According to mutational analysis, the acetylation status of Swi4 does not change its binding to DNA target sites, however, the transcription of SBF-regulated genes was significantly decreased in the deacetyl-mimic mutant. The two lysines belong to the Swi6 binding domain, so likely their acetylation contributes to efficient SBF complex formation. (Kaluarachchi Duffy et al., 2012)

Transcriptional repressors are also targets of acetylation-dependent regulation. The zinc-cluster Ume6 protein is a transcriptional repressor located at Early Meiotic Genes promoters in mitosis and recruiting histone deacetylase and chromatin remodelers in order to ensure inactivated state of the genes. Gcn5 acetylates several lysines within the zinc cluster in order to loosen DNA binding, likely by removal of the electrostatic bonds between the repressor and DNA. This step promotes further ubiquitination-dependent degradation of Ume6. The expression of the Ume6 non-acetylatable allele caused a delay in the expression of Early Meiotic Genes. (Law et al., 2014)

3.2.2. Kinase acetylation

Cdc28 was found to be acetylated on conserved K40 position in the catalytic ATP-binding pocket, and mutations of this lysine either to arginine (to mimic constitutive deacetylation) or to glutamine (to mimic constitutive acetylation) were not able to support growth underlining the functional significance of this lysine (Choudhary et al., 2009). The analogous site in mammalian CDK9 (K48) is considered to be important for orienting phosphate groups of ATP and for magnesium ion binding (De Bondt et al., 1993). Interestingly, CDK9 in complex with cyclin T1 was shown to primarily phosphorylate the C-terminal domain of RNA Pol II at serine 5 (Gibbs et al., 2017) in *Drosophila*, and K48 acetylation by GCN5 and P/CAF inhibits its kinase activity (Sabò et al., 2008) in U2OS cells.

3.2.3. Nuclear pore acetylation

The studies of nuclear pore acetylation pointing to the functional significance of nuclear pore acetylation have just started to emerge in recent years, even though acetylation of nuclear pore components has been known since the beginning of 2010s both for budding yeasts (Downey et al., 2015; Henriksen et al., 2012) and for higher

eukaryotes (Beli et al., 2012; Y. Chen et al., 2012; Choudhary et al., 2009; Lundby et al., 2012; Sol et al., 2012; Weinert et al., 2011, 2013). Several nucleoporins from different parts of the NPC have been consistently found in these studies to yield acetylated peptides (see Table 1, Supplementary tables 1 and 2), but the effects of nuclear pore acetylation on cell physiology remain largely unexplored.

Table 1 Nucleoporins grouped by location and function within the NPC. *Adapted from (Lange & Corbett, 2013). Nucleoporins that yielded acetylated peptides at least in one of the acetylome studies in bold; nucleoporins that were found to be acetylated in the same position in at least 2 studies are underlined. References point to the studies where acetylated peptide(s) for corresponding nucleoporins were detected.*

Budding yeast *(S. cerevisiae)*	Mammalian	Location within NPC	Motifs/domains	Predicted function
Nup1(Downey et al., 2015; Henriksen et al., 2012), **Nup60**(Downey et al., 2015; Henriksen et al., 2012)	**Nup153**(Beli et al., 2012; Y. Chen et al., 2012; Choudhary et al., 2009; Lundby et al., 2012; Weinert et al., 2013)	Nuclear	FG	Structure; transport
Nup2(Downey et al., 2015; Henriksen et al., 2012)	**Nup50/Npap60**(Beli et al., 2012; Y. Chen et al., 2012; Choudhary et al., 2009; Lundby et al., 2012; Sol et al., 2012; Weinert et al., 2013)	Nuclear	FG	Transport
Mlp1(Downey et al., 2015; Henriksen et al., 2012), Mlp2	**Tpr**(Beli et al., 2012; Y. Chen et al., 2012; Choudhary et al., 2009; Lundby et al., 2012; Sol et al., 2012; Weinert et al., 2013)	Nuclear	Coiled-coil	Structure; transport
Nup1 complex: **Nsp1**(Henriksen et al., 2012), **Nup49**(Henriksen et al., 2012), Nup57	*Nup62 complex*: Nup45, Nup54, Nup58, Nup62	Symmetric	FG, coiled-coil	Structure; transport
Nic96 complex: Nic96, **Nup53**(Downey et al., 2015; Henriksen et al., 2012), Nup59, Nup157,	*Nup93 complex*: Nup35/53, **Nup93**(Sol et al., 2012; Weinert et al., 2013), **Nup155**(Lundby et al., 2012),	Symmetric	β-Propeller, α-solenoid, FG	Structure; transport

Nup170(Henriksen et al., 2012), Nup188, Nup192	**Nup188**(Choudhary et al., 2009; Lundby et al., 2012), **Nup205**(Beli et al., 2012; Choudhary et al., 2009)			
Nup84 complex: Nup84, Nup85, Nup120, Nup133, Nup145C, Sec13, Seh1	*Nup107–160 complex*: ALADIN, Nup37, Nup43, Nup75/85, Nup96, **Nup107**(Y. Chen et al., 2012; Lundby et al., 2012), **Nup133**(Y. Chen et al., 2012; Lundby et al., 2012; Sol et al., 2012; Weinert et al., 2013), **Nup160**(Y. Chen et al., 2012), Sec13, Seh1	Symmetric	β-Propeller, α-solenoid	Scaffold
Pom152	Gp210	Transmembrane	TMH	Transport
Ndc1	Ndc1	Transmembrane	TMH	Structure
–	**Pom121**(Choudhary et al., 2009)	Transmembrane	TMH, FG	Structure
Pom34	–	Transmembrane	TMH	Structure
Nup100(Downey et al., 2015), Nup116, Nup145N	**Nup98**(Y. Chen et al., 2012; Choudhary et al., 2009)	Symmetric	FG, Nup98 fold	Transport
Gle2	**RAE1**(Weinert et al., 2013)/Gle2	Symmetric	β-Propeller	Transport
Nup82	**Nup88**(Lundby et al., 2012)	Cytoplasmic	β-Propeller, coiled-coil	Structure
Nup159(Downey et al., 2015)	**Nup214**(Choudhary et al., 2009; Lundby et al., 2012; Weinert et al., 2013)	Cytoplasmic	β-Propeller, coiled-coil, FG	Structure
–	Nup358	Cytoplasmic	FG	Structure; transport
Nup42	NLP1/CG1	Cytoplasmic	FG	Structure; transport

The most consistently acetylated nucleoporins between budding yeast and mammals reside in the nuclear basket, making it reasonable that most studies so far have concentrated on acetylation of Nup60 and Nup1 (mammalian Nup153), Nup2 (mammalian Nup50) and Mlp1/2 (Tpr).

Acetylation of *Arabidopsis thaliana* Nup50 conserved residue K18 was shown to be decreased upon treatment with KDAC inhibitors TSA and apicidin (Hartl et al., 2017). The analogous residue of murine Nup50 K8 is located within the binding segment 1 and responsible for complex formation with importin-α, and the crystal structure of the complex suggests that K8 approaches a negatively charged amino acid in the acidic linker of Nup50 located right next to the binding segment 1. This interaction likely contributes to the formation of the β-turn that intrudes the NLS binding site of importin-α and accelerates the importin-cargo complex disassembly upon entry; the mechanism is predicted to be affected by K8 acetylation (Füßl et al., 2018). Acetylation of Nup2, the yeast functional homologue of Nup50, was shown to at least partially depend on SAGA (Downey et al., 2015; Henriksen et al., 2012).

Even though Tpr presents the highest number of conserved acetylation sites among nucleoporins (see Supplementary table 2), so far there are no studies examining their functional relevance. The significance of acetylation sites within yeast Nup1 is still cryptic as well. Acetylation of Nup153 and its yeast homologue Nup60, on the other hand, has been investigated slightly more extensively.

The functional significance of budding yeast Nup60 acetylation has been studied in recent years by two groups including ours (Kumar et al., 2018; Meinema et al., 2022). I will discuss the work by (Meinema et al., 2022) in the Discussion section of the thesis, and here I will briefly list the findings relative to the functional consequences of NPC deacetylation by Hos3 and some nucleoporin substrates identified as its targets.

Our group has shown that Hos3 deacetylase localizes to the daughter nuclear baskets in anaphase, where it deacetylates a number of nuclear pore components including Nup60, Nup49, and Nup57. Their deacetylation synergistically delays Start in daughter cells through at least two independent mechanisms. On one hand, nucleoporin acetylation regulates the transport of the G1-phase transcription repressor Whi5. Indeed, Whi5 concentration is higher in daughter cells than in mother cells at the moment of cell birth and this asymmetry is decreased in acetyl-mimic mutants Nup60K467N, Nup49-K(382,383)N and their combination. On the other hand, Nup60 acetylation also modulates the association of the *CLN2* gene locus with the nuclear periphery. Constitutive localization of Hos3 to the nuclear periphery of both mother and daughter cells at all cell cycle stages led to changes in the distribution of RNA (Mtr2, Mex67, Los1) and protein (Kap95) transport factors. (Kumar et al., 2018)

Interestingly, three acetylation sites (K228, K262, and K272) have been detected in Nup2 within the FG-repeat region (Adams et al., 2015; Downey et al., 2015; Henriksen

et al., 2012), and one low-confidence acetylation site at K51 - right next to the Kap binding domain (Cibulka et al., 2022). At the same time, its mammalian homologue Nup50 is a verified target of regulation by acetylation, however, in addition to K8, there are 2 more acetylation sites within the importin binding domain (K59, K83) and K162, within the domain responsible for NPC (Nup153, the yeast Nup60/Nup1 homologue, or MEL28/ELYS) binding (Holzer et al., 2021).

Nup60 may also be regulated by acetylation at other sites except for the one we characterize. Several other low-confidence acetylation sites are located within or next to a predicted motif with so far uncharacterized function (K358, K363 (Cibulka et al., 2022; Henriksen et al., 2012)), and another one maps to the FG-repeat region (Henriksen et al., 2012).

3.2.4. Protein acetylation in connection with metabolism, cell cycle entry, and growth

Acetyl-coenzyme A, the compound that the cell uses as a source of acetyl groups for protein acetylation, is the downstream metabolite of various carbon sources that serve as an integrative metabolic signal that drives growth and cell proliferation. The studies in budding yeast under conditions of continuous glucose-limited growth showed that upon synchronous entry into the growth phase cellular concentration of acetyl-CoA peaks within minutes and that is associated with an increase in expression of genes important for amino-acid synthesis, ribosome production, RNA and sulfur metabolism, followed by an increase in G1-S related gene expression (such as *CLN2*). They also showed that this burst of acetyl-CoA results in Gcn5-dependent acetylation of Spt7, Sgf73, and Ada3 components of the SAGA complex and concomitant rapid increase in histone H3 acetylation at promoters of genes activated at this stage, sometimes together with increased SAGA localization to the same sites. (Cai et al. 2011; Tu et al. 2005)

Since acetyl-CoA is membrane impermeable and unstable, it is thought to be synthesized in the same subcellular compartment where it is used. This implies that acetyl-CoA used by KATs in the nucleus should be generated in the nucleoplasm. A recent study in human cultured cancer cells showed a role for nuclear pyruvate dehydrogenase complex (PDC) specifically in G1-S transition. The evidence is that the PDC complex is translocated from mitochondria to the nucleus in G1-S and this correlates with G1-S specific dependent histone H3 acetylation (H3K9, H3K18) and precedes cyclin A accumulation. (Sutendra et al., 2014)

KATs require for their activity acetyl-CoA, which is a ubiquitous molecule used in energy metabolism, lipid metabolism, and amino acid metabolism. Nuclear acetyl-CoA in budding yeast is generated from acetate in the nucleus majorly by acetyl-CoA synthase Acs2 or by a related enzyme Acs1, in media with non-fermentable carbon sources; although cytoplasm-generated acetyl-CoA may as well pass through the NPC. Acs2-dependent acetyl-CoA synthesis seems to be a rate-limiting stage of histone acetylation since *acs2-ts* mutant rapidly loses histone acetylation of H3 K9,14 and H4 K5,8,12,16 (but not H3 K56) at the restrictive temperature (Takahashi et al., 2006). Acs2 was shown to promote rDNA locus silencing and downregulate the number of ERC, and *acs2* mutant cells have significantly decreased replicative life span (RLS) (Falcón et al., 2010). Interestingly, Acs2 physically interacts with histone H3 (Gilmore et al., 2012) and with Ulp1, a protease that localizes to the nuclear pore basket (Sung et al., 2013).

NuA4 acetyltransferase directly regulates acetyl-CoA levels via Acc1 catalytic activity regulation (Rollins et al., 2017). Since the activity of Gcn5 is competitively inhibited by CoA *in vitro (Tanner et al., 2000)*, NuA4 could directly modulate its enzymatic activity through modulation of the local acetyl-CoA:Co-A ratio via Acc1. On the contrary, bulk levels of H4 acetylation also depend on Gcn5 which led to a proposal that NuA4 acetyltransferase activity may be influenced by SAGA under certain circumstances. (L. Cai et al., 2011; Tu et al., 2005)

Lysine acetylation depends on the availability of metabolites that are essential, as substrates or regulators, for the activity of KATs and KDACs. For instance, class I and IIa HDACs are inhibited by fatty acid hydrolysis products (butyrate, β-hydroxybutyrate), while sirtuins are activated by their cofactor NAD^+ and inhibited by its precursor, nicotinamide (NAM) (X. Li et al., 2018).

A certain part of protein acetylation observed in living cells that largely depends on cell metabolism is non-enzymatic acetylation. The first *in vivo* evidence of such came when increased levels of acetylation were observed in growth-arrested metabolically active yeast cells, and changes in acetyl-CoA levels caused by genetic or nutritional perturbations lead to corresponding proportional changes in acetylation levels (Weinert et al., 2014). One of the factors that influences levels of non-enzymatic acetylation is the pH of the compartment since for this mechanism the side chain of lysine has to be deprotonated (Paik et al., 1970). In this respect perinuclear space of the nucleoplasm could be favoring non-enzymatic acetylation since the nucleus has been shown to display a higher pH than the cytoplasm that is generated thanks to K^+/H^+ exchange mechanism in

the nuclear envelope in rat astrocytes and murine cells (Masuda et al., 1998; Seksek & Bolard, 1996).

3.3. Budding yeasts lysine acetyltransferases

3.3.1. Classification and targets

Many lysine acetyltransferases were first described as proteins with transcription-related functions. In budding yeasts, there are 11 acetyltransferase enzymes, out of which only Esa1 (the yeast homologue of mammalian Tip60) is essential (see Table 2). These enzymes can be subdivided into 3 groups according to sequence homology: GNAT (Gcn5-related N-acetyltransferase) family - Gcn5, Hat1, Hpa2, Hpa3, Elp3, Eco1, Spt10; MYST family (named after the founding members, MOZ, Tbf/Sas3, Sas2 and Tip60, the human homologue of yeast Esa1) - Sas3, Sas2, Esa1; and an acetyltransferase unique for fungi, Rtt109.

Table 2 Classification and targets among histone proteins and non-histone proteins, functions.

HAT/functional complex	Function	Identified histone substrates	Non-histone substrates
Gcn5/SAGA, Ada, etc.	Transcriptional co-activation and elongation, transcriptional repression, chromatin architecture regulation	H3K9, H3K14	Sin1, Rsc4, Snf2, Spt7, Gcn5, others
Esa1/NuA4, piccolo NuA4	Transcriptional activation, DNA repair, cell cycle progression	H4, H2A	
Hat1/Hat1-Hat2-Hif1	Telomeric silencing, DNA repair	H4K5, H4K12	Nop53
Hpa2	?	H3K14, H4K5, H4K12	small basic proteins
Hpa3	Overcoming the toxicity of D-aminoacids	H4K8	D-aminoacids
Elp3	Transcriptional	H3K14, H4K8	tRNA

	elongation, tRNA wobble uridine acetylation		
Sas2/SAS (Sas2-Sas4-Sas5)	Telomeric silencing (*sir1* background), euchromatin-hetero chromatin border maintenance	H4K16	
Sas3/NuA3 (Sas3-Taf30-Yng1-Pdp3)	Silencing, transcriptional elongation (*sir1* background)	H3K14, H3K23	
Rtt109/Rtt109-Vps75, Rtt109-Asf1	DNA repair, nucleosome assembly	H3K9, H3K27, H3K56	
Eco1	Sister chromatid cohesion, DSB repair, nuclear organization	-	Mps3, Smc3, Mcd1
Spt10/Spt10-Spt21	Transcriptional activation and silencing	H3K56, H3K18, H3K9	-

3.3.2. Gcn5

Gcn5 (named for General Control Non-repressible 5) is the founding member of the GNAT superfamily. It was initially identified genetically as a transcriptional co-activator (Georgakopoulos & Thireos, 1992), and after the elucidation of its catalytic activity became the first characterized nucleosome modifying lysine acetyltransferase. Gcn5 exerts its activity in the cell as the component of several multisubunit complexes, out of which the first one described was SAGA (Spt-Ada-Gcn5-acetyltransferase) complex. (Helmlinger et al., 2021) However, at least 8 proteins were found differentially acetylated between *ada2* and *ada2 gcn5* mutants indicating that some targets of Gcn5 may be independent of any of the known Gcn5-containing complexes (Downey et al., 2015).

The bridging function between the chromatin-bound transcription factors and the transcription machinery requires co-activators to exert several functions such as histone modification, incorporation of specific histone variants, and nucleosome remodeling. It is likely that in order to coordinate these functional activities at the transcription site the

multimodular complexes such as SAGA have evolved. (Helmlinger et al., 2021) Table 3 gives a list of SAGA subunits and of the components of the ADA and SLIK complexes that share subunits with SAGA.

Table 3 List of SAGA, SLIK subunits, and functional modules.

ADA subunits	SAGA or SLIK subunits	SAGA Modules
Gcn5	Gcn5	HAT module
Ada2	Ada2	
Ada3	Ada3	
Sgf29	Sgf29	
	Ubp8	DUB module
	Sgf11	
	Sgf73	
	Sus1	
	Taf5	Core structural module
	Taf6	
	Taf9	
	Taf10	
	Taf12	
	Spt7 (modified in SLIK)	
	Ada1	
	Ada5/Spt20	
	Spt3	TBP binding
	Spt8 (absent from SLIK)	
	Tra1	TF binding module
Ahc1		
Ahc2		
	Rtg2 (SLIK)	

Each module of SAGA serves a specific function. HAT module comprises the catalytic subunit Gcn5, which alone can acetylate free histones but not nucleosomes (Grant et al., 1997; Kuo et al., 1996). The DUB module harbors the second enzymatic

activity of the complex which is deubiquitination by the ubiquitin protease Ubp8 (Sanders et al., 2002). The fully functional DUB module composed of Ubp8, Sgf73, Sgf11, and Sus1 is known to be active toward monoubiquitinated histone H2B (Daniel et al., 2004). Mutations in the core structural module components cause loss of SAGA structural integrity and lead to severe growth phenotypes, implying that likely proper localization of SAGA and its other functions are more important for cell function than acetylation (Horiuchi et al., 1997; Sterner et al., 1999). Finally, SAGA contains the TBP binding module (Sterner et al., 1999) and a large subunit Tra1 which is shared with NuA4 complex (Allard et al., 1999) and interacts with specific transcription activators in higher eukaryotes (McMahon et al., 1998) and in budding yeast (Reeves & Hahn, 2005).

SAGA is mostly studied in the context of transcriptional regulation. It shares several subunits with the transcription factor TFIID, and rapid depletion of both complexes severely affects the transcription of ~13% of the genome, while the rest is sensitive to the rapid loss of TFIID but not that of SAGA (Donczew et al., 2020). However, chronic loss of SAGA is more severe, and evaluation of the different SAGA component deletion mutants indicates that it plays a global role in RNA Pol II-dependent transcription, affecting ~4500 genes in *S.cerevisiae*. These changes are only visible when nascent transcription is assessed since the steady state mRNA levels are not significantly changed due to a compensatory increase in transcript half-lives. Transcription is most affected by the loss of both acetyltransferase and TBP delivery functions of SAGA, and the latter is also performed by SAGA for the majority of RNA Pol II transcribed genes. (Baptista et al., 2018)

The substrate specificity of Gcn5 is partially overlapping with Rtt109 - these are the only acetyltransferases that acetylate histone H3K9 (Fillingham et al., 2008; Kuo et al., 1996). The genome-wide study looking at acetylation patterns of Gcn5, Elp3, Hat1, Hpa2, Sas3, and Esa1 showed that Gcn5 and Esa1 are the major acetyltransferases responsible for H3 and H4 acetylation, respectively (Durant & Pugh, 2006). The exact biological roles of Gcn5 in the context of different functional complexes are not always well characterized. However, a lot is known about the Gcn5 function in different contexts. For example, Gcn5 promotes replication-coupled nucleosome assembly together with Rtt109, likely via acetylation of histone H3 tail. Cells lacking both Gcn5 and Rtt109 are hypersensitive to DNA-damaging agents, and cells expressing N-terminally mutated H3 do not incorporate newly synthesized H3 as efficiently as wild-type cells (Burgess et al., 2010). The role of Gcn5 in transcription has also been extensively studied. Its catalytic activity, specifically on nucleosomal histones, has been

tightly linked to its ability to potentiate transcription (L. Wang et al., 1998). Gcn5 was reported to be recruited to promoter regions by Swi/Snf complex or transcription factors such as Gal4 or Gcn4, and to promote transcription factor binding and the recruitment of RNA Pol II (Han et al., 2008; Huisinga & Pugh, 2004; Marcus et al., 1994). There is some evidence that Gcn5 participates in transcriptional elongation (Johnsson et al., 2009). Paradoxically, under some contexts, Gcn5 and increased histone H3 acetylation at the gene promoter may be associated with a repressed state (Ricci et al., 2002). Another interesting point is that Gcn5 may have distinct roles in various chromatin contexts. A recent preprint reveals the role of Gcn5 in the regulation of heterochromatin structure, gene silencing, and nucleotide excision repair (NER) at the heterochromatic HML locus. (H. Chen et al., 2021)

In addition to histone substrates, Gcn5 is known to target many non-histone proteins. One possible example is the acetylation of Sin1, a negative regulator of transcription required for RNA polyadenylation. *GCN5* and *SIN1* interact genetically and Gcn5 has been shown to acetylate Sin1 *in vitro*. (Pollard & Peterson, 1997) Significant input of new information in this respect was obtained thanks to global acetylome studies. Downey *et al*. identified 39 high-confidence Gcn5-regulated acetylation sites from 34 proteins with functions in RNA metabolism, Pol I/II transcription, ribosome biogenesis, metabolism, DNA replication and repair, chromatin structure, and protein synthesis (Downey et al., 2015). Some targets, such as Snf2 (J.-H. Kim et al., 2010) and Rsc4 (VanDemark et al., 2007), were previously identified. Interestingly, Rsc4 acetylation was independent of Ada2 pointing towards the possibility of SAGA/SLIK/ADA independent acetylation, the same was true for 7 more proteins, whereas Ada2 was important for acetylation of histones and SAGA/SLIK component Sgf73. For 2 proteins, Net1 and Nhp2, Ada2 even seemed to inhibit Gcn5-dependent acetylation. (Downey et al., 2015) Another peculiar fact is that Gcn5 acetylates lysine 348 of Hif1, a component of the HAT-B histone acetyltransferase complex (Downey et al., 2015), which raises the possibility of Gcn5 regulating Hat1 activity.

ADA complex is another Gcn5-containing complex that consists of all SAGA HAT module subunits and 2 more, namely Ahc1 and Ahc2. The evidence that it can act as a complex distinct from SAGA came from the demonstration that deletion of Ahc1 leads to specific loss of the ADA complex but not SAGA. The classic Ada^- phenotype of cells with *ADA2*, *ADA3*, or *GCN5* deletions (defects in response to Gal4-VP16 activator (Berger et al., 1992)) was not seen for *ahc1* mutant cells pointing to its association with the activity of SAGA but not ADA complex. (Eberharter et al., 1999) In vitro, ADA was

found to acetylate histone H3 (Grant et al., 1999), but no reports of the in vivo activity specific to ADA have been published now. Ahc1/2 localizes to both the nucleus and the cytoplasm, hence chances are that this complex is responsible for the acetylation of some of the non-histone Gcn5 targets.

SLIK (SAGA-like) complex is structurally very similar to SAGA, except it contains a C-terminally trimmed form of Spt7, lacks Spt8, and contains an additional subunit Rtg2 (Pray-Grant et al., 2002). This SLIK component was initially discovered as part of a retrograde response pathway that links mitochondria dysfunction with changes in nuclear gene expression (Liao & Butow, 1993). It is possible that the function of Rtg2 in transcriptional activation may be connected to its ability to associate with the SLIK complex. (Pray-Grant et al., 2002) However, since Gcn5 mostly localizes to the nucleus, and Rtg2 is predominantly cytoplasmic, it is possible as well that at least some SLIK targets are non-nuclear. This hypothesis is somewhat reinforced by a recent biochemical and structural study comparing SAGA and SLIK, in which no difference was detected at the levels of domain organization, DNA binding, or TBP binding. (Adamus et al., 2021)

3.3.3. Esa1/NuA4

Esa1 is the only essential acetyltransferase in budding yeast. This KAT is performing its functions as part of the multisubunit complex NuA4 which participates in many processes such as histone H4 tail acetylation (Smith et al., 1998), modulation of transcription (Ginsburg et al., 2009), DNA repair (Bird et al., 2002; Noguchi et al., 2019) and cell cycle progression (Clarke et al., 1999). Recent reports indicate that a KAT module of NuA4, termed piccolo NuA4, may serve an independent function in both yeast and human cells (Lu et al., 2022). The different NuA4 subunits are listed in Table 4.

Table 4 NuA4 subunits and functional modules.

NuA4 subunits	Functional parts
Esa1	Catalytic submodule (equivalent to piccolo NuA4)
Yng2	
Epl1	
Tra1	Transcription, DNA repair recruitment module
Eaf1 (HSA/SANT)	
Eaf3	
Eaf5	
Eaf7	

Eaf2	
Arp4	
Yaf9	
Act1	
Eaf6	

One of the roles of NuA4 is to recruit TFIID to the promoters, and most of RNA Pol II transcribed genes depend on TFIID (Warfield et al., 2017). The recruitment of NuA4 itself to the promoter regions depends on the Eaf1 component of the complex. In the absence of NuA4, this function can be performed by SAGA. (Uprety et al., 2015) RNA Pol II occupancy depends on both Gcn5 and Esa1, however, it is more significantly decreased upon Esa1 depletion in genes that were previously annotated in (Huisinga & Pugh, 2004) as "TFIID-dominated" than in "SAGA-dominated" genes (Bruzzone et al., 2018). According to (Huisinga & Pugh, 2004), SAGA-dominated genes are mostly stress-induced, constitute ~10% of the measurable genome, and have a consensus TATA-box sequence within the promoter region, while TFIID-dominated genes lack a TATA-box sequence and form the majority of genes. Several lines of evidence indicate that NuA4 binding to the promoter region and subsequent promoter region remodeling precedes gene activation (Nourani et al., 2004).

The main chromatin acetylation targets of NuA4 are histones H4, H2A and its variant, histone H2A.Z. (Babiarz et al., 2006; Doyon & Côté, 2004) H2A.Z variant is known to be enriched one nucleosome downstream of the transcription start sites (TSS) of both actively transcribed and silent genes, being important for rapid transcriptional activation (Bagchi et al., 2020). In particular, *CLN2* and *CLB5* cell cycle gene expression is delayed upon the deletion of the yeast gene encoding H2A.Z, *HTZ1*; Htz1 was shown to localize to their promoter regions. (Dhillon et al., 2006) *GAL1-10* bidirectional promoter (regulating expression of *GAL1* and *GAL10* genes) is induced in the glucose-deprived medium upon galactose availability depending on H2A.Z presence for binding of RNA Pol II, TBP, and Mediator and for SAGA recruitment (Adam et al., 2001; Lemieux et al., 2008). This data is well correlated with cell cycle entry being delayed in cells lacking H2A.Z. The role of H2A.Z in genome integrity support was as well established in the study of *HTZ1* deletion mutants: *htz1* cells are delayed in DNA replication due to untimely origin firing and experience problems in S phase progression. Replication checkpoint depending on Rad53 was essential in cells lacking Htz1. (Dhillon et al., 2006) The importance of NuA4-dependent H2A.Z acetylation was demonstrated

for the spreading of heterochromatin. Non-acetylatable version of this protein could not perform this function and slowed down cellular growth in combination with the deletion of the non-essential NuA4 component (Babiarz et al., 2006). The deposition of H2A.Z is known to be promoted by NuA4 in several organisms indicating the conservation of this function for the acetyltransferase complex. *In vitro* data from budding yeast-based system shows that the exchange of H2A-H2B dimer for H2A.Z-H2B by SWR1 chromatin remodeling complex is mediated by NuA4 dependent acetylation of H4 and H2A N-terminal tails. Interestingly, mutations in both H4 and H2A tails are synthetically lethal (Altaf et al., 2010; Bieluszewski et al., 2022), the same as the analogous combination of H4 and H2A.Z mutations (Babiarz et al., 2006). SWR1 complex itself is strikingly similar to NuA4 in its components, although it lacks all of the piccolo NuA4 subunits including Esa1, but has 3 additional subunits such as Bdf1 containing two bromodomains important for recognition of acetylated H4/H2A, and Vps71 and Vps72 requires for nucleosome and H2A.Z binding correspondingly (Giaimo et al., 2019; Watanabe et al., 2013; Wu et al., 2005).

The activities of NuA4 and piccolo NuA4 towards histone substrates are different, while nothing is known about the preferential acetylation of non-histone substrates by either complex. In terms of histone acetylation, piccolo NuA4 *in vivo* performs non-targeted global acetylation and prefers nucleosomal histones, while NuA4 acts in a locus-specific manner and is equally efficient towards free histones and nucleosomes. For example, upon glycolytic burst in stationary phase cells, Esa1 is preferentially found in the form of piccolo NuA4 and drives global acetylation of histone H4 at K5, 8 and 12 (Friis et al., 2009). NuA4 *in vitro* acetylated all lysines available in the N-terminal tail of histone H4 - positions K5, 8, 12, and 16 (Allard et al., 1999).

Some known functions of Esa1/NuA4 are likely ensured via the acetylation of non-histone targets. For example, NuA4 under glucose deprivation stress promotes the formation of stress granules (SG) - cytoplasmic aggregates of RNA and protein with so far cryptic functions. However, it is known that stress granule formation is important under several stress conditions. Upon glucose removal, the stress granules are formed rapidly, within 5 to 10 minutes, in wild-type cells, while in NuA4 mutant cells such as temperature-sensitive *esa1-ts* catalytic subunit mutants and deletion mutants *eaf1*, *eaf3*, *eaf5,* and *eaf7* SG formation is significantly decreased. (Rollins et al., 2017) Another more robustly established role of NuA4 in glucose deprivation response is the acetylation of phosphoenolpyruvate carboxykinase Pck1 (reversed by deacetylase Sir2), a key enzyme in the gluconeogenesis pathway. Pck1 acetylation promotes its enzymatic activity

in the formation of phosphoenolpyruvate from oxaloacetate, and its acetyl mimic mutant *pck1-K514Q* rescues decreased activity of Pck1 isolated from *esa1* mutant cells in the enzymatic assay. The evolutionary conservation proved to be the case for this target of NuA4, as human hepatocellular carcinoma (HepG2) cells decreased glucose secretion to the glucose-free medium upon the knockdown *TIP60* in agreement with the hypothesis of decreased enzymatic activity of human homologue of yeast Pck1, *PEPCK*. (Lin et al., 2009)

The role of NuA4 in supporting genome integrity is at least in part mediated by histone H4 acetylation which is specifically important for the repair of DSB but not other types of DNA damage. Acetylation of either lysine of four available in the H4 N-terminal tail is sufficient for providing wild-type levels of resistance to DSB and rescuing G2/M cell cycle defect, both of which are associated with the inability to acetylate H4. (Bird et al., 2002; Megee et al., 1995) One of the possible explanations for the importance of lysine acetylation in DSB repair is that it makes chromatin more open, which in turn allows access to chromatin remodelers and DNA repair factors. (Koyama et al., 2002)

Esa1 has been shown to be responsible for the acetylation of certain cell cycle and RNA metabolism-related proteins, however, the exact functions of acetylation in these proteins have not been elucidated. A Proteome microarray study (in which 5800 yeast proteins were immobilized on nitrocellulose slide and probed with NuA4 complex for isotope-labeled acetyl-CoA incorporation) showed NuA4-dependent *in vitro* acetylation of Cdc34 and Rpt5 proteins that promote cell cycle progression, and of Brx1 protein that participates in 60S ribosomal subunit rRNA component maturation. These substrates were later validated *in vivo*. However, some of the substrates in this study were not followed up for *in vivo* validation, among which are the major cell cycle entry transcriptional repressor Whi5 and RNA-interacting proteins, such as polyadenylated RNA binding protein Nab3 and putative RNA helicases Dbp6,10. (Lin et al., 2009)

Global acetylome mass spectrometry study revealed some additional targets of Esa1, such as the Tho2 component of the THO transcriptional elongation complex, the Ssn2 component of the Mediator complex, and Sfp1 protein, known to modulate cell size and directly bind promoters of ribosomal protein genes. Yng2 and Epl1 components of the NuA4 catalytic module and of piccolo NuA4 are also acetylated by Esa1. (Downey et al., 2015)

3.3.4. Hat1

Hat1 is the first lysine acetyltransferase identified and it is the sole KAT in the group of "type B" KATs, which historically denominated acetyltransferases with cytoplasmic localization and with the ability to acetylate free non-nucleosomal histones. In fact, Hat1 turned out to be ubiquitous and can be found both in the nucleus and the cytoplasm. Hat1 can be found as the component of several distinct complexes, but all of them contain the Hat2 protein. Hat2 increases the catalytic activity of Hat1 and appears to increase the interaction between Hat1 and histone H4 has been proposed to be responsible for the nuclear localization of the complex (Parthun et al., 1996). *In vivo* functions of Hat1 include DSB repair and telomeric silencing. The study using the single double-strand break induced by HO nuclease in the *MAT* locus shows that adjacent chromatin is rapidly acetylated at H4 tail lysines. However of the 4 lysines acetylated in the tail only acetylation of the H4K12 site depended on Hat1, which was likely recruited after histone H2A S129 phosphorylation and alongside Rad52 recombinational repair factor. (Qin & Parthun, 2006) Nevertheless, this study did not show the requirement for H4K12 acetylation for DNA repair. The role in telomeric silencing, on the opposite, is quite elegantly demonstrated in a study looking at *HAT1*/*HAT2* deletions combined with mutations of histone H3 N-terminal lysines. Concurrent loss of Hat1 activity and H3 mutants mimicking non-acetylated histone lead to a major telomeric silencing defect, which according to further mutational analysis was mostly due to loss of H4K12 acetylation. (Kelly et al., 2000) A later study identified another subunit of the Hat1-containing complex termed Hif1. It interacts both with Hat1 and histone H4, this binding being mediated by Hat2. Hif1 binding does not affect Hat1 catalytic activity, however, it influences telomeric silencing (Poveda et al., 2004). Hat1-Hat2-Hif1 was shown to acetylate free non-nucleosomal histone H4 at positions K5 and K12 and to physically interact with Asf1 (Fillingham et al., 2008).

Hat1 may target non-histone proteins; one known example is Nop53, a nucleolar ribosome assembly factor that was found to be reproducibly under-represented in *hat1* mutant in the large-scale acetylome study (Downey et al., 2015).

3.3.5. Hpa2, Hpa3

Hpa2, and Hpa3 are closely related KATs belonging to the GNAT superfamily. Hpa2, the most recently described yeast KAT, demonstrated *in vitro* acetyltransferase activity towards histones H3 and H4, with preferential targeting of H3K14, H4K5, and H4K12, and is capable of autoacetylation. (Angus-Hill et al., 1999; Sampath et al., 2013).

Hpa3 only acetylated histone H4 at the K8 position and, same as Hpa2, autoacetylated (Angus-Hill et al., 1999; Sampath et al., 2013). Additional substrates were found for both proteins: Hpa2 acetylated small basic proteins such as nuclear Nhp6a, Nhp6b, Hmo1, Hmo2, and mitochondrial Abf2, while Hpa3 targeted free D-aminoacids (Sampath et al., 2013). D-amino acids corresponding to L-amino acid protein building blocks are toxic and inhibit growth. Hpa3 dependent N^{α}-acetylation of D-amino acids and their further secretion to the medium allowed cells to avoid protein synthesis inhibition (Yow et al., 2006). Deletion of either protein does not confer any growth phenotype, but overexpression is toxic for the cells (Sampath et al., 2013).

3.3.6. Elp3

Elp3 is the lysine acetyltransferase subunit of the Elongator complex that acetylates histones H3 and H4 while being associated with the elongating form of RNA polymerase II. Elongator complex binds to both naked and nucleosomal DNA and acetylates predominantly histones H3 at K14 and H4 at K8. The acetyltransferase activity of Elp3 depends on 3 other Elongator subunits - Elp4, Elp5, and Elp6. (Winkler et al., 2002) The functional consequence of Elp3-dependent H3 acetylation was evaluated in a study looking at the transcription of *SSA3* and *SSA4* genes and proved to positively regulate transcriptional elongation (Han et al., 2008).

This enzyme is distinct from other KATs in a way that in addition to a KAT domain, it has an N-terminal domain similar to the catalytic domain of S-adenosylmethionine radical enzymes (rSAM, able to generate 5'-deoxyadenosyl radical, 5'-dA•). Such dualistic nature of the protein is conserved in evolution and thus acetyltransferase activity and modification with concurrent formation of 5'-dA• radical was thought to be directed to the same substrate. (Chinenov, 2002) While there is no evidence that this is happening for histone substrates, this is true for the mechanism revealed for Elp3-dependent acetylation of wobble uridine-34 (U^{34}) C5 within tRNA in *Methanocaldococcus infernus* (Selvadurai et al., 2014). Wobble uridine acetylation is a modification conserved in eukaryotes and essential for viability in some metazoans and strain backgrounds of *S.cerevisiae* (Björk et al., 2007; Schaffrath & Leidel, 2017).

3.3.7. Sas2

As the name of the protein (*SAS* stands for "something about silencing") suggests, *Sas2*, the lysine acetyltransferase from MYST family, was originally identified in a screen for defects in epigenetic silencing in *SIR1* deacetylase mutant cells. However,

the effect was not the same for all silenced loci, since Sas2 promoted silencing at *HML* locus while decreasing silencing at *HMR* locus. One of the modes of Sas2 action as a silencer proposed in the same study suggests inhibition of the ORC (Origin Recognition Complex) machinery via its components' acetylation. However, this does not explain the difference in the effect of Sas2 loss on *HMR* and *HML* silencing since they are equally derepressed in ORC mutants. (Ehrenhofer-Murray et al., 1997) A later study confirmed the positive role of Sas2 in DNA replication and cell cycle progression, indicated that Sas2 increases the strength of silencers independently of their position and genomic context, and demonstrated the role of this acetyltransferase in the maintenance of transcriptionally silent chromatin structure (Zou & Bi, 2008). Sas2 in the cell forms part of the trimeric complex called SAS, containing additionally Sas4 and Sas5. It targets exclusively H4K16 lysine, in striking contrast with NuA4 promiscuity relative to histone H4 tail lysines. (Shia et al., 2005) Paradoxically, SAS was as well described as an "anti silencer" in the context of telomeres, where it antagonizes Sir2 and via H4K16 acetylation promotes the incorporation of a histone variant H2A.Z thus limiting the spreading of Sir proteins in the nearby euchromatin (Shia et al., 2006).

3.3.8. Sas3

SAS3 is the homologue of MOZ leukemia gene encoding another lysine acetyltransferase belonging to MYST family. Sas3 acts as the component of a conserved multisubunit NuA3 (nucleosomal acetyltransferase of histone H3) complex. It was shown to acetylate histones in vitro (Takechi & Nakayama, 1999) and to specifically target H3K14 and H3K23 (Howe et al., 2001) *in vivo*. Histone acetylation repertoire is overlapping with Gcn5; however Sas3 was shown to support acetylation of H3K14 in the absence of Gcn5, but not of H3K9 (Vicente-Muñoz et al., 2014). Sas3 is not just a KAT, it serves a core function for the NuA3 complex integrity (John et al., 2000). Deletion of *SAS3* alone is not associated with any phenotype, although, same as *sas2* mutation, *sas3* mutants in *sir1* mutant background restore silencing of *HMR* locus, but not at telomeres (Reifsnyder et al., 1996). ChIP analysis of Sas3 distribution showed that it preferentially binds to 5'-half of the target genes coding regions, pointing toward a possible role in transcriptional elongation (Vicente-Muñoz et al., 2014).

3.3.9. Rtt109

Rtt109 is the fungal lysine acetyltransferase known for acetylating nascent histone H3 at positions K9 (Fillingham et al., 2008) and K27 (Burgess et al., 2010) in the

histone tail, and K56 (J. Schneider et al., 2006) within the histone-fold domain. These modifications play an important role in replication- and repair-coupled de novo nucleosome assembly (Burgess et al., 2010; Yang & Freudenreich, 2010). Rtt109 acetyltransferase uniquely works together with histone chaperones, which defines its specificity. Vps75 directs Rtt109 activity towards H3K9 and H3K27 acetylation, while Asf1 drives H3K56 acetylation. (D'Arcy & Luger, 2011) The mechanisms of activation are distinct for two chaperones: Rtt109-Vps75 can acetylate histone dimer H3-H4, H3 alone, or the H3 tail peptide (Berndsen et al., 2008), whereas Rt109-Asf1 is only active towards the H3-H4 dimer (Tsubota et al., 2007); in addition, Rtt109 forms a strong complex with Vps75 (Albaugh et al., 2010), but interacts only transiently with Asf1 (Tsubota et al., 2007). Rtt109, same as Asf1, was reported to play a role in error-free replication of CAG/CTG repeats, which indicated at H3K56 playing a role in DNA repeat stabilization through proper nucleosome assembly at the replication fork (Yang & Freudenreich, 2010). One of the known roles of H3K56 acetylation is that it directly promotes the interaction of H3 with the chromatin assembly factor CAF-1 and Rtt106, which take part in newly synthesized histone deposition on the replicating DNA (Q. Li et al., 2008).

3.3.10. Eco1

Eco1 is the only yeast acetyltransferase that does not target histones in vitro (Ivanov et al., 2002). It is required for the establishment of sister chromatid cohesion during DNA replication and belongs to Gcn5-related N-acetyltransferase (GNAT) superfamily. *In vitro* it targets cohesin components Scc1, Scc3, and Pds5, however, no evidence was found that these subunits are targeted in vivo (Ivanov et al., 2002). The important function for cohesion is the acetylation of two conserved lysines of the cohesin complex subunit Smc3. The expression of non-acetylatable version of Smc3 causes a loss of sister chromatid cohesion and an increase in genome instability. (J. Zhang et al., 2008) The Mcd1 subunit of the cohesin complex is acetylated by Eco1 in order to protect cohesin from Wpl1-dependent cohesin removal at sites of double-strand breaks (DSB). (Heidinger-Pauli et al., 2009) Another target of Eco1 is Mps3, a nuclear envelope SUN-domain protein. Its acetylation adjacent to the transmembrane domain is important for correct sister chromatid cohesion and for the recruitment of chromosomes to the nuclear membrane, making it important for the nuclear organization. (Ghosh et al., 2012)

3.3.11. Spt10

Spt10 acetyltransferase belongs to the GNAT superfamily and shares several acetyltransferase motifs with Gcn5. It contains a zinc-finger motif pointing to the possibility of direct binding to specific DNA sequences (Neuwald & Landsman, 1997). Under some conditions, however, Spt10 binding requires additional partners. It was shown to physically interact and cooperate with Spt21 to promote G1/S specific transcription of histone genes *HTA2* and *HTB2*, even though Spt10 binds all histone promoter regions. The cell cycle phase specificity in this case is achieved by G1/S specific transcription of Spt21. (Hess et al., 2004) Lysine acetylation at H3K56, H3K18, and H3K9 was found to be specifically enriched in promoter regions of histone genes and mediated by this Spt10 (Xu et al., 2005). An interesting role at histone gene promoters specific for Spt10 and Spt21 is to be removed from DNA under replicative stress to inhibit corresponding mRNA synthesis. This mechanism is not conserved in mammalian cells, where histone mRNAs are degraded under replicative stress conditions. (Bhagwat et al., 2021) Several other genes have been shown to be affected by mutations in Spt10 and/or Spt21, including *CUP1* (C.-H. Shen et al., 2002) and others (Natsoulis et al., 1991). Spt10 and Spt21 however are likely to play distinct roles in some circumstances: *spt10* mutant cells are synthetically lethal with loss of either MBF or SBF, but at the same time *swi4*, *mbp1,* and *swi6* suppress the Spt$^-$ phenotype of *spt21* mutant cells. Another suppressor of *spt21-dependent* Spt$^-$ phenotype is a mutation in the *GTR1* gene, which encodes a RanGDP regulator. (Hess & Winston, 2005) More recent studies also showed that Spt10 and Spt21 promote silencing at telomeres and *HMLα* locus, while their mutations relieve silencing at the rRNA by altering chromatin accessibility (Chang & Winston, 2011).

3.3.12. Functional redundancy

As it can be deduced from substrate specificities, which are more established for histones, certain acetyltransferases may have overlapping functions in vivo. Some combinations with diverse phenotypes can be found in the literature.

For example, the *sas3 elp3* double mutant does not have growth phenotype, while the *gcn5 elp3* double mutant, though alive has significantly decreased H3 acetylation, which correlated with the transcription state: the less H3 within ORF is acetylated, the lower transcription. (Kristjuhan et al., 2002) The nucleosome density in the regions of intragenic H3 hypoacetylation was not different from that of the wild-type cells. This indicates that transcriptional activity does not directly correlate with

nucleosome occupancy (Kristjuhan & Svejstrup, 2004) Another consequence of H3 hypoacetylation in this double mutant is that Sir3 protein normally localized at the telomere tips spreads to subtelomeric DNA and causes loss of histone H4K16 acetylation. The growth defect of the *gcn5 elp3* mutant can be rescued by deletion of any of the *SIR1-4* genes, arguing that under conditions of hypoacetylated histone H3 Sir proteins are toxic. (Kristjuhan et al., 2003), and by the simultaneous deletion of *HDA1* and *HOS2* deacetylases (Wittschieben et al., 2000).

Interestingly, loss of Gcn5 together with Sas3 is lethal and leads to a global decrease in H3 acetylation and arrest in the G2/M cell cycle stage, with replicated DNA. (Howe et al., 2001)

3.4. Budding yeasts lysine deacetylases

The enzymes that reverse lysine acetylation are called lysine deacetylases. This chapter aims to give a brief overview of their classes based on the mechanism of catalysis referencing yeast lysine deacetylases and their functions and make a special emphasis on Hos3, a unique lysine deacetylase that has a cell cycle-dependent localization.

3.4.1. Classification, examples of functions, and targets

The first lysine deacetylase isolated was mammalian HDAC1, which turned out to be homologous to a known yeast transcriptional regulator Rpd3. All currently known lysine deacetylases are divided into 4 classes: class I (or Rpd3-like), class II (or Hda1-like, further subdivided into classes IIa and IIb) and class IV (or Hos-like) are Zn-dependent enzymes inhibited by trichostatin A, and class III deacetylases (called sirtuins) which require NAD^+ as a cofactor for enzymatic activity. (Taunton et al., 1996) Budding yeast deacetylases are Zn-dependent Rpd3, Hda1, Hos1-3, and NAD^+-dependent sirtuins, heterochromatin associated Sir2 and Hst1-4 (Moazed, 2001; Rundlett et al., 1996).

3.4.2. Role of lysine deacetylation in gene expression

Generally the role of lysine deacetylase activity towards histones in gene expression is considered inhibitory since they are counteracting the largely activatory role of histone acetyltransferases. However, there are several exceptions. For example, the comparison of gene expression profiles of *rpd3* and *hda1* mutant cells with the *WT* cells treated with TSA allows us to propose that these two deacetylases may act both as direct transcriptional inhibitors and as activators, however, the latter seems to be specific for

sub-telomeric regions. The mechanism of Rpd3-dependent transcriptional activation likely depends on its ability to deacetylate H4 at the K12 position, which in the case of subtelomeric genes ensures interaction with the repressive SIR complex (formed by Sir2-4). (Bernstein et al., 2000) The sirtuin consensus sequences (acetylome of triple mutant *hst1 hst2 sir2* was evaluated) are largely overlapping with that of Gcn5 acetyltransferase, resulting in a subset of possibly co-regulated targets (Downey et al., 2015).

An exception compared to other deacetylases, Hos2 does not associate with the promoter but with the coding regions, and binds highly active but not silent genes. It locally deacetylates histones H3 and H4 and is required for robust and switch-like gene activation. (A. Wang et al., 2002) The possible explanation for the unconventional direction of gene expression changes upon histone deacetylation is that this process is important for reverting the chromatin structure disrupted by the passage of transcriptional machinery (Kurdistani & Grunstein, 2003). The hypothesis is supported by the fact that hypoacetylated chromatin arrays are more readily remodeled *in vitro* by SWI/SNF complex (Logie et al., 1999) and that SWI/SNF induces long-range interactions between promoter and coding regions (Y. Kim & Clark, 2002).

3.4.3. Role of lysine deacetylation in supporting genome integrity

Sirtuins Hst3 and Hst4 deacetylate H3K56 before G2/M. Double deletion mutants of these deacetylases are prone to spontaneous DNA damage, chromosome loss, and sensitivity to genotoxic stress. (Celic et al., 2006)

Hos1 likely acts as the antagonist of Eco1 in the process of the establishment of sister chromatid cohesion which is important for error-less genome transfer to the progeny. *HOS1* deletion mutants form ~20% more cohesin dimers which are contributing to cohesion. This adds Hos1-dependent deacetylation of the cohesin complex to the mechanism involving another known negative regulator of cohesion Wpl1 in mitosis. (D. Shi et al., 2020)

3.4.4. The role of lysine deacetylation in silencing

Telomeric silencing is largely ensured by Sir proteins and depends on Rap1. Rap1 binds DNA in its corresponding binding sites in the telomeric regions, where it recruits Sir4. Sir3 and Sir2 are further recruited by Sir4, and lysine of histone H4 at position K16 is deacetylated. After the initial binding SIR spreads along the chromatin in a mechanism dependent on the N-termini of both histones H3 and H4, in a repetitive

circle. Sir3 can bind to the deacetylated tail of H4 and recruit Sir4, which in turn recruits Sir2 to start the next cycle. Similarly SIR complex functions in rDNA and mating locus silencing (Hoppe et al., 2002; Luo et al., 2002; Rusché et al., 2002)

3.4.5. Hos3

Hos3 is a class IV deacetylase with wide *in vitro* histone specificity with deacetylation sites in histones H4, H3, H2A, and H2B (Carmen et al., 1999). In an intergenic microarray study, the loss of Hos3 was found to preferentially cause hyperacetylation of ribosomal DNA (Robyr et al., 2002).

Hos3 is unique among KDACS (which are usually nuclear) in its localization pattern. Hos3 localizes specifically to the daughter nuclear periphery at the end of mitosis (Kumar et al., 2018). Hos3 deacetylase cell-cycle dependent localization and its determinants were carefully described in (Kumar et al., 2018). Briefly, Hos3 is distributed homogeneously in the nucleus and cytoplasm during most of the cell cycle and is recruited to the daughter side of the septin ring (located at the mother-bud neck) in mitosis and to the daughter nuclear periphery during anaphase, until 1-2 minutes before cytokinesis, when Hos3 is again localized throughout the cell. If the septin ring formation is perturbed, the asymmetric distribution of Hos3 is abolished. Hos3 targeting the daughter nuclear periphery coincides with the nuclear passage through the bud neck and depends on it, since in the *dyn1* mutant that completes the division within the mother cell, Hos3 only moves to the daughter nucleus as it migrates to the bud. Hos3 is targeted to the septin ring in a Hsl7-dependent manner, and targeting to the nuclear periphery depends on an importin Mtr10. In the daughter nuclear periphery, Hos3 associates with the Nup60 component of the NPC nuclear basket.

Hos3 together with Rpd3 was earlier linked with cell cycle progression inhibition through their interaction with Whi5. Rpd3 is required for the dose-dependent effect of Whi5 on cell size. (Huang et al. 2009; Wang et al. 2009) In addition to earlier identified chromatin-related functions, Hos3 was found to deacetylate a number of nucleoporins within the NPC basket and central channel. The functional consequences of the NPC deacetylation were multiple, seen at the level of diverse nuclear transport receptors cellular distribution between the nucleus/nuclear periphery and cytoplasm, at the level of Whi5 protein transport, and at the level of *CLN2* gene localization. (Kumar et al., 2018).

Hos3 is likely to be important for additional processes beyond the regulation of the G1/S transition. For example, under non-stressed conditions, deletion of *HOS3* but

not any other deacetylase leads to a 2-fold increase in stress granule formation. However, the exact Hos3 targets responsible for this phenotype are not identified. (Rollins et al., 2017). Additionally, hos3 is localized to the spindle pole bodies and plays a role in the spindle orientation checkpoint (Wang and Collins 2014).

4. Regulation of gene expression

Regulation of gene expression is a complex process that comprises the interaction of general and gene-specific transcription factors with the promoter region and the formation of the pre-initiation complex, followed by the regulation of the transcribing polymerase that leads to the formation of an mRNA. The mRNA has to be properly processed and exported through the nuclear pore in order to be translated into protein in the cytoplasm. At all stages, mRNA is bound by multiple proteins that ensure its stability or target it for degradation, and all stages present the points of gene expression control. Here I will briefly introduce the main commonly known details about gene expression, focusing on the transcription of protein-coding genes.

4.1. Promoter region

Within every promoter region of a protein-coding gene one can find the transcription start site (TSS), the TATA-box, and the sequences bound by transcription regulators. The first to constitute the core promoter element of about 100bp. The TATA-box is the AT-rich sequence upstream of the TSS that TBP can bind. Other sequences important for transcription are the ones bound by transcriptional activators and silencers (or repressors). While transcriptional activators promote transcription and may be bound proximally upstream or distantly, to the enhancer sequence that interacts with the promoter region, transcriptional repressors are inhibiting transcription through different mechanisms, including interfering activator binding, recruitment of transcriptional apparatus or modifying chromatin structure. (T. I. Lee & Young, 2000)

4.2. Preinitiation complex formation

The preinitiation complex (PIC) is formed at the promoter region and is important for RNA polymerase II (or RNA Pol II) to initiate transcription. It consists of the general transcription factors, both are constitutively present at PICs (including RNA polymerase II, TFIIB, and the TATA-binding protein, or TBP) and the ones that are not always present, as reviewed in (T. I. Lee & Young, 2000). In vitro these factors can form stable associates with the DNA, however, there is still debate on whether partial PICs can be formed in living cells (Buratowski et al., 1989; Petrenko et al., 2019). The Srb/Mediator complex, a separate part of the preinitiation complex, is thought to integrate signals from regulators of transcription, its composition being dynamic and

responsive to the changes in the environment (T. I. Lee & Young, 2000). Mediator is essential for RNA Pol II transcription, however, not all of its subunits are essential on their own (Petrenko et al., 2017).

The first PIC protein thought to bind the promoter is TBP, as this is the only protein that can bind the DNA on its own in vitro (Buratowski et al., 1989), although in the promoter it is thought to be either on its own or as the component of TFIID complex, which additionally contains TBP-associated factors. SAGA complex is reported to promote PIC formation in budding yeast and metazoans (X.-F. Chen et al., 2012; Shukla et al., 2006), and the mechanism likely includes TBP delivery to the promoter (Papai et al., 2020). NuA4 is another KAT that contributes to the PIC assembly, in particular, it recruits TFIID to ribosomal protein genes, and this is dependent on its KAT activity. (Uprety et al., 2015) Overall, two options for PIC assembly and TBP delivery, in particular, are proposed. (Bruzzone et al., 2018) The first one is that for a certain group of genes that strongly depend on Mediator but are unresponsive to NuA4 TBP is deposited and PIC is formed solely upon SAGA activity (which is well correlated with SAGA being unable to bind DNA on its own); while for the rest of the genes, the main role in TBP delivery and PIC formation is played by NuA4 and TFIID. The alternative proposal is that for every PIC all three actors - SAGA, Mediator, and NuA4-TFIID - contribute, yet to a different extent. (Bruzzone et al., 2018)

As stated above, chromatin remodeling may be required for proper PIC formation. For example, HO gene activation in budding yeast requires the recruitment of the Swi/Snf chromatin modification complex and SAGA complex prior to the association of another activator, SBF (Cosma et al., 1999).

4.3. Switch that triggers elongation

The largest subunit of RNA Pol II, Rpb1 in budding yeast, contains a conserved C-terminal domain (CTD) consisting of ~27 tandem heptad repeats with the amino acid sequence $Y^1S^2P^3T^4S^5P^6S^7$ that is essential for viability (Corden, 1990). The CTD phosphorylation state is intimately connected with the transition to elongation. Non-phosphorylated C-terminus is tightly bound by Mediator (Robinson et al., 2016) while transcribing forms of RNA Pol II binds hyperphosphorylated CTDs. Serine 5 phosphorylation in the CTD of Pol II likely causes dissociation of Mediator complex from the promoter thus allowing Pol II to escape the promoter region, while later on this residue phosphorylation is decreased and Serine 2 is increasingly phosphorylated (Jeronimo & Robert, 2014; Komarnitsky et al., 2000).

4.4. mRNA processing

During transcription, while mRNA is being processed, multiple RNA binding proteins (RBPs) bind at specific recognition sites located mostly in 3' UTR (3' untranslated region) and in 5' UTR, and within introns. (Ainger et al., 1997; Sharma et al., 2021)

The very first mRNA processing step is 5' capping. As soon as the growing transcript reaches the length of 22-25 nucleotides and exits the channel of RNA Pol II, it is modified with 7-methylguanosine (m7GpppN) by three sequential enzymatic reactions performed in yeast by Cet1, Ceg1, and Abd1. (Mao et al., 1995; Shibagaki et al., 1992; Tsukamoto et al., 1997).

Introns are sequences within the ORF that are not eventually translated into protein and have to be excised before leaving the nucleus in a process called splicing. Most budding yeast genes are intronless, except for the limited number of highly transcribed ones. The total number of introns only reaches a few hundred per more than 6000 genes in *S.cerevisiae*, and one gene usually has not more than one intron defined by conserved sequences and removed by the complex ribonucleoprotein apparatus collectively called the spliceosome. (Stevens & Abelson, 2002) Interestingly, some introns accumulate as linear RNAs under saturated growth conditions. They stay associated with the spliceosome components and inhibit growth through the TOR signaling pathway. (J. T. Morgan et al., 2019)

The last step of mRNA processing is 3' polyadenylation. polyA tail length regulates mRNA stability and is important for mRNA nuclear export and surveillance in the cytoplasm (Ito-Harashima et al., 2007; Sachs, 1990). Two steps are required for polyadenylation, and both are performed by the cleavage and polyadenylation factor in budding yeast: first, the nascent mRNA 3'-UTR is cleaved at the polyadenylation site by a nuclease module, and then the 3' end is polyadenylated by Pap1 polyA polymerase until the process is terminated, as reviewed in (Stewart, 2019).

4.5. mRNA export factors

Nuclear export of fully processed mature eukaryotic mRNA is the last step before it is accessed by the cellular translation machinery, which naturally makes it the convenient regulatory point important for selective mRNA export and for mRNA quality control. These functions are ensured thanks to certain proteins that bind to the mRNA in the nucleus and form the export-competent messenger ribonucleoprotein particle

(mRNP). For simplicity nuclear export can be described in a number of stages: first comes the interaction between the mRNP and the NPC basket in the nucleoplasm, then follows the passage of the mRNA through the NPC channel and simultaneous remodeling of the mRNP, and the last step is the mRNP release into the cytoplasm at the cytoplasmic filaments.

One of the first proteins to bind mRNA is the capping binding complex (CBC) composed of the heterodimer Cbc1/Cbc2. It is important for pre-mRNA splicing and transcription termination (J. D. Lewis et al., 1996; C.-M. Wong et al., 2007) and promotes the accumulation of gene-specific activators at promoters of highly transcribed genes (T. Li et al., 2016), but it was not shown to play a direct role for mRNA export in yeast. However, CBC was shown to genetically and physically interact with **Npl3** (E. C. Shen et al., 2000), a factor essential for efficient mRNA export that also associates among the first ones with the growing transcript. It physically associates with RNA Pol II independently of RNA, genetically interacts with TATA-binding protein Spt15, and also binds the DNA upstream of the gene coding sequence as found by ChIP, all of which points to Npl3 loading being coupled to the beginning of transcript elongation (Lei et al., 2001).

The next mRNA export protein to bind the transcript is **Yra1**, which was the first RNA-binding protein identified (Strässer & Hurt, 2000). Its binding to mRNA depends on 3'-end processing and, in the case of intron-containing transcripts, on splicing (Lei & Silver, 2002). Same as Nlp3, it was found associated with chromatin, but at later stages of transcript elongation (Lei et al., 2001). Yra1 was proposed to be an adaptor protein for **Mex67**, another protein essential for mRNA export that does not bind mRNA directly (Hurt et al., 2000). Yra1 forms a complex with Mex67 and to binds RNA *in vitro* (Strässer & Hurt, 2000), however, Yra1 homologues Aly/REF in flies and *C.elegans* are dispensable for mRNA export (Gatfield & Izaurralde, 2002; Longman et al., 2003) and Yra1 does not associate with all yeast mRNAs bound by Mex67 (Hieronymus & Silver, 2003), which pointed to the existence of other adaptor proteins. It turned out that **Nab2**, an essential polyA binding protein (Anderson et al., 1993), directly binds Mex67 and this interaction is strengthened by Yra1 (Iglesias et al., 2010).

Important steps of mRNP structural remodeling are induced by Sub2 and coupled with TREX complex sequential binding and dissociation from the mature mRNP. These rearrangements lead to the removal of Yra1 and the introduction of the Mex67-Mtr2 complex to the mRNP structure. The mature transcripts need to reach the

nucleoplasmic side of the NPC, where they face the rate-limiting step. Nab2 interacts with Mlp1 and could facilitate the following export (Fasken et al., 2008).

There is another important player with multiple intricate reported functions called the TREX-2 complex. It is thought to couple SAGA-dependent gene expression to mRNA export by promoting gene interaction with the nuclear basket. In the nuclear basket, it interacts with Nup1, while it is known to interact with Mex67:Mtr2 heterodimer (Jani et al., 2014) bound to the mRNP. TREX-2 contains a scaffold Sac3 protein, that interacts with Nup1 through the Sac3 CID (centrin binding) region; subunit Thp1 known for its role in transcription elongation, 2 Sus1 subunits (shared with SAGA complex), Sem1 and Cdc31. (Fischer et al., 2002; Jani et al., 2014; Rodríguez-Navarro et al., 2004)

Once the mRNA particle reaches the nuclear pore channel, Mex67:Mtr2 coat engages in interaction with the FG nucleoporins to ensure the passage through the barrier (Strässer et al., 2000). Interestingly, a recent study indicates that mRNA moving through the NPC with a certain directionality, 5' end exiting first (Ashkenazy-Titelman et al., 2022). The directionality of mRNA export is primarily ensured by the steps on the cytoplasmic side of the pore, including the Dbp5-dependent removal of Mex67:Mtr2 from the mRNP and replacement of Nab2 polyA binding protein for Pab1, characteristic for cytoplasmic mRNPs. Dbp5 is a unique DEAD-box protein that functions in the nucleus, at the cytoplasmic part of the NPC, and in the cytoplasm, via displacing specific proteins by generating kinks locally in the mRNP structure. However, only the activity of Dbp5 at the cytoplasmic filaments is essential for cell viability, where it releases Nab2 (Tran et al., 2007) and Mex67 (Lund & Guthrie, 2005) from the mRNA. The activity of Dbp5 is very much enhanced by Gle1 and Nup42 cytoplasmic nups (Alcázar-Román et al., 2006; Weirich et al., 2006), which implies that if some modifications of the NPC cause removal of these components, mRNA export could be less efficient.

It needs to be told that the mechanism described is just the tip of the iceberg. Yra1 and Mex67 collectively bind roughly 36% of mRNAs transcribed each (1000 and 1050 mRNAs respectively), and out of those only ~350 mRNAs are bound by both of them. Interestingly, Yra1 binding of mRNAs correlates with their transcriptional frequency, whereas this is not true for Mex67. Certain connections were found between the export factor binding and the classes of proteins encoded by bound mRNAs, as well as with transcription factors regulating gene expression. This indicates that different export mechanisms are used for different mRNA groups based on encoded messages. For example, *CLN2* mRNA was not is not bound by either Yra1 or Mex67, whereas *CLN1* mRNA is bound by Yra1 but not Mex67. (Hieronymus & Silver, 2003)

However, some of the commonly accepted views on mRNA export may be revisited with the new facts being uncovered. For example, Mex67 has recently been proposed to be a bona fide nucleoporin and to interact with the mRNA exclusively within the NPC channel (Derrer et al., 2019).

4.6. mRNA quality control

It is highly important that the mRNPs that reach the cytoplasm and are translated there are properly processed and fully mature. Even though most budding yeast genes do not contain introns, it's the most expressed genes that do have them, which results in roughly half of the transcripts requiring splicing, while all genes are supposed to be polyadenylated before export.

In the case of splicing, the mechanism that prevents non-spliced transcripts from leaving the nucleus was proposed to promote their degradation by the exosome. Interestingly, the mechanism that controls the retainment of such mRNAs is also dependent on polyA binding protein Nab2 and nuclear basket component Mlp1, in addition to splicing factors such as U1 small nuclear RNP component Mud2 (Misra & Green, 2016; Soucek et al., 2016). While the involvement of both Nab2 and Mud2 implies the connection between polyadenylation and splicing machinery, Mlp1 involvement may either suggest that it promotes the export of spliced mRNA or that it retains the non-spliced ones. In the case of polyadenylation it is proposed that its termination itself triggers changes in polyadenylation machinery that, once transmitted to TREX complex, promote Yra1 association with the processed mRNP and activation of Sub2, thus leading to Mex67:Mtr2 attachment (Iglesias et al., 2010; Johnson et al., 2009). Interestingly, the aberrantly polyadenylated mRNAs are retained next to the transcription sites (Thomsen et al., 2003), and this requires nuclear exosome activity (Hilleren et al., 2001).

4.7. mRNA degradation

The mRNA processing quality control aims to target defective mRNAs that cannot be properly processed for nuclear (or cytoplasmic) degradation, reviewed in (Parker, 2012). Unspliced (or mis-spliced) mRNAs are proposed to be cleaved at a specific RNaseIII site and degraded by exonucleases (Danin-Kreiselman et al., 2003) within the nucleus, or exported to the cytoplasm and be degraded by exosome or Xrn1 (Parker, 2012). Indeed, multiple experiments observe cytoplasmic degradation of unspliced pre-mRNAs by nonsense-mediated decay (NMD) - a cytoplasmic mechanism

monitoring aberrantly translated mRNAs (Kawashima et al., 2009), or by NMD-independent pathways (Sayani et al., 2008). It is suggested that this is both part of the surveillance mechanism (for unspliced and incorrectly spliced pre-mRNAs) and a regulatory pathway that is for example utilized by splicing factors to autoregulate their own transcript levels (Ni et al., 2007).

Not all transcripts from cells with defects in 3' end processing machinery have the same fate. Some may have normal polyA length and export; some may be hypo- or hyper adenylated and nevertheless, a high proportion of both is stable, suggesting their retainment in the nucleus; and some are degraded (Hilleren & Parker, 2001; Mandart & Parker, 1995; Rougemaille et al., 2007).

Cytoplasmic degradation is performed by two general mRNA decay pathways, both of which start with the deadenylation step performed by the Ccr4/Not/Pop2 complex or Pan2/Pan3 complex and are followed by either decapping and exonucleolytic decay, or directly exonucleolytic decay. Another group is specialized pathways. (Parker, 2012)

4.8. Structure of pre-translational mRNPs

The structure of pre-translational mRNPs was studied by electron microscopy in budding yeast (Batisse et al., 2009) and salivary glands of *Chironomus tentans (Skoglund et al., 1983)* and by proximity in mammalian cells (Metkar et al., 2018). All lines of evidence speak in favor of the conserved co-transcriptional rod-like mRNP formation, with a thickness that does not largely depend on the mRNA class. In the case of yeast data, (Batisse et al., 2009) the study design implies that specifically pre-export mRNAs are isolated, pointing towards the picture in which rod-shaped mRNPs would be the ones to interact with the NPC basket. The RBPs that bind the RNA along its synthesis and processing is not just the export factors and proteins marking the maturation stage of the mRNA, but also a vast majority of the proteins that define the mRNA destiny including its stability, localization, translation and, eventually, degradation (Hentze et al., 2018).

4.9. Role of different nucleoporins in mRNA export

Once the mRNA interacts with the NPC, it does not mean that it will be definitely exported. Recent mRNA live imaging study in mammalian cells looking at mRNP particle dynamics at the NPC showed that it may be rejected and come back to the nuclear interior at all stages of passing through the different parts of the NPC - the nuclear basket, the central scaffold and the cytoplasmic fibrils, which raises the question about the roles of other nucleoporins except for the ones belonging to the nuclear basket

impacting the efficiency of mRNA export. The study however focused on the roles of different basket nucleoporins in the mRNA export process that proved to be distinct. Nup153 (possibly together with Nup50, since it is mislocalized from the NPCs upon Nup153 depletion) was found to be important for ensuring efficient nuclear mRNA export, 4 out of 8 copies of it per nuclear pore being sufficient for reaching the maximum export efficiency values. Tpr turned out to only play a critical role in the mRNP docking at the nuclear basket thus increasing the probability of mRNA entry to the NPC channel. Nup50 on the other hand likely does not play a significant part in ensuring efficient export or facilitating mRNP docking. In addition to the efficiency, the mRNA routes within the NPC were assessed and found to be changed in the basket upon depletion of either Nup153 or Tpr, but to a different extent. Depletion of Tpr mildly affected the mRNA paths, while depletion of Nup153 shifted most trajectories to the central axial channel pointing towards passive diffusion to the central channel, likely due to the absence of FG repeats in the basket devoid of Nup153 and Nup50. (Y. Li et al., 2021)

A comprehensive study in budding yeast aimed at deciphering the roles of specific FG domains in mRNA export showed that the combination of symmetric GLFG domains (Nup57 and Nup49) and FXFG domains (Nup1 and Nup2) is required for polyA mRNA export. The proposed mechanism implies the impaired recruitment and/or translocation of Mex67 through the NPC. Interestingly, FG repeats identified as important for a number of key karyopherins are different from those important for mRNA export. (Terry & Wente, 2007)

4.10. Gene gating

Nuclear periphery has been long thought to serve as a heterogeneous surface reflecting diverse adjacent genomic regions. The heterogeneity was thought to largely depend on the non-random distribution of nuclear pore complexes (Blobel 1985), which have been proven to be additionally different in composition (Bensidoun et al., 2022; Meinema et al., 2022). The gene gating hypothesis proposed that actively transcribed genes associate with the nuclear pore complexes both in order to organize the genome in 3D and to gate the genes to the cytoplasm thus bringing it in close proximity with the entry point of transcription and mRNA export factors from the cytoplasm, as well as the exit point for the resulting mRNA. The model also assumed that transcripts originating from gated genes would be exported through the nuclear pores situated next to the gene position. (Blobel, 1985) Some evidence in favor of this hypothesis has been drawn recently from live mRNA imaging in mammalian cells where indeed some nuclear pore

clusters exporting the same type of mRNA species were observed (Ashkenazy-Titelman et al., 2022).

4.11. Role of Gcn5/SAGA in mRNA export

Not much is known about the role of SAGA in mRNA export. SAGA complex associated with TREX-2 at the nuclear periphery. Sus1 is the component of TREX-2 and at the same time belongs to the DUB module of SAGA. Interestingly, Sus1 and Ubp8 depend on each other for the recruitment to the *GAL1* locus upon its activation, meaning that TREX-2 complex association with the active gene depends on the DUB module of SAGA. Additionally, the mRNA export defect of *sus1* mutant cells is aggravated by *SGF11* deletion implying that Sgf11 has DUB-independent functions in mRNA export (Köhler et al., 2006), and this data from yeast is supported by evidence from Drosophila (Gurskiy et al., 2012).

Sus1 could play completely independent roles in the DUB module and TREX-2; alternatively, it could be the element dynamically bridging these two complexes. The HAT module plays a role in the SAGA-TREX-2 association through its Sgf29 component that recruits TREX-2 to SAGA. On the opposite, disruption of the DUB module via Ubp8 deletion does not affect the SAGA binding of TREX-2. The data above argues that SAGA-bound Sus1 does not directly mediate SAGA-TREX-2 binding; however, it is still possible that there is a dynamic exchange of Sus1 between the two complexes coupled to the NPC binding/release, coordinated with transcriptionally-dependent changes in the chromatin-mRNA complex bound by SAGA and TREX-2. Such mechanism provides an explanation for activated *GAL1* locus dynamic behavior at the nuclear periphery and may be subject to regulation, specifically by post-translational protein modifications. (Klöckner et al., 2009) Another member of the DUB module, Sgf11 in *Drosophila* interacts with the 5' cap-binding protein Cbp80 and thus is recruited to the growing transcript. It is shown to be highly important for general mRNA export. (Gurskiy et al., 2012)

Interestingly, the Sgf73 subunit of the SAGA DUB module is acetylated by SAGA/ADA. Little is known however about the functional relevance of this modification; unpublished data from the Barral lab indicate that Sgf73-K401 acetylation promotes DNA circle retention in the mother cell.

4.12. NPC in gene expression

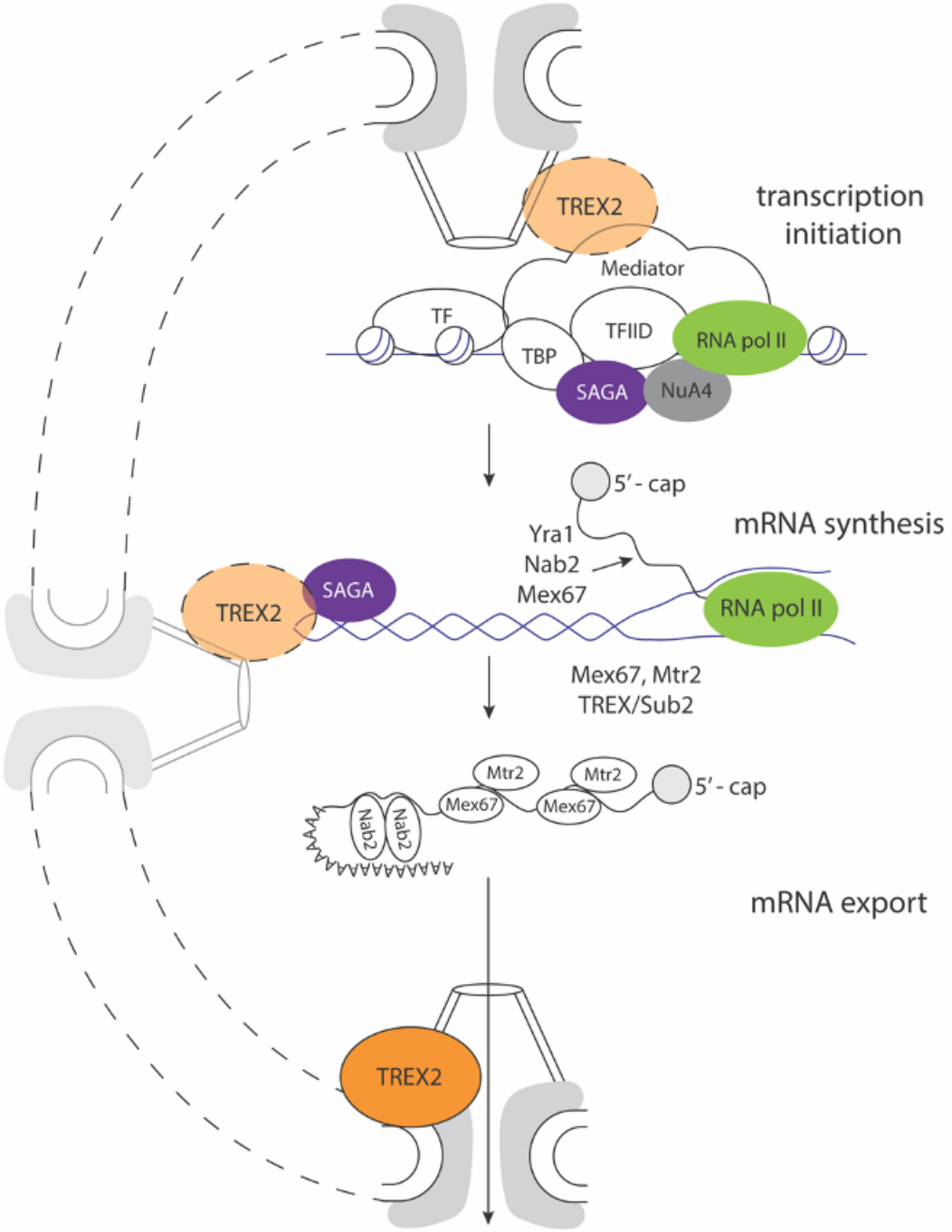

Figure 4 Initiation of transcription, mRNA synthesis, and export *Scheme of gene expression until the moment of mRNA export. TREX-2 complex is shown to promote the formation of the pre-initiation complex, transcription, and mRNA export, Sac3 mediates interactions between the nuclear pore basket and Mediator, SAGA, Mex67:Mtr2 at the promoters.*

The NPC has been proposed to regulate and coordinate transcript elongation, pre-mRNA processing, and export (Ibarra & Hetzer, 2015; Sood & Brickner, 2014). The way to do that is to directly interact with the transcription sites and to accumulate in the

vicinity diverse regulatory factors that either participate in transcription or interact with the proteins associated with the transcribed gene promoters or mRNAs (Figure 4). In particular, Sac3, the component of the TREX-2 complex, is docked at the nuclear basket through Nup1 and interacts directly with Mex67:Mtr2 heterodimers, while another TREX-2 component Thp1 is involved in transcription elongation. Mutations of both Sac3 and Thp1 lead to the mRNA export defect. (Fischer et al., 2002; Gallardo & Aguilera, 2001) Importantly, SAGA interacts both with the NPC and with the gene promoters, and these interactions are conserved (Denoth-Lippuner et al., 2014; Kurshakova et al., 2007; Meinema et al., 2022). Notably, despite sharing a Sus1 subunit, TREX-2, and SAGA are likely forming solely separate protein complexes (Ellisdon et al., 2010). TREX-2 in association with the NPC directly interacts with Mediator and modulates its interaction with RNA Pol II phosphorylated on Ser5. TREX-2 and Mediator co-regulate a group of genes, including *GAL1*. (M. Schneider et al., 2015)

One of the processes that may be associated with gene activation and recruitment to the NPC is sumoylation. Inositol-3-phosphate synthase gene *INO1*, a target of the unfolded protein response pathway, is recruited to the nuclear membrane upon transcriptional activation in a Hac1 transcription activator-dependent manner. Hac1 is negatively regulated by a transcriptional repressor Opi1 and is constitutively expressed in *opi1* cells. Its activation requires an integral nuclear membrane protein Scs2 or else just the recruitment to the nuclear periphery since artificial anchoring to the nuclear periphery via FFAT-Lac repressor interaction with LacO upstream of the *INO1* promoter permits its activation in *scs2* mutant cells. (J. H. Brickner & Walter, 2004) In the case of induction of *INO1* sumoylation is important for gene recruitment to the NPC, and further desumoylation by a nuclear basket interacting isopeptidase Ulp1 is contributing to continuous NPC localization and normal expression of this gene. (Saik et al., 2020) Once activated and repressed, *INO1* stays at the periphery for several generations and can get reactivated the second time quicker than for the first time. The phenomenon is defined as transcriptional memory and depends on a short sequence within the promoter region that ensures perinuclear targeting and the incorporation of H2A.Z upon repression. In cells where NPC targeting of *INO1* is perturbed either by Nup100 or the targeting DNA sequence, transcriptional memory is lost. (Light et al., 2010)

The *GAL1* gene is another example of a gene activated at the nuclear periphery. Activation of the GAL locus comprising *GAL1*, *GAL10,* and *GAL7*, leads to its sterical confinement in the nuclear periphery. While the locus is not active, it is located mostly within the nuclear interior and moves in a sub-diffusive manner, while in the activated

state, it becomes anchored to the nuclear periphery and moves largely along its surface. Perinuclear localization of the gene is associated with higher expression levels and depends on Sus1 and Ada2 (but not Gcn5), and on Sac3, which in the simplest case belong to SAGA and TREX-2. Interestingly, the positive transcriptional effect of the localization next to the nuclear periphery association is not lost upon the loss of peripheral localization (in *nup1* or *ada2* mutants), and vice versa, transcriptional activation is not enough to be recruited to the periphery (*sus1* and *sac3* mutants both transcribe *GAL1*, however, the locus is not at the periphery). Interestingly, Mlp1 and Nup60 are not directly involved in the gene targeting the pore. (Cabal et al., 2006) *GAL1*, similarly to *INO1*, is regulated by a nuclear basket-associated Ulp. If Ulp1 is no more constrained at the nuclear periphery but instead redistributed in the nucleoplasm, this leads to *GAL1* derepression, presumably because of the desumoylation of Tup1 and Ssn6 transcriptional repressors in the *GAL1* promoter. (Texari et al., 2013) Another report indicates that there is a connection between gene anchoring at the periphery and Mlp1 or Mex67, for *GAL* locus and *HSP104*. Mex67 was recruited to the genes co-transcriptionally, but independently of the nascent mRNA. Interestingly, the Mex67-5 mutant protein did not associate with the transcribing genes and the gene was not anchored. (Dieppois et al., 2006)

5. Cell cycle entry regulation in budding yeast

Unicellular organisms, such as budding yeasts, aims to reproduce as fast as possible as long as the conditions allow it. The decision to divide and give progeny, in the case of yeast cells by asymmetric cell division, is a step known as the Start in budding yeasts, happening in the late G1 phase of the cell cycle. This is one of the major cell-cycle transitions, and it requires that the external (such as nutrient availability) and internal (such as reaching the appropriate size) conditions are satisfied in order for the cell to irreversibly commit to DNA synthesis and further division.

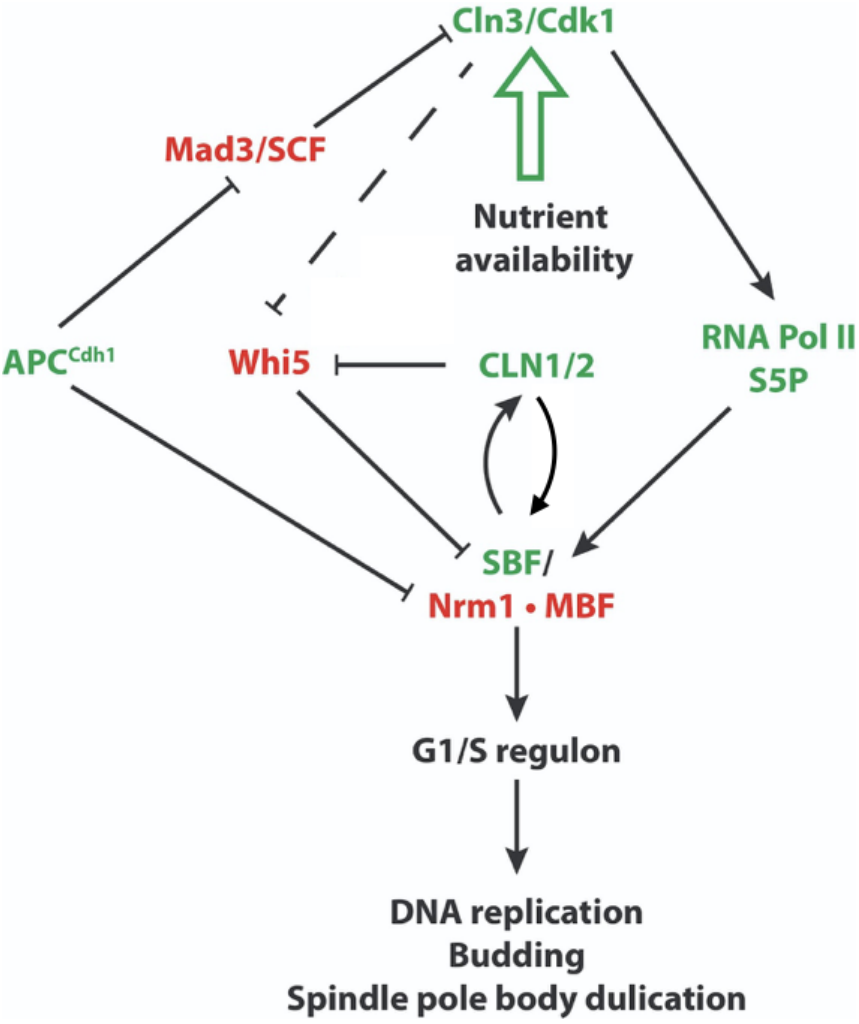

Figure 5 G1/S transition circuitry *The scheme represents the general scheme of G1/S transition, with activatory nodes depicted in green and inhibitory nodes in red; nutrient availability signals to Cln3 to promote G1/S, while the poorer carbon source, the more Whi5 in the next cell cycle the cell will get.* *(Sommer et al. 2021)*

5.1. Cell cycle progression depends on the activation of Cdk1

Progression through the cell cycle is governed by Cdk (cyclin-dependent kinase). Cdk is a serine/threonine protein kinase that requires one among multiple cyclins (separate regulatory protein subunits) for the activity and specificity towards its substrates. Cdk activity can also be inhibited by multiple specific inhibitors. Cyclins and Cdk inhibitors are in turn modulated during the cell cycle by synthesis and degradation. (Frolov and Dyson 2004) The abundance of certain cyclins oscillates during the cell cycle, and these cyclins together with corresponding Cdks orchestrate cell cycle progression. While mammalian cells have several cell-cycle regulating Cdks, each one able to bind one or few cyclins, budding yeasts have two proteins, Cdc28 (or Cdk1) and Pho85, binding respectively 9 and 10 cyclins. Cdc28 is the only essential Cdk in budding yeasts, although Pho85 is indispensable under some conditions including growth after starvation. (Malumbres 2014) Cdks serve as a point of integration of extracellular and intracellular cues to regulate gene expression and drive the cell cycle (D. O. Morgan 1997).

5.2. The G1/S transition relies on a Cdk-dependent transcriptional wave

The centerpiece of Start is the activation of G1/S cyclin-Cdk1 complexes - Cln1/Cln2-Cdc28. They directly activate events needed for cell cycle entry such as SPB duplication and budding, and indirectly, through relieving the inhibition of S cyclin-Cdk1 complexes, promote DNA replication. The switch-like activation of G1/S cyclin-Cdk1 depends on positive feedback loops and other mechanisms ensuring irreversible cell cycle entry. G1/S cyclins Cln1 and Cln2 and S cyclins Clb5 and Clb6 belong to the G1/S transcriptional regulon of about 200 genes activated by the late G1 cyclin Cln3-Cdk1 complex. Cln3-Cdk1 is thought to phosphorylate the major cell cycle repressor protein Whi5 to drive it away from the nucleus allowing the transcription of genes activated at the G1/S transition (Bertoli, Skotheim, and de Bruin 2013). Whi5 deletion mutant is small, consistent with its role in repression of G1/S transition and hence prolonging G1 (Costanzo et al. 2004; de Bruin et al. 2004), the part of the cell cycle contributing mostly to growth (Johnston, Pringle, and Hartwell 1977); increased Whi5 concentration in the cell leads to the dose-dependent increase in cell size (Schmoller et al. 2015). Whi5 has orthologs in the higher eukaryotes, such as human pRB which is a G1/S transition repressor and turns out to be inactivated in many tumors. (Frolov and Dyson 2004)

However, the primary role of Whi5 phosphorylation in Start and Whi5 being the target of Cln3-Cdk1, in particular, has been recently disputed, as explained later in this chapter (Kõivomägi et al. 2021). One of the facts supporting the doubts of Whi5 phosphorylation and nuclear export being paramount for cell cycle entry is that non-phosphorylatable Whi5 mutant does stay in the nucleus and the cells are delayed in Start, but viable (Wagner et al. 2009).

5.3. SBF and MBF transcription activators drive Start-specific gene expression

The G1/S regulon comprises genes encoding G1/S and S cyclins and other components of cell-cycle machinery responsible for late G1 and S phase events, including enzymes and other proteins required for DNA synthesis and budding. Genes to be activated at the G1/S border have common motifs in their promoter regions that direct binding of transcriptional activators SCB (Swi4/Swi6-regulated cell cycle boxes (Andrews and Herskowitz 1989)), MCB (MluI cell cycle box (McIntosh et al. 1991)) or both. SCB is bound by the SBF transcription factor (SCB-binding factor, a heterodimer of Swi4 and Swi6) and MCB is bound by the MBF transcription factor (MCB-binding factor, a heterodimer of Mbp1 and Swi6). DNA specificity for these factors is determined by Swi4 and Mbp subunits. Even though it is generally considered that SBF regulates transcription of *CLN1/2* and cell wall synthesis and budding regulating genes, and MBF regulates transcription of *CLB5/6* and DNA metabolism-regulating genes, one transcription factor (TF) can replace another (and vice versa) for many genes. (Bean, Siggia, and Cross 2005)

The repressed state of SBF-controlled loci is ensured via Whi5-dependent recruitment of Rpd3 deacetylase, likely through local histone modification. MBF-regulated genes recruit Rpd3 as well, although this depends on Stb1, another transcription regulator present in both SBF and MBF-bound promoters. Upon G1/S genes activation SBF and MBF recruit FACT chromatin remodeling complex that promotes rapid nucleosome eviction to facilitate transcription. (Takahata, Yu, and Stillman 2009)

CLN2 expression depends on SBF (Iyer et al. 2001), and the Cln2 protein regulates the transcription of its own gene creating a positive feedback loop. Cln2 binds Cdc28; this cyclin-Cdk1 complex activates *CLN2* transcription and transcription of the rest of the G1/S regulon through definitive phosphorylation and inactivation of Whi5. (Skotheim et al. 2008)

Despite sharing the Swi6 subunit and being induced with a similar temporal pattern, the mechanism of SBF and MBF action is different: while SBF functions as a transcription activator, promoting gene expression in G1-S transition, while MBF renders genes under its control silent outside of G1, reviewed in (Bertoli, Skotheim, and de Bruin 2013).

This implies different modes of regulation for SBF- and MBF-dependent genes in the cell cycle. For example, SBF-dependent genes are not active in *swi4* mutant cells. Their activation at the end of G1 depends on Whi5 dissociation from SBF, which in turn depends on Cln1/2-Cdc28 activity (Costanzo et al. 2004; de Bruin et al. 2004). SBF component Swi4 is reported to double its concentration with growth in glucose, which likely contributes to Whi5/SBF ratio in the nucleus and G1/S transition (Dorsey et al. 2018).

On the other hand, MBF-dependent genes are constitutively active in *mbp1* mutant cells. Inactivation of their transcription in wild-type cells is ensured by MBF-dependent expression of a co-repressor Nrm1. (de Bruin et al. 2006) At the end of G1 Nrm1 is degraded in an APC-Cdh1-dependent fashion (Ostapenko and Solomon 2011) contributing to the coordinated transcription of genes activated at the G1/S border.

5.4. The role of Cln3 in Start

Cln3 protein is an early G1 cyclin, one of the most prominent Start modulators. It was originally thanks to the gain-of-function mutation that conferred small size and resistance to α-factor G1 arrest via truncation of the protein degradation signal (Cross 1988). Even though any of the Cln1-3 cyclins is sufficient to drive the G1/S transition (Richardson et al. 1989), there are a number of indications that Cln3 is the upstream and major regulatory molecule. Transcriptome-wide analysis shows that *CLN3* deletion leads to a delayed Start with normal progression through later stages of G1-S transition, while these were particularly affected by *CLN1-2* deletion (Teufel et al. 2019).

The long-standing image of Start control implies that the primary and core action of the Cln3-Cdc28 complex in promoting cell cycle entry is Whi5 phosphorylation and its dissociation from the promoter regions of regulated genes (de Bruin et al. 2004; Costanzo et al. 2004). However, this is challenged by the recent finding that low-level phosphorylation of Whi5 present in G1 is likely not connected with Cln3-Cdc28 activity since it is not lost upon Cln3 anchor-away from the nucleus. The hyperphosphorylated Whi5 form, on the other hand, is not found in *cdc34-ts* blocked cells that only have *CLN3* out of 3 G1 cyclin genes. The authors argue that it is serine 5 in Pol II C-terminal domain

that is being phosphorylated by Cln3-Cdc28, leading to transcription activation of SBF-regulated genes. This study also links CDK function to transcription kinases regulated in a cell cycle-independent manner. (Kõivomägi et al. 2021)

The Cln3-dependent pathway of SBF-/MBF-target genes activation is partially redundant with the Bck2-driven mechanism of cell cycle entry. (Wijnen and Futcher 1999). The intriguing finding is that Bck2 activates gene expression of a variety of cell-cycle regulated targets across different cell cycle stages in a mechanism that depends on other molecules except for SBF and MBF transcription factors (Ferrezuelo, Aldea, and Futcher 2009),

5.5. Pathways that control Cln3 accumulation

There are multiple pathways that have been shown to control Cln3 protein abundance and in turn Cln3-CDK activity. For example, *CLN3* mRNA is possibly downregulated by Whi3, an ER-associated protein binding GCAU motifs in its 3'-untranslated region (3'-UTR), which promotes interaction with Ccr4-Not complex and leads to mRNA deadenylation; on the other mRNA end, 5′-untranslated region (5'-UTR) GCAU motifs attract Whi3 and may hinder translation (Garí et al. 2001; Y. Cai and Futcher 2013). Interestingly, Whi3 forms aggregates in old cells that segregate to mothers in mitosis, making them less sensitive to pheromone arrest (Schlissel et al. 2017).

However, *CLN3* mRNA, unlike that of *CLN1-2*, is only mildly oscillating in the cell cycle (Nash et al. 1988; Wittenberg, Sugimoto, and Reed 1990), implying that regulation of Cln3 activity is largely co- or post-translational. One of the known mechanisms is that Cln3 protein is retained in the ER in a Cdc28-dependent manner in early G1 and released by a Ydj1 chaperone from the ER in late G1 (Vergés et al. 2007).

Cln3 levels peak shortly before budding, regulated post-translationally by an elaborate network as shown recently in (Pérez et al. 2022). Cln3 is degraded both in the cytoplasm and in the nucleus by Skp1–Cullin–F-box (SCF), and its degradation depends on Mad3 centromeric-signaling protein. Mad3 in its turn is degraded by anaphase promoting complex (APC) together with Cdh1. This level of control brings a "timer" component to the budding yeast Start mechanism - meaning that the molecular event (Start) is triggered as a function of time, independent of size.

Another control mechanism for Cln3-CDK activity comes from Cip1, a functional ortholog of mammalian p21, which is expressed in G1 and inhibits G1-S transition both by targeting G1 cyclin-CDK complexes and by inhibiting the activity of

Ccr4-Caf120. Both pathways under Cip1 control rely on Whi5 inhibition (Y.-L. Chang et al. 2017; P. Li et al. 2020).

5.6. Cln2 regulation beyond the transcriptional level

CLN2 gene expression is regulated at several levels. One of them is the level of mRNA export, which may be partially dependent on the Ssd1 protein. Ssd1 shuttling between nucleus and cytoplasm is important for cytoplasmic localization of bound mRNAs (Ohyama, Kasahara, and Kokubo 2010; Kurischko et al. 2011), and *CLN2* expression under stress conditions is promoted by Ssd1 binding its 5' UTR (Ohyama, Kasahara, and Kokubo 2010; Kurischko et al. 2011).

At the level of protein, Cln2 degradation is induced by CDK-driven phosphorylation (Lanker, Valdivieso, and Wittenberg 1996), meaning that Cln2-Cdc28 regulates itself through a negative feedback loop. Interestingly, despite significant redundancy in Cln1 and Cln2 sequences and similar lifetimes, they display differences in their degradation mechanisms: Cln1 is predominantly degraded by SCF-Grr1, whereas Cln2 is degraded both by SCF-Grr1 and SCF-Cdc4, the difference coming from N-terminal domain which is different from the one which targets these proteins for degradation. (Quilis and Igual 2017).

5.7. G1/S-Cdks promote S-Cdks activation

Cln3-Cdk drives the expression of SBF-dependent genes, and they are in turn inactivated thanks to an intricate feedback loop involving the degradation of Sic1 inhibitor leading to activation of S-phase cyclin (Clb5/6)-Cdc28.

CLB5/CLB6 transcription depends on MBF (Schwob and Nasmyth 1993); Clb5-Cdc28 is inhibited by Sic1 binding (Schwob et al. 1994; B. L. Schneider, Yang, and Futcher 1996). Cln1/2-Cdc28 phosphorylates Sic1, priming it for further phosphorylation by Clb5-Cdc28 and leading to its SCF/Cdc4-mediated degradation (Verma et al. 1997; Kõivomägi et al. 2011). Once Sic1 is degraded, S-phase CDK Clb5/6-Cdc28 promotes initiation of DNA replication and dissociation of SBF from its targets (Koch et al. 1996).

5.8. S-Cdks inactivate APC^{Cdh1} after Start

APC^{Cdh1}, the initial driver of Start events, is inactivated approximately 12 minutes after Whi5 export (Ondracka, Robbins, and Cross 2016) through several mechanisms including CDK-dependent phosphorylation of Cdh1 and pseudosubstrate inhibition by Acm1 protein. It was proposed that both Clb5/6-Cdc28 (J. N. Huang et al.

2001) and Cln1/2-Cdc28 (Amon 1997) could potentially phosphorylate Cdh1 in order to inactivate APC^{Cdh1}, but the analysis of partially phosphorylatable Cdh1 mutants indicates that the primary role belongs to Clb5/6-Cdc28 (Ondracka, Robbins, and Cross 2016). *ACM1* expression depends on SBF/MBF and the protein appears in late G1. It contains motifs specific for APC substrates (KEN-box and D-box), but is not ubiquitinated by APC. On the contrary, it competes with APC^{Cdh1} substrates as it binds Cdh1. The stability of Acm1 is increased by Cdc28-dependent phosphorylation. (Martinez et al. 2006; Ostapenko et al. 2008)

5.9. How irreversible is Start?

Even though Whi5 eviction from the nucleus marking Start has been long considered a moment of irreversible commitment to cell cycle entry, recent data suggests that there may be another decision-making point in the cell cycle between Whi5 exit and the beginning of replication. Post-Start yeast cells can dephosphorylate and reimport Whi5 upon glucose starvation if the stress occurs within 20 minutes after Whi5 nuclear export that is, likely before the replication is initiated. These cells largely regain pre-Start identity, since they become alpha-factor responsive and initiate a second wave of *CLN2* expression once the stress is over. (Irvali et al. 2021)

5.10. Cell size control

Since most growth in budding yeasts (and many other cell types) happens over G1, they keep control over how much they need to grow before they commit to division, at Start. A number of factors promoting and inhibiting cell cycle entry have been identified over the years, mutations in which correspondingly cause cells to grow longer before Start and to have bigger mean cell size, and vice versa (Soifer and Barkai 2014). However, the cell size control defined by the cell size distribution across the population (approximated by the mean divided by the variation coefficient) is strikingly the same across deletion mutants. This would mean that, while changing the cell size, the cells change the distribution of sizes proportionally, keeping “control” over how much they grow on average (Yuping Chen et al. 2020).

Two molecules have been proposed to serve as cell size/growth sensors, Whi5 as the one to record the past environmental conditions, meaning in particular nutrient availability (Qu et al. 2019), and Cln3 on the other hand - as a readout of current environmental conditions, since its transcription, translation, and localization depend on nutrient availability (Hall et al. 1998; Polymenis and Schmidt 1997; L. Shi and Tu 2013).

Accordingly, two models of cell size control have been proposed based on how much Whi5 is diluted by growth, or on an increase in protein synthesis in pre-Start cells leading to Cln3 concentration reaching a limiting point (Schmoller et al. 2015; Litsios et al. 2019). The underlying features of both proposals have been challenged in follow-up studies (Litsios et al. 2022; Schmoller et al. 2022).

Additionally, since each of the models is based solely on changes in concentration of one of the molecules, be that Whi5 or Cln3, the critical experiment was to look at the cell size distributions under conditions where the abundance of these cell cycle regulators is independent of cell size, keeping the overall expression at the wild-type level. This was achieved by expressing Whi5 or Cln3 from the galactose-driven promoter, and the cell size distributions (and diverse cell cycle correlated growth parameters for Whi5) turned out to be indistinguishable from those of the wild type. Such results for the Start players with an established role in cell size control implied that a more complicated model should be devised. (Barber, Amir, and Murray 2020)

The results of a global study lead to the proposal of a comprehensive model of cell size control that attempts to make peace between the Whi5 dilution and increased Cln3 synthesis models. It turns out that there is a striking correlation at the mRNA level: many activators increase their abundance with cell growth, while inhibitors, on the other hand, are less abundant in bigger cells. This allowed to propose a hypothesis of collective cell size determination by activators that increase and inhibitors that decrease their concentrations with cell growth. The model is supported by the fact that cell size control is perturbed (i.e. the distribution of cell sizes is broadened) if the mRNA of one of the leading activators of Start (*CLN2*) subscales instead of super scaling as in wild type. This is achieved by a simple *CLN2* promoter exchange to the one belonging to an inhibitor (*WHI5*). (Yuping Chen et al. 2020)

5.11. The role of NPC acetylation in Start

The connection between the NPC acetylation state and the cell cycle progression was reported in a recent paper from our group. I briefly mentioned some of the major findings in sections considering the role of NPC acetylation and Hos3, but here I would like to highlight them again to show the connection to the questions that I am addressing in this thesis, before going into the results.

The paper from Kumar *et al.* centers around the role of Hos3 deacetylase in NPC deacetylation and the consequences on cell cycle progression, and the key findings are outlined in the following sections of the introduction: Nuclear pore acetylation, Hos3

(Protein acetylation and its role in regulation of gene expression) and Nup60 (Nuclear pore complex). Briefly, it is shown that Hos3 lysine deacetylase associates specifically with the nuclear pores of daughter cells in mitosis until late anaphase and that its catalytic activity on the central channel and nuclear basket components of the nuclear pore drives daughter-specific cell cycle delay in G1. The analysis of acetyl-mimic mutants (lysine to asparagine) showed that they undergo an advanced G1/S transition, suggesting that they may be targeted by Hos3 at the nuclear periphery.

It was proposed that deacetylation of the daughter NPC regulates the cell cycle entry through modulation of the canonical NPC function such as protein and mRNA transport and gene gating. Accumulation of Whi5 in daughter cells depends on Hos3 and on the acetylation state of the nucleoporins, indicating that protein transport of certain cargoes may be affected by nuclear pore acetylation. This possibility remains open for future studies.

With regard to the proposed role in gene expression and gating, *hos3* cells were found to express the GFP reporter gene under the *CLN2* promoter earlier than wild-type cells which indicates at a possible connection between Hos3 and *CLN2* expression timing (Kumar et al. 2018). This could arise from Hos3 being associated with Whi5 to downregulate transcription. (D. Huang et al. 2009) The position of the *CLN2* gene, which encodes one of the major drivers of G1/S transition, was shown to be dependent on the cell cycle stage: *CLN2* locus was shown to be mostly at the nuclear periphery in G1 cells (when *CLN2* is repressed) and to be localized mostly in the nucleoplasm interior in cells that transitioned to S phase. This distribution was perturbed in *hos3* mutant cells and in nucleoporin acetylation mutants, which implies the possibility of a role of the NPC in the transcription and/or export of mRNA, the processes proposed to be facilitated by gene gating. In addition, in a screen with *hos3-NLS* mutant that is constitutively localized to the nucleus, many nuclear transport receptor molecules were found mislocalized, including the Mex67 mRNA export factor that normally associates with the nuclear periphery but was displaced by Hos3. These and other findings indicate that gene expression and, specifically, mRNA export could be modulated by NPC acetylation. (Kumar et al. 2018)

This study opened many questions, and we started giving our answers in the publication central to this thesis. The two main questions we were eager to answer are

1) What is the acetyltransferase that counteracts Hos3 at the nuclear periphery?

2) What is the mechanistic link that connects the nuclear pore complex acetylation state and the cell cycle progression?

6. Articles

Article 1

Nuclear pore complex acetylation regulates mRNA export and cell cycle commitment in budding yeast

This article reveals a previously undescribed pathway contributing to the regulation of gene expression in budding yeast. Esa1/NuA4 acetyltransferase, a well-established player in the field of transcription control, acetylates the Nup60 component of the nuclear pore basket, which promotes mRNA export. We describe the mechanistic link between these two processes and identify the functional role of Nup60 acetylation in G1/S cell cycle transition and in cellular adaptation to a new carbon source.

This work is largely a result of my collaboration with a former postdoc Merce Gomar with a very much appreciated participation of other contributors. My contribution to this project consisted of strain construction and experimental design, analysis, and interpretation of the data with the consequent contribution to the manuscript, before and after the final revision. The experiments that were directly performed by me are reflected in: Fig.1D; Fig.2C,E; Fig.3, EV2B; EV3A,C; EV4; S2; S3D; S6; S13. I also contributed with the macro code for high-throughput analysis of the Spinning disk microscopy images and with the MatLab code for the analysis of microscopy data from microfluidics chamber experiments and with the training of Celia Schaal and Bogdan Cichocki who also made contributions to the final manuscript.

Article

SOURCE DATA | TRANSPARENT PROCESS | OPEN ACCESS

THE EMBO JOURNAL

Nuclear pore complex acetylation regulates mRNA export and cell cycle commitment in budding yeast

Mercè Gomar-Alba[1,2,†], Vasilisa Pozharskaia[1,†], Bogdan Cichocki[1], Celia Schaal[1], Arun Kumar[3], Basile Jacquel[1], Gilles Charvin[1,4,5,6], J Carlos Igual[2] & Manuel Mendoza[1,4,5,6,*]

Abstract

Nuclear pore complexes (NPCs) mediate communication between the nucleus and the cytoplasm, and regulate gene expression by interacting with transcription and mRNA export factors. Lysine acetyltransferases (KATs) promote transcription through acetylation of chromatin-associated proteins. We find that Esa1, the KAT subunit of the yeast NuA4 complex, also acetylates the nuclear pore basket component Nup60 to promote mRNA export. Acetylation of Nup60 recruits the mRNA export factor Sac3, the scaffolding subunit of the Transcription and Export 2 (TREX-2) complex, to the nuclear basket. The Esa1-mediated nuclear export of mRNAs in turn promotes entry into S phase, which is inhibited by the Hos3 deacetylase in G1 daughter cells to restrain their premature commitment to a new cell division cycle. This mechanism is not only limited to G1/S-expressed genes but also inhibits the expression of the nutrient-regulated *GAL1* gene specifically in daughter cells. Overall, these results reveal how acetylation can contribute to the functional plasticity of NPCs in mother and daughter yeast cells. In addition, our work demonstrates dual gene expression regulation by the evolutionarily conserved NuA4 complex, at the level of transcription and at the stage of mRNA export by modifying the nucleoplasmic entrance to nuclear pores.

Keywords G1-S transition; Hos3; mRNA export; NuA4; nuclear pore complex
Subject Categories Cell Cycle; Post-translational Modifications & Proteolysis; RNA Biology
DOI 10.15252/embj.2021110271 | Received 24 November 2021 | Revised 16 May 2022 | Accepted 19 May 2022 | Published online 23 June 2022
The EMBO Journal (2022) 41: e110271

Introduction

Nuclear pores are macromolecular assemblies composed of approximately 30 different nucleoporins that form a channel across the nuclear envelope (Knockenhauer & Schwartz, 2016; Hampoelz *et al*, 2019; Raices & D'Angelo, 2021). The central channel mediates communication between the nucleus and cytoplasm. Other NPC substructures include the cytoplasmic filaments and the nuclear basket, associated with the cytoplasmic and nuclear sides of the central channel, respectively. The nuclear basket regulates gene expression through interactions with active genes (Casolari *et al*, 2004; Cabal *et al*, 2006; Light *et al*, 2010; Brickner *et al*, 2019) and with regulators of transcription (Texari *et al*, 2013; Schneider *et al*, 2015) and mRNA export (Fischer *et al*, 2002; Dieppois *et al*, 2006). These and other studies have suggested that NPCs can act as regulatory sites for the coordination of transcript elongation, processing and export (Sood & Brickner, 2014; Ibarra & Hetzer, 2015).

The nuclear basket also recruits lysine acetyltransferases (KATs) and deacetylases (KDACs). Acetylation of histones is tightly associated with transcription, and KATs and KDACs, often residing in large multiprotein complexes, are thought to target nucleosomes to regulate transcriptional activity (Sterner & Berger, 2000; Lee & Workman, 2007). In addition, acetylation of non-histone proteins is common in eukaryotes and has been implicated in a variety of biological processes in addition to transcription, such as DNA damage repair, cell division and signal transduction (Kaluarachchi Duffy *et al*, 2012; Narita *et al*, 2019). Among the best-characterised yeast KATs are Esa1 and Gcn5, contained in the NuA4 and SAGA complexes, respectively. Esa1 (known as Kat5 or Tip60 in mammals) is the only essential KAT in budding yeast and is involved in DNA transcription and repair (Allard *et al*, 1999; Clarke *et al*, 1999; Doyon & Côté, 2004; Bruzzone *et al*, 2018). Gcn5 (also known as KAT2A) is not essential but plays a role in the transcription of most yeast genes (Baptista *et al*, 2017; Bruzzone *et al*, 2018). KATs and KDACs known to associate with NPCs include Gcn5 and the type II deacetylases Hos3 (in yeast) and HDAC4 (in mammals) (Cabal *et al*, 2006; Kurshakova *et al*, 2007; Kehat *et al*, 2011; Kumar *et al*, 2018). Despite their presence at NPCs, how KATs and KDACs act to regulate gene expression at these sites is poorly understood.

1 Institut de Génétique et de Biologie Moléculaire et Cellulaire, Illkirch, France
2 Institut de Biotecnologia i Biomedicina (BIOTECMED) and Departament de Bioquímica i Biologia Molecular, Universitat de València, Burjassot, Spain
3 Department of Cell Biology, Universitat Pompeu Fabra (UPF), Barcelona, Spain
4 Centre National de la Recherche Scientifique, UMR7104, Illkirch, France
5 Institut National de la Santé et de la Recherche Médicale, U964, Illkirch, France
6 Université de Strasbourg, Strasbourg, France
*Corresponding author. Tel: +33 3 88653313; E-mail: manuel.mendoza@igbmc.fr
†These authors contributed equally to this work

Regulatory principles of the G1/S transition (known as Start in yeast) are evolutionarily conserved: activation of cyclin-dependent kinase (CDK) drives the transcription of hundreds of genes involved in the start of S phase (Bertoli *et al*, 2013). Indeed, defects in G1/S control are tightly associated with oncogenesis. For example, pRB is a repressor of the G1/S transition thought to be functionally inactivated in most tumour cells (Frolov & Dyson, 2004). In both yeast and animal cells, inhibition of premature G1/S transition involves the targeting of KDACs to chromatin, generating an environment that is unfavourable for transcription (Frolov & Dyson, 2004; Huang *et al*, 2009; Takahata *et al*, 2009; Wang *et al*, 2009). We recently discovered that in budding yeast, NPC acetylation regulates the G1/S transition (Kumar *et al*, 2018; Gomar-Alba & Mendoza, 2019). The KDAC Hos3 is cytoplasmic during interphase, but associates with the yeast division site (the mother-bud neck) in mitosis and then binds to daughter cell NPCs as they traverse the bud neck during anaphase, leading to Hos3 association with the nuclear basket specifically in daughter cells (Fig 1A). Hos3-dependent deacetylation of central pore channel nucleoporins in daughter cells enhances nuclear accumulation of the main Start inhibitor (the transcriptional

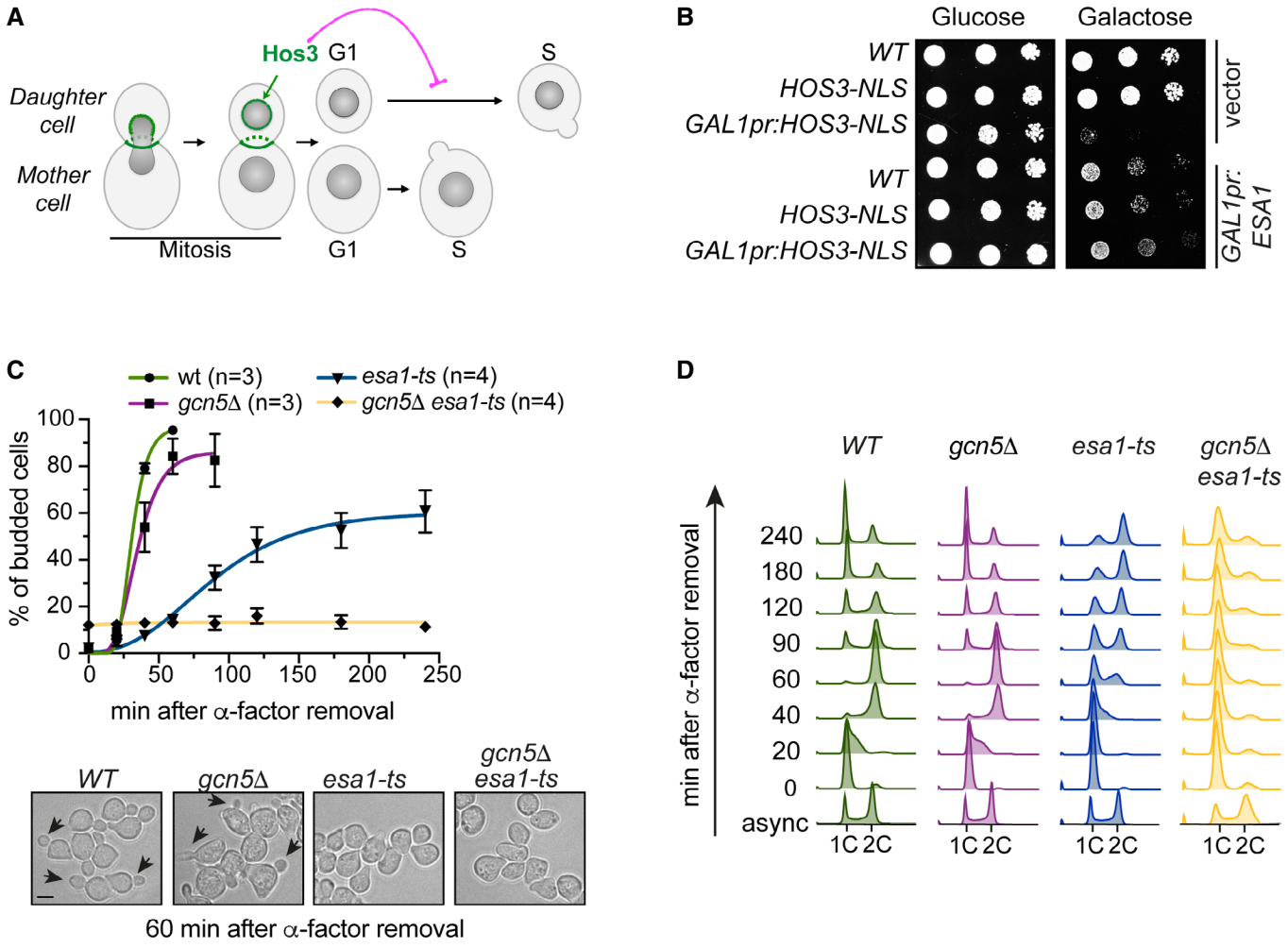

Figure 1. KATs Esa1 and Gcn5 counteract the KDAC Hos3 to promote the G1/S transition.

A Localisation and function of the Hos3 deacetylase during mitotic division. Hos3 (in green) associates with the bud neck and with daughter cell NPCs during nuclear migration into the bud. Hos3 delays the G1/S transition specifically in daughter cells through deacetylation of NPCs (Kumar *et al*, 2018).

B Growth inhibition upon overexpression of *HOS3-NLS* driven by the *GAL1* promoter is suppressed by overexpression of the KAT Esa1. 10-fold serial dilutions of the indicated strains transformed with an empty vector or with the indicated plasmids were spotted onto SC-Glu and SC-Gal medium (to activate the *GAL1* promoter) and incubated at 25°C for 3 days. Note that *HOS3-NLS* (under the control of the native *HOS3* promoter) does not affect cell growth.

C *esa1-ts* and *gcn5Δ esa1-ts* mutants have bud emergence defects. (*Top*) Cells of the indicated strains were arrested in G1 by treatment with α-factor for 2.5 h at 25°C, shifted to 37°C for 1 h and released from the G1 arrest at 37°C. Cells were fixed at the indicated times, and the presence of buds was assessed by microscopy. Mean and SEM are derived from n = number of independent experiments. At least 200 cells were scored for each strain and time point. (*Bottom*) Bright-field images of the indicated strains 60 min after the α-factor washout. Arrowheads point to cell buds. Scale bar, 4 μm.

D Inactivation of *ESA1* and *GCN5* delays DNA replication. Cells of the indicated genotypes were synchronised as in panel C, and DNA content was evaluated by flow cytometry. Numbers indicate time in minutes after the release. This experiment was repeated three times with similar results; one experiment is shown.

Source data are available online for this figure.

repressor Whi5, functional analog of pRB). In addition, deacetylation of the nuclear basket nucleoporin Nup60 has relatively minor effects on Whi5 nuclear accumulation but is associated with the perinuclear tethering of a key cell cycle control gene (encoding the G1/S cyclin Cln2, homologue of mammalian Cyclin E) (Kumar *et al*, 2018). Thus, acetylation of specific nucleoporins promotes different aspects of nuclear pore function necessary for S-phase entry, and their deacetylation in daughter cells reinforces cell size control mechanisms that prevent premature S phase in small daughters (Turner *et al*, 2012). However, the identity of the KAT(s) targeting the NPC for acetylation is unknown, and the molecular mechanism by which NPC acetylation status affects S-phase entry remains unclear.

Here, we show that the KAT Esa1 acetylates the nuclear basket component Nup60 to promote mRNA export and the G1/S transition. Furthermore, we demonstrate that Hos3-dependent deacetylation of Nup60 displaces mRNA export complexes from daughter cell NPCs to inhibit Start. We propose that, in addition to modulating cell cycle entry and preventing premature division of daughter cells, this pathway regulates general mRNA export. Thus, the evolutionarily conserved NuA4 complex drives gene expression and cell cycle progression not only by acetylating chromatin and promoting transcription but also by acetylating the nucleoplasmic entrance to NPCs to facilitate export of nuclear mRNA, thereby dually controlling the gene expression state of the cell.

Results

Esa1 is the main lysine acetyltransferase promoting cell cycle entry

To understand how NPC acetylation regulates the G1/S transition (Start), we sought to identify the lysine acetyltransferases (KATs) counteracting the activity of the Hos3 deacetylase. Hos3 displays asymmetric distribution between mother and daughter cells in wild-type *Saccharomyces cerevisiae*. Overexpression of a version of Hos3 fused to a nuclear localisation signal (*GAL1pr-HOS3-NLS*) leads to targeting of Hos3 to mother and daughter cell nuclei, deacetylation of nucleoporins and inhibition of cell proliferation (Kumar *et al*, 2018). We tested whether this inhibition could be relieved by overexpression of yeast KATs, including Eco1, Elp3, Esa1, Gcn5, Hat1, Hpa2, Hpa3, Rtt109, Sas2 and Spt10. Overexpression of Elp3, Gcn5 and Spt10 was toxic in wild-type cells, and therefore, their potential role in opposing Hos3 could not be established using this assay (Fig EV1). However, we found that of the remaining KATs, only Esa1 and Hat1 overexpression suppressed Hos3-NLS lethality (Figs 1B and EV1B).

Inactivation of Hos3 leads to premature onset of S phase in daughter cells (Kumar *et al*, 2018). We thus tested whether inactivation of Esa1 or Hat1 (alone or in combination) inhibits the G1/S transition, as would be expected of KATs counteracting the KDAC Hos3. We also tested the role of Gcn5, since its loss was previously reported to cause a mild delay in the G1/S transition (Kishkevich *et al*, 2019). The non-essential genes *HAT1* and *GCN5* were deleted, whereas Esa1 was inactivated using the well-characterised thermosensitive (ts) mutation *esa1-L254P* (hereafter called *esa1-ts*) (Clarke *et al*, 1999). Wild-type and mutant cells were arrested in G1 at 25°C by addition of alpha factor, shifted to the restrictive temperature for *esa1-ts* (37°C), and released from the cell cycle arrest by alpha-factor removal. The fraction of S-phase cells at different times after alpha-factor washout was determined by monitoring bud emergence. More than 95% of wild-type cells budded within 60 min of alpha-factor removal, and *gcn5*Δ cells exhibited a 15-min delay in budding as previously reported (Kishkevich *et al*, 2019). In contrast, budding was strongly delayed in *esa1-ts* cells: on average, only 10% of these cells had formed a bud after 60 min, and approximately 40% lacked a bud after 4 h. Moreover, cells lacking both Esa1 and Gcn5 had stronger defects in budding than either single mutant: *esa1-ts gcn5*Δ cells remained unbudded after 4 h of alpha-factor washout (Figs 1C and EV2A). Deletion of *HAT1* did not delay budding of either wild-type, *gcn5*Δ or *esa1-ts* cells (Fig EV2B). Thus, *HAT1* does not play a role in Start and was not characterised further. DNA replication, assayed by flow cytometry, was also delayed in Esa1-deficient cells. Whereas most wild-type cells replicated their DNA 40 min after alpha-factor removal, replication was still incomplete after 4 h in *esa1-ts* cells, and was undetectable in *esa1-ts gcn5*Δ (Fig 1D). In summary, Esa1 promotes budding and DNA replication, which are hallmarks of the G1/S transition. In the absence of Esa1, these functions can be partially compensated by Gcn5.

Esa1 acts through Nup60 acetylation to promote Start

These data raised the possibility that Esa1, Gcn5 and Hos3 regulate the G1/S transition, at least in part, by modulating the acetylation level of shared target proteins. Proteomic studies have indicated that budding yeast nucleoporins are targeted by multiple KATs, including Esa1 and Gcn5, although the role of these modifications remained unclear (Henriksen *et al*, 2012; Downey *et al*, 2015). Furthermore, Hos3-dependent deacetylation of the nuclear basket component Nup60 lysine 467 is important for inhibition of Start in daughter cells (Kumar *et al*, 2018). Therefore, we investigated whether Esa1 and Gcn5 promote Start through Nup60 acetylation. Nup60-GFP was immunoprecipitated from cells expressing Esa1 or Gcn5 under the control of the inducible *GAL1* promoter, and its acetylation state was assayed with an anti-acetyl-lysine (AcLys) antibody. This revealed increased Nup60 acetylation after addition of galactose in *GAL1pr-ESA1* and *GAL1pr-GCN5* cells (Fig 2A). Thus, Esa1 and Gcn5 can acetylate Nup60.

We next tested whether acetylation of Nup60 can mediate the G1/S function of Esa1 and Gcn5. Lysine (K) 467 of Nup60 was replaced with an asparagine (N) residue, whose biophysical properties resemble those of acetylated lysine, to generate the acetyl-mimic Nup60-KN. Cells were released from a G1 block, and their budding efficiency was determined as previously. Expression of Nup60-KN partially rescued the budding efficiency of the single mutant *esa1-ts* (Fig 2B), although it was not sufficient to restore budding in cells lacking both Esa1 and Gcn5 (Fig EV3A). Furthermore, the replacement of Nup60 K467 with arginine (R) to mimic the lack of acetylation (Nup60-KR) led to the opposite phenotype of Nup60-KN, further delaying the budding of *esa1-ts* (Fig EV3B). These results suggest that Esa1 promotes the G1/S transition in part by acetylation of Nup60.

Start is marked by the transcription of hundreds of genes of the G1/S regulon, which are required for budding and DNA replication.

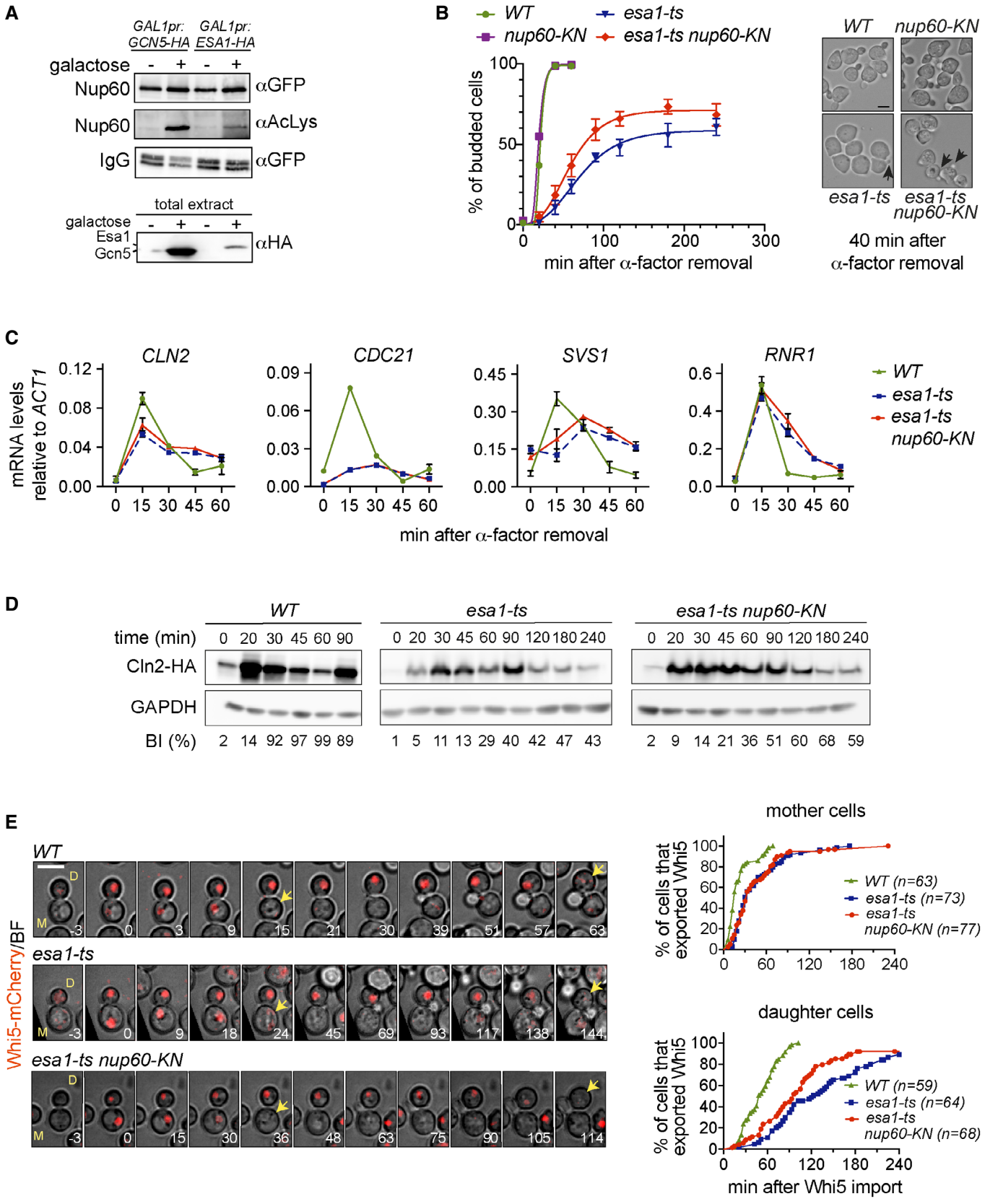

Figure 2.

Figure 2. Acetyl-mimic Nup60 partially rescues the Start defects of *esa1-ts* cells.

A Overexpression of Esa1 and Gcn5 KATs leads to increased acetylation levels of the nuclear basket nucleoporin Nup60. *(Top)* Nup60-GFP was immunoprecipitated from extracts of the indicated strains, and its acetylation state probed with anti-AcLys antibodies. *(Bottom)* Total extracts probed with anti-HA antibodies to verify KAT overexpression.

B *nup60-KN* partially rescues the budding defect of *esa1-ts* cells. *(Left)* Budding of cells of the indicated strains was determined as in Fig 1C. At least 200 cells were scored for each strain and time point. Data from three independent experiments are represented as mean and SEM (*esa1-ts*, *esa1-ts nup60-KN*). *(Right)* Bright-field images of the indicated strains 40 min after the α-factor washout. Arrowheads point to cell buds. Scale bar, 4 μm.

C mRNA levels of *CLN2*, *CDC21*, *SVS1* and *RNR1* were determined for cells of the indicated strains after G1 arrest and release at restrictive temperature, with samples collected at indicated times. Data from three independent experiments are represented as mean and SEM.

D *nup60-KN* mutation partially rescues the delay in synthesis of the G1/S cyclin Cln2 in *esa1-ts* cells. Cells of the indicated strains were processed as in (B), and the amount of Cln2-HA protein at the indicated times was assessed by Western blot. % of budded cells (budding index, BI) is indicated below for each corresponding strain and time point. Note the slow, inefficient budding in *esa1-ts* mutants. In *WT*, the reduction in Cln2 at 60 min and its increase at 90 min reflect the start of a second cycle, which is absent in *esa1-ts* cells.

E *nup60-KN* partially rescues the Whi5 export defect of *esa1-ts* daughter cells. Composite of bright field and Whi5-mCherry (*left*) and quantification of Whi5 nuclear export (*right*) in mother (M) and daughter (D) cells of the indicated strains. Whi5 export (arrows) is delayed in *esa1-ts* mothers and daughters compared to *WT* ($P < 0.001$, log-rank Mantel–Cox test); *esa1-ts nup60-KN* advances Whi5 export relative to *esa1-ts* in daughters ($P = 0.0105$), but not in mothers ($P > 0.05$). 3 z-confocal slices spaced 0.5 μm were acquired every 3 min; maximum projections of selected timepoints are shown. Time is indicated in minutes; $t = 0$ marks Whi5 nuclear import. Scale bar, 5 μm. n = number of cells, pooled from two independent experiments with similar results.

Source data are available online for this figure.

To gain insight into how Nup60 acetylation promotes the G1/S transition, we first determined the mRNA levels of four representative regulon genes (*CLN2*, *CDC21*, *SVS1* and *RNR1*) during the G1/S transition using quantitative reverse transcription PCR (RT–qPCR) in KAT-deficient cells. In wild-type synchronous cultures, *CLN2*, *CDC21*, *SVS1* and *RNR1* are induced 15 min after alpha-factor removal, and their mRNA levels decrease as cells enter S phase (Fig 2C, *WT*). In agreement with the observed budding and DNA replication defects, transcription of G1/S genes was impaired in *esa1-ts* cells. *CLN2* was induced at lower levels and with slower kinetics than in wild type, whereas *CDC21* and *SVS1* mRNA levels did not oscillate during the experiment, and *RNR1* was induced at normal levels but its mRNA remained unusually stable (Fig 2C, *esa1-ts*). As previously reported (Kishkevich *et al*, 2019), deletion of *GCN5* did not affect the mRNA levels of any of the tested genes. However, the double mutant *gcn5*Δ *esa1-ts* showed stronger transcriptional defects than the *esa1-ts* single mutant (Fig EV3C). Together, these results indicate that Esa1 drives the coordinated induction of G1/S genes and that Gcn5 can partially compensate for the absence of Esa1. Notably, the acetyl-mimic version of Nup60, which partially rescued budding efficiency of the *esa1-ts* mutant (Fig 2B), did not improve its transcriptional defects (Fig 2C, *esa1-ts nup60-KN*). To understand how Nup60-KN promotes budding of Esa1-deficient cells, western blotting was used to determine the protein levels of the G1/S cyclin Cln2 in *esa1-ts* and *esa1-ts nup60-KN*. Cln2 plays a critical role in driving activation of CDK in late G1 and robust, irreversible G1/S transition *via* positive feedback (Skotheim *et al*, 2008; Charvin *et al*, 2010). As expected, Cln2 protein synthesis occurred later and at lower levels in *esa1-ts* than in wild-type cells released from a G1 block. Importantly, the delay in Cln2 protein synthesis was alleviated in *esa1-ts nup60-KN* (Fig 2D and Appendix Fig S1). This suggests that Nup60 acetylation promotes Cln2 expression at the post-transcriptional level.

Finally, we examined the requirement for Esa1 and Nup60 acetylation in the G1/S transition of mother (M) and daughter (D) cells, using time-lapse microscopy of freely cycling cells. To determine the time of the G1/S transition in single cells, we monitored the nuclear localisation changes of the Whi5 transcriptional repressor, a G1 marker. Whi5 is imported into the nucleus of M and D cells in late anaphase, and its export in G1, driven by CDK phosphorylation, marks the irreversible commitment to S phase (Costanzo *et al*, 2004; de Bruin *et al*, 2004; Charvin *et al*, 2010). Cells were incubated at 37°C and imaged at 3-min intervals. In wild-type cells, nuclear export of Whi5-mCherry occurred first in mothers and later in daughters relative to Whi5 import (median times, 15 min [M cells] and 59 min [D cells]; note that the duration of G1 phase in cells synchronised with alpha factor is not directly comparable with that of freely cycling cells) (Fig 2E, *WT* and Appendix Fig S2). This dichotomy is due to both cell size control in small daughters and size-independent mechanisms that delay Start specifically in daughters, including NPC deacetylation (Di Talia *et al*, 2007; Kumar *et al*, 2018). In *esa1-ts* cells, Whi5 export was markedly delayed in both M and D cells (median times: 30 min [M] and 123 min [D]; Fig 2E, *esa1-ts*). Furthermore, the presence of Nup60-KN partially restored the delay in Whi5 export caused by Esa1 inactivation, specifically in daughter cells (median times: 33 min [M] and 96 min [D]; Fig 2E, *esa1-ts nup60-KN*). Thus, Esa1 promotes Start in both mother and daughter cells, but constitutive Nup60 acetylation advances Start specifically in Esa1-deficient daughters. This is consistent with daughter-specific Nup60 deacetylation caused by asymmetric inheritance of the Hos3 KDAC (Kumar *et al*, 2018), and further supports the hypothesis that acetylation of Nup60 in mothers is reversed by Hos3 in daughter cells.

Esa1 and Nup60-KN promote the export of *CLN2* mRNA

Next, we used time-lapse microscopy to determine *CLN2* mRNA localisation, by inserting PP7 stem loops in its 3' UTR. PP7 stem loops bind to the bacteriophage coat protein fused to a nuclear localisation signal and GFP (PCP-GFP-NLS), allowing visualisation of *CLN2* mRNA foci (Neurohr *et al*, 2018). We used Whi5-tdTomato to monitor the G1/S transition in the same cells. Freely cycling cells (wild type, *esa1-ts* and *esa1-ts nup60-KN*) were incubated at 37°C and imaged at 5-min intervals for up to 6 h. We restricted our analysis to daughter cells, which are most affected by inactivation of Esa1. In wild type, a single bright perinuclear focus indicative of *CLN2* transcription was detected for 1–2 consecutive frames at the time of Whi5 nuclear export. This occurred approximately 30 to

50 min after Whi5 was imported into the nucleus (Fig 3A–C). *CLN2* transcription was followed by the appearance of 5–20 mRNA foci in the cytoplasm (Fig 3A and D). In *esa1-ts*, nuclear mRNA foci appeared later (relative to Whi5 import) than in wild-type cells (Fig 3B); short-lived nuclear foci could be detected during the extended G1 phase in these cells (see example in Fig 3A). Importantly, the fraction of cells with nuclear *CLN2* mRNA foci peaked in both wild-type and *esa1-ts* at the time of Whi5 export, indicating that Whi5 export is associated with *CLN2* transcription even in the absence of Esa1 (Fig 3C). However, the fluorescence intensity of nuclear foci was lower in *esa1-ts* than in wild type (Fig 3E). Thus, Esa1 promotes the synthesis of *CLN2* mRNA. Inactivation of Esa1 was also associated with changes in the localisation of *CLN2* transcripts; nuclear mRNA foci were associated with the nuclear periphery in 95% of wild-type cells, compared to 80% in *esa1-ts* (Fig 3F). In addition, the number of cytoplasmic foci at the time of Whi5 export was lower in *esa1-ts* than in wild-type cells (Fig 3A and E). Strikingly, Nup60-KN did not alter the intensity of *CLN2* nuclear foci in *esa1-ts* cells, but rescued the fraction of cells with perinuclear mRNA, and increased the number of *CLN2* cytoplasmic foci (Fig 3D and E). These results raised the possibility that Nup60 acetylation is specifically required for the nuclear export of *CLN2* mRNA.

Together, these findings suggest two distinct roles for Esa1 in driving cell cycle commitment. First, a major function of Esa1 in promoting the G1/S transition is to drive the timely transcription of genes required for cell cycle entry. This is in keeping with an established role of Esa1 in promoting transcription of most yeast genes (Bruzzone *et al*, 2018). Second, Esa1 may play additional positive roles in Start, independently of transcription, that are mediated by Nup60 acetylation and may include mRNA export. To further test the hypothesis that Nup60 acetylation plays mostly a post-transcriptional role in gene regulation, we determined genome-wide mRNA levels in wild-type, *nup60-KN* and *nup60-KR* cells by RNA sequencing. With the exception of minor changes in a handful of subtelomeric genes, this analysis found no significant changes in transcription among these strains (Fig EV4). A non-transcriptional role of Nup60 acetylation in gene expression could also explain why Nup60-KN rescues the Start defect of *esa1-ts* but not those of the double mutant *esa1-ts gcn5*Δ. Indeed, levels of G1/S mRNAs in this mutant may be too low to promote S phase, even in the presence of increased mRNA export efficiency promoted by Nup60-KN.

Esa1 and Nup60 acetylation promote bulk mRNA export

Nuclear basket components are required for the efficient export of nuclear mRNA through their association with the Transcription and Export 2 (TREX-2) complex (Fischer *et al*, 2002). Our previous findings raised the possibility that Nup60 acetylation promotes mRNA export. We therefore tested whether the cell proliferation defect of *GAL1pr-HOS3-NLS* cells, in which Nup60 and other nucleoporins are deacetylated, can be alleviated by increased levels of mRNA export factors (Fig 4A). Indeed, we found that the growth of *GAL1pr-HOS3-NLS* cells was restored by overexpression of the mRNA export receptors Mtr2 and Mex67, which escort mRNA molecules through the NPC (Strässer *et al*, 2000; Strawn *et al*, 2001) (Fig 4B). Likewise, overexpression of the scaffolding subunit of the TREX-2 complex, Sac3 (Fischer *et al*, 2002; Jani *et al*, 2014), also restored growth of *GAL1pr-HOS3-NLS* cells (Fig 4C). Note that a truncated Sac3 version was used, since overexpression of full-length Sac3 is toxic (Appendix Fig S3A–C). This further suggests that Hos3, possibly *via* Nup60 deacetylation, prevents cell proliferation by inhibiting export of nuclear mRNA. Overexpression of Mtr2 and Mex67 did not rescue the growth of Esa1-deficient cells, confirming that mRNA export is not the only essential function of this KAT (Appendix Fig S3D).

To directly test whether Nup60 deacetylation inhibits bulk mRNA export, we imaged polyadenylated mRNA by fluorescence *in situ* hybridisation (FISH) using a poly-dT probe. This was done in wild type and in cells in which Nup60 acetylation was reduced by overexpression of nuclear Hos3 (*GAL1pr:HOS3-NLS*) or by inactivation of Esa1 and Gcn5 (*esa1-ts*, *gcn5*Δ). As expected, all wild-type cells showed mRNA localisation diffusely in both nucleus and cytoplasm. In contrast, approximately 15% of cells exhibited nuclear mRNA accumulation upon induction of *GAL1pr:HOS3-NLS* (Fig 4D and Appendix Fig S4A). Nuclear accumulation of mRNA was dependent on Hos3 KDAC activity, as it was not observed upon overexpression of a catalytically inactive mutant ($Hos3^{EN}$-NLS) (Fig 4D). Furthermore, inactivation of Esa1 (*esa1-ts*) led to accumulation of nuclear mRNA in up to 20% of cells, and this fraction rose to 30% in the double mutant *esa1-ts gcn5*Δ (Fig 4E and Appendix Fig S4B).

Figure 3. Esa1 and Nup60-KN promote the nuclear export of *CLN2* mRNA.

A Composite of bright field and Whi5-tdTomato (BF/Whi5) and *CLN2-PP7* mRNA labelled with PCP-NLS-GFP (*CLN2* mRNA) in mother (M) and daughter (D) cells of the indicated strains. Arrows indicate nuclear foci. Brighter GFP nucleoplasmic areas may correspond to the nucleolus. Insets show enhanced-contrast images to visualise cytoplasmic mRNA particles (arrowheads). Numbers indicate minutes relative to Whi5 nuclear import. Maximum projections of whole-cell Z-stacks are shown for Whi5 and *CLN2* mRNA except in the inset and in selected *esa1-ts* images, where single Z-slices are shown for clarity. Scale bar, 4 μm (inset: 1 μm).

B Fraction of cells of the indicated strains with nuclear *CLN2-PP7* mRNA foci, aligned relative to Whi5 import. Symbols represent individual values; lines were generated by smoothing of the nearest three neighbouring values (0^{th} order polynomial).

C Fraction of cells of the indicated strains with nuclear *CLN2-PP7* mRNA foci, aligned relative to Whi5 export.

D Mean fluorescence intensity of nuclear *CLN2* mRNA foci at the time of Whi5 export, normalised relative to the nuclear background.

E Number of cytoplasmic *CLN2-PP7* mRNA foci in early G1 (5 min after Whi5 import) and at the G1/S transition (5 min after Whi5 export).

F The position of nuclear *CLN2-PP7* foci (marked with arrowheads in the examples) was scored relatively to the nuclear periphery (visualised with PCP-NLS-GFP) in the indicated strains. The fraction of non-perinuclear *CLN2*-PP7 foci is significantly increased in *esa1-ts* cells compared to the *WT* and rescued by *nup60-KN* mutation (two-sided Fisher's exact test, $P = 0.0209$ and $P = 0.0227$). Scale bar, 1 μm.

Data information: In (D and E), boxes include 50% of data points, lines represent the median, and whiskers extend to maximum and minimum values. ****, $P \leq 0.0001$; **, $P \leq 0.01$; and n.s., $P > 0.05$, ordinary one-way ANOVA with Tukey's multiple comparisons test. Adjusted *P*-values in (D): *WT* vs. *esa1-ts*, $P < 0.0001$; *WT* vs. *esa1-ts nup60-KN*, $P < 0.0001$; and *esa1-ts* vs. *esa1-ts nup60-KN*, $P = 0.9845$; and in (E): *WT* vs. *esa1-ts*, $P < 0.0001$; and *esa1-ts* vs. *esa1-ts nup60-KN*, $P = 0.002$. Foci were scored in individual Z-slices spanning the entire cell volume. *n* = number of cells, pooled from two independent experiments with similar results.
Source data are available online for this figure.

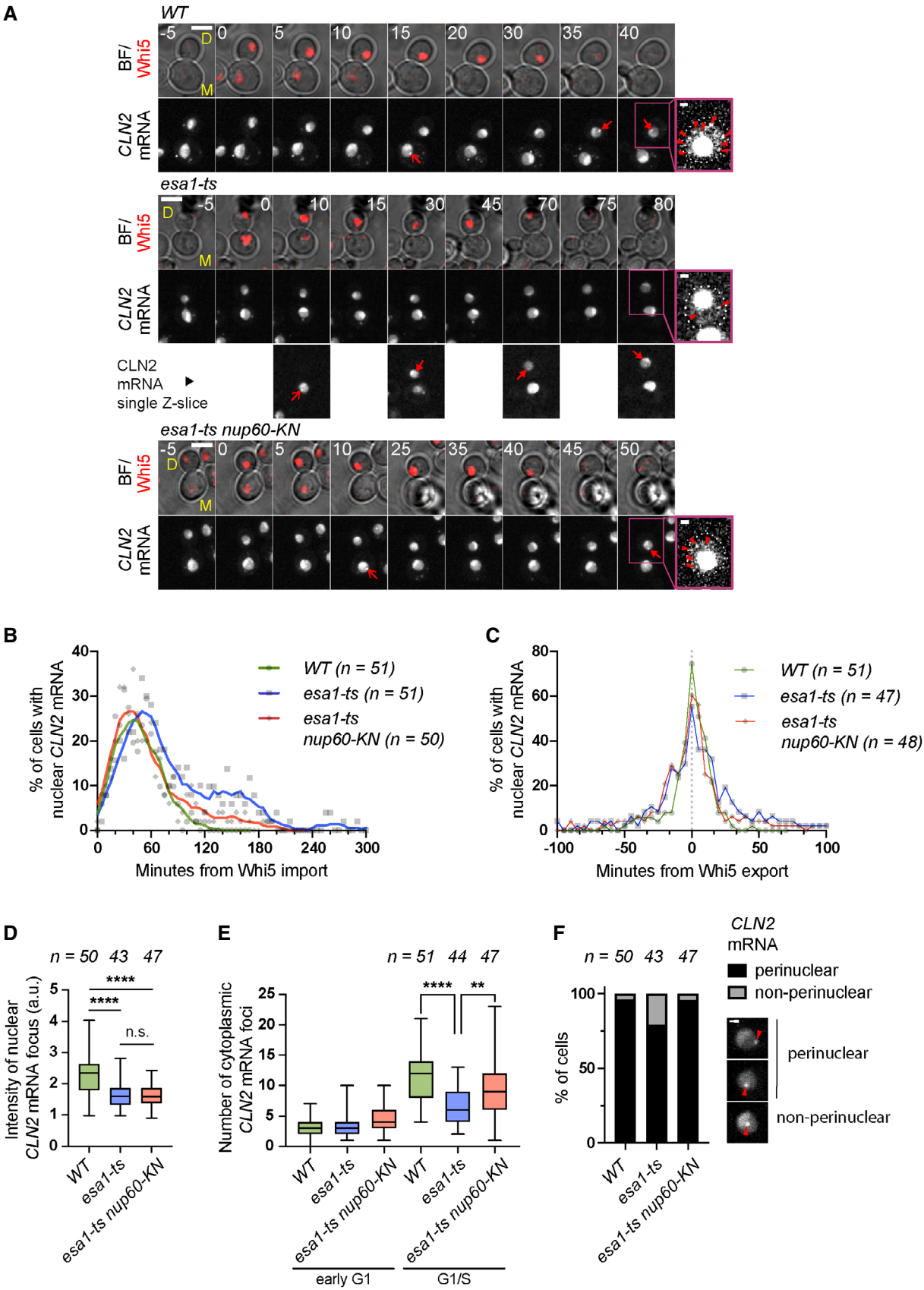

Figure 3.

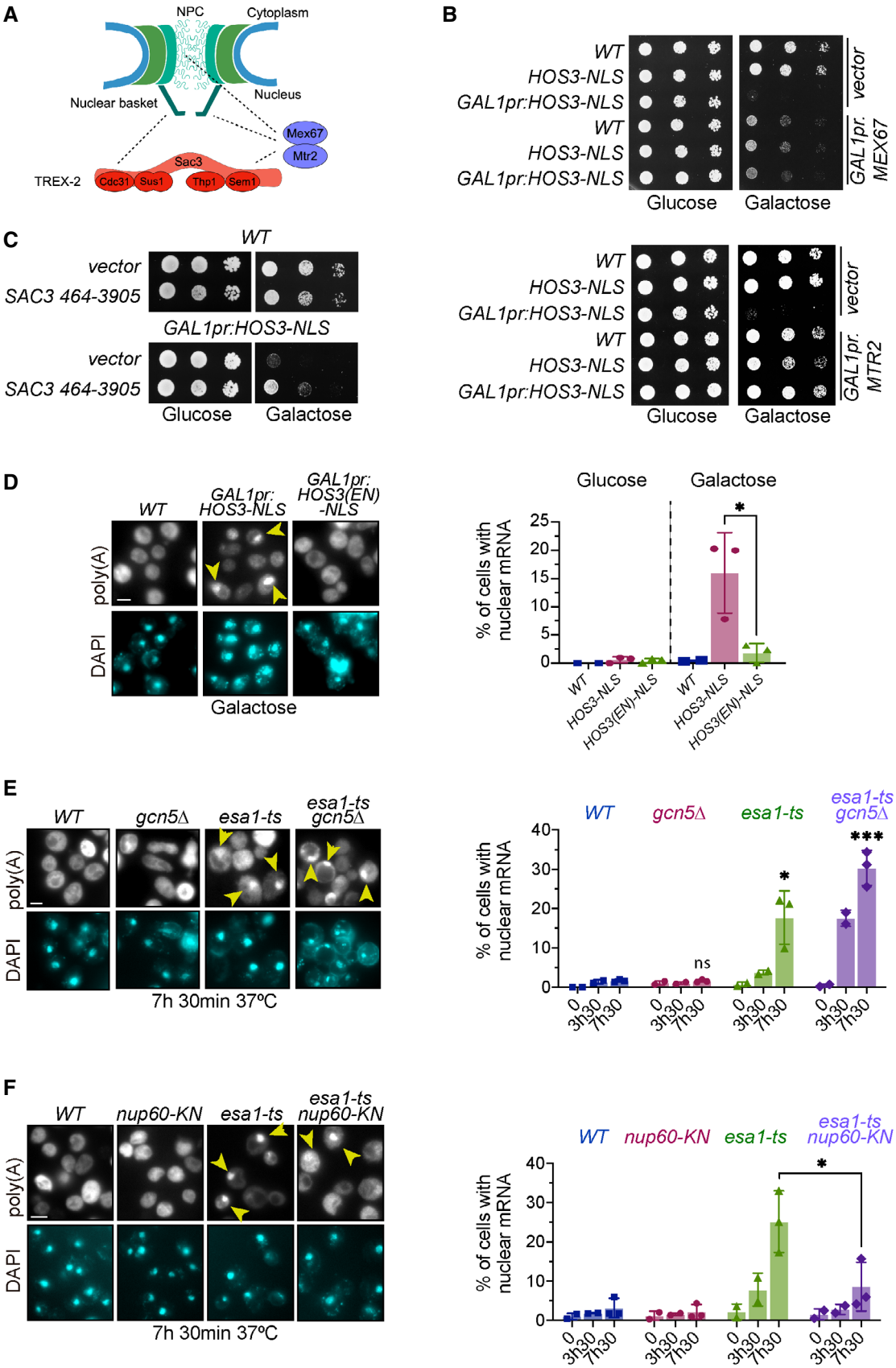

Figure 4.

Figure 4. Nuclear export of mRNA is inhibited by the KDAC Hos3 and promoted by the KAT Esa1 and Nup60 acetylation.

A Illustration of the physical interactions (dashed lines) of the NPC with mRNA export factors.

B Overexpression of *MEX67* and *MTR2* rescues the lethality of Hos3-NLS overexpression. 10-fold serial dilutions of the indicated strains transformed with the indicated plasmids spotted onto SC-Glu and SC-Gal medium and incubated at 25°C for 3 days.

C A high-copy plasmid containing *SAC3* rescues the lethality of Hos3-NLS overexpression. Strains carrying a high-copy plasmid containing the *SAC3* ORF (nucleotides 467–3,905), or the empty vector, were grown as in (B).

D Overexpression of Hos3-NLS promotes nuclear accumulation of mRNA. (*Left*) Cultures of the indicated strains were treated with galactose overnight to induce *HOS3-NLS* expression, cells were fixed, and FISH was performed using Cy3-Oligo(dT). (*Right*) The fraction of cells with nuclear mRNA accumulation was determined for the indicated strains and conditions.

E Inactivation of Esa1 impairs export of poly(A) RNA. (*Left*) Cultures of the indicated strains were incubated at 37°C. (*Right*) The fraction of cells with nuclear mRNA accumulation was determined for the indicated strains and conditions as in (D).

F *nup60-KN* mutation partially rescues the mRNA export defects of *esa1-ts*. Cells of the indicated strains were processed as in (E).

Data information: In (D–F), arrows point to polyadenylated RNA in the nucleus, which was visualised by DAPI staining. Data from three independent biological replicates (7h30) are represented as mean and s.d., and data from two independent biological replicates (0 and 3h30) as mean and range. *, $P \leq 0.05$; ***, $P \leq 0.001$; and ns, $P > 0.05$, two-tailed unpaired *t*-test. At least 200 cells were scored for each time point and condition. Scale bar, 4 μm.
Source data are available online for this figure.

Notably, deletion of *GCN5* alone did not cause nuclear mRNA accumulation, suggesting that this KAT does not play an important role in promoting mRNA export. The Esa1 function in RNA export appeared to be specific for mRNA, since depletion of Esa1 (alone or in combination with Gcn5) did not affect export of ribosomal RNA (Appendix Fig S5A and B). Importantly, the fraction of Esa1-deficient cells with nuclear mRNA accumulation was significantly reduced in *esa1-ts* cells carrying the acetyl-mimic Nup60 mutation (Fig 4F). These results suggest that acetylation and deacetylation of Nup60, mediated by Esa1 and Hos3, respectively, regulate mRNA export.

Nup60 acetylation recruits the TREX-2 complex to the nuclear basket to promote Start

We previously found that constitutive nuclear localisation of Hos3 (Hos3-NLS) reduces the amount of NPC-associated mRNA export factors, such as Sac3, that localise to the nuclear periphery (Kumar *et al*, 2018). This suggests that in wild-type cells, Nup60 acetylation facilitates the recruitment of Sac3 to NPCs and this is inhibited in G1 daughter cells *via* Hos3-dependent Nup60 deacetylation. To test this prediction, we measured the nuclear intensity of GFP-tagged Sac3 relative to that of the structural NPC component Nup49-mCherry in mother (M) and daughter (D) nuclei immediately after cytokinesis. Interestingly, loss of Hos3 (*hos3*Δ) lead to an increase in Sac3 nuclear localisation in D cells, and expression of acetyl-mimic Nup60 (*nup60-KN*) caused an increase in nuclear Sac3 in both M and D cells (Fig 5A, nucleus). Importantly, cellular Sac3 levels were not affected by mutations in *HOS3* or *NUP60* (Fig 5A, whole cell; see also Appendix Fig S6 for analysis of Sac3 levels by Western blotting). As wild-type D cells entered S phase (and Nup60 was acetylated), their nuclear Sac3 levels increased; in contrast, Sac3 levels remained constant from G1 to S phase in *hos3* and *nup60-KN* daughter cells (Fig EV5). We conclude that Hos3 and deacetylation of Nup60 reduce the enrichment of Sac3 in G1 daughter cell nuclei. We then tested whether Esa1 promotes the localisation of Sac3 to the nuclear basket. To avoid potential confounding effects due to Esa1 inactivation during S phase, cells were treated with the microtubule polymerisation inhibitor nocodazole at 25°C, to arrest *esa1-ts* cells in mitosis in the presence of Esa1 function. Nocodazole was then removed, cells were shifted to 37°C to inactivate Esa1, and the nuclear intensity of Sac3-GFP, normalised to that of Nup49-mCherry, was determined in the following G1. This revealed that nuclear enrichment of Sac3 is significantly reduced in

Figure 5. Nup60 deacetylation in daughter cells displaces Sac3 from NPCs and delays Start.

A Depletion of Hos3 or expression of acetyl-mimic Nup60 (*nup60-KN*) increases the nuclear localisation of Sac3 in G1. Cells of the indicated strains were imaged by time-lapse microscopy, and the fluorescence levels of the indicated proteins were determined in G1 (after cytokinesis). The NPC component Nup49 was used as a control for nuclear pore complex protein levels. Fluorescence intensity was measured in sum projections of whole-cell Z-stacks, by segmentation of either the nuclear area in the mCherry channel or the whole cell in the bright-field channel. The ratio of Sac3 to Nup49 intensities was then normalised relative to the mean intensity of wild-type mothers.

B Inactivation of Esa1 decreases Sac3 nuclear levels. Wild-type (*WT*) and *esa1-ts* cells were arrested in mitosis by treatment with nocodazole at 25°C, shifted to 37°C, released from the mitosis block in fresh medium at 37°C and imaged by time-lapse microscopy. Fluorescence levels were quantified in G1 as in (A).

C Rapamycin-dependent dimerisation abolishes Sac3 mother/daughter asymmetries. *NUP60-mCherry-FKBP SAC3-GFP-FRB* cells were incubated with rapamycin (RAPA) to trigger FRB-FKBP heterodimerisation, or with DMSO as control. Fluorescence levels were quantified in G1 cells as in (A), 15 to 30 min after addition of the drug.

D Sac3 anchoring to the nuclear basket advances Start in *esa1-ts* daughter cells. Composite of bright field and Whi5-mGFP (*top*) and quantification of Whi5 nuclear export timing (*bottom*) in wild-type (*WT*) and *esa1-ts* mother (M) and daughter (D) cells treated with either rapamycin (RAPA) or DMSO and expressing Nup60-FRB and Sac3-mCherry-FKBP. Sac3 anchoring to Nup60 does not alter Whi5 export timing in *WT* mother or daughter cells (DMSO vs. RAPA, $P > 0.05$, log-rank Mantel–Cox test), but it advances Whi5 export in *esa1-ts* daughters ($P = 0.0001$). Whi5 export efficiency was slightly improved also in mother cells ($P = 0.0374$). 8 z-confocal slices spaced 0.4 μm were acquired every 3 min; maximum projections are shown. Time is indicated in minutes; $t = 0$ marks Whi5 nuclear import. Scale bar, 5 μm.

Data information: In (A–C), arrowheads point to daughter cells, and in (D), to Whi5 export. In (A–C), boxes include 50% of data points, the line represents the median, and whiskers extend to maximum and minimum values. ****, $P \leq 0.0001$; **, $P \leq 0.01$; and ns, $P > 0.05$, two-tailed unpaired *t*-test. Scale bar, 2 μm. *n* = number of cells, pooled from three independent experiments with similar results.
Source data are available online for this figure.

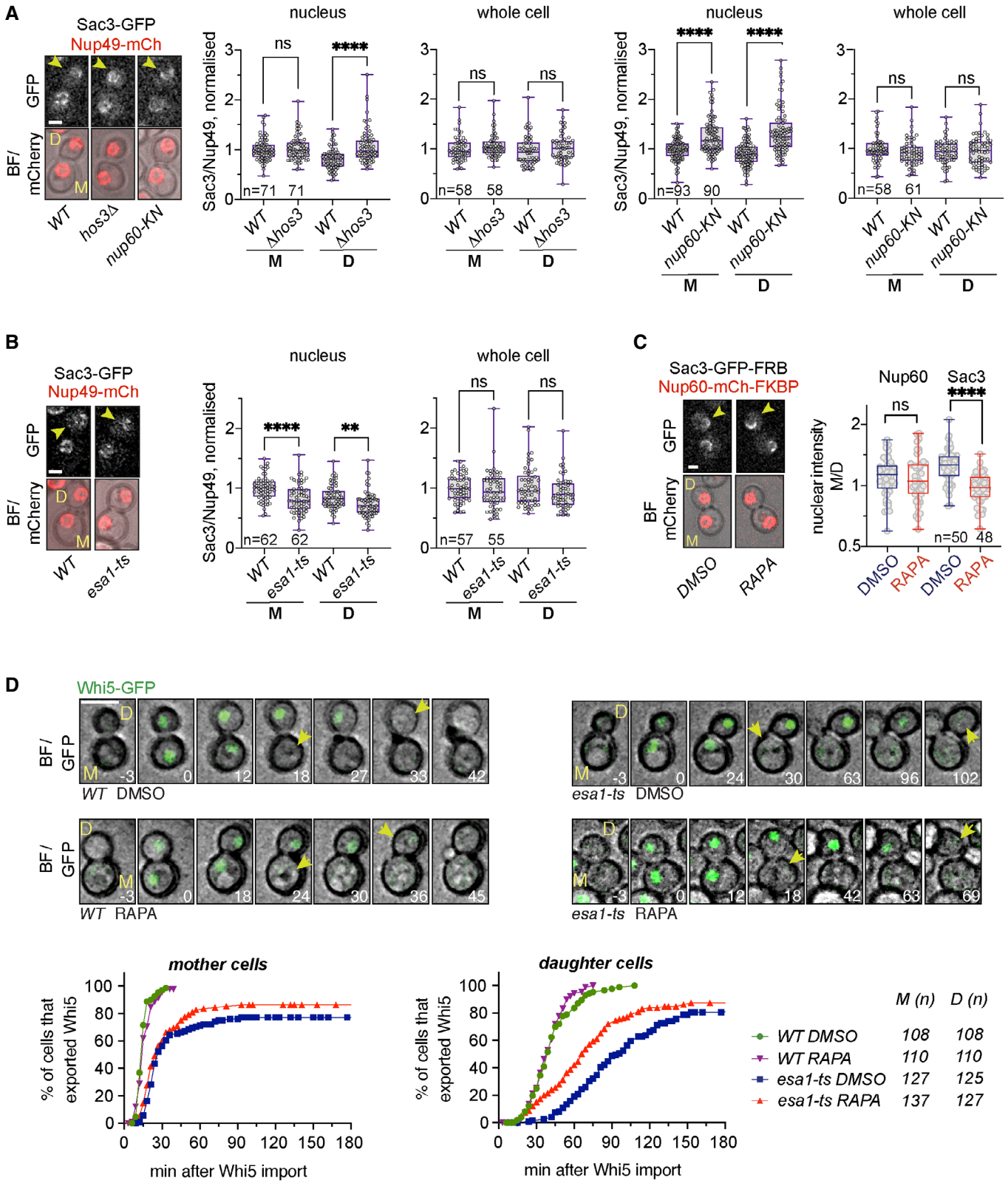

Figure 5.

both M and D *esa1-ts* cells, while total cellular levels of Sac3 were not affected (Fig 5B and Appendix Fig S6). Together, these data indicate that Nup60 acetylation, driven by Esa1 and inhibited by Hos3 in G1 daughter cells, is important for perinuclear recruitment of the mRNA export factor Sac3.

Sac3 is tethered to the nuclear pore basket, and this localisation is required for its mRNA export function (Fischer *et al*, 2002). To test whether Esa1 promotes Start by targeting Sac3 to NPCs, we asked whether artificially anchoring Sac3 to the nuclear basket is sufficient to rescue their Start delay in Esa1-deficient cells. We used the anchor-away system, which triggers dimerisation of FK506-binding protein (FKBP) and FKBP–rapamycin binding (FRB) in the presence of rapamycin (Gallego *et al*, 2013) to anchor Sac3-FKBP and Nup60-FRB protein fusions. Consistent with results in Fig 5A, the distribution of fluorescently labelled Sac3-FRB and Nup60-FKBP was biased towards mother cells, with a higher bias for Sac3 than for Nup60 ($P < 0.005$, unpaired *t*-test) (Fig 5C). The addition of rapamycin did not alter the accumulation of Nup60-FKBP in mother cells. In contrast, rapamycin altered the asymmetric localisation of Sac3-FRB: whereas Sac3 accumulated preferentially in mother cell nuclei in DMSO-treated cells, it was partitioned equally to M and D nuclei in the presence of rapamycin (Fig 5C). Thus, rapamycin increases the localisation of Sac3-FRB in daughter cells. G1 duration was then determined by time-lapse microscopy of *esa1-ts* cells expressing Whi5-GFP, as in Fig 2E, in the presence of either rapamycin or DMSO. Rapamycin slightly increased Whi5 export efficiency in *esa1-ts NUP60-FRB SAC3-FKBP* mother cells, and specifically advanced Whi5 export in daughter cells (Fig 5D). This is consistent with Hos3-dependent Nup60 deacetylation in daughter cells (Kumar *et al*, 2018). We conclude that acetylation of Esa1 and Nup60 promotes Start, at least in part, by targeting Sac3 to the nuclear basket, where it mediates mRNA export. Consistent with the requirement of mRNA export to trigger Start, we find that inactivation of the essential mRNA export factor Mex67 is sufficient to prevent entry into S phase (Appendix Fig S7).

Nup60 acetylation regulates expression of the inducible *GAL1* gene

Our results indicate that Nup60 deacetylation inhibits mRNA export and reduces the NPC recruitment of Sac3 to delay Start in daughter cells, presumably by inhibiting the export of mRNAs required for S phase. Next, we asked whether Nup60 acetylation can also affect the expression of genes that are not required for the G1/S transition, such as the inducible galactokinase (*GAL1*) gene. To measure *GAL1* expression, fast-folding, destabilised GFP (*sfGFP*) was placed under the control of the *GAL1-10* promoter (*GAL1pr*) and inserted next to the endogenous *GAL1* locus. Thus, measuring GFP fluorescence with time-lapse microscopy allows tracking of *GAL1* expression in single cells. Wild-type and Nup60 acetyl-mimic (*nup60-KN*) were placed in a microscope chamber, and *GAL1* expression was induced with galactose (Fig 6A). GFP fluorescence appeared earlier and increased to higher levels in *nup60-KN* than in wild-type cells, indicating that Nup60 acetylation promotes *GAL1* expression (Fig 6B and Appendix Fig S8). Notably, mRNA levels of *GAL1* (measured by RT–qPCR) were comparable in wild type and *nup60-KN*. This indicates that Nup60 acetylation promotes *GAL1* expression at the post-transcriptional level (Fig 6C). Nup60 levels were equivalent throughout all experiments, suggesting that Nup60 acetylation is unlikely to affect gene expression through changes in Nup60 stability (Appendix Fig S9A and B).

Because Nup60 acetylation is inhibited in daughter cells, we tested whether *GAL1* expression occurs with different strengths in mothers and daughters. Indeed, *GAL1* expression levels were higher in wild-type mother cells than in their daughters, and these differences were absent in cells lacking Hos3 or expressing Nup60-KN (Fig 6D). We conclude that acetylation of Nup60 in mother cells promotes *GAL1* expression, whereas its deacetylation in daughter cells inhibits expression. Expression of *GAL1* was slightly increased in the double mutant *hos3*Δ *nup60-KN* relative to either *hos3*Δ and *nup60-KN* single mutants (Fig 6D). This suggests that Hos3 inhibits *GAL1* expression in daughters largely, but not entirely through deacetylation of Nup60 at Lys 467.

Induction of *GAL1* by galactose is associated with tethering of its gene locus to the NPC (Cabal *et al*, 2006). To test whether NPC association is required for *GAL1* regulation by acetylated Nup60, we induced the *GAL1* gene in wild-type and *nup60-KN* cells with an oestradiol-dependent hybrid transactivator (the DNA binding domain of Gal4 fused to the hormone-binding domain of the human oestrogen receptor and the activation domain of the viral transcriptional activator VP16; GEV) that does not induce gene tethering (Appendix Fig S10). In cells expressing the GEV hybrid protein, addition of oestradiol led to similar *GAL1* induction profiles in wild-type, *hos3*Δ and *nup60-KN* cells. This was in contrast to *GAL1*

Figure 6. Daughter cell-specific Nup60 deacetylation inhibits *GAL1* expression.

A Time-lapse microscopy of *WT* and *nup60-KN* cells expressing *GAL1pr:sfGFP* and Nup60-mCherry at the indicated times of galactose induction. Scale bar, 4 μm.

B Depletion of Hos3, and expression of acetyl-mimic Nup60 (*nup60-KN*) enhance *GAL1* expression. WT, *hos3Δ*, *nup60-KN* and *nup60-KN hos3Δ* cells were shifted to galactose and imaged by time-lapse microscopy to monitor *GAL1pr:sfGFP* expression during 7 h. Nuclear fluorescence was scored by segmentation of the nuclear area in the mCherry channel, and mean fluorescence of nuclear GFP and Nup60-mCherry was quantified from sum projections of whole-cell Z-stacks at the indicated times. At least 200 cells were scored for each strain and time point. Shaded areas indicate the SEM.

C mRNA levels of *GAL1* were determined for wild-type (*WT*) and *nup60-KN* cells at the indicated times after galactose addition. One of two independent experiments with similar results is shown (mean and SEM from three technical replicates).

D The GFP intensity of mother/daughter pairs for cells in (B), at 5-min intervals after galactose addition (*left*) and 425 min after galactose addition (*right*). Boxes include 50% of data points, the line represents the median, and whiskers extend to maximum and minimum values. ****, $P \leq 0.001$; and ns, $P > 0.05$, two-tailed paired *t*-test. *N* = number of cells. One of two independent experiments with similar results is shown.

E Expression of *GAL1pr:sfGFP* induced with galactose (*left*) or ß-oestradiol (*right*), in the presence of the ß-oestradiol-dependent transactivator Gal4-ER-VP16. Smooth lines show GFP fluorescence intensity (left *x* axis); lines with circles show the difference in GFP intensity between the indicated strains (right *x* axis). The difference between wild type and *hos3*Δ, and between wild type and *nup60-KN*, increases continuously over time in response to galactose, but not to ß-oestradiol.

Source data are available online for this figure.

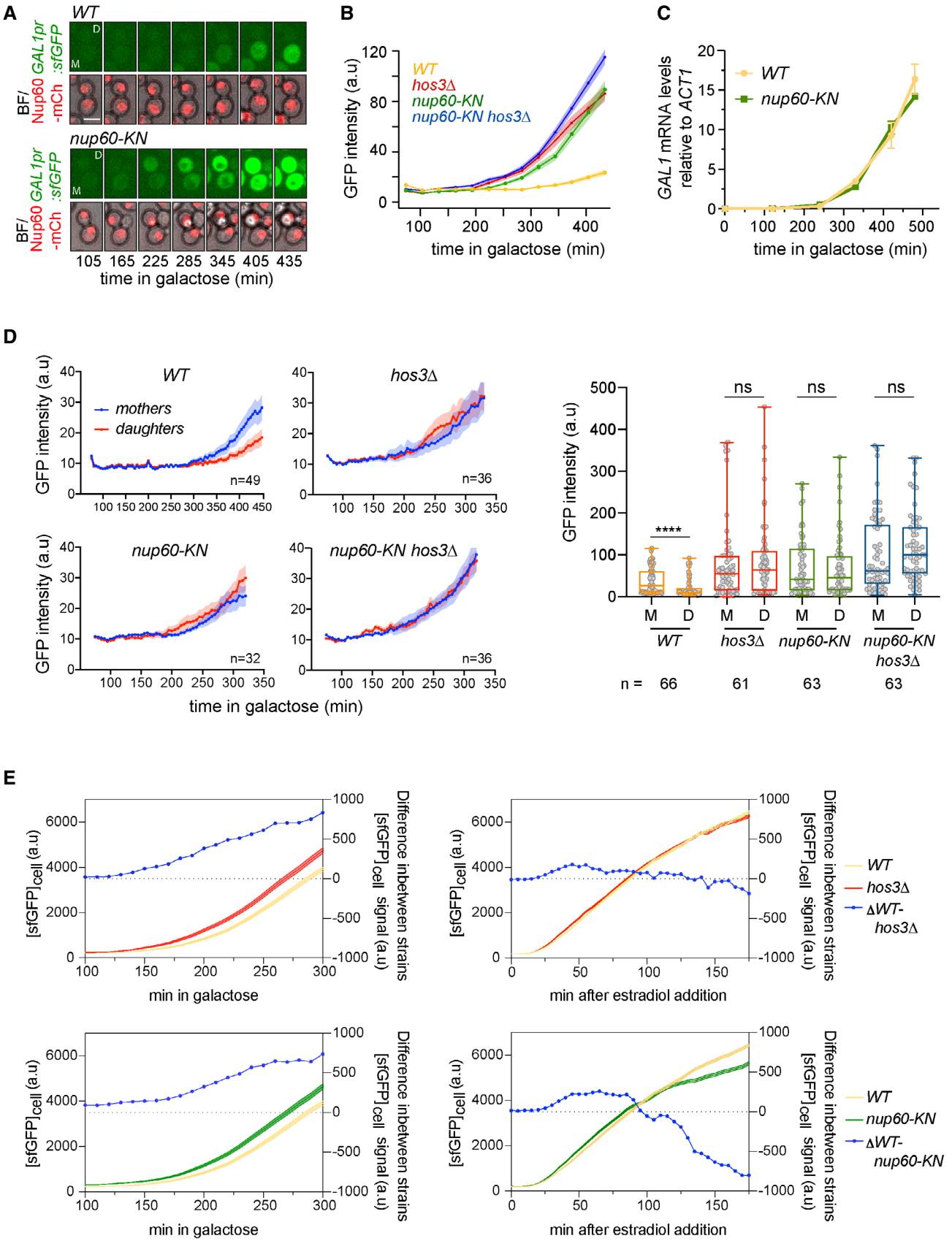

Figure 6.

expression upon galactose addition, in which *hos3*Δ and *nup60-KN* induced *GAL1* more strongly than wild type (Fig 6E and Appendix Fig S11A and B). Note that the effect of *hos3* and *nup60-KN* on *GAL1* expression in response to galactose was milder in GEV than in non-GEV strains, probably due to differences in genetic background. GEV strains are derived from W303, which carries a functional copy of the galactose permease *GAL2*. Non-GEV strains in Fig 6A–D are derived from S288c, which is *gal2*- and relies on lower-affinity permeases to import galactose (Mortimer & Johnston, 1986; Donnini *et al*, 1992). Thus, Nup60 acetylation may be particularly important when galactose availability is limited. These data suggest that for optimal regulation of *GAL1* expression by Nup60 acetylation, the *GAL1* gene must be associated with the NPC. Furthermore, forcing the symmetric distribution of the mRNA export factor Sac3 to the nuclear basket of mother and daughter nuclei using the FRB-FKBP system (as in Fig 5C) increased *GAL1* expression specifically in daughter cells (Fig 7A and B and Appendix Fig S12). These data further support the notion that Hos3-dependent deacetylation of Nup60 inhibits general mRNA export in daughter cells.

Discussion

Our data indicate that in budding yeast, the lysine acetyltransferase subunit of the NuA4 complex (Esa1) promotes cell cycle entry. In the absence of Esa1, the KAT subunit of the SAGA complex (Gcn5) can partially fulfil this function. Given that the G1/S transition depends on the coordinated expression of hundreds of genes, the involvement of NuA4 and SAGA components in this cell cycle transition is in line with their common role as transcriptional coactivators with known functional overlaps. Indeed, NuA4 and SAGA complexes share the targeting subunit Tra1 (Helmlinger & Tora, 2017) and are thought to drive gene expression mainly through acetylation of histone H3 (for SAGA) and H4 (for NuA4) and subsequent chromatin decompaction (Sterner & Berger, 2000; Lee & Workman, 2007). However, we demonstrate that Esa1 is required not only for gene transcription but also for mRNA export. Also in this case, Gcn5 can partially compensate for the absence of Esa1. Importantly, expression of an acetyl-mimic Esa1/Gcn5 substrate, the nuclear pore component Nup60, partially alleviates the G1/S transition and mRNA export defects of Esa1-defective cells.

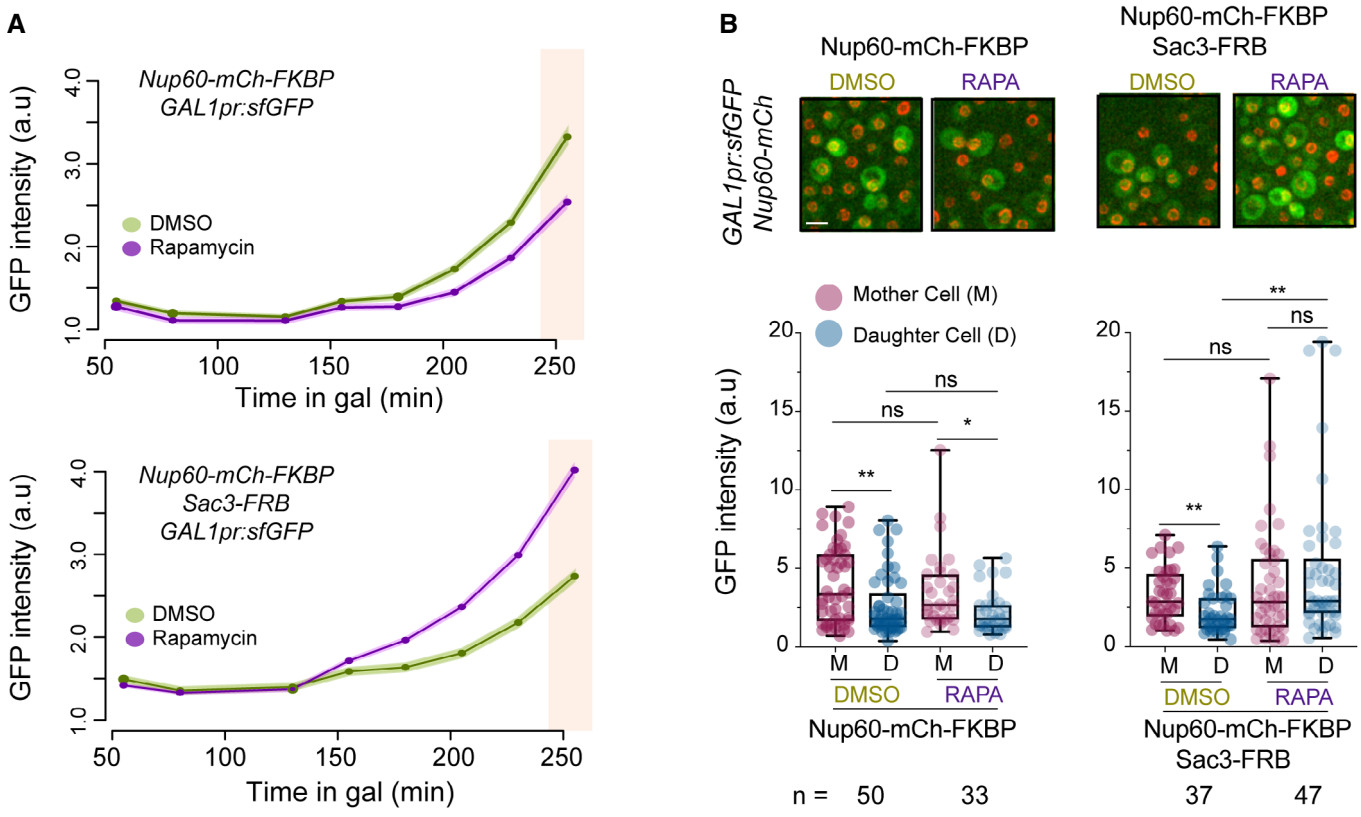

Figure 7. Sac3 anchoring to Nup60 promotes *GAL1* expression.

A Cells of the indicated strains were incubated with galactose in the presence of either rapamycin (RAPA) to induce FRB-FKBP heterodimerisation, or DMSO as control. *GAL1pr:sfGFP* expression was monitored over time as in Fig 6B.

B (*Top*) Representative images of the indicated cells in rapamycin or DMSO, 250 min after galactose addition. Scale bar, 4 μm. (*Bottom*) Mother/daughter pairs were quantified as in Fig 6D at 250 min after galactose addition (pink shaded area in A). Boxes include 50% of data points, the line represents the median, and whiskers extend to maximum and minimum values. **, $P \leq 0.01$; *, $P \leq 0.05$; and ns, $P > 0.05$, two-tailed paired *t*-test for M-D comparisons, unpaired for comparisons between strains. *n* = number of cells. One of two independent experiments with similar results is shown.

Source data are available online for this figure.

Thus, we propose that Esa1 is the main KAT driving transcription of G1/S genes (most likely through acetylation of chromatin proteins) and that it also promotes mRNA export by acetylation of Nup60. To our knowledge, this is the first time that a KAT is linked to post-transcriptional regulation of gene expression by modification of NPCs. Esa1 may acetylate other NPC components in addition to Nup60 to promote mRNA export (Henriksen *et al*, 2012; Kumar *et al*, 2018). Importantly, we show that Esa1 activity and Nup60 acetylation facilitate the nuclear enrichment of the TREX-2 complex scaffolding subunit Sac3, which promotes mRNA export at the nucleoplasmic side of the nuclear pores, thereby driving mRNA export and cell cycle entry (Fig 8). Our finding that Nup60 acetylation promotes the Sac3-dependent expression of *GAL1*, which is not required for cell cycle entry, further suggests that Esa1 and acetylation of Nup60 are part of a pathway promoting general mRNA export during the entire cell cycle.

Our results also indicate that Esa1-dependent mRNA export, which may be constitutively active in mother cells, is specifically inhibited in daughter cells to restrain their G1/S transition. This inhibition is caused by the KDAC Hos3, which deacetylates Nup60 in G1 daughters, contributing to their prolonged G1 phase and enforcing cell size control. Nup60 acetylation in daughter cells is restored in S phase, presumably due to removal of Hos3 from NPCs in G1 (Kumar *et al*, 2018), thus allowing resumption of normal mRNA export in daughter cells later in the cell cycle. These observations reveal an additional level of control of the G1/S transition, which is also regulated by the differential scaling of Start inhibitors and activators with cell size (Schmoller *et al*, 2015; Chen *et al*, 2020) and by the daughter-specific inheritance of transcriptional regulators (Di Talia *et al*, 2009; Kumar *et al*, 2018). Notably, our data suggest that gene expression at the G1/S transition is controlled not only through transcription but also at the level of mRNA export. We speculate that the Hos3-Nup60 pathway downregulates mRNA export during G1, because Nup60 deacetylation is largely restricted to this cell cycle phase. Moreover, it is possible that Nup60 deacetylation does not specifically inhibit expression of the G1/S regulon, because Hos3 also inhibits expression of the nutrient-responsive *GAL1* gene.

Esa1-deficient yeast cells arrest in late S phase or early mitosis in a manner dependent on the DNA damage checkpoint (Clarke *et al*, 1999). This cell cycle arrest probably masked the role of Esa1 in earlier cell cycle stages, which we reveal here through analysis of both synchronised populations and freely cycling cells. Moreover, our results raise the possibility that DNA damage in *esa1-ts* cells may stem (at least in part) from replicative stress during S phase caused by inefficient synthesis and/or export of G1/S mRNAs. Supporting this hypothesis, DNA replication (although delayed) seems to proceed in many unbudded *esa1-ts* cells (Fig 1C and D). In addition, lack of Esa1 activity is associated with aberrant nucleolar fragmentation (Clarke *et al*, 1999). Although the molecular basis of the nucleolar defect in Esa1-defective cells is unclear, it is interesting that nucleolar fragmentation is also observed after inactivation of mRNA export factors, provided that mRNA synthesis is ongoing (Kadowaki *et al*, 1994; Schneiter *et al*, 1995). Thus, nucleolar fragmentation after inactivation of Esa1 may be caused by abnormal accumulation of mRNA in the cell nucleus.

mRNA export factors, including Mex67 and Sac3, contribute to NPC tethering of active yeast genes and may contribute to their optimal expression (Cabal *et al*, 2006; Dieppois *et al*, 2006; Brickner *et al*, 2019). Our data indicate that Esa1 promotes the perinuclear enrichment of Sac3, but whether this localisation affects the interaction of chromosomal loci with NPCs is not known. Interestingly, the *CLN2* locus interacts with NPCs specifically in G1, and this interaction is stabilised by Nup60 deacetylation in daughter cells (Kumar

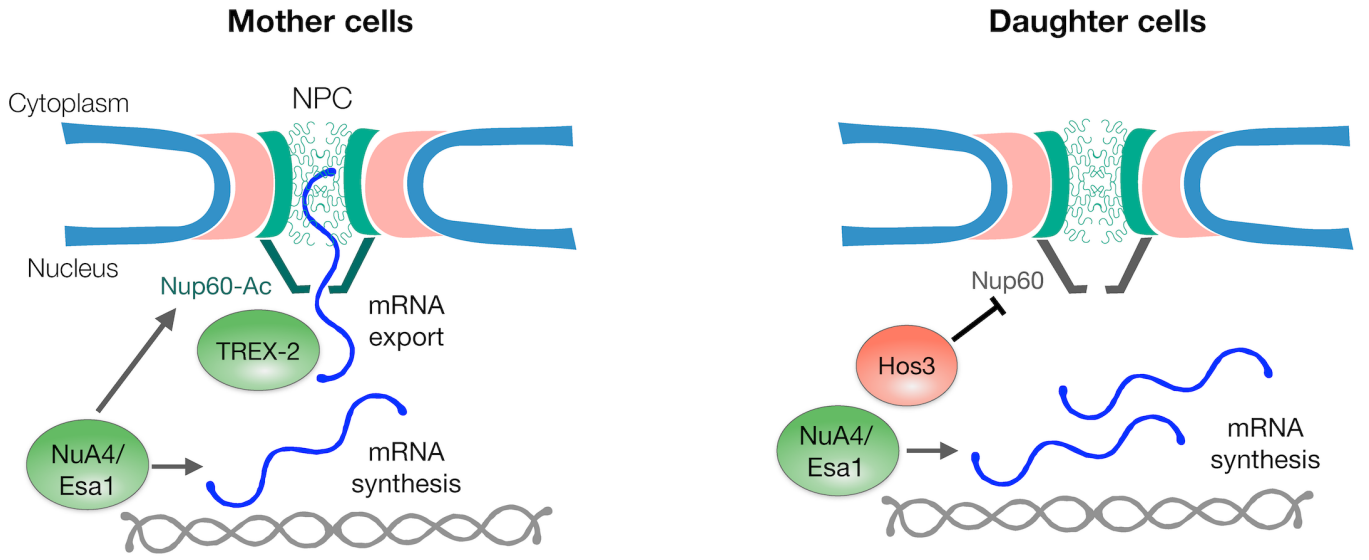

Figure 8. Esa1 coordinates mRNA synthesis and export during the G1/S transition through Nup60 acetylation.

In mother cells, Esa1 promotes both mRNA synthesis and export. Mechanistically, mRNA export is promoted by acetylation of Nup60, which increases the association between the mRNA export factor TREX-2 and the nuclear pore basket. In daughter cells, Hos3 deacetylates Nup60, which reduces TREX-2 association with the NPC, and thus mRNA export. Inhibition of Nup60 acetylation in daughter cells contributes to their longer G1 phase, possibly by delaying the export of mRNAs required for entry into S phase such as *CLN2*, and inhibits the expression of the *GAL1* gene in response to galactose.

et al, 2018). It will be of interest to establish how NPC tethering of G1/S genes such as *CLN2* is related to the elongation and export state of their respective mRNAs, and whether stabilisation of gene tethering by Nup60 deacetylation corresponds to primed or active transcriptional conditions.

Whether the role of NuA4 in NPC acetylation and mRNA export is evolutionarily conserved is not known. As in yeast, the TREX-2 complex is associated with the nuclear pore basket in human cells (Umlauf *et al*, 2013) and promotes export of a subset of mRNAs together with the basket component TPR (Wickramasinghe *et al*, 2010, 2014; Aksenova *et al*, 2020). Furthermore, human nucleoporins are acetylated, including TPR and the Nup60 homologue Nup153 (Choudhary *et al*, 2009), and TPR physically interacts with Tip60/KAT5, the mammalian homologue of Esa1 (Chen *et al*, 2013); however, the physiological relevance of these modifications and interactions has not been determined. Our findings raise the possibility that mammalian nucleoporins represent a novel category of substrates for KATs and for the multiprotein complexes in which these enzymes reside, with important roles in gene expression. Testing this possibility, and identifying the molecular mechanisms by which KATs such as NuA4 and SAGA regulate mRNA export in mammalian cells (e.g. by acetylation of non-histone proteins such as nucleoporins) remain therefore a key subject for future studies.

In summary, these data reveal a novel role in mRNA export for the evolutionarily conserved KAT-containing coactivator complex, NuA4. They also demonstrate that differences in Nup60 acetylation determined by the interplay between a KAT (in mother cells) and a KDAC (in daughter cells) allow the modulation of mRNA export capabilities of NPCs in different cell types, shaping their gene expression and cell proliferation profiles. Furthermore, our findings on the regulation of *GAL1* expression by Nup60 acetylation indicate that differences in NPC acetylation between mother and daughter cells contribute to the development of heterogeneous gene expression responses among a population of genetically identical cells. This type of phenotypic variability (often interpreted as a bet-hedging strategy) could provide a growth advantage for a clonal population upon sudden changes in environmental conditions (Veening *et al*, 2008). Thus, while specifically assessing the role of NPC acetylation in cell cycle entry, our study raises the possibility that acetylation of nuclear pores and regulation of mRNA export define an important regulatory step in cell identity establishment. Analogous mechanisms may also contribute to cell differentiation during the development of multicellular organisms.

Materials and Methods

Strains, plasmids and cell growth

Saccharomyces cerevisiae strains are derivatives of S288c or BY4741 except when indicated (Appendix Table Table S1). Gene deletions and insertions of C-terminal tags were generated by standard one-step PCR-based methods (Longtine *et al*, 1998; Janke *et al*, 2004). The acetyl-mimic *nup60-KN* mutant was generated using CRISPR/Cas9 to replace the acetylated lysine 467 by asparagine, as described (Kumar *et al*, 2018). The deacetyl-mimic *nup60-KR* mutant was obtained by homologous recombination with a PCR product generated from a *nup60-KR* strain, a gift from Dr. Yves Barral. The *esa1-ts* thermosensitive strain carrying the *L254P* mutation (Clarke *et al*, 1999) linked to the kanamycin-resistance cassette *KanMX* (Li *et al*, 2011) was used to obtain the *esa1-ts-kanMX* cassette and integrate the *ts* allele in the corresponding S288c-derived strains. The *mex67-ts* strain is a gift from Dr. M. del Olmo (Estruch *et al*, 2009).

pBG1805 2μ multicopy plasmids expressing KATs, Mtr2, Mex67 or Sac3 under the control of the *GAL1* promoter and carrying a HA C-terminal tag (Gelperin *et al*, 2005) were obtained from the Yeast ORF collection (Thermo Scientific Open Biosystems, YSC3868). pGP565 2μ multicopy plasmids (Jones *et al*, 2008) containing Sac3, Sus1, Cdc31, Sem1 and Thp1 are a gift from Dr. S. Leon (Yeast Genomic Tiling Collection, Open Biosystems). The pUC57 vector containing the superfolder (sf) GFP fused to the CLN2-PEST degron under the control of *GAL1pr* (AP2) is described in Goulev *et al* (2019), and the Rpl25-GFP plasmid is a gift from Dr. H. Schmidt.

Cells were grown in exponential conditions (below OD_{600} = 1) at 25°C in standard yeast extract–peptone–dextrose medium supplemented with adenine 70 μg/ml (YPDA) or synthetic complete (SC) medium with 2% glucose, 2% raffinose (SC-Raf) or 2% galactose (SC-Gal). Where indicated, cells were incubated in the presence of 15 μg/ml nocodazole and 15 μg/ml α-factor, or transferred to 37°C. For growth assays in solid media, 10-fold serial dilutions of exponential cultures were spotted onto SC-Glu and SC-Gal medium and incubated at 25°C for 3 days.

For G1 arrest, exponential cells growing in YPDA medium were synchronised with 15 μg/ml α-factor (GenScript, Cat. No: RP01002) for 2 h at 25°C, supplemented with additional α-factor (5 μg/ml) and incubated 30 min more at 25°C. Then, cells were shifted to 37°C during 1 h, washed three times with pre-warmed YPDA and released in fresh pre-warmed YPDA medium at 37°C. For the nocodazole arrest, cells were incubated during 2 h with nocodazole 15 μg/ml, washed three times and then released in fresh pre-warmed YPDA medium at 37°C.

For the analyses of *GAL1pr*-driven expression of the sfGFP reporter, the *GAL1pr:sfGFP-CLN2-PEST* cassette was integrated between the *GAL1* and *FUR4* loci using the following oligonucleotides:

GALsfGFP-Fw (5'-AAAGTCATTTGCGAAGTTCTTGGCAAGTTGCCAACTGACGtACGGATTAGAAGCCGCCGA-3′) and GALsfGFP-Rv (5'-AGGACAAAAAGTTTCAAGACGGCAATCTCTTTTTACTGCAATGGttagaaaaactcatcgag-3′) and the AP2 plasmid as a PCR template. For induction of the *GAL1pr:sfGFP* reporter (Fig 6), exponential cells were grown in glucose, washed three times with SC-Gal and resuspended in SC-Gal (2% galactose, 0.1% glucose) for time-lapse imaging. For Nup60-GFP IP assays (Fig 2A), cells were grown in glucose until exponential phase, diluted and incubated in SC-Raf (2% raffinose, 0.1% glucose) overnight until exponential phase, and 2% galactose was added to induce *GAL1pr:GCN5-HA* and *GAL1pr:ESA1-HA* expression for 2 h.

For analysis of Gal1-LacO gene tethering, cells were grown in glucose, washed three times with SC-Gal and resuspended in SC-Glu, SC-Glu + 90 μM oestradiol or SC-Gal for time-lapse imaging.

For tethering of Sac3 to Nup60, we used inducible dimerisation of FK506-binding protein (FKBP) and FKBP–rapamycin binding (FRB) domain, as described in Gallego *et al* (2013). Sac3 and Nup60 were tagged at the C-terminus. The background of the anchoring

strains harbours the *tor1-1* mutation and lacks the endogenous FPR1 gene rendering growth insensitive to rapamycin. Exponential cells were incubated with 20 μM rapamycin (Sigma-Aldrich, Cat. No R8781) throughout the imaging experiment. Association between Sac3-GFP-FRB and Nup60-mCherry-FKBP was checked by measuring the disruption of Sac3 asymmetries within 15–30 min of rapamycin addition (Fig 5C). Similar results were obtained for Sac3-mCherry-FKBP and Nup60-FRB. For the induction of *GAL1pr:sfGFP*, cells were grown in glucose, washed three times with SC-Gal and shifted to SC-Gal (2% galactose, 0.1% glucose) with rapamycin or DMSO for the time-lapse imaging (Fig 7). For inactivation of *esa1-ts*, cells were imaged at 37°C at the moment of rapamycin or DMSO addition (Fig 5D).

Fluorescence microscopy

For time-lapse microscopy, cells were grown overnight in 50-ml flasks containing 10 ml of SC medium at 25°C, then diluted to OD600 = 0.1–0.3 in fresh medium, grown at least for 4 h to mid-log phase and plated in minimal synthetic medium on concanavalin A-coated (Sigma-Aldrich) Lab-Tek chambers (Thermo Fisher Scientific). Images were acquired on a Nikon TiE inverted microscope (or on a Leica DMi8 for Fig 3) equipped with a X1 Yokogawa Spinning disk confocal head using a Leica HC PL APO 100× NA1.4 objective. The excitation/emission parameters were as follows: for GFP laser excitation at 488 nm/bandpass emission filter 525/50 nm and for tdTomato laser excitation at 561 nm/bandpass emission filter 605/64 nm. Images were captured with a Photometrics Prime 95B sCMOS camera. Laser power and camera exposure times were modulated depending on the samples. A Tokai Hit Environmental Chamber maintained the sample temperature at 37°C. Time-lapse series of 4-μm stacks spaced 0.2–0.3 μm were acquired every 2–5 min. For Sac3-GFP, a maximum of 13 z-stacks were taken; for Whi5-GFP, 8 z-stacks spaced by 0.4 μm were taken; for Whi5-tdTomato/*CLN2*-PP7, 16 z-stacks spaced by 0.25 μm were taken; and in case of Whi5-mCherry due to low protein abundance and poor fluorophore stability, 3 z-stacks spaced by 0.5 μm were used. Red channel images (Whi5-mCherry, Whi5-tdTomato) were subject to Gaussian blur (radius = 2 px), and Whi5-GFP images were subject to median filtering (radius = 1 px) to remove noise. The images were processed and analysed on 2D maximum or sum projections (unless mentioned otherwise) using Fiji (https://imagej.net/software/fiji/). In Figs 2E and 5D, only cells that imported Whi5 30 min after the start of imaging were included in the analysis. Maximum projections are shown throughout, except in Figs 5A–C and EV5, where sum projections are shown.

Nuclear *CLN2*-PP7 focus intensity (Fig 3D) was calculated by determining the mean fluorescence of nuclear foci during Whi5 export in a single confocal Z-slice, normalised by the mean fluorescence of the whole nucleus in the same slice. Fluorescent levels of Sac3-GFP, and Nup49- or Nup60-mCherry were determined in background-subtracted 2D sum projections of whole-cell Z-stacks, with the nuclear area defined by Nup49-mCherry or by Nup60-mCherry. For Sac3 (Fig 5A), G1 mother and daughter cells were quantified in G1, defined as the first 30–45 min after completion of anaphase and the absence of bud. For the *GAL1pr:sfGFP* reporter, the GFP mean fluorescence was determined (Fig 6). For mother/daughter measurements (Figs 6D *right* and 7B), mother/daughter pairs with individual nuclei at the moment of galactose shift were tracked and their fluorescence was measured at the indicated times. For the quantification of *GAL1pr:sfGFP* activation over time (Figs 6B and 7A), a custom Fiji macros segmented the nuclear signal (Nup60-mCherry), and after manual correction of ROI, total fluorescence and mean fluorescence of the mCherry and GFP channels were automatically determined for all the individual cells. For measuring GAL1pr-GFP fluorescence in mother and daughter cells over time (Fig 6D *left*), sequences of bright-field / fluorescence confocal images were processed using DetecDiv (preprint: Aspert *et al*, 2021) as follows: cells were segmented using a pre-trained deep learning-based pixel classification model, after training it using 14 manually annotated images. Then, the model was deployed on all (roughly ~1,000) images and slight post-processing (i.e. small object removal and watershed) was applied to refine cell segmentation. We then used a tracking routine based on the Hungarian method for assignment to map individual cell trajectories over time, which allowed us to quantify the dynamics of their mean cytoplasmic fluorescence.

Conventional epifluorescence microscopy was carried out with a Leica DM4000B widefield microscope equipped with HCX PL APO 100X/1.40 OIL PH3 CS objective, and image acquisition was performed with Hamamatsu ORCA-Flash4.0 LT digital CMOS camera with the help of Leica Application Suite X (LAS X) software. For DNA staining, cells were fixed for 5 min by addition of 70% ethanol and resuspended in 1 μg/ml DAPI (4′,6-diamidino-2-phenylindole). Budding index was scored manually using the transmitted light images and the cell-counter plug-in of Fiji.

Microfluidics

Microfluidics devices (Fig 6E and Appendix Fig S11) were fabricated and handled as in Jacquel *et al* (2021). Cells were imaged with a Zeiss Axio Observer Z1 microscope. Before image acquisition, cells were washed for 1 h with SC-Glu media, and afterwards, the media flow was changed either to SC-Glu + 90 μM oestradiol or to SC-Gal. Raw images were processed using MATLAB-based software PhyloCell (Goulev *et al*, 2017). Imaged cells of all time points were segmented by the software, and the mean intensity of each segment was calculated.

Western blotting

Approximately 10 ml of exponential growing cells (OD_{600} = 0.3–0.6) was collected, resuspended in 200 μl of 0.1 M NaOH and incubated for 5 min at room temperature. Cells were collected by centrifugation, resuspended in 50 μl of Laemmli buffer and incubated for 5 min at 95°C. Extracts were clarified by centrifugation, and equivalent amounts of protein were resolved in an SDS–PAGE and transferred onto a nitrocellulose membrane. Membranes were blocked with milk powder 5% in TBS–Tween 0.01% or FBS 10% in TBS–Tween 0.1% (anti-AcLys) and incubated overnight with primary antibodies. Primary antibodies were anti-HA peroxidase 3F10 (Roche Diagnostics, Cat. No: 12013819001) diluted 1:5,000, anti-GFP (Roche Diagnostics, Cat. No: 11814460001) diluted 1:5,000, anti-GAPDH (Thermo Fisher Scientific Cat. No: MA5-15738) diluted 1:2,000, anti-G-6-PDH diluted 1:20,000 (Sigma, Cat. No: A9521), anti-AcLys diluted 1:1,000 (Cell Signalling, Cat. No: 9681), and anti-Cdc28 (anti-

Cdk1/cdc2 (PSTAIR)) (Merck, Cat. No: 06–923) diluted 1:2,000. Blots were developed with anti-mouse IgG and anti-rabbit IgG horseradish peroxidase conjugate (Thermo Fisher Scientific, Cat. No: 170–6,516 or 31,460 respectively) diluted 1:20,000 using the SuperSignal West Femto Maximum Sensitivity Substrate (Thermo Scientific). Bands were acquired with ImageQuant™ LAS 4000 mini biomolecular imager (GE Healthcare) and quantified in ImageJ.

Protein Immunoprecipitation assays

Approximately 100 ml of exponential growing cells (OD_{600} = 0.5–0.8) expressing Nup60-GFP were collected and resuspended in 300 µl of Lysis Buffer (50 mM Tris–HCl, pH 8, 250 mM NaCl, 5 mM EDTA, 1% Triton X-100, 1 mM PMSF, 2.5 mM benzamidine, and 0.1% (w/v) sodium deoxycholate) with Complete Mini Protease Inhibitor (Roche Diagnostics) and histone deacetylase inhibitors (iHDAC) 5 µM trichostatin A (Sigma-Aldrich), 10 mM nicotinamide (Sigma-Aldrich) and 10 mM sodium butyrate (Sigma-Aldrich). Cells were broken with vigorous shaking in the presence of glass beads, the cellular debris was removed, and the supernatant was clarified by centrifugation at 13,400 *g* for 5 min. 50 µl Dynabeads Protein G magnetic beads (Invitrogen) were incubated with anti-GFP antibody (Roche Diagnostics) for 20 min at room temperature and after washing with phosphate-buffered saline (PBS) containing Tween 0.02%, incubated with the cell extract for 2 h at 4°C. After washing the beads four times with PBS Tween 0.02%, the immunoprecipitated Nup60 was eluted by boiling the beads for 5 min with 100 µl of Laemmli buffer 2× and analysed by SDS–PAGE followed by Western blot analysis.

PolyA fluorescence *in situ* hybridisation

Cells were grown in SC to exponential phase at 25°C, and the culture was divided into two to incubate half of the culture at 25°C or 37°C or in SC or SC-gal during the indicated times. Approximately 10 ml of exponential cultures (OD_{600} = 0.5–1) was fixed with 4% (v/v) formaldehyde (Sigma-Aldrich) during 15 min at room temperature or 37°C. Cells were collected and resuspended in 0.1 M potassium phosphate (KPi), pH = 6.4/4% formaldehyde and fixated for 1 h in agitation at room temperature. The fixation agent was removed by washing two times with 0.1 M KPi, pH 6.4. Cells were washed one time with ice-cold washing buffer (0.1 M KPi (pH = 6.4)/1.2 M sorbitol) and resuspended in 200 µl of ice-cold washing buffer, and subsequently, cell wall was digested by incubating 100 µl of cells with 0.4 mg/ml of Zymolyase 100T (SEIKAGAKU CORPORATION) at 30°C for 5–15 min. Partially spheroplasted cells were recovered by centrifugation (3,000 *g* for 5 min), washed one time with washing buffer and resuspended in 30 µl 0.1 M KPi (pH = 6.4)/1.2 M sorbitol. Samples were then applied on Teflon slides with wells previously coated with poly-L-lysine. Non-adhering cells were removed by aspiration, cells were rehydrated with 2X SSC (0.15 M NaCl and 0.015 M sodium citrate) and incubated with prehybridisation buffer (formamide 50%, dextran sulphate 10%, 125 µg/ml of *Escherichia coli* tRNA, 4× SSC, 1× Denhardt's solution and 500 µg/ml herring sperm DNA) for 1 h at 37°C in a humid chamber. The hybridisation was incubated overnight at 37°C in a humid chamber with 20 µl of prehybridisation buffer supplemented with 1 µM of Cy3-end-labelled oligo(dT), 1 mM DTT and RNasin (Promega) 4 U/ml. After hybridisation, slides were washed with 2× SSC and 1× SSC at room temperature for 5 min, and subsequently, cells were incubated for 1 min with 2 µl of DAPI 2.5 mg/ml. Cells were washed twice with 1× SSC, washed with 0.5× SSC, air-dried and mounted with 50% glycerol. Detection of Cy3-oligo(dT) and DAPI was performed using a Leica DM4000B fluorescence microscope.

Flow cytometry

DNA content analysis was performed according to the protocol from Rosebrock (2017). Briefly, cells were fixed in two volumes of 100% ethanol (overnight −20°C), rehydrated with PBS and digested with proteinase K (20 µg/ml, Thermo Scientific) and RNase A (10 µg/ml) for 2 h at 50°C in the presence of SYTOX Green (0.5 µM, Invitrogen). Flow cytometry was performed on a LSRII (BD) instrument, and the data were analysed with the FlowJo software. Gating strategies are shown in Appendix Fig S13.

RT–qPCR

Samples for gene expression analysis containing approximately 4×10^8 cells were frozen in liquid nitrogen and stored at −80°C. RiboPure-Yeast (Invitrogen) kit was used to isolate total RNA according to the manufacturer's protocol. Briefly, cells were broken in a Disruptor Genie (Scientific Industries) with Zirconia Beads in Lysis Buffer with one volume of phenol:chloroform. The lysate was centrifuged at 16,100 *g* for 10 min, and the aqueous phase was separated and mixed with corresponding amounts of 100% ethanol and binding buffer. The resulting solution was drawn through the column filter, which was further washed with wash solutions. RNA was eluted from the filter with 2 × 50 µl of elution buffer and 1 × 50 µl with DEPC-treated Molecular Biology Grade Water (Merck). RNA samples were quantified with NanoDrop 2000 Spectrophotometer (Thermo Scientific). 2.5 µg of RNA was incubated with ezDNase, and cDNA was obtained with SuperScript IV VILO Master Mix (both Invitrogen) following the manufacturer's instructions. cDNA was analysed in triplicate by quantitative RT–PCR with LightCycler 480 SYBR Green I Master Mix (Roche) using the Roche LightCycler 480 II instrument. mRNA levels of genes of interest were quantified relative to *ACT1* mRNA by the ΔCt method.

RNA-seq

Cells were harvested by centrifugation, and RNA was extracted from snap-frozen pellets using the RiboPure-Yeast Kit (Ambion). RNA concentrations were determined using NanoDrop 1000 (Thermo Scientific), while quality and integrity were checked using a Bioanalyzer 2100 (Agilent Technologies). RNA sequencing (RNA-seq) was performed on a HiSeq 4000 (Illumina). Single-end reads were preprocessed using cutadapt (Martin, 2011) to remove adapters, polyA and low-quality sequences. Reads longer than 40 bp were aligned to the reference *S. cerevisiae* genome (R64) using STAR version 2.5.3a (Dobin *et al*, 2013). Gene expression was quantified from uniquely aligned reads using HTSeq-count (Anders *et al*, 2014), v.0.6.1p1, with annotations from Ensembl release 94 and union mode. TPM was calculated from raw read counts, and average TPM in each condition was performed and transformed using log2.

Statistical methods and reproducibility

Graphs and statistical analysis (two-tailed unpaired/paired *t*-test, one-sample *t*-test, ANOVA with Tukey's multiple comparisons test and log-rank Mantel–Cox test) were performed with GraphPad Prism software and R. For all the strains used in this work, at least two independent clones were tested with similar results. All data were obtained from at least two independent biological replicates. Each experiment was repeated on at least two different days. For most experiments, at least 100 cells were counted for each replicate (50 cells for time-lapse microscopy). Given two populations of cells, and two behaviours (0 and 1), a sample size of 100 cells can detect a difference between the two populations with $P < 0.05$ of more than five cells (more than 5%) and with $P < 0.001$ of more than 10 cells (more than 10%) (Fisher's exact test).

Data availability

All strains, plasmids and data are available from the authors upon request. RNA-seq raw data are available at: https://www.ncbi.nlm.nih.gov/geo/query/acc.cgi?acc=GSE199740

Expanded View for this article is available online.

Acknowledgements
We are grateful to the IGBMC Imaging Centre and Flow Cytometry Facility; Kenny Schumacher for assistance with RT–qPCR; Damien Plassard for analysis of RNA-seq data; Didier Devys, Gabriel Neurohr, Snezhana Oliferenko, Laszlo Tora and all members of the Mendoza Lab for helpful comments; and Life Science Editors for editorial assistance. This study was supported by Ministerio de Ciencia e Innovación, Spain, and co-financed by the European Regional Development Fund from the European Union, grant numbers BFU2017-88692 and PID2020-119793GB-I00 to JCI; by the Fondation ARC pour la recherche sur le cancer www.fondation-arc.org and "Équipe FRM" EQU202003010561 to MM; and by the grant ANR-10-LABX-0030-INRT, which is a French state fund managed by the Agence Nationale de la Recherche under the frame programme Investissements d'Avenir ANR-10-IDEX-0002-02 to the IGBMC. MGA was a Postdoctoral Fellow from the Generalitat Valenciana (APOSTD/2017/094) and is a recipient of a Juan de la Cierva Incorporación Fellowship (IJC2018-036206-I) from the Ministerio de Ciencia e Innovación, Spain. VP was supported by "Fin de thèse" FRM fellowship FDT202106012921.

Author contributions
Mercè Gomar-Alba: Conceptualization; validation; investigation; visualization; methodology. **Vasilisa Pozharskaia:** Conceptualization; validation; investigation; visualization; methodology. **Bogdan Cichocki:** Investigation. **Celia Schaal:** Investigation. **Arun Kumar:** Conceptualization. **Basile Jacquel:** Investigation. **Gilles Charvin:** Conceptualization; supervision; investigation; methodology. **J Carlos Igual:** Conceptualization; supervision. **Manuel Mendoza:** Conceptualization; supervision.

In addition to the CRediT author contributions listed above, the contributions in detail are:

MG-A, VP, AK, GC, JCI and MM conceptualised the study. MG-A, VP, BC, CS, BJ and GC investigated the study. MGA, VP, BC, CS, GC and MM performed the formal analysis. MGA, VP and MM wrote the original draft. MGA, VP, GC, JCI and MM wrote, reviewed and edited the manuscript. JCI and MM acquired funding. GC, JCI and MM supervised the study.

Disclosure and competing interest statement
The authors declared that they have no conflict of interest.

References

Aksenova V, Smith A, Lee H, Bhat P, Esnault C, Chen S, Iben J, Kaufhold R, Yau KC, Echeverria C, *et al* (2020) Nucleoporin TPR is an integral component of the TREX-2 mRNA export pathway. *Nat Commun* 11: 4577

Allard S, Utley RT, Savard J, Clarke A, Grant P, Brandl CJ, Pillus L, Workman JL, Côté J (1999) NuA4, an essential transcription adaptor/histone H4 acetyltransferase complex containing Esa1p and the ATM-related cofactor Tra1p. *EMBO J* 18: 5108–5119

Anders S, Pyl PT, Huber W (2014) HTSeq—a Python framework to work with high-throughput sequencing data. *Bioinformatics* 31: 166–169

Aspert T, Hentsch D & Charvin G (2021) DetecDiv, a deep-learning platform for automated cell division tracking and replicative lifespan analysis. *bioRxiv* https://doi.org/10.1101/2021.10.05.463175 [PREPRINT]

Baptista T, Grünberg S, Minoungou N, Koster MJE, Timmers HTM, Hahn S, Devys D, Tora L (2017) SAGA is a general cofactor for RNA polymerase II transcription. *Mol Cell* 68: 130–143

Bertoli C, Skotheim JM, de Bruin RAM (2013) Control of cell cycle transcription during G1 and S phases. *Nat Rev Mol Cell Biol* 14: 518–528

Brickner DG, Randise-Hinchliff C, Lebrun Corbin M, Liang JM, Kim S, Sump B, D'Urso A, Kim SH, Satomura A, Schmit H, *et al* (2019) The role of transcription factors and nuclear pore proteins in controlling the spatial organization of the yeast genome. *Dev Cell* 49: 936–947

de Bruin RAM, Mcdonald WH, Kalashnikova TI, Yates J, Wittenberg C (2004) Cln3 activates G1-specific transcription via phosphorylation of the SBF bound repressor Whi5. *Cell* 117: 887–898

Bruzzone MJ, Grünberg S, Kubik S, Zentner GE, Shore D (2018) Distinct patterns of histone acetyltransferase and Mediator deployment at yeast protein-coding genes. *Genes Dev* 32: 1252–1265

Cabal GG, Genovesio A, Rodriguez-Navarro S, Zimmer C, Gadal O, Lesne A, Buc H, Feuerbach-Fournier F, Olivo-Marin J-C, Hurt EC, *et al* (2006) SAGA interacting factors confine sub-diffusion of transcribed genes to the nuclear envelope. *Nature* 441: 770–773

Casolari JM, Brown CR, Komili S, West J, Hieronymus H, Silver PA (2004) Genome-wide localization of the nuclear transport machinery couples transcriptional status and nuclear organization. *Cell* 117: 427–439

Charvin G, Oikonomou C, Siggia ED, Cross FR (2010) Origin of irreversibility of cell cycle start in budding yeast. *PLoS Biol* 8: e1000284

Chen PB, Hung J-H, Hickman TL, Coles AH, Carey JF, Weng Z, Chu F, Fazzio TG (2013) Hdac6 regulates Tip60-p400 function in stem cells. *elife* 2: e01557

Chen Y, Zhao G, Zahumensky J, Honey S, Futcher B (2020) Differential scaling of gene expression with cell size may explain size control in budding yeast. *Mol Cell* 78: 359–370

Choudhary C, Kumar C, Gnad F, Nielsen ML, Rehman M, Walther TC, Olsen JV, Mann M (2009) Lysine acetylation targets protein complexes and co-regulates major cellular functions. *Science* 325: 834–840

Clarke AS, Lowell JE, Jacobson SJ, Pillus L (1999) Esa1p is an essential histone acetyltransferase required for cell cycle progression. *Mol Cell Biol* 19: 2515–2526

Costanzo M, Nishikawa JL, Tang X, Millman JS, Schub O, Breitkreuz K, Dewar D, Rupes I, Andrews B, Tyers M (2004) CDK activity antagonizes Whi5, an inhibitor of G1/S transcription in yeast. *Cell* 117: 899–913

Di Talia S, Skotheim JM, Bean JM, Siggia ED, Cross FR (2007) The effects of molecular noise and size control on variability in the budding yeast cell cycle. *Nature* 448: 947 – 951

Di Talia S, Wang H, Skotheim JM, Rosebrock AP, Futcher B, Cross FR (2009) Daughter-specific transcription factors regulate cell size control in budding yeast. *PLoS Biol* 7: e1000221

Dieppois G, Iglesias N, Stutz F (2006) Cotranscriptional recruitment to the mRNA export receptor Mex67p contributes to nuclear pore anchoring of activated genes. *Mol Cell Biol* 26: 7858 – 7870

Dobin A, Davis CA, Schlesinger F, Drenkow J, Zaleski C, Jha S, Batut P, Chaisson M, Gingeras TR (2013) STAR: ultrafast universal RNA-seq aligner. *Bioinformatics* 29: 15 – 21

Donnini C, Lodi T, Ferrero I, Algeri A, Puglisi PP (1992) Allelism of IMP1 and GAL2 genes of *Saccharomyces cerevisiae*. *J Bacteriol* 174: 3411 – 3415

Downey M, Johnson JR, Davey NE, Newton BW, Johnson TL, Galaang S, Seller CA, Krogan N, Toczyski DP (2015) Acetylome profiling reveals overlap in the regulation of diverse processes by sirtuins, gcn5, and esa1. *Mol Cell Proteomics* 14: 162 – 176

Doyon Y, Côté J (2004) The highly conserved and multifunctional NuA4 HAT complex. *Curr Opin Genet Dev* 14: 147 – 154

Estruch F, Peiró-Chova L, Gómez-Navarro N, Durbán J, Hodge C, Del Olmo M, Cole CN (2009) A genetic screen in *Saccharomyces cerevisiae* identifies new genes that interact with mex67-5, a temperature-sensitive allele of the gene encoding the mRNA export receptor. *Mol Gen Genomics* 281: 125 – 134

Fischer T, Strässer K, Rácz A, Rodriguez-Navarro S, Oppizzi M, Ihrig P, Lechner J, Hurt E (2002) The mRNA export machinery requires the novel Sac3p-Thp1p complex to dock at the nucleoplasmic entrance of the nuclear pores. *EMBO J* 21: 5843 – 5852

Frolov MV, Dyson NJ (2004) Molecular mechanisms of E2F-dependent activation and pRB-mediated repression. *J Cell Sci* 117: 2173 – 2181

Gallego O, Specht T, Brach T, Kumar A, Gavin A-C, Kaksonen M (2013) Detection and characterization of protein interactions *in vivo* by a simple live-cell imaging method. *PLoS One* 8: e62195

Gelperin DM, White MA, Wilkinson ML, Kon Y, Kung LA, Wise KJ, Lopez-Hoyo N, Jiang L, Piccirillo S, Yu H, *et al* (2005) Biochemical and genetic analysis of the yeast proteome with a movable ORF collection. *Genes Dev* 19: 2816 – 2826

Gomar-Alba M, Mendoza M (2019) Modulation of cell identity by modification of nuclear pore complexes. *Front Genet* 10: 1301

Goulev Y, Matifas A, Heyer V, Reina-San-Martin B, Charvin G (2019) COSPLAY: an expandable toolbox for combinatorial and swift generation of expression plasmids in yeast. *PLoS One* 14: e0220694

Goulev Y, Morlot S, Matifas A, Huang B, Molin M, Toledano MB, Charvin G (2017) Nonlinear feedback drives homeostatic plasticity in H_2O_2 stress response. *elife* 6: e23971

Hampoelz B, Andres-Pons A, Kastritis P, Beck M (2019) Structure and assembly of the nuclear pore complex. *Annu Rev Biophys* 48: 515 – 536

Helmlinger D, Tora L (2017) Sharing the SAGA. *Trends Biochem Sci* 42: 850 – 861

Henriksen P, Wagner SA, Weinert BT, Sharma S, Bacinskaja G, Rehman M, Juffer AH, Walther TC, Lisby M, Choudhary C (2012) Proteome-wide analysis of lysine acetylation suggests its broad regulatory scope in *Saccharomyces cerevisiae*. *Mol Cell Proteomics* 11: 1510 – 1522

Huang D, Kaluarachchi S, van Dyk D, Friesen H, Sopko R, Ye W, Bastajian N, Moffat J, Sassi H, Costanzo M, *et al* (2009) Dual regulation by pairs of cyclin-dependent protein kinases and histone deacetylases controls G1 transcription in budding yeast. *PLoS Biol* 7: e1000188

Ibarra A, Hetzer MW (2015) Nuclear pore proteins and the control of genome functions. *Genes Dev* 29: 337 – 349

Jacquel B, Aspert T, Laporte D, Sagot I, Charvin G (2021) Monitoring single-cell dynamics of entry into quiescence during an unperturbed life cycle. *elife* 10: e73186

Jani D, Valkov E, Stewart M (2014) Structural basis for binding the TREX2 complex to nuclear pores, GAL1 localisation and mRNA export. *Nucleic Acids Res* 42: 6686 – 6697

Janke C, Magiera MM, Rathfelder N, Taxis C, Reber S, Maekawa H, Moreno-Borchart A, Doenges G, Schwob E, Schiebel E, *et al* (2004) A versatile toolbox for PCR-based tagging of yeast genes: new fluorescent proteins, more markers and promoter substitution cassettes. *Yeast* 21: 947 – 962

Jones GM, Stalker J, Humphray S, West A, Cox T, Rogers J, Dunham I, Prelich G (2008) A systematic library for comprehensive overexpression screens in *Saccharomyces cerevisiae*. *Nat Methods* 5: 239 – 241

Kadowaki T, Hitomi M, Chen S, Tartakoff AM (1994) Nuclear mRNA accumulation causes nucleolar fragmentation in yeast mtr2 mutant. *Mol Biol Cell* 5: 1253 – 1263

Kaluarachchi Duffy S, Friesen H, Baryshnikova A, Lambert J-P, Chong YT, Figeys D, Andrews B (2012) Exploring the yeast acetylome using functional genomics. *Cell* 149: 936 – 948

Kehat I, Accornero F, Aronow BJ, Molkentin JD (2011) Modulation of chromatin position and gene expression by HDAC4 interaction with nucleoporins. *J Cell Biol* 193: 21 – 29

Kishkevich A, Cooke SL, Harris MRA, de Bruin RAM (2019) Gcn5 and Rpd3 have a limited role in the regulation of cell cycle transcripts during the G1 and S phases in *Saccharomyces cerevisiae*. *Sci Rep* 9: 1 – 9

Knockenhauer KE, Schwartz TU (2016) The nuclear pore complex as a flexible and dynamic gate. *Cell* 164: 1162 – 1171

Kumar A, Sharma P, Gomar-Alba M, Shcheprova Z, Daulny A, Sanmartín T, Matucci I, Funaya C, Beato M, Mendoza M (2018) Daughter-cell-specific modulation of nuclear pore complexes controls cell cycle entry during asymmetric division. *Nat Cell Biol* 20: 432 – 442

Kurshakova MM, Krasnov AN, Kopytova DV, Shidlovskii YV, Nikolenko JV, Nabirochkina EN, Spehner D, Schultz P, Tora L, Georgieva SG (2007) SAGA and a novel *Drosophila* export complex anchor efficient transcription and mRNA export to NPC. *EMBO J* 26: 4956 – 4965

Lee KK, Workman JL (2007) Histone acetyltransferase complexes: one size doesn't fit all. *Nat Rev Mol Cell Biol* 8: 284 – 295

Li Z, Vizeacoumar FJ, Bahr S, Li J, Warringer J, Vizeacoumar FS, Min R, VanderSluis B, Bellay J, Devit M, *et al* (2011) Systematic exploration of essential yeast gene function with temperature-sensitive mutants. *Nat Biotechnol* 29: 361 – 367

Light WH, Brickner DG, Brand VR, Brickner JH (2010) Interaction of a DNA zip code with the nuclear pore complex promotes H2A.Z incorporation and INO1 transcriptional memory. *Mol Cell* 40: 112 – 125

Longtine MS, McKenzie A, Demarini DJ, Shah NG, Wach A, Brachat A, Philippsen P, Pringle JR (1998) Additional modules for versatile and economical PCR-based gene deletion and modification in *Saccharomyces cerevisiae*. *Yeast* 14: 953 – 961

Martin M (2011) Cutadapt removes adapter sequences from high-throughput sequencing reads. *EMBnetjournal* 17: 10 – 12

Mortimer RK, Johnston JR (1986) Genealogy of principal strains of the yeast genetic stock center. *Genetics* 113: 35 – 43

Narita T, Weinert BT, Choudhary C (2019) Functions and mechanisms of non-histone protein acetylation. *Nat Rev Mol Cell Biol* 20: 156 – 174

Neurohr GE, Terry RL, Sandikci A, Zou K, Li H, Amon A (2018) Deregulation of the G1/S-phase transition is the proximal cause of mortality in old yeast mother cells. *Genes Dev* 32: 1075 – 1084

Raices M, D'Angelo MA (2021) Structure, maintenance, and regulation of nuclear pore complexes: the gatekeepers of the eukaryotic genome. *Cold Spring Harb Perspect Biol* 14: a040691

Rosebrock AP (2017) Analysis of the budding yeast cell cycle by flow cytometry. *Cold Spring Harb Protoc* 2017 https://doi.org/10.1101/pdb.prot088740

Schmoller KM, Turner JJ, Kõivomägi M, Skotheim JM (2015) Dilution of the cell cycle inhibitor Whi5 controls budding-yeast cell size. *Nature* 526: 268 – 272

Schneider M, Hellerschmied D, Schubert T, Amlacher S, Vinayachandran V, Reja R, Pugh BF, Clausen T, Köhler A (2015) The nuclear pore-associated TREX-2 complex employs mediator to regulate gene expression. *Cell* 162: 1016 – 1028

Schneiter R, Kadowaki T, Tartakoff AM (1995) mRNA transport in yeast: time to reinvestigate the functions of the nucleolus. *Mol Biol Cell* 6: 357 – 370

Skotheim JM, Di Talia S, Siggia ED, Cross FR (2008) Positive feedback of G1 cyclins ensures coherent cell cycle entry. *Nature* 454: 291 – 296

Sood V, Brickner JH (2014) Nuclear pore interactions with the genome. *Curr Opin Genet Dev* 25: 43 – 49

Sterner DE, Berger SL (2000) Acetylation of histones and transcription-related factors. *Microbiol Mol Biol Rev* 64: 435 – 459

Strässer K, Bassler J, Hurt E (2000) Binding of the Mex67p/Mtr2p heterodimer to FXFG, GLFG, and FG repeat nucleoporins is essential for nuclear mRNA export. *J Cell Biol* 150: 695 – 706

Strawn LA, Shen T, Wente SR (2001) The GLFG regions of Nup116p and Nup100p serve as binding sites for both Kap95p and Mex67p at the nuclear pore complex. *J Biol Chem* 276: 6445 – 6452

Takahata S, Yu Y, Stillman DJ (2009) The E2F functional analogue SBF recruits the Rpd3(L) HDAC, via Whi5 and Stb1, and the FACT chromatin reorganizer, to yeast G1 cyclin promoters. *EMBO J* 28: 3378 – 3389

Texari L, Dieppois G, Vinciguerra P, Contreras MP, Groner A, Letourneau A, Stutz F (2013) The nuclear pore regulates GAL1 gene transcription by controlling the localization of the SUMO protease Ulp1. *Mol Cell* 51: 807 – 818

Turner JJ, Ewald JC, Skotheim JM (2012) Cell size control in yeast. *Curr Biol* 22: R350 – R359

Umlauf D, Bonnet J, Waharte F, Fournier M, Stierle M, Fischer B, Brino L, Devys D, Tora L (2013) The human TREX-2 complex is stably associated with the nuclear pore basket. *J Cell Sci* 126: 2656 – 2667

Veening J-W, Smits WK, Kuipers OP (2008) Bistability, epigenetics, and bet-hedging in bacteria. *Annu Rev Microbiol* 62: 193 – 210

Wang H, Carey LB, Cai Y, Wijnen H, Futcher B (2009) Recruitment of Cln3 cyclin to promoters controls cell cycle entry via histone deacetylase and other targets. *PLoS Biol* 7: e1000189

Wickramasinghe VO, Andrews R, Ellis P, Langford C, Gurdon JB, Stewart M, Venkitaraman AR, Laskey RA (2014) Selective nuclear export of specific classes of mRNA from mammalian nuclei is promoted by GANP. *Nucleic Acids Res* 42: 5059 – 5071

Wickramasinghe VO, McMurtrie PIA, Mills AD, Takei Y, Penrhyn-Lowe S, Amagase Y, Main S, Marr J, Stewart M, Laskey RA (2010) mRNA export from mammalian cell nuclei is dependent on GANP. *Curr Biol* 20: 25 – 31

Expanded View Figures

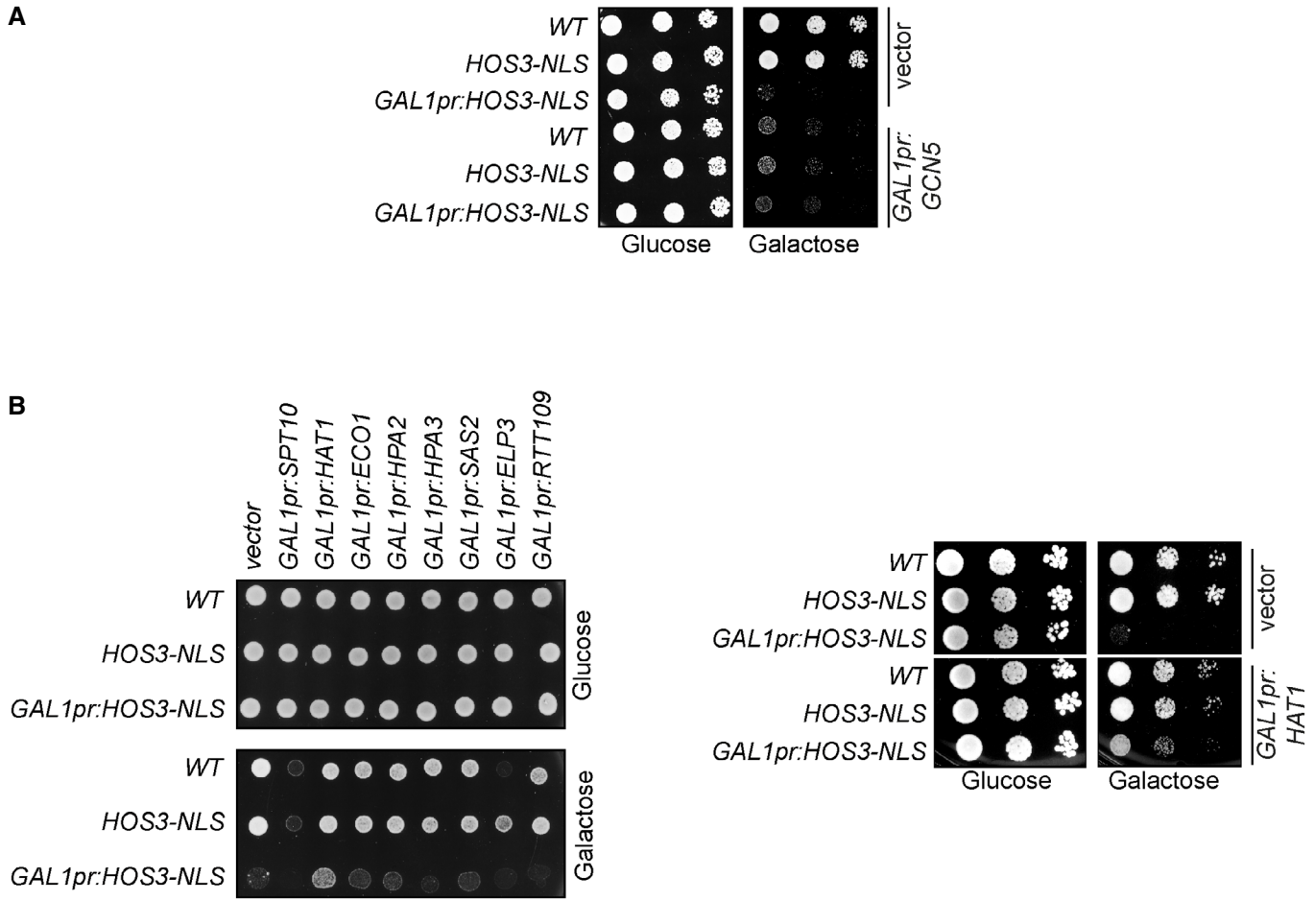

Figure EV1. Effect of KAT overexpression in Hos3-NLS-dependent growth inhibition.

A Overexpression of the KAT Gcn5 is toxic. 10-fold serial dilutions of wild-type (*WT*), *HOS3-NLS-GFP* and *GAL1pr:HOS3-NLS-GFP* (single copy at the endogenous locus) transformed with an empty vector or the *GAL1pr:GCN5-HA* plasmid were spotted onto SC-Glu and SC-Gal medium and incubated at 25°C for 3 days.

B Role of KAT overexpression in cell viability and ability to rescue growth in the presence of overexpressed *HOS3-NLS*. (*Left*) Exponential cultures of the indicated strains transformed with an empty vector or plasmids overexpressing the KATs Spt10, Eco1, Hpa2, Hpa3, Sas2, Elp3 or Rtt109 were spotted onto SC-Glu and SC-Gal medium and incubated at 25°C for 3 days. (*Right*) The effect of *HAT1* overexpression was also assessed in 10-fold serial dilutions as in (A).

Figure EV2. Role of *ESA1*, *GCN5* and *HAT1* in Start.

A *esa1-ts* and *gcn5Δ esa1-ts* mutants have bud emergence defects. Cells of the indicated strains were arrested in G1 by treatment with α-factor for 2.5 h at 25°C, shifted to 37°C for 1 h and released from the G1 arrest at 37°C. Cells were fixed at the indicated times, and the presence of buds (arrowheads) was assessed by microscopy.

B *HAT1* is not involved in Start. Bright-field images of cells of the indicated strains, treated as in (A) and scored at the indicated times after α-factor washout. The left subpanel shows the fraction of budded cells in one of two independent experiments with similar results. At least 200 cells were scored for each strain and time point. Arrowheads point to cell buds. Scale bars in (A and B), 5 μm.

Source data are available online for this figure.

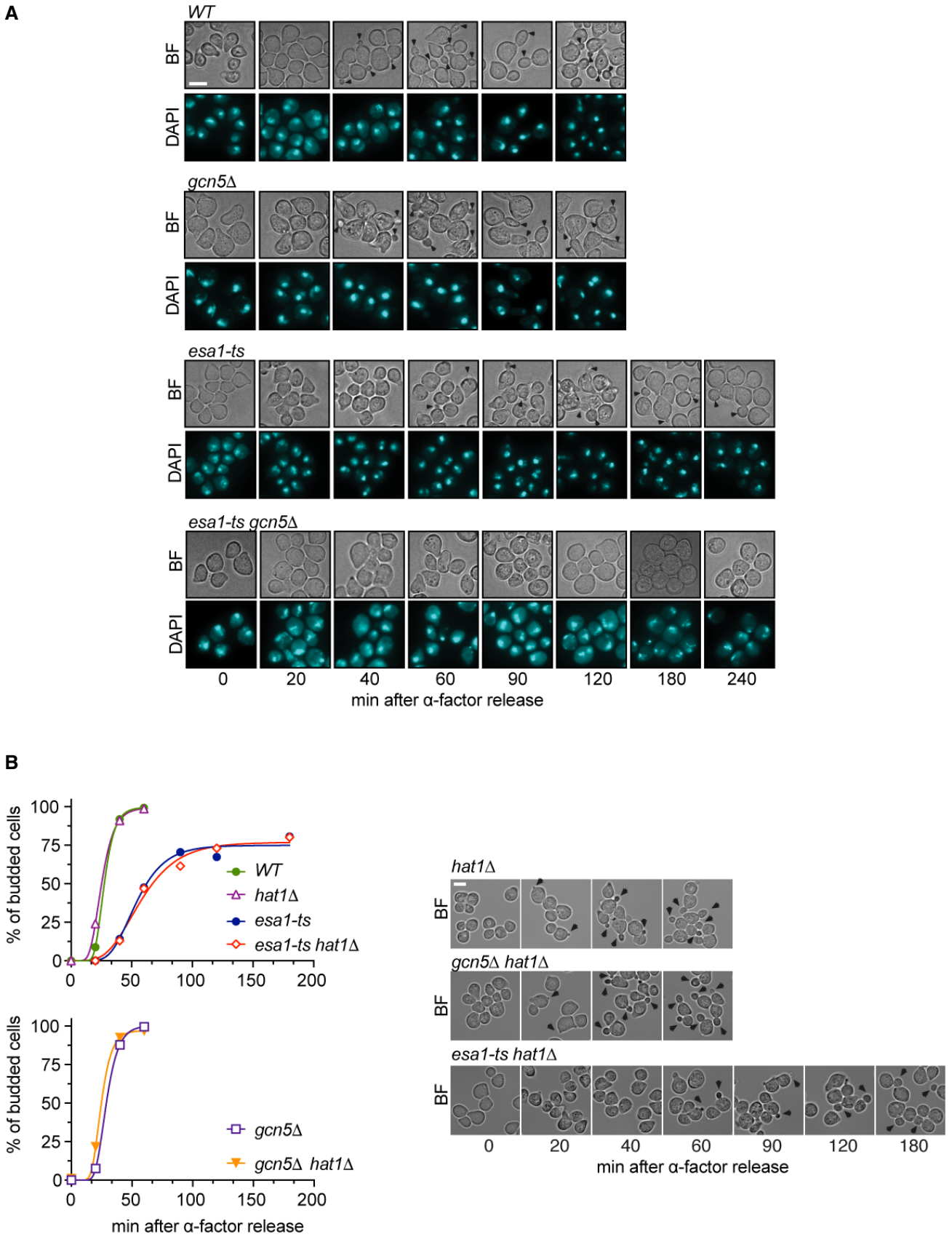

Figure EV2.

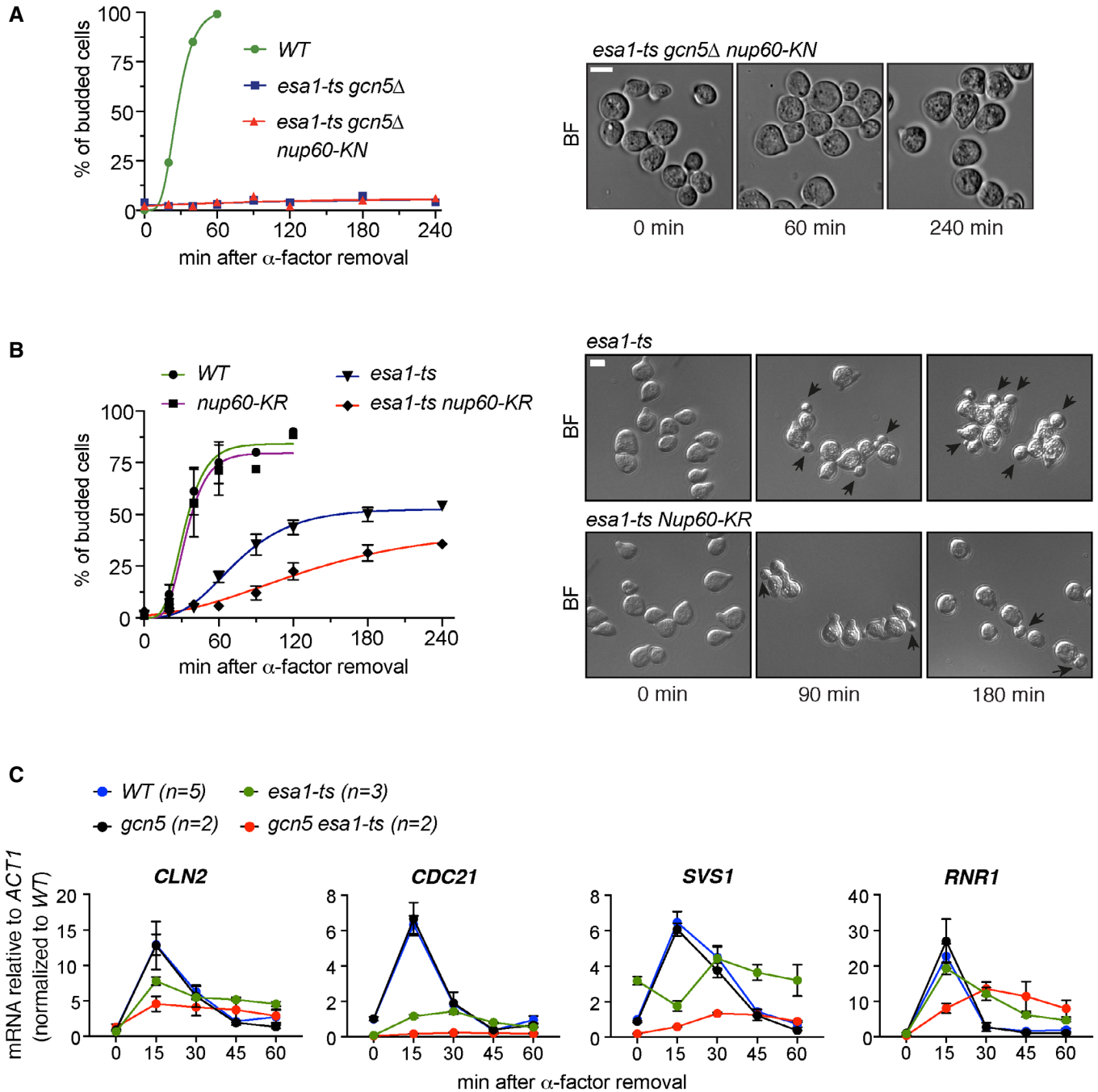

Figure EV3. G1/S transition in KAT and Nup60 KN/KR mutants.

A Acetyl-mimic Nup60-KN does not rescue the budding defect of the double mutant *esa1-ts gcn5*Δ. Cells were arrested in G1 by treatment with α-factor for 2.5 h at 25°C, shifted to 37°C for 1 h and released from the G1 arrest at 37°C. Cells were fixed at the indicated times, and the presence of buds was assessed by microscopy. The left subpanel shows the fraction of budded cells in one of two independent experiments with similar results.

B Non-acetylatable Nup60-KR increases the budding defect of *esa1-ts* cells. In (A and B), at least 200 cells were scored for each strain and time point. In (B), data from three independent experiments are represented as mean and SEM. In bright-field images of cells at the indicated times after α-factor washout, arrowheads point to cell buds.

C mRNA levels of *CLN2*, *CDC21*, *SVS1* and *RNR1* were determined for cells of the indicated strains after G1 arrest and release at restrictive temperature, with samples collected at indicated times. Data from $n > 2$ independent experiments are represented as mean and SEM (*WT*, *esa1-ts*) and data from $n = 2$ independent experiments (*gcn5*Δ, *gcn5*Δ *esa1-ts*) as mean and range. The $2^{\Delta Ct}$ values were then normalised relative to the wild-type value at 0 min.

Data information: (A, B) Scale bar, 4 μm.
Source data are available online for this figure.

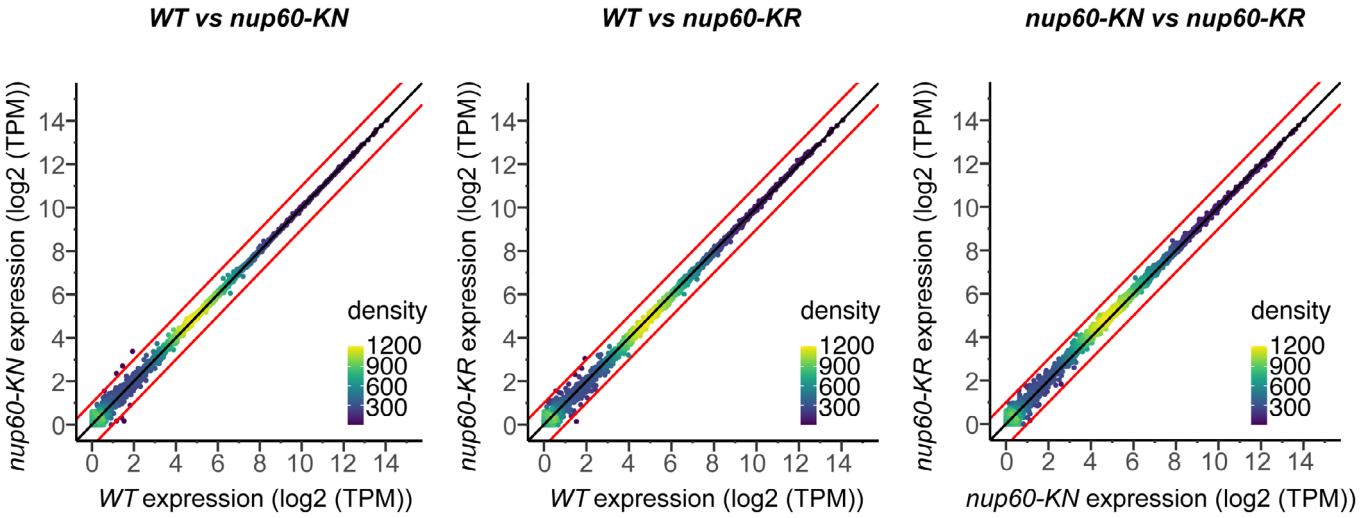

Figure EV4. Nup60-KN and Nup60-KR alleles do not alter mRNA levels.

Expression levels in *nup60-KN* and *nup60-KR* strains compared to expression in the wild-type strain (*WT*) and to each other. Red lines show a fold change of 1. Genes with FC > 1 are *YCR107W*, *YCR106W* and *YGL263W* (subtelomeric); genes with FC < −1 are *YFL065C* (subtelomeric), *YLR124W* and *tF(GAA)F* (phenylalanine tRNA).

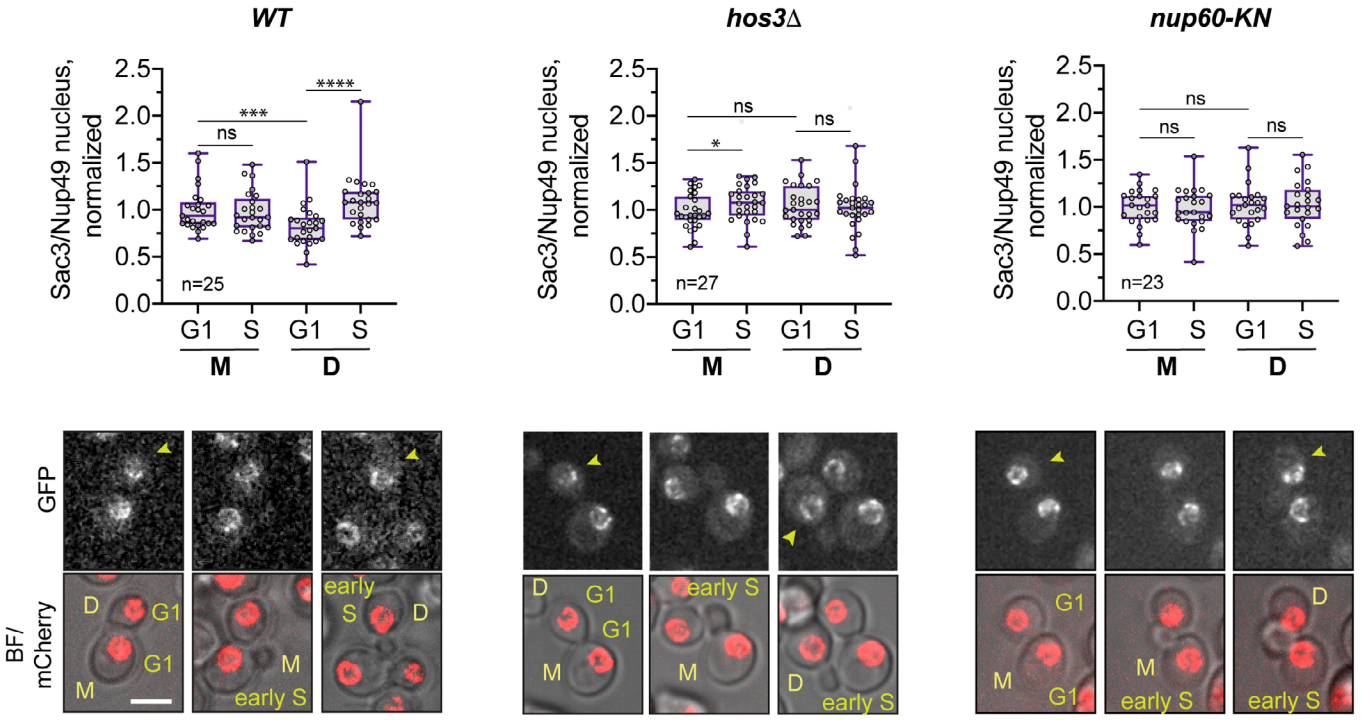

Figure EV5. Sac3 recruitment to daughter cell nuclei in G1 and S phase.

Cells of the indicated strains were imaged by time-lapse microscopy, and the fluorescence levels of Sac3-GFP and Nup49-mCherry were determined in G1 (unbudded cells after cytokinesis) and S phase (cells with small buds). The NPC component Nup49 was used as a control for nuclear pore complex protein levels. Fluorescence intensity was measured in sum projections of whole-cell Z-stacks, by segmentation of the nuclear area in the mCherry channel. The ratio of Sac3 to Nup49 intensities was then normalised relative to the mean intensity of wild-type mothers. Boxes include 50% of data points, the line represents the median, and whiskers extend to maximum and minimum values. ****, $P \leq 0.0001$; ***, $P < 0.001$, *, $P \leq 0.05$; and ns, $P > 0.05$, two-tailed paired *t*-test. Scale bar, 4 μm. *n* = number of cells, pooled from three independent experiments with similar results. Arrows point to daughter cells.

Source data are available online for this figure.

Appendix

Nuclear Pore Complex Acetylation Regulates mRNA Export and Cell Cycle Commitment in Budding Yeast

Mercè Gomar-Alba, Vasilisa Pozharskaia *et al*.

Table of contents

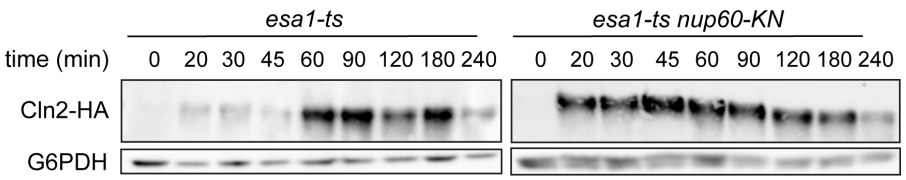

Appendix Figure S1.

***nup60-KN* mutation partially rescues the delay in synthesis of the G1/S cyclin Cln2 in *esa1-ts* cells.**

Independent biological replicates of the experiment shown in Figure 2D. Cells of the indicated strains were arrested in G1 by treatment with α-factor for 2.5 h at 25 ºC, shifted to 37 ºC for 1 h and released from the G1 arrest at 37 ºC. Samples for total protein extracts were collected at the indicated times after α-factor washout and the amount of Cln2-HA protein was assessed by western blot. G6PDH was used as loading control.

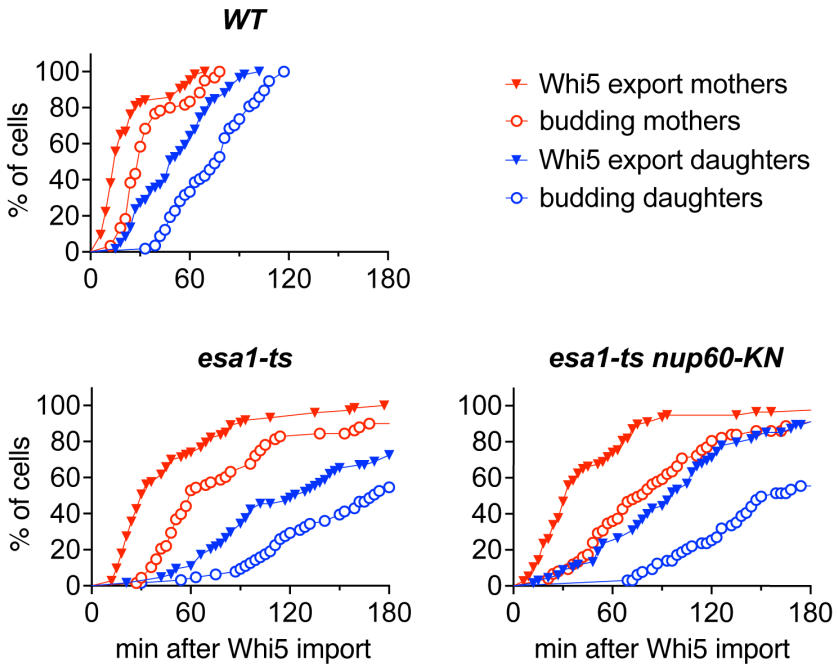

Appendix Figure S2.

Whi5-mCherry nuclear export and budding for cells in Figure 2E.
Whi5-mCherry nuclear export was scored in the fluorescence channel, and budding was scored in bright-field images (maximum projections of 3 z-confocal slices spaced 0.5 µm).

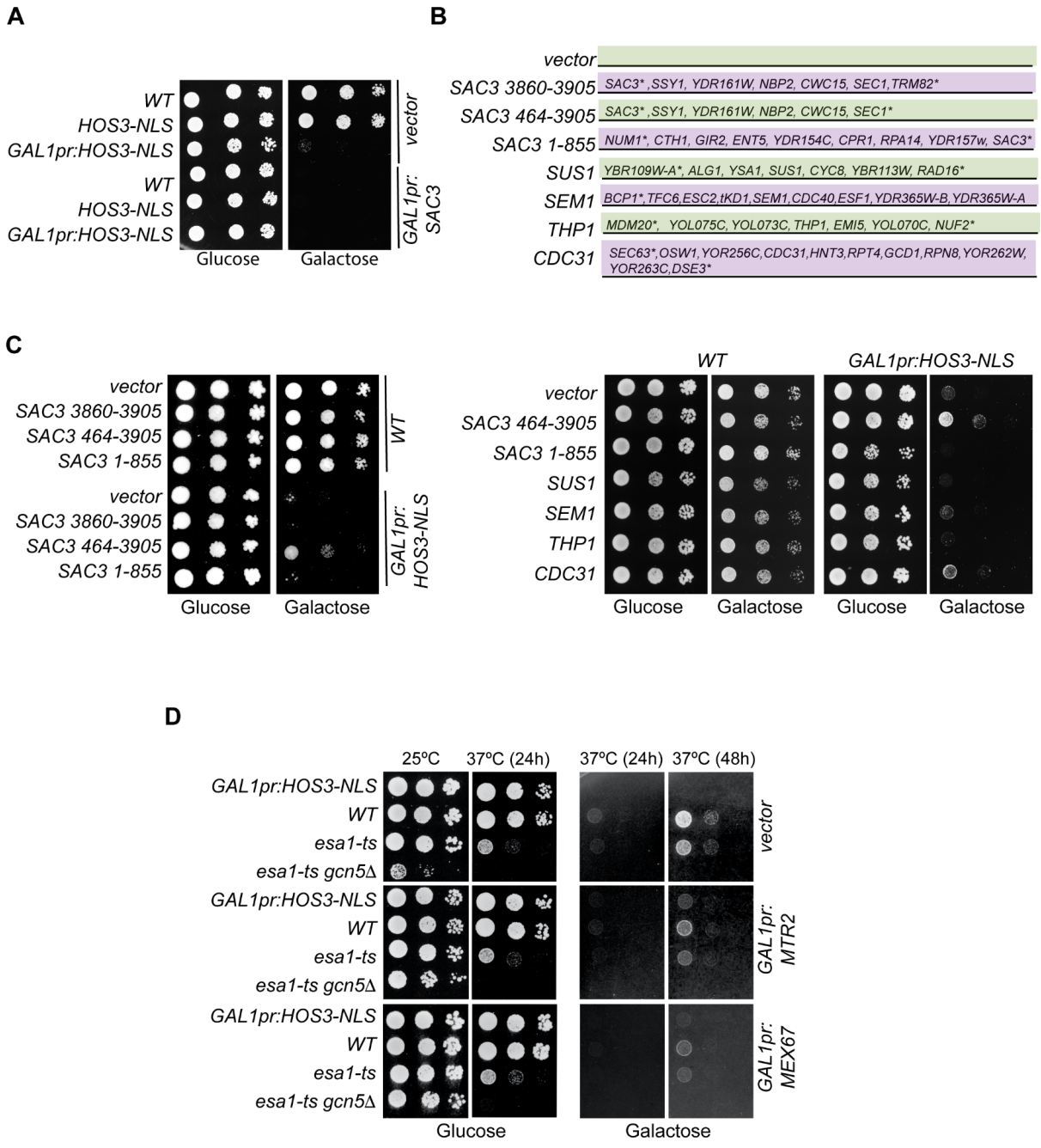

Appendix Figure S3.

Overexpression of the TREX-2 complex component Sac3 rescues the toxicity of *HOS3-NLS* overexpression.

(A) Toxicity of full-length *SAC3* overexpression. 10-fold serial dilutions of wild-type (*WT*), *HOS3-NLS-GFP* and *GAL1pr:HOS3-NLS-GFP* cultures transformed with an empty vector or the *GAL1pr:SAC3-HA* plasmid were spotted onto SC-Glu and SC-Gal medium and incubated at 25 °C for 3 days.

(B) List of high-copy (2μ) plasmids from a tiling genome library (Jones et al., 2008) containing TREX-2 complex genes (*SAC3*, *SUS1*, *CDC31*, *SEM1* and *THP1*) together with

neighboring genes. Asterisks (*) indicate that the corresponding ORFs are incomplete. Nucleotides of *SAC3* (full length 3905 nt) included in each plasmid are indicated.

(C) A high-copy plasmid containing *SAC3(464-3905)* is not toxic and relieves the toxicity of *HOS3-NLS* over-expression. 10-fold serial dilutions of wild-type (*WT*) and *GAL1pr:HOS3-NLS-GFP* cultures, transformed with an empty vector or the indicated multicopy plasmids, were spotted onto SC-Glu and SC-Gal medium and incubated at 25 °C for 3 days. Note that *SAC3(464-3905)* rescues growth of *GAL1pr:HOS3-NLS* but that the overlapping plasmid *SAC3(3860-3905)*, lacking all of *SAC3* ORF but 45 nucleotides at its 3', does not. The "vector" and *SAC3(464-3905)* sections of the left image are also shown in Figure 3C for simplicity.

(D) Overexpression of *MEX67* and *MTR2* does not rescue the growth defect of *esa1-ts* and *esa1-ts gcn5*Δ cells. 10-fold serial dilutions of the indicated strains transformed with the indicated plasmids spotted onto SC-Glu and SC-Gal medium. Due to poor growth at 37 °C on SC-gal, plates were pre-incubated for 24 or 48h at 25 °C and later incubated at indicated temperatures for up to 5 days from plating.

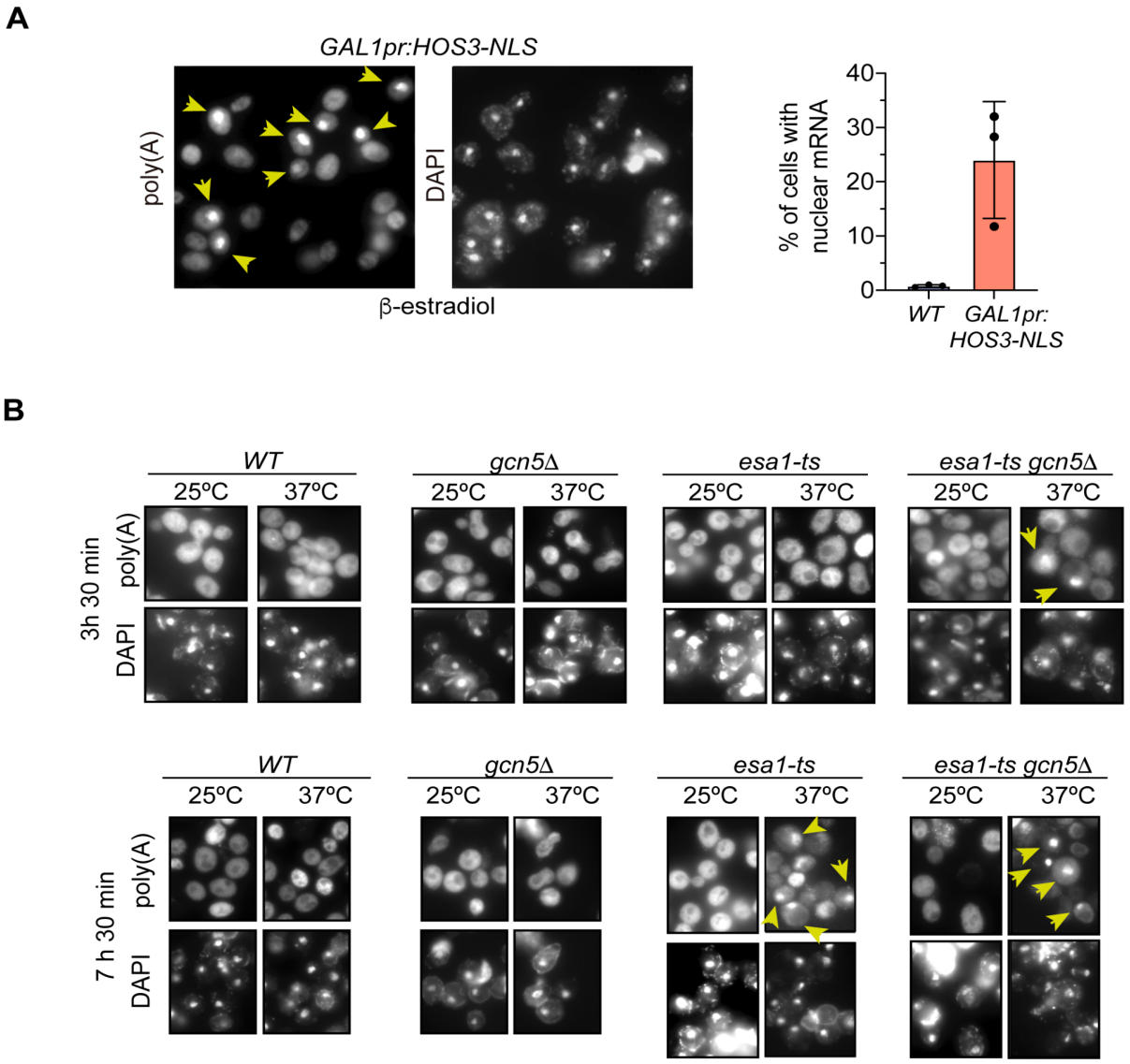

Appendix Figure S4.

Hos3-NLS overexpression or depletion of Esa1 impairs export of poly(A) RNA.
(A) Overexpression of Hos3-NLS promotes nuclear accumulation of mRNA. Cultures of the indicated strains were treated with β-estradiol (90 nM) to induce Hos3-NLS. After induction overnight, cells were fixed and FISH was performed using a Cy3-Oligo(dT) probe. Arrows point to polyadenylated RNA in the nucleus, which was visualized by DAPI staining (*left*). The fraction of cells with nuclear mRNA accumulation was determined for the indicated strains and conditions (*right*).
(B) Representative images of cells processed for poly(A) FISH as in (A) after incubation in the indicated conditions. Associated with Figure 3E.

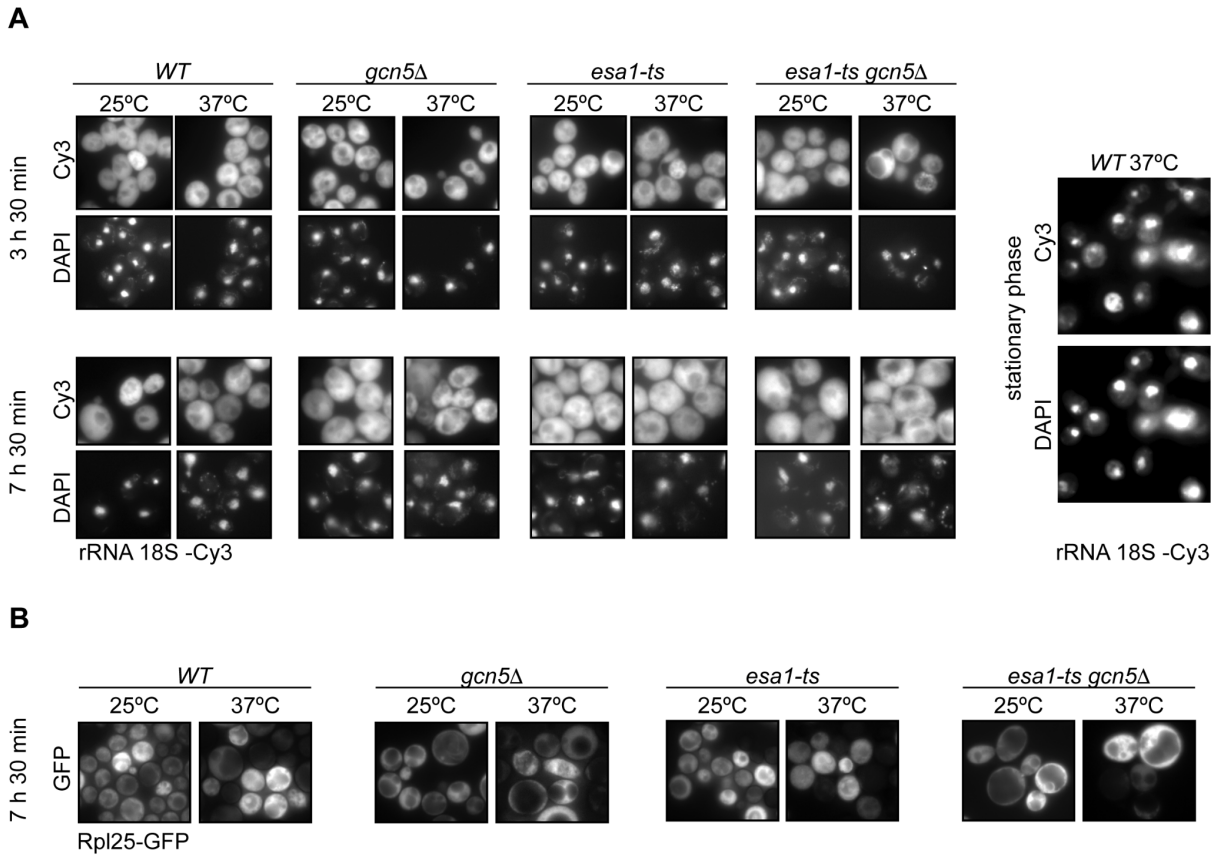

Appendix Figure S5.

Depletion of Esa1 or Gcn5 does not affect export of rRNA.

(A) Wild-type, *gcn5*Δ, *esa1-ts* and *gcn5*Δ *esa1-ts* cultures were incubated at 25ºC or 37ºC at the indicated times. In all cases, cells were fixed and in situ hybridization was performed using Cy3-TXGTTCCTCGTTAAGGXATTTACATTGTACTXCC-Cy3 to target 18S rRNA and monitor ribosomal 40S subunit nucleo/cytoplasmic distribution. DNA was visualized by DAPI staining. Cells from stationary cultures exposed to heat shock during 4h were used as positive control for nuclear accumulation of 18S rRNA.

(B) Wild-type, *gcn5*Δ, *esa1-ts* and *gcn5*Δ *esa1-ts* cultures transformed with an Rpl25-GFP plasmid as a reporter for ribosomal 60S subunit nucleo/cytoplasmic distribution were incubated at 25ºC or 37ºC for 7h and 30 min and imaged at the indicated conditions using fluorescence microscopy.

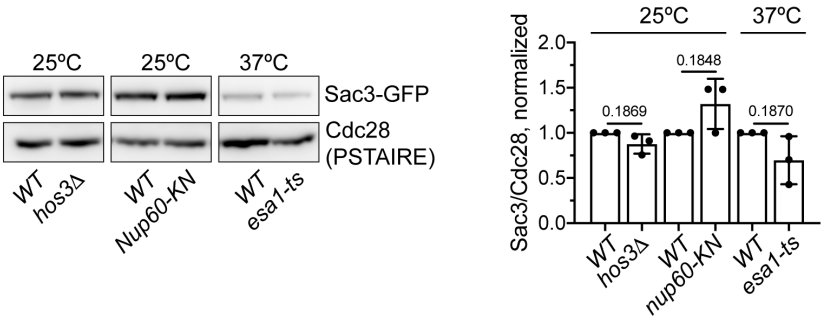

Appendix Figure S6.

Sac3 protein levels are not significantly affected by *HOS3* deletion, *nup60-KN* mutation and Esa1 inactivation.

Cells of the indicated strains were grown at 25 ºC (and shifted to 37 ºC for 2 h when indicated), and then collected for total protein extraction. Experiment was repeated three times, the result of one representative western blot is shown (*left*). The amount of Sac3-GFP protein was assessed by western blot, normalized to Cdc28 (PSTAIR) and further normalized to the WT at the corresponding temperature (*right*). Exact *p*-values from one sample t-test are given.

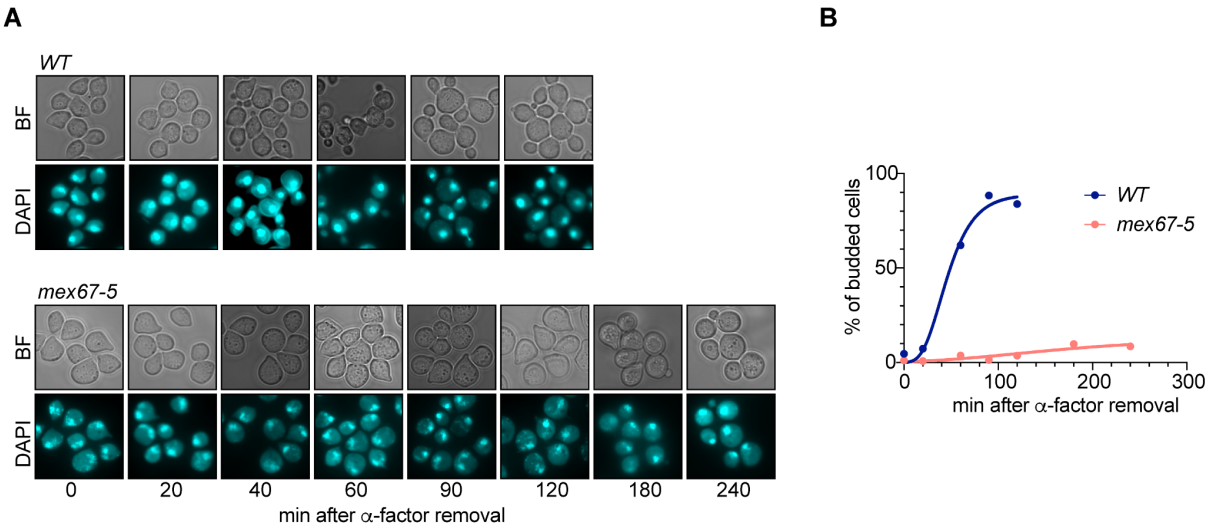

Appendix Figure S7.

Bud emergence defects in the *mex67-5* thermosensitive mutant.

(A) Bright field (BF) images of wild type (*WT*) and *mex67-5* cells at the indicated times after the α-factor washout. Cells were arrested in G1 by treatment with α-factor for 2.5 h at 25 ºC, shifted to 37 ºC for 1 h and released from the G1 arrest at 37 ºC. The DNA was visualized by DAPI staining.

(**B**) Cells were fixed at the indicated times and the presence of buds was assessed by microscopy. At least 200 cells were scored for each strain and time point.

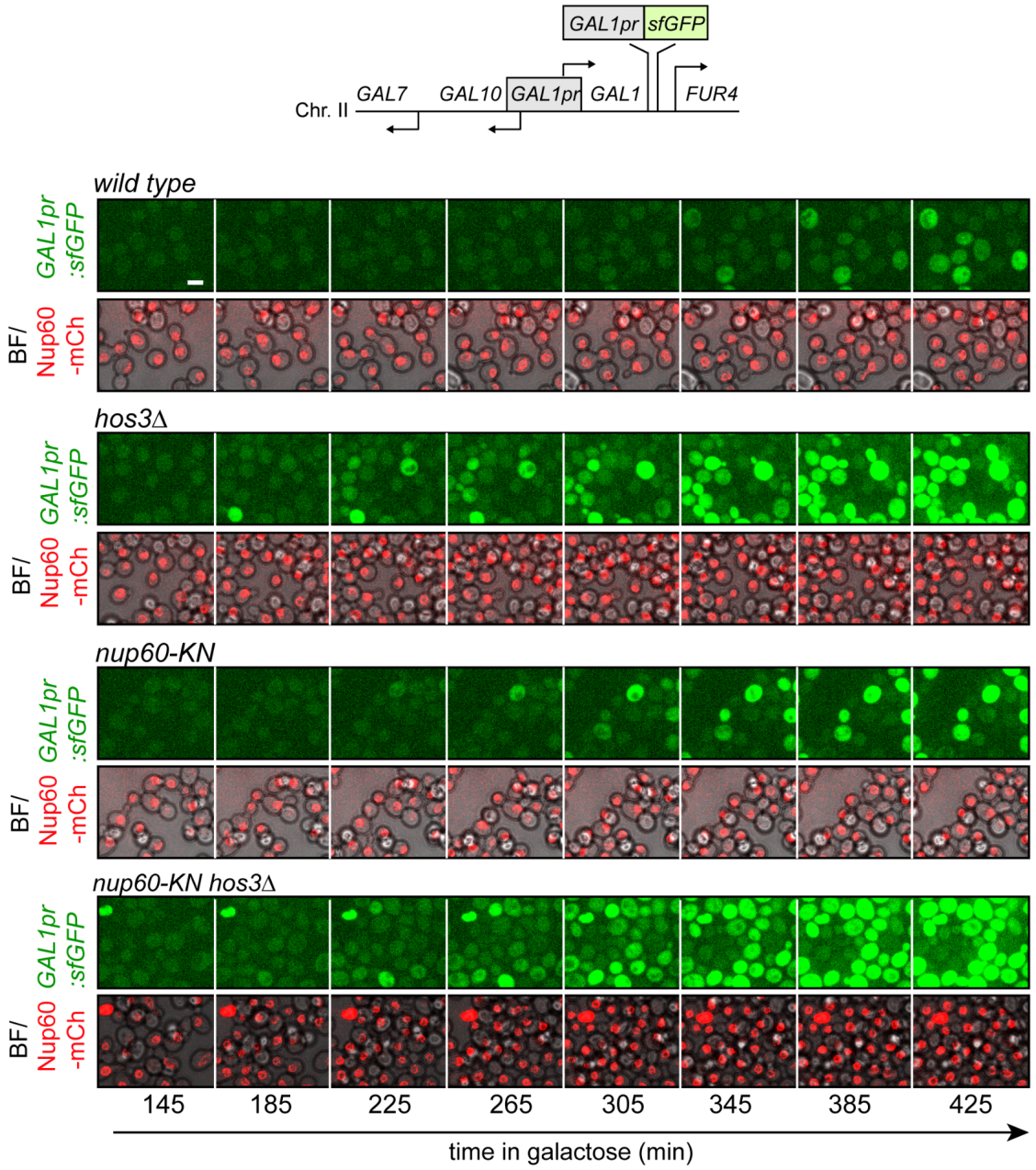

Appendix Figure S8.

Daughter-cell specific Nup60 deacetylation inhibits *GAL1* expression.
(*Top*) The *GAL1pr:sfGFP* reporter was integrated on Chr. II between the *GAL1* and *FUR4* loci. (*Bottom*) Time Lapse microscopy of *WT, hos3*Δ, *nup60-KN hos3*Δ and *nup60-KN* cells expressing *GAL1pr:sfGFP* and Nup60-mCherry at the indicated times of galactose induction. Scale bar, 4 µm.

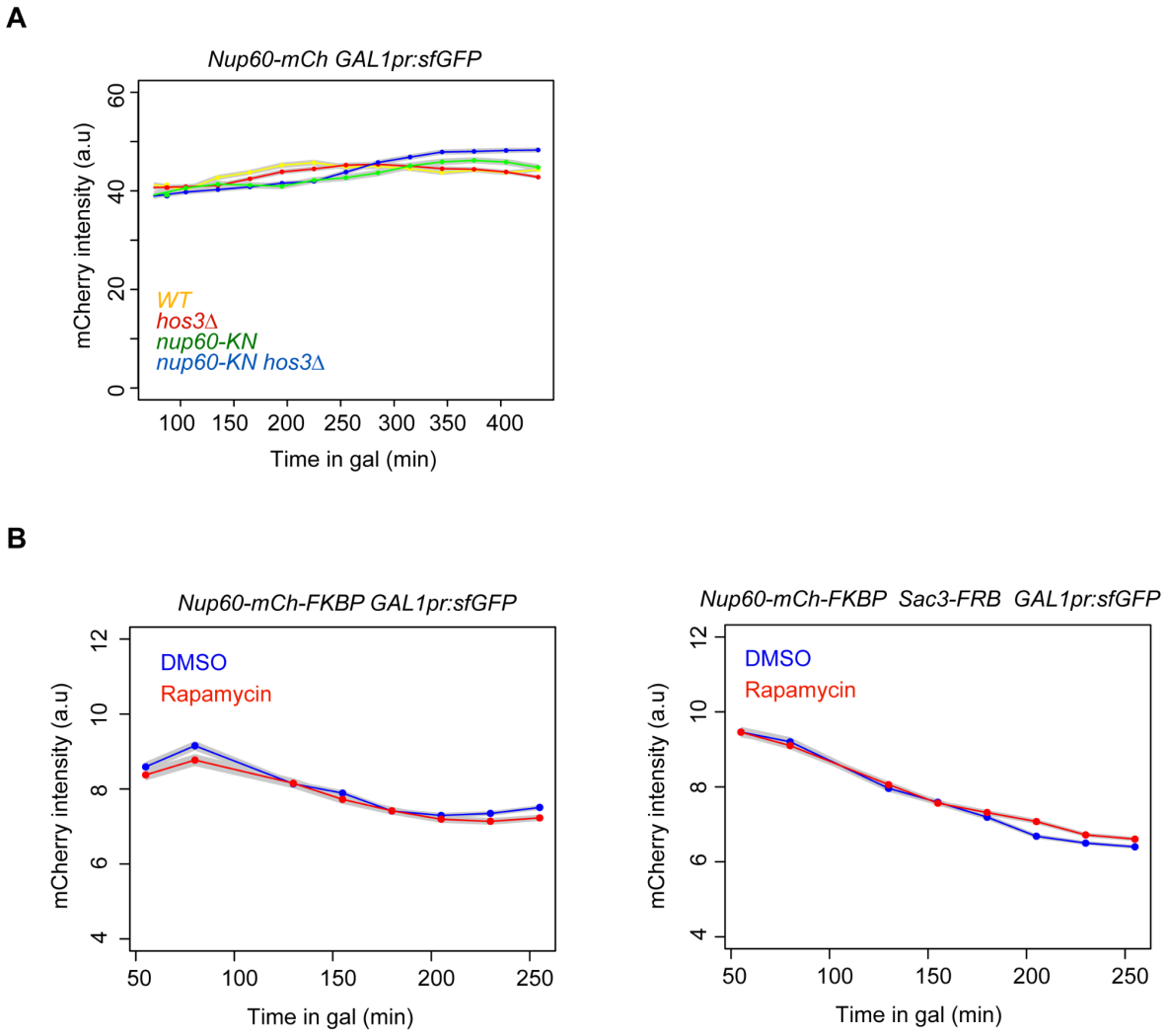

Appendix Figure S9.

Nup60 protein levels upon galactose induction of *GAL1pr:sfGFP* are not changed by the acetyl-mimic allele of Nup60 (*nup60-KN*) or Hos3 and Sac3 anchoring to NPCs.

(**A**) Cultures of *WT*, *hos3Δ, nup60-KN* and *nup60-KN hos3Δ* were shifted to galactose and imaged by Time Lapse microscopy to monitor *Nup60-mCherry* fluorescence during 7 hours of galactose induction of *GAL1pr:sfGFP* expression. Nuclear fluorescence was scored by segmentation of the nuclear area in the mCherry channel and total fluorescence of Nup60-mCherry was quantified as in Figure 6B . At least 200 cells were scored for each strain and time point. Shaded areas indicate the SEM.

(B) Cells expressing either *Nup60-mCherry-FKBP GAL1pr:sfGFP* or *Nup60-mCherry-FKBP Sac3-FRB GAL1pr:sfGFP* were incubated with rapamycin for FRB-FKBP heterodimerization or DMSO as control as in Figure 7A. Cells were imaged upon rapamycin and galactose addition and the *Nup60-mCherry* fluorescence over time was monitored as in A.

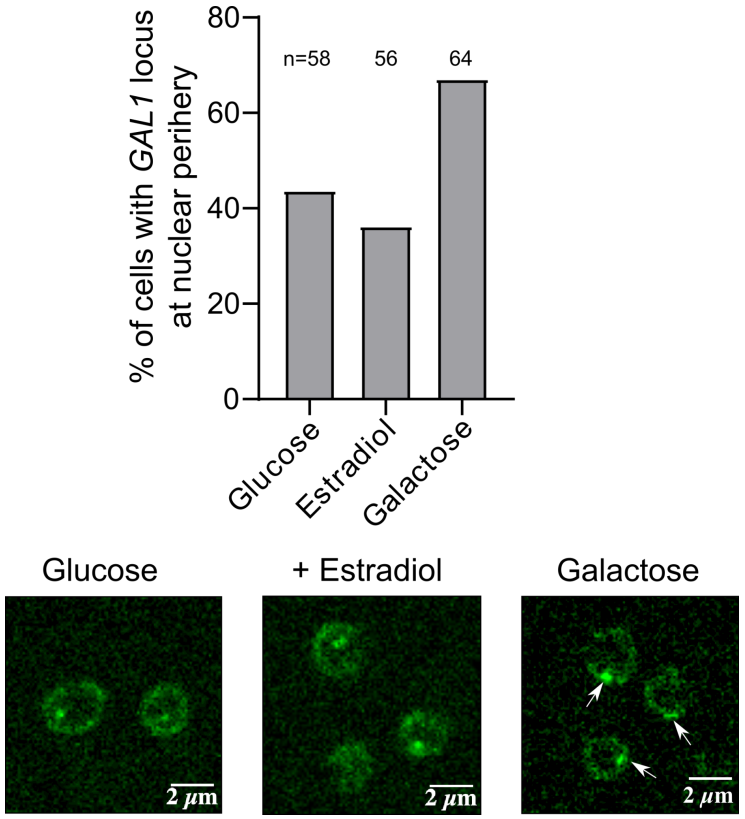

Appendix Figure S10.

The ß-estradiol-dependent GAL4-VP16 transactivator does not increase the perinuclear localization of *GAL1,10* locus.

GAL1 locus localization in cells incubated with 2% glucose (repression), or 30 minutes after addition of 2% galactose or 90 µM ß-estradiol (induction). Localisation was scored by time-lapse microscopy of *GAL10::LacO* cells expressing LacI-GFP and the ß-estradiol-dependent transactivator (GEV). Gene localization was scored as "perinuclear" (arrows) when the nuclear focus was in contact with the nuclear periphery signal (Nup49-GFP). *n* indicates the number of cells scored, which were pooled from two independent experiments.

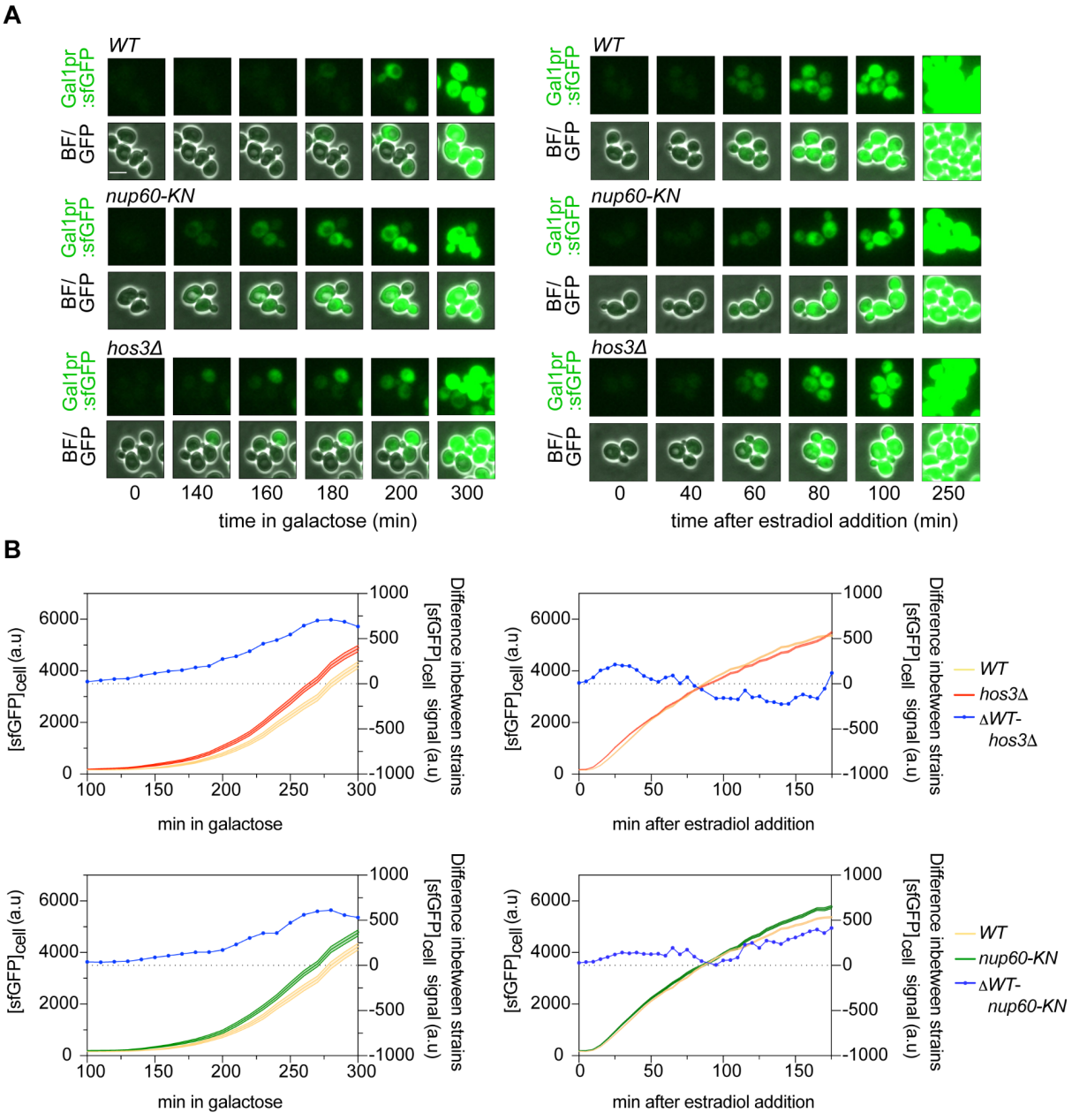

Appendix Figure S11.

Independent biological replicate of the microfluidics time lapse microscopy experiment shown in Figure 5E.

(A) GFP images, and composite of bright field and GFP, from time-lapse microscopy of *WT*, *nup60-KN* and *hos3Δ* cells expressing *GAL1pr:sfGFP* at the indicated times after addition of galactose (left panels) or ß-estradiol (right panels). Scale bar, 4 µm.

(B) sfGFP expression of *WT*, *hos3Δ* and *nup60-KN* strain after switching to 2% galactose

(top) or estradiol (bottom) containing media was monitored. Mean intensity of the sfGFP signal quantified from sum projections for each strain (*WT*, *hos3Δ* and *WT*, *nup60-KN* – left and right panel correspondingly) and the difference of mean intensity in between the strains (Δ WT-*hos3Δ* and Δ WT-*nup60-KN*)) is displayed. At least 450 cells have been quantified for each strain and time point. Shaded areas indicate the SEM.

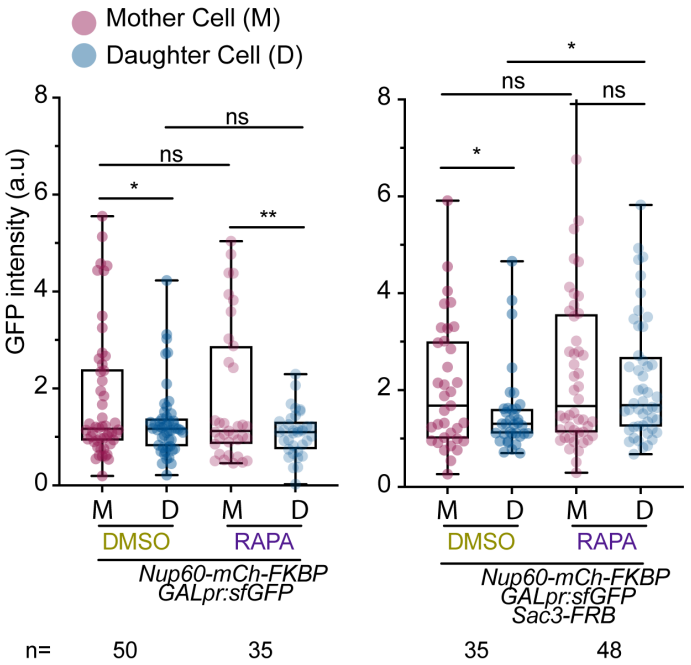

Appendix Figure S12.

Mother/daughter pairs were quantified as in Figure 7B at 200 min after galactose addition.

Boxes include 50% of data points, the line represents the median and whiskers extend to maximum and minimum values. ***, $p \leq 0.001$; **, $p \leq 0.01$; *, $p \leq 0.05$; ns, $p > 0.05$, two-tailed paired t-test for M-D comparisons, unpaired for comparisons between strains.

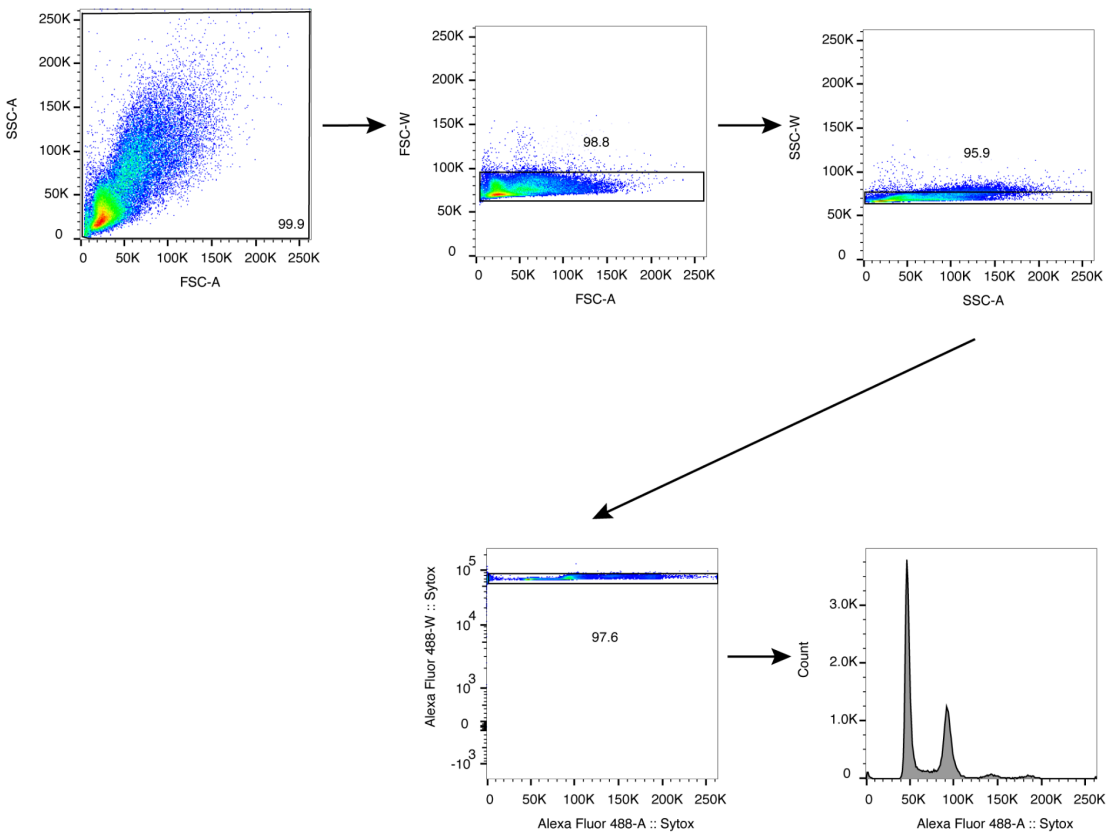

Appendix Figure S13.

Gating FACS strategy used in Figure 1D.

Shown are wild-type cells 240 minutes after the release from alpha factor block.

Appendix Table S1.

***Saccharomyces cerevisiae* strains used in this work.**

Name	Strain	Genotype	Genetic background	Source
YMM1	*wild type (WT)*	*MATa ura3-52 his3Δ200 leu2 lys2-801 ade2-101 trp1Δ63*	*S288c*	
YMM5088	*wild type (WT)*	*MATa his3 leu2 met15 ura3*	*BY4741*	
YMM5737	*gcn5Δ*	*MATa ura3-52 his3Δ200 leu2 lys2-801 ade2-101 trp1Δ63 gcn5Δ::kanMX6*	*S288c*	This study
YMM5671	*esa1-ts*	*MATa ura3-52 his3Δ200 leu2 lys2-801 ade2-101 trp1Δ63 esa1-L254P::KANMX*	*S288c*	This study
YMM5686	*gcn5Δ esa1-ts*	*MATa ura3-52 his3Δ200 leu2 lys2-801 ade2-101 trp1Δ63 esa1-L254P::KANMX gcn5Δ::kanMX6*	*S288c*	This study
YMM2936	*HOS3-NLS-GFP*	*MATa ura3-52 his3Δ200 leu2 ls2-801 ade2-101 trp1Δ63 HOS3-GFP::KAN*	*S288c*	Kumar et al., 2018
YMM3073	*GAL1pr:HOS3-NLS-GFP MYO1-mCherry*	*MATa ura3-52 his3Δ200 leu2 lys2-801 ade2-101 trp1Δ63 natNT2::GAL1pr-HOS3-NLS-GFP::KAN MYO1-mCherry::hphNT1*	*S288c*	Kumar et al., 2018
YMM5121	*GAL1pr:HOS3-NLS-GFP*	*ura3-52 his3Δ200 leu2 lys2-801 ade2-101 trp1Δ63 natNT2::GAL1pr-HOS3-NLS-GFP::KAN*	*S288c*	This study
YMM5123	*GAL1pr:HOS3(EN)-NLS-GFP*	*ura3-52 his3Δ200 leu2 lys2-801 ade2-101 trp1Δ63 natNT2::GALpr-hos3-EN(H196E D231A)-NLS-GFP::KAN*	*S288c*	This study
YMM3861	*GAL1pr:HOS3-NLS-GFP MYO1-mCherry ADGEV*	*MATa ura3-52 his3Δ200 leu2 lys2-801 ade2-101 trp1Δ63 natNT2::GAL1pr-HOS3-NLS-GFP::KAN MYO1-mCherry::hphNT1 ADHpr:GAL4-ER-VP16::URA3 (ADGEV)*	*S288c*	Kumar et al., 2018
YMM5761	*NUP60-GFP*	*MATa ura3-52 his3Δ200 leu2 lys2-801 ade2-101 trp1Δ63 NUP60-GFP::HIS3MX6*	*S288c*	This study
YMM5763	*nup60-KN-GFP*	*MATa ura3-52 his3Δ200 leu2 lys2-801 ade2-101 trp1Δ63 nup60(K467N)-GFP::HIS3MX6*	*S288c*	This study
YMM5769	*esa1-ts NUP60-GFP*	*ura3-52 his3Δ200 leu2 lys2-801 ade2-101 trp1Δ63 NUP60-GFP::HIS3MX6 esa1-L254P::kanMX*	*S288c*	This study
YMM5771	*esa1-ts nup60-KN-GFP*	*ura3-52 his3Δ200 leu2 lys2-801 ade2-101 trp1Δ63 nup60(K467N)-GFP::HIS3MX6 esa1-L254P::kanMX*	*S288c*	This study
YMM5027	*CLN2-HA*	*MATa ura3-52 his3Δ200 leu2 lys2-801 ade2-101 trp1Δ63 CLN2-6xHA::HIS3*	*S288c*	This study
JCY2452	*esa1-ts NUP60-GFP CLN2-HA*	*MATa ura3-52 his3Δ200 leu2 lys2-801 ade2-101 trp1Δ63 NUP60-GFP::HIS3MX6 esa1-L254P::kanMX CLN2-6xHA::hphNT1*	*S288c*	This study

JCY2450	*esa1-ts nup60-KN-GFP CLN2-HA*	*MATa ura3-52 his3Δ200 leu2 lys2-801 ade2-101 trp1Δ63 nup60(K467N)-GFP::HIS3MX6 esa1-L254P::kanMX CLN2-6xHA::hphNT1*	*S288c*	This study
YMM5036	*mex67-5*	*MATa leu2Δ1 ura3-52 trp1Δ63 mex67-5::natNT2*	*FY86*	Scarcelli et al., 2007
YMM5117	*SAC3-GFP NUP49-3xmCherry*	*MATa ura3-52 his3Δ200 leu2 lys2-801 ade2-101 trp1Δ63 SAC3-GFP::KAN NUP49-3xmCherry::hphNT1*	*S288c*	This study
YMM5119	*hos3Δ SAC3-GFP NUP49-3xmCherry*	*MATa ura3-52 his3Δ200 leu2 lys2-801 ade2-101 trp1Δ63 SAC3-GFP::KAN NUP49-3xmCherry::hphNT1 hos3Δ::natNT2*	*S288c*	This study
YMM5351	*SAC3-GFP NUP49-3xmCherry*	*MATα ura3-52 his3Δ200 leu2 lys2-801 ade2-101 trp1Δ63 SAC3-GFP::TRP NUP49-3xmCherry::hphNT1*	*S288c*	This study
YMM5353	*SAC3-GFP nup60-KN NUP49-3xmCherry*	*ura3-52 his3Δ200 leu2 lys2-801 ade2-101 trp1Δ63 SAC3-GFP::TRP NUP49-3xmCherry::hphNT1 nup60(K467N)*	*S288c*	This study
YMM5675	*SAC3-GFP NUP49-3xmCherry esa1-ts*	*MATα ura3-52 his3Δ200 leu2 lys2-801 ade2-101 trp1Δ63 SAC3-GFP::TRP1 NUP49-3xmCherry::hphNT1 esa1-L254P::kanMX*	*S288c*	This study
YMM5549	*GAL1pr:sfGFP-CLN 2PEST nup60-mCherry*	*MATa his3 leu2 met15 ura3 GAL1pr:sfGFP-CLN2PEST::KAN NUP60-mCherry::hphNT1*	*BY4741*	This study
YMM5622	*hos3Δ GAL1pr:sfGFP-CLN 2PEST nup60-mCherry*	*MATa his3 leu2 met15 ura3 GAL1pr:sfGFP-CLN2PEST::KAN hos3Δ::natNT2 NUP60-mCherry::hphNT1*	*BY4741*	This study
YMM5557	*GAL1pr:sfGFP-CLN 2PEST nup60-KN-mCherry*	*MATa his3 leu2 met15 ura3 GAL1pr:sfGFP-CLN2PEST::KAN nup60(K467N)-mCherry::hphNT1*	*BY4741*	This study
YMM5721	*hos3Δ GAL1pr:sfGFP-CLN 2PEST nupP60-KN-mCherr y*	*MATa his3 leu2 met15 ura3 GAL1pr:sfGFP-CLN2PEST::KAN hos3Δ::natNT2 nup60(K467N)-mCherry::hphNT1*	*BY4741*	This study
YMM5653	*nup60-mCherry-FK BP SAC3-FRB-GFP*	*MATα his3Δ1 leu2Δ0 ura3Δ0 LYS+, Can1::Ste2pr-Leu2, Lyp1::, tor1-1, Fpr1::Ura NUP60-mCherry-FKBP::natNT2 SAC3-FRB-GFP::KAN*	*BY4742*	This study
YMM5637	*GAL1pr:sfGFP-CLN 2PEST NUP60-mCherry-FK BP*	*MATα his3Δ1 leu2Δ0 ura3Δ0 LYS+, Can1::Ste2pr-Leu2, Lyp1::, tor1-1, Fpr1::Ura NUP60-mCherry-FKBP::natNT2 GAL1pr:sfGFP-CLN2PEST::KAN*	*BY4742*	This study
YMM5657	*GAL1pr:sfGFP-CLN 2PEST NUP60-mCherry-FK BP SAC3-FRB*	*MATα his3Δ1 leu2Δ0 ura3Δ0 LYS+, Can1::Ste2pr-Leu2, Lyp1::, tor1-1, Fpr1::Ura NUP60-mCherry-FKBP::natNT2 GAL1pr:sfGFP-CLN2PEST::KAN SAC3-FRB::hphNT1*	*BY4742*	This study

YMM5844	*SAC3-mCherry-FKBP NUP60-FRB WHI5-GFP esa1-ts*	*MATα his3Δ1 leu2Δ0 ura3Δ0 LYS+, Can1::Ste2pr-Leu2, Lyp1::, tor1-1, Fpr1::Ura SAC3-mCherry-FKBP::natNT2 NUP60-FRB::hphNT1 esa1-L254P::kanMX WHI5-GFP::HIS3MX6*	*BY4742*	This study
YMM5848	*SAC3-mCherry-FKBP NUP60-FRB WHI5-GFP*	*MATα his3Δ1 leu2Δ0 ura3Δ0 LYS+, Can1::Ste2pr-Leu2, Lyp1::, tor1-1, Fpr1::Ura SAC3-mCherry-FKBP::natNT2NT2 NUP60-FRB::hphNT1 WHI5-GFP::HIS3MX6*	*BY4742*	This study
YMM5850	*NUP60-GFP WHI5-mCherry*	*MATa ura3-52 his3Δ200 leu2 lys2-801 ade2-101 trp1Δ63 NUP60-GFP::HIS3MX6 WHI5-mCherry::hphNT1*	*S288c*	This study
YMM5854	*NUP60-GFP WHI5-mCherry esa1-ts*	*MATa ura3-52 his3Δ200 leu2 lys2-801 ade2-101 trp1Δ63 esa1-L254P::kanMX NUP60-GFP::HIS3MX6 WHI5-mCherry::hphNT1*	*S288c*	This study
YMM5860	*nup60-KN-GFP WHI5-mCherry esa1-ts*	*MATa ura3-52 his3Δ200 leu2 lys2-801 ade2-101 trp1Δ63 nup60(K467N)-GFP::HIS3MX6 WHI5-mCherry::hphNT1 esa1-L254P::kanMX*	*S288c*	This study
YMM5773	*gcn5Δ esa1-ts NUP60-GFP*	*MATa ura3-52 his3Δ200 leu2 lys2-801 ade2-101 trp1Δ63 NUP60-GFP::HIS3MX6 esa1-L254P::kanMX gcn5Δ::kanMX6*	*S288c*	This study
YMM5775	*gcn5Δ esa1-ts nup60-KN-GFP*	*MATa ura3-52 his3Δ200 leu2 lys2-801 ade2-101 trp1Δ63 nup60-KN-GFP::HIS3MX6 esa1-L254P::kanMX gcn5Δ::kanMX6*	*S288c*	This study
YMM5019	*CLN2-PP7 NLS-PCP-EGFP WHI5-tdTomato*	*MATa, ADE2, leu2-3, ura3, trp1-1, his3-11,15, can1-100, psi+, WHI5- tdTOMATO::KAN, URA::NAT::pCYC1-NLS-PCP-GFP-ADH1term::ura3 CLN2- 24xPP7SL::loxP*	*W303*	Neurohr et al., 2018
YMM6020	*CLN2-PP7 NLS-PCP-EGFP WHI5-tdTomato NUP60-6xHA*	*MATa, ADE2, leu2-3, ura3, trp1-1, his3-11,15, can1-100, psi+, WHI5- tdTOMATO::KAN, URA::NAT::pCYC1-NLS-PCP-GFP-ADH1term::ura3 CLN2- 24xPP7SL::loxP NUP60-6xHA::HIS3MX6*	*W303*	This study
YMM6022	*CLN2-PP7 NLS-PCP-EGFP WHI5-tdTomato NUP60-6xHA esa1-ts*	*MATa, ADE2, leu2-3, ura3, trp1-1, his3-11,15, can1-100, psi+, WHI5- tdTOMATO::KAN, URA::NAT::pCYC1-NLS-PCP-GFP-ADH1term::ura3 CLN2- 24xPP7SL::loxP NUP60-6xHA::HIS3MX6 esa1-ts::hphNT1*	*W303*	This study
YMM6026	*CLN2-PP7 NLS-PCP-EGFP WHI5-tdTomato nup60-KN-6xHA esa1-ts*	*MATa, ADE2, leu2-3, ura3, trp1-1, his3-11,15, can1-100, psi+, WHI5- tdTOMATO::KAN, URA::NAT::pCYC1-NLS-PCP-GFP-ADH1term::ura3 CLN2- 24xPP7SL::loxP nup60(K467N)-6xHA::HIS3MX6 esa1-ts::hphNT1*	*W303*	This study
YMM6077	*NUP60-GFP*	*MATa ura3-52 his3Δ200 leu2 lys2-801 ade2-101 trp1Δ63 NUP60-GFP::HIS3MX6*	*S288c*	This study

YMM6081	*nup60-KR-GFP*	*MATa ura3-52 his3Δ200 leu2 lys2-801 ade2-101 trp1Δ63 nup60(K467R)-GFP::HIS3MX6*	*S288c*	This study
YMM6085	*NUP60-GFP esa1-ts*	*MATa ura3-52 his3Δ200 leu2 lys2-801 ade2-101 trp1Δ63 NUP60-GFP::HIS3MX6 esa1-ts::kanMX*	*S288c*	This study
YMM6087	*nup60-KR-GFP esa1-ts*	*MATa ura3-52 his3Δ200 leu2 lys2-801 ade2-101 trp1Δ63 nup60(K467R)-GFP::HIS3MX6 esa1-ts::kanMX*	*S288c*	This study
YMM6070	*hat1*Δ	*MATa ura3-52 his3Δ200 leu2 lys2-801 ade2-101 trp1Δ63 hat1Δ::natNT2*	*S288c*	This study
YMM6072	*gcn5Δ hat1*Δ	*MATa ura3-52 his3Δ200 leu2 lys2-801 ade2-101 trp1Δ63 gcn5Δ::kanMX6 hat1Δ::natNT2*	*S288c*	This study
YMM6070	*esa1-ts hat1*Δ	*MATa ura3-52 his3Δ200 leu2 lys2-801 ade2-101 trp1Δ63 hat1Δ::natNT2 esa1-ts::kanMX*	*S288c*	This study
YMM3836	*Gal10-LacO LacI-GFP NUP49-GFP*	*MATa ura3-52 his3Δ200 leu2 lys2-801 ade2-101 trp1Δ63 LacI-GFP::HIS Gal10-LacO::TRP NUP49-GFP*	*W303*	Susan Gasser lab
YMM6104	*Gal10-LacO LacI-GFP NUP49-GFP Gal4-ER-VP16 (ADEGV)*	*MATa ura3-52 his3Δ200 leu2 lys2-801 ade2-101 trp1Δ63 LacI-GFP::HIS Gal10-LacO::TRP NUP49-GFP Adh1pr-Gal4-ER-VP16::URA*	*W303*	This study
YMM6101	*Gal4-ER-VP16(ADE GV)*	*MATα leu2-3,112 trp1-1 can1-100 ura3-1 ade2-1 his3-11,15 Gal4-ER-VP16::ADE*	*W303*	This study
YMM6140	*sfGFP-CLN2PEST Nup60-mCherry Gal4-ER-VP16(ADE GV)*	*MATα leu2-3,112 trp1-1 can1-100 ura3-1 ade2-1 his3-11,15 GAL1pr:sfGFP-CLN2PEST::KAN Nup60mCherry::hphNT1 Gal4-ER-VP16::ADE*	*W303*	This study
YMM6142	*sfGFP-CLN2PEST Nup60KN-mCherry Gal4-ER-VP16(ADE GV)*	*MATα leu2-3,112 trp1-1 can1-100 ura3-1 ade2-1 his3-11,15 GAL1pr:sfGFP-CLN2PEST::KAN Nup60(K467N)mCherry::hphNT1 Gal4-ER-VP16::ADE*	*W303*	This study
YMM6144	*sfGFP-CLN2PEST hos3Δ Nup60-mCherry Gal4-ER-VP16(ADE GV)*	*MATα leu2-3,112 trp1-1 can1-100 ura3-1 ade2-1 his3-11,15 hos3Δ::natNT2 GAL1pr:sfGFP-CLN2PEST::KAN Nup60mCherry::hphNT1 Gal4-ER-VP16::ADE*	*W303*	This study
YMM6138	*NUP60-GFP gcn5Δ*	*MATa ura3-52 his3Δ200 leu2 lys2-801 ade2-101 trp1Δ63 NUP60-GFP::HIS3 gcn5Δ::kanMX6*	*S288c*	This study

Article 2

Impact of chromosome fusions on 3D genome organization and gene expression in budding yeast

In this article, we used budding yeast chromosome fusions and 3D chromatin modeling to reveal mild but consistent and genomewide transcription changes upon global changes in nuclear organization. These changes are well correlated with changes in distance from the periphery and are most prominent for subtelomeric genes. Once the chromosomes are fused, one of the centromeres needs stay active (this chromosome is termed donor), while others need to be inactivated (termed acceptor). Some predictions of the interphase chromatin bead-and-string polymer model upon chromosome fusions include that the donor chromosomes are displaced from the SPB; that chromosome regions next to the telomeres are displaced from the periphery; and that the distance between chromosome loci in the donor chromosome are reduced, implying higher level of compaction upon increased physical constraints of interphase chromatin.

Here I did a minor contribution in finishing strain construction of some of the strains and performing the microscopy experiments and data analysis for Fig.6C,D in order to validate the results of the modeling.

Impact of Chromosome Fusions on 3D Genome Organization and Gene Expression in Budding Yeast

Marco Di Stefano,[*,†,1] Francesca Di Giovanni,[†,1] Vasilisa Pozharskaia,[‡,§,,††] Mercè Gomar-Alba,[‡,§,**,††] Davide Baù,[*,†] Lucas B. Carey,[‡‡,§§,2] Marc A. Marti-Renom,[*,***,2] and Manuel Mendoza[†,‡,§,**,††,†††,2]**

[*]CNAG-CRG, The Barcelona Institute of Science and Technology (BIST), 08028 Barcelona, Spain, [†]Centre for Genomic Regulation (CRG), The Barcelona Institute of Science and Technology (BIST), 08003 Barcelona, Spain, [‡]Institut de Génétique et de Biologie Moléculaire et Cellulaire, 67404 Illkirch, France, [§]Centre National de la Recherche Scientifique, UMR7104, 67404 Illkirch, France, [**]Institut National de la Santé et de la Recherche Médicale, U964, 67404 Illkirch, France, [††]Université de Strasbourg, 67000 Strasbourg, France, [‡‡]Center for Quantitative Biology and [§§]Peking-Tsinghua Center for the Life Sciences, Academy for Advanced Interdisciplinary Studies, Peking University, 100871 Beijing, China, [***]ICREA, 08010 Barcelona, Spain, and [†††]Universitat Pompeu Fabra (UPF), 08002 Barcelona, Spain

ORCID IDs: 0000-0001-6195-4754 (M.D.S.); 0000-0002-6091-9129 (V.P.); 0000-0002-7210-0364 (M.G.-A.); 0000-0002-7245-6379 (L.B.C.); 0000-0001-5522-4878 (M.M.)

ABSTRACT The three-dimensional (3D) organization of chromosomes can influence transcription. However, the frequency and magnitude of these effects remain debated. To determine how changes in chromosome positioning affect transcription across thousands of genes with minimal perturbation, we characterized nuclear organization and global gene expression in budding yeast containing chromosome fusions. We used computational modeling and single-cell imaging to determine chromosome positions, and integrated these data with genome-wide transcriptional profiles from RNA sequencing. We find that chromosome fusions dramatically alter 3D nuclear organization without leading to strong genome-wide changes in transcription. However, we observe a mild but significant and reproducible increase in the expression of genes displaced away from the periphery. The increase in transcription is inversely proportional to the propensity of a given locus to be at the nuclear periphery; for example, a 10% decrease in the propensity of a gene to reside at the nuclear envelope is accompanied by a 10% increase in gene expression. Modeling suggests that this is due to both deletion of telomeres and to displacement of genes relative to the nuclear periphery. These data suggest that basal transcriptional activity is sensitive to radial changes in gene position, and provide insight into the functional relevance of budding yeast chromosome-level 3D organization in gene expression.

KEYWORDS budding yeast; computational modeling; gene expression; nuclear organization; single-cell imaging

CHROMOSOMES in interphase nuclei are spatially distributed in a nonrandom manner. Indeed, chromosomes are organized in distinct structural units and their organization influences nuclear functions such as transcription, replication, and DNA damage repair [reviewed in Gibcus and Dekker (2013), Furlan-Magaril *et al.* (2015), Lemaître and Bickmore (2015), and Denker and De Laat (2016)]. In animal cells, individual chromosomes tend to occupy defined nuclear regions termed "chromosome territories" (CTs) (Cremer *et al.* 1982; Haaf and Schmid 1991; Cremer and Cremer 2001; Branco and Pombo 2006), and the spatial distribution of CTs can be size- and gene density-dependent. In several cell types, gene-poor chromosomes associate preferentially with the nuclear periphery, whereas gene-rich chromosomes are enriched in the nuclear interior (Croft *et al.* 1999; Boyle *et al.* 2001). In addition, distinct structural domains at the subchromosomal level have been identified by microscopy, termed chromosomal domains (Markaki *et al.* 2010). Chromosomal domains may correspond to

doi: https://doi.org/10.1534/genetics.119.302978
Manuscript received August 9, 2019; accepted for publication January 1, 2020; published Early Online January 6, 2020.
Available freely online through the author-supported open access option.

Supplemental material available at figshare: https://doi.org/10.25386/genetics.11516508.
[1]These authors contributed equally to this work.
[2]Corresponding authors: Peking University, 5 Yiheyuan Road, 100871 Beijing, China. E-mail: lucas.carey@pku.edu.cn; Parc Científic de Barcelona – Torre I (10th Floor), Baldiri Reixac, 4, 08028 Barcelona, Spain. E-mail: martirenom@cnag.crg.eu; and Institut de Génétique et de Biologie Moléculaire et Cellulaire, 1 rue Laurent Fries, Illkirch 67404, France. E-mail: mendozam@igbmc.fr

subchromosomal units defined by their increased interaction frequencies with each other or with the nuclear lamina. In particular, the nuclear periphery is a transcriptionally repressive environment in yeast and metazoans (Andrulis *et al.* 1998; Pickersgill *et al.* 2006; Guelen *et al.* 2008; Green *et al.* 2012), and gene repositioning from the nuclear interior to the periphery leads to repression of some, but not all, genes tested (Kosak *et al.* 2002; Zink *et al.* 2004; Kumaran and Spector 2008; Reddy *et al.* 2008; Finlan *et al.* 2008). Notably, individual genes can display mobility within chromosomal and subchromosomal domains, and this has been correlated with changes in their expression levels during cell differentiation (Peric-Hupkes *et al.* 2010). However, it remains unclear if the position of individual genes within the nucleus affects their expression, and/or their ability to be silenced or activated in response to different stimuli, or if these expression-related properties are merely correlated with spatial organization.

Studies in the budding yeast *Saccharomyces cerevisiae* have provided insight into the functional role of nuclear spatial organization [reviewed in Taddei *et al.* (2010), Zimmer and Fabre (2011), and Taddei and Gasser (2012)]. In this organism, chromosome organization is highly stereotypical. The 16 centromeres localize around the spindle pole body (SPB, the equivalent of the animal cell centrosome), whereas the 32 telomeres cluster in three to eight different foci at the nuclear periphery. Chromosome arms thus extend away from the SPB toward the nuclear periphery where telomeres are anchored, and their specific distribution is linked to their length. Finally, the nucleolus is positioned on the opposite side of the SPB, and is organized around 100–200 repeats of ribosomal DNA (rDNA) located in chromosome XII. Certain aspects of nuclear organization can have an impact on gene expression in budding yeast. On one hand, artificial tethering of reporter genes to subtelomeric regions and to the nuclear periphery can lead to their repression (Gottschling *et al.* 1990; Andrulis *et al.* 1998; Pryde and Louis 1999; Taddei *et al.* 2009). Moreover, perinuclear tethering of the *CLN2* cyclin gene in daughter cells mediates its repression during the G1 phase (Kumar *et al.* 2018). The association of silent information regulator (SIR) factors with telomeres also contributes to perinuclear repression (Taddei *et al.* 2009). Accordingly, genes within 20 kb of telomeres are poorly expressed, and this depends at least partially on SIR proteins and telomere anchoring to the nuclear periphery (Wyrick *et al.* 1999; Taddei *et al.* 2009). On the other hand, some inducible genes translocate from the nuclear interior to the periphery upon activation, where they interact with nuclear pore complexes (Casolari *et al.* 2004, 2005; Schmid *et al.* 2006; Taddei *et al.* 2006; Akhtar and Gasser 2007), and artificial targeting of genes to nuclear pores can also lead to their transcriptional activation (Brickner and Walter 2004; Menon *et al.* 2005; Taddei *et al.* 2006). Thus, the yeast nuclear periphery appears to harbor transcriptionally repressing and activating domains. How the three-dimensional (3D) organization of the yeast genome shapes global transcription levels remains largely unexplored.

To study the effect of nuclear organization on transcription in budding yeast, we took advantage of previously described strains bearing fusion chromosomes (FCs) (Neurohr *et al.* 2011; Titos *et al.* 2014). These cells have a grossly altered nuclear organization in interphase that is not associated with dramatic genome-wide changes in transcription, consistent with previous observations in yeast cells with extensively fused chromosomes (Luo *et al.* 2018; Shao *et al.* 2018). However, we find that displacement of FC genes away from the nuclear periphery does lead to mild, but consistent and reproducible, changes in expression across a large number of genes; on average a 10% shift away from the nuclear periphery leads to a 10% increase in expression. These effects are associated with both deletion of telomeric sequences and with displacement away from the nuclear periphery. These results suggest that radial chromosome-level spatial organization plays a limited, but significant, role in transcriptional regulation in budding yeast.

Materials and Methods

Polymer modeling

Each yeast chromosome of wild-type and FC strains was modeled using a bead-and-spring polymer model previously used and validated for modeling chromatin fibers (Rosa and Everaers 2008). This model consists of three different energy contributions, each describing a general physical property of the chain:

1. Excluded volume (purely repulsive Lennard-Jones potential). Each particle occupies a spherical volume of diameter equal to 30 nm and cannot overlap with any other particle in the system. Considering the typical compaction ratio of the chromatin fiber in yeast (Bystricky *et al.* 2004, 2005), each particle contains ~3.2 kb of DNA.
2. Chain connectivity (finite extensible nonlinear elastic potential). Consecutive particles on the chain are connected with elastic potential, which allows a maximum bond extension of 45 nm. The simultaneous action of the excluded volume and the chain connectivity prevents chain crossing.
3. Bending rigidity (Kratky–Porod potential). The bending properties of an ensemble of polymer chains are usually described in terms of the *persistence length*, which is the length scale where the chain changes its behavior from rigid to flexible. According to the bending properties experimentally measured for the yeast chromatin fiber (Cui and Bustamante 2000; Bystricky *et al.* 2004; Langowski 2006), the persistence length of each model chain was set to 61.7 nm for internal regions of the chromosomes and to 195.0 nm for the terminal ones. The regions of the chains corresponding to the telomeres (the 20 kb at the chromosomes ends), in fact, are more compact and rigid (Dekker 2008).

Since the modeling aims to describe the chromosomal configuration of haploid strains, the total number of beads

in the system is 4062, resulting from the presence of one copy of each yeast chromosome (Supplemental Material, Tables S5–S6). Each chromosome is initially folded in a solenoidal arrangement, where a rosette pattern is repeatedly stacked to yield an overall linear, rod-like conformation, see Figure 1 (Rosa and Everaers 2008; Di Stefano *et al.* 2013, 2016).

The chromosome chains are consecutively placed inside a sphere of radius 1.0 centered in the origin (0,0,0). This sphere, describing the typical shape of the yeast nucleus in G1, according to imaging data, interacts with the chromosome particles as a rigid wall. To obtain the initial chromosome nuclear locations, the positions of the chromosome centers are picked in a random, uniform way inside the nucleus, and the orientation of the rod axis is chosen randomly. The iterative placement proceeds from the longest to the shortest chromosome in a way that the newly added chromosomes must not clash with previously placed ones. In case of a clash, the placement attempt is repeated. Next, the following biological restraints (i–iii) are satisfied using a short preliminary run of Langevin dynamics, spanning 60 τ_{LJ}, where τ_{LJ} is the Lennard-Jones time and is used as the time unit in Large-scale Atomic/Molecular Massively Parallel Simulator (LAMMPS):

1. To simulate the tethering of the centromeres to the SPB, the motion of the centromere particles was restrained into a spherical compartment of radius R_{SPB} = 150 nm centered in c_{SPB} = (−850,0.0,0.0).
2. rDNA particles were restrained to a region occupying 10% of the total nuclear volume and located at the opposite side of the SPB, to simulate the nucleolus. Nucleolar volume was derived from experimental measurements. This region was defined by the intersection of the nuclear sphere with a sphere of radius R_{NUCL} = 640.92 nm whose center is located at c_{NUCL} = (1000,0.0,0.0). Conversely, the other no-rDNA particles of the chromosome models were restrained to stay out of the same nucleolar region.
3. Finally, to represent the tendency of the telomeres to stay anchored to the nuclear envelope (NE), the periphery of the sphere (a shell within R_{PER} = 126 nm from the NE, which accounts for one-third of the nuclear volume) was set to be attractive for the terminal particles of the chromosome chains. This effect, unexplored so far, was accomplished using a Lennard-Jones attraction (Jones 1924). It is important to note that telomeres were not strictly confined at the nuclear periphery of our models, but they were only favored to be close to the NE using a short-range interaction, which could be overcome by forces acting in the telomeres of chromosomes. Indeed, the first and last beads of each chromosome (telomeres) were not always peripheral in our simulations. If the nucleus was divided into three concentric spherical shells of the same volume, telomeres occupied the medium or central parts of the nucleus in ∼40% of the models, as shown in Figure S7.

The restraints listed above were imposed, applying on each of the involved particles a force F, only when the particle did not satisfy the confinement conditions, using the option indent of the software LAMMPS (Plimpton 1995):

$$F(r) = -10(r - R)^2,$$

where r is the distance from the particle to the center of the sphere and R is the radius of the sphere.

In the FC strains, the chromosomes involved in the fusion were attached to each other using additional connectivity bonds (chain connectivity in point 2 above) between the telomeres involved in the fusion process. These telomeres, which were attracted to the periphery in the wild-type strain models, behaved as internal chromosomal sequences in the FC strains and lost the telomeric attraction to the NE.

Finally, the system was relaxed using a run of Langevin dynamics of 30,000 τ_{LJ}, and one conformation every 3000 τ_{LJ} (10 models per trajectory) was retained for analysis. Replicating the complete simulation 1000 times generated 10,000 genome-wide conformations per strain.

Analysis of the genome-wide models and calculation of changes in % peripheral

Various measures were performed to characterize the generated structural models:

1. Building on the representations in Tjong *et al.* (2012), two-dimensional (2D) localization probability density plots of chromosomes were generated. For each chromosome, the Cartesian coordinates (x, y, z) of the particles were collected and then projected into a 2D reference frame made of an axial coordinate (along the SPB-to-nucleolus direction of the model nucleus that is x-axis in this work) and a radial one: (a, ρ)=(x, $\sqrt{y^2 + z^2}$). In the 2D (a, ρ) plan, the points are represented in a grid to produce the final heatmap. The grid size was 2×2 μm and the cell dimension was 10 nm. Once a point (a_c, ρ_c) is mapped onto the grid, since the particle is larger than the pixel of the grid, a Gaussian blur ($\sigma = 30nm$) is applied centered at the corresponding pixel. The values of the heatmap are finally normalized from 0 to 1 (Figure 1A and Figure 4).
2. To characterize the nuclear positioning of each locus, the volume of the model nucleus was divided into three concentric shells, each spanning one-third of the total nuclear volume. In each simulation, all chromosome particles (3.2-kb loci) were next categorized as central, middle, or peripheral depending on which of the three shells they occupied. This measure was used to generate the plots of the predicted percentage in periphery per particle and the percentage of shell occupation per terminal (telomeres) particle (Figure S9). The latter quantities were averaged over the ensemble of 10,000 model conformations.
3. By mapping the annotated genes on the 3D models, the predicted percentage in the periphery for each gene was computed as the average of the constitutive particles. Subtracting the percentage in periphery computed in the wild-type to the value in the FC strain and taking the absolute

value, the decrease in percentage in the periphery was then calculated (Figure 7).

4. The "displacement from NE" and the "difference in distance to the NE" the for 10-kb regions of the models were computed as follows. First, the distance between each particle and the NE was computed for each strain. Next, each chromosome was partitioned in groups of three consecutive particles (which correspond to about 10 kb) and the distance of each 10-kb locus from the NE was computed as the average distance of the particles within the locus. The displacement and the difference in the distance were then computed comparing the FC strains to the wild-type one (Figure 5).
5. The genomic locations of the *LYS4* and *TRP4* genes were mapped on the models, and the distances from the NE (or from SPB or between the two genes) were computed as the average of the corresponding particle-based distances (Figure 6).
6. The contact maps were computed for the wild-type strain using a distance cutoff between particles of 120 nm and binning at 32 kb (corresponding to 10 model particles) of resolution. The 3C (Chromosome Conformation Capture) interaction maps (used for model validation, not as input for modeling) were obtained by downloading the data sets from Duan *et al.* (2010) obtained using the *Hin*dIII restriction enzyme and the raw reads from Gene Expression Omnibus (GEO) accession number SRR5077790 from Lazar-Stefanita *et al.* (2017). The latter was next analyzed using the TADbit (Serra *et al.* 2017) pipeline to obtain the raw interaction maps and the OneD procedure (Vidal *et al.* 2018) to normalize it (Figure S1).
7. The median telomere–telomere (terminal particle of the chromosome model) distance was computed for each of the 60 telomere pairs considered in Therizols *et al.* (2010) (Figure S2) and correlated with the experimental measures performed therein.
8. The displacement of model particles from the SPB in Figure S4 was computed as follows: (i) for each strain and all model conformations, the distances between each particle individually and the SPB were computed; (ii) the average particle–SPB distances were computed for each particle in each strain; (iii) for each FC strain, the difference in the (average) distance to the SPB with respect to the wild type were computed for each particle; and (iv) the difference was computed such that positive values indicated a (typical) displacement away from the SPB in the FC strains and negative values indicated displacement toward the SPB in FC strains.

Previously published modeling approaches

The *S. cerevisiae* genome has been previously modeled using two main restraint-based approaches. First, 3C data sets have been used as input restraints to reconstruct the 3D conformation of the yeast genome (Duan *et al.* 2010; Lesne *et al.* 2014; Lazar-Stefanita *et al.* 2017). Second, and in a similar approach to that used in our work, models were built using genome tethering to nuclear elements as restraints (Tjong *et al.* 2012; Wong *et al.* 2012). The differences between our approach and these previously published studies are minimal. For example, in this work, the genome was represented as a series of spherical beads compared to cylinders previously used by Wong *et al.* (2012). Moreover, the initial conditions of the simulation, the confinement of the genome, and the minimization protocols were different in our work compared to those used by Tjong *et al.* (2012). However, these differences are likely to minimally change the final conclusions of our modeling approach compared to those previously published.

Strains, cell growth, and microscopy

S. cerevisiae strains are derivatives of S288c. TetO/LacO cells and chromosome fusions were previously described. Briefly, FC chromosomes were obtained by successive rounds of homologous recombination between subtelomeric regions of two chromosomes, by transformation of haploid yeast cells with a PCR-generated DNA fragment containing a resistance cassette flanked by sequences homologous to the subtelomeric regions of two different chromosomes. Formation of dicentric chromosomes was avoided through activation of a *GAL1,10* promoter inserted next to centromere 4 and selection of FC recombinants in galactose. When fusing three or four chromosomes, one of the centromeres was deleted and fusion with another chromosome was repeated. To allow the reuse of selection markers, the *URA3* cassette was deleted by homologous recombination and ura- recombinants were selected on 5-FOA. Finally, the conditional *CEN4* locus was deleted or replaced with a wild-type copy to ensure robust growth in glucose. Strains were confirmed by PCR, and by the segregation timing of *TRP1* and *LYS4* loci by time-lapse imaging, as previously described in detail (Neurohr *et al.* 2011; Titos *et al.* 2014). Live-cell microscopy was carried out on a confocal spinning disk (Nikon, Garden City, NY) equipped with an HCX plan APO 100X objective and a Photometrics Prime 95B camera. Eleven 0.2-μm thick z-sections were collected. Distances were measured between local maxima (*i.e.*, the brightest pixels of fluorescent spots or the center of the nuclear rim) on single planes using ImageJ (http://rsb.info.nih.gov/ij/), although for clarity, figures are represented as 2D maximum projections of whole-cell Z-stacks. Graphs and statistical analysis (Student's *t*-test allowing for unequal variance) were performed with R and Excel (Microsoft).

Immunofluorescence and FISH

To make FISH probes, a 6-kb PCR fragment in the *TEL4R* region was amplified from genomic DNA with primers: 5′-ATCTTTCCTTACACATAAACTGTCAAAGGAAGTAACCAGG-3′ and 5′-GTAACATACAAACTCAACGCCTACTAAGATTAATACATCA-3′, and labeled with Alexa Fluor 488 by nick translation using the FISH Tag-DNA Multicolor Kit (Invitrogen, Carlsbad, CA). FISH-immunofluorescence was performed essentially as

described (Gotta *et al.* 1999), with minor modifications. First, 1–2^9 cells of exponential cultures (OD_{600} = 0.5–1) were collected, resuspended in 500 μl of 0.1 M EDTA/KOH pH 8.0 and 10 mM DTT, and incubated for 10 min at 30°. Cells were collected and resuspended in 0.1 M KPi (pH = 6.4)/1.2 M sorbitol and digested with 0.4 mg/ml Zymolyase 100T (Seikagatu) for 5–15 min at 30° in 0.1 M KPi (pH = 6.4)/1.2 M sorbitol. This treatment allowed the cells not to be completely converted into spheroplasts, but instead partially retain their cell walls, to help stabilize their 3D structure. Partially spheroplasted cells were fixed for 20 min with 3.7% paraformaldehyde in YPD/1.2 M sorbitol at room temperature. Cells were recovered by centrifugation (1000 × *g* for 5 min), washed three times in YPD/1.2 M sorbitol, resuspended in 0.1 M KPi (pH = 6.4)/1.2 M sorbitol, and spotted on Teflon slides; after being left to air-dry for 5 min, they were immersed in cold methanol for 6 min and in cold acetone for 30 sec. Slides were then rinsed in PBS containing 0.1% Triton X-100 (PBS-T) and 1% BSA, and incubated for 30 min at room temperature. Spots of the slide were dried and incubated overnight at 4° (or for 1 hr at 37°) with anti-Nuclear Pore Complex antibody (Mab414, ab24609, Abcam), diluted 1:2 in PBS-T 1% BSA. Slides were then washed in PBS-T and incubated with anti-mouse Alexa 647 (A-21236, Life Technologies) diluted 1:200 in PBS-T and 1% BSA at 37° for 1 hr. Next, slides were fixed again in PBS containing 3.7% paraformaldehyde for 20 min and incubated overnight in 4× SSC, 0.1% Tween 20, and 20 μg/ml of RNase A at room temperature. Slides were then washed in water, sequentially immersed for 1 min in 70, 80, 90, and 100% ethanol at −20°, and air-dried. Slides were then denatured at 72° with 70% formamide and 2× SSC, immersed for 1 min sequentially in 70, 80, 90, and 100% ethanol at −20°, and air-dried. The hybridization solution (50% formamide, 10% dextran sulfate, 2× SSC, 0.05 mg/ml labeled probe, and 0.2 mg/ml single-stranded salmon sperm DNA) was then applied and slides were incubated at 10 min at 72°. Slides were incubated for 48 hr at 37° to allow probe hybridization, and washed twice for 10 min each at 42° in 0.05× SSC and twice in buffer (0.15 M $NaHCO_3$ and 0.1% Tween 20, pH 7.5) with 0.05% BSA for 30 min. After three washes in BT buffer, 2 μl of DAPI (Roche Diagnostics) 2.5 mg/ml were added and incubated for 1 min. Slides were washed twice with 0.05× SSC and mounted in 1× PBS, 50% glycerol, and 24 μg/ml 1,4diazabicyclo-2,2,2,octane, pH 7.5.

RNA sequencing

Cells were harvested by centrifugation and RNA was extracted from fresh pellets using the RiboPure Yeast Kit (Ambion). RNA concentrations were determined using a NanoDrop 1000 (Thermo Scientific), while quality and integrity were checked using a Bioanalyzer 2100 (Agilent Technologies). RNA sequencing (RNA-seq) was performed on a HiSeq2000 (Illumina). Paired-end reads of 50 bp were aligned to the reference *S. cerevisiae* genome (R64-1-1) using kallisto quant -i orf_coding_all.idx -o output -b 100 read1_file.fastq.gz read2_file.fastq.gz.

To obtain a robust and accurate wild-type expression level for each gene, we averaged across strains. For each strain in which the gene was predicted to increase or decrease time spent in the nuclear periphery by < 1%, we took the median expression value across all strains (four independent RNA-seq replicate experiments per strain). Fold-change in expression was calculated as the log2 ratio of expression in the FC strain divided by expression in this median expression value. Similar results were obtained if expression for the wild-type control strain was used, but as many of the genes were expressed at very low levels, and hence represented by very few reads, averaging across strains was more robust to random counting noise.

Data availability

Yeast strains are available upon request. Data and codes are available at https://github.com/Lcarey/DiGiovanni_DiStefano_FC. RNA-seq raw data are available at https://www.ncbi.nlm.nih.gov/geo/query/acc.cgi?acc=GSE108261 with GEO accession Nr GSE108261. Supplemental material available at figshare: https://doi.org/10.25386/genetics.11516508.

Results

A computational model to study the impact of yeast nuclear organization in gene expression

To study how the 3D organization of the genome affects gene expression, we first sought to establish how gene position correlates with transcription levels in wild-type budding yeast cells. To estimate gene position, we built computational models of chromosomes in the interphase G1 nucleus, a strategy that has proven useful in recapitulating chromosome-level nuclear organization in budding yeast (Tjong *et al.* 2012; Wong *et al.* 2012; Dultz *et al.* 2016). We modeled chromosomes as bead-and-spring chains, an approach previously validated for modeling the general physical properties of chromatin fibers (Rosa and Everaers 2008; Di Stefano *et al.* 2013). Details of the polymer modeling process are found in the *Materials and Methods* and summarized in Figure 1A. Briefly, chromosomes were confined inside a sphere of 2 μm diameter corresponding to the interphase nuclear size. Centromeres were confined to a spherical region of radius 150 nm at one pole of the nuclear sphere to account for the tethering of centromeres to the SPB by microtubules (O'Toole *et al.* 1999). The dynamic association of telomeres with the NE was modeled with the periphery of the sphere attracting the terminal beads of chromosome chains. Finally, to reproduce the confinement of the rDNA in the nucleolus, the particles corresponding to rDNA were restrained to a region located at the opposite side of the SPB. An ensemble of chromosomal polymer models was generated using Brownian motion dynamics. A total of 10,000 model conformations satisfying all the imposed restraints were then selected, and analyzed for the likelihood of particular loci and chromosomes being positioned in specific regions of the cell nucleus (Figure 1B).

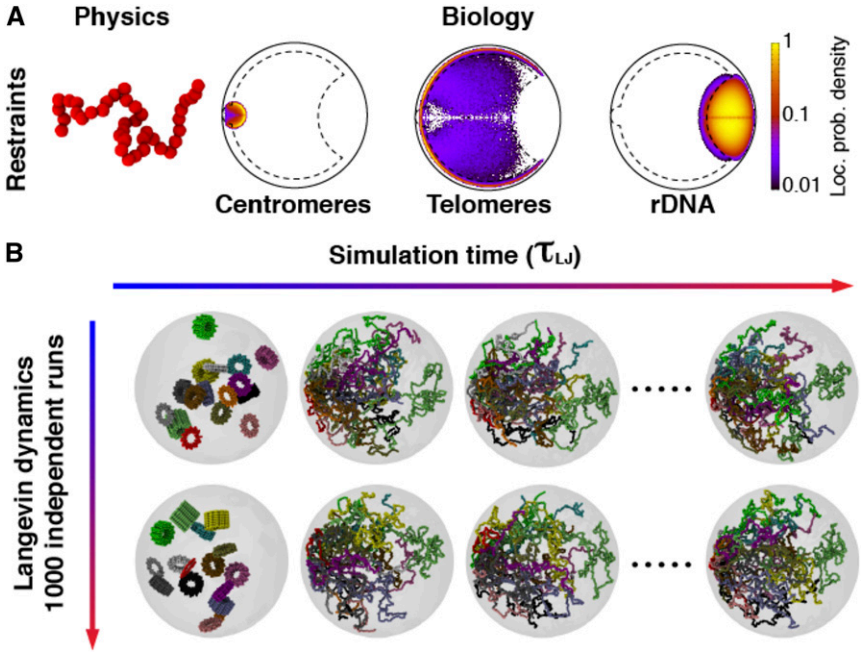

Figure 1 Computational modeling of the haploid budding yeast nucleus in interphase. (A) The 16 chromosomes were modeled as bead-and-spring chains with 30-nm beads each comprising 3.2 kb of DNA. The chains were confined into the nucleus (1-μm radius sphere) and beads corresponding to centromeres were constrained in a sphere of radius 150 nm attached to the nuclear envelope to mimic the attachment to SPB-mediated by microtubules. The rDNA was restrained in a region occupying 10% of the nuclear volume at the opposite side of the nucleus with respect to the SPB. The telomeres were attracted to the nuclear envelope to have higher propensity to occupy the nuclear periphery, which is defined as the spherical shell, that is the closest to the nuclear envelope and occupies one-third of the total volume of the nucleus (*Materials and Methods*). (B) The chromosomal polymer models, representing the genome-wide chromosome arrangement, were initialized as cylindrical solenoids of radius 150 nm. The solenoid chromosome states serve the sole purpose of obtaining an initial chain conformation that is compact, yet not entangled, without making any claim to reproducing any specific quantitative features of mitotic yeast chromosomes. Next, the restraints on centromeres, rDNA, and telomeric particles were satisfied using a short preliminary run of Langevin dynamics, spanning 60 τ_{LJ}. Finally, the system was relaxed with a 30,000 τ_{LJ} run of Langevin dynamics, in which all the spatial restraints are in place. This run is used to obtain 10 steady-state conformations per trajectory (one every 3000 τ_{LJ}). Each strain was modeled in 1000 independent replicates to obtain 10,000 genome-wide conformations per strain (*Materials and Methods*). rDNA, ribosomal DNA; SPB, spindle pole body.

As an orthogonal validation of our model, we compared the probability of contact among all chromosomal particles in the wild-type models with the experimentally measured intra- and interchromosomal contact frequencies observed by a 3C-derived technique (Duan *et al.* 2010; Lazar-Stefanita *et al.* 2017). Specifically, we compared the internal correlations between models' and experimental contact matrices (Imakaev *et al.* 2012) and the correlations between matrix elements grouped by genomic distance (Figure S1B and C) and found in both cases significant similarities between models and experiments. In addition, we compared the predicted median telomere–telomere distances from our models with analogous experimental data obtained using imaging (Therizols *et al.* 2010). In both comparisons, we found that our models, based on the physical properties of chromatin and minimal biological restraints, accurately described wild-type yeast nuclear organization (Figures S1–S2). This confirms the validity of polymer-based modeling to reproduce nuclear organization features (Tjong *et al.* 2012; Wong *et al.* 2012).

To determine if our computational models were consistent with the experimentally measured low gene expression at the nuclear periphery, the predicted gene position relative to the nuclear periphery was correlated with genome-wide messenger RNA (mRNA) levels obtained by RNA-seq. Genomic regions within 30 kb of the ends of wild-type chromosomes were poorly expressed, consistent with previous reports (Wyrick *et al.* 1999) (Figure 2, A and B). Importantly, lower expression was also correlated with gene peripheral localization, as predicted by polymer modeling (Figure 2B). Because most subtelomeric sequences are also restricted to the perinuclear region, the above analysis confounds the contributions of sequence proximity to chromosome ends [one-dimensional (1D) effect] and proximity to the nuclear periphery (3D effect) to steady-state mRNA levels. However, we found that, while distance to the telomere and predicted location in the nuclear periphery were correlated, they were imperfectly so (Figure 2C). Especially for genes with low expression, the fraction of modeled nuclei in which a gene was predicted to be at the nuclear periphery was more highly correlated with expression than distance to the telomere in both linear (correlation = −0.093) and log space (Figure 2D and Figure S3). Furthermore, in a linear model that predicts expression from both of the two variables, % peripheral is a slightly more important feature (Table S1). These data open the possibility that localization to the periphery, and not only distance from the telomere, is partially responsible for low expression.

Computational modeling and cell imaging validate nuclear reorganization after chromosomal rearrangements

To experimentally determine if spatial organization affects expression, we next examined how large-scale chromosome rearrangements affect nuclear reorganization. In previously described FC strains, up to three "donor" chromosomes were sequentially fused to the end of a "recipient" chromosome (Neurohr *et al.* 2011; Titos *et al.* 2014). Centromeres were simultaneously removed from donor chromosomes to avoid formation of toxic dicentrics; telomere elements at the site of the fusion were also removed. Thus, like normal chromosomes,

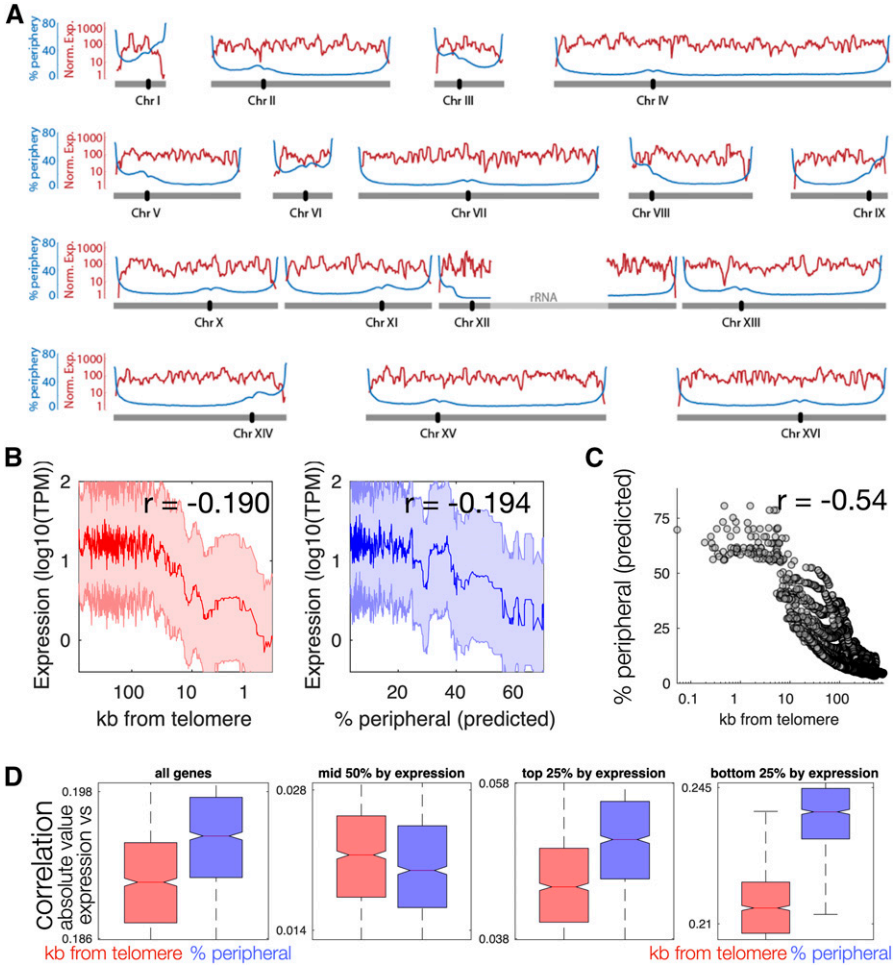

Figure 2 Localization in the nuclear periphery is associated with lower expression. (A) mRNA expression (red) and predicted time spent in the nuclear periphery (blue) are shown for each chromatin bead along each of the 16 yeast Chrs. (B) Median expression level for genes binned by distance to the telomere (red) or by predicted % peripheral (blue). Correlation values are for Pearson correlation on unbinned data. (C) Predicted % peripheral is not perfectly correlated with distance from the telomere. (D) The *y*-axis values are absolute values of the correlation of either kb from the telomere (red) or % peripheral (blue), with gene expression. The two distributions (red and blue) are generated by randomly sampling the data 1000 times. Across all but one grouping, gene expression is more strongly correlated with predicted % peripheral (blue) than with log(distance to the telomere) (red). The difference is larger with linear distance to the telomere (not shown). Boxplots show median correlation across 1000 random samplings of 90% of genes. All distributions are significantly different from each other due to the large number of computational samplings. The statistical differences and effect size are largest in genes in the bottom 25% of expression. Chr, chromosome; mRNA, messenger RNA; TPM, transcripts per million.

FCs contain two telomeres and one centromere (Figure 3, A and B). These chromosome fusions only minimally changed the genomic content relative to wild-type strains, since only 5 to 26 subtelomeric ORFs are lost during the fusion procedure (Table S2). However, we hypothesized that FC strains would display dramatically altered interphase chromosome organization. Indeed, this is dependent on chromosome number and length, centromere attachment to SPBs, and telomere anchoring to the NE, all of which are altered in FC strains. Importantly, chromosome fusions led to a maximal reduction in chromosome and centrosome number from 16 to 13, reduction of telomere number from 32 to 26, and lengthening of the longest chromosome arm (excluding chromosome XII, containing the variable rDNA array) from 1 to almost 4 Mb (Figure 3B).

We then applied the principles used in modeling wild-type nuclei to determine nuclear organization in the 10 different FC strains (Figure 3B). FCs used in this study are named using the following convention: FC is followed by the chromosomes that comprise the fusion indicated in brackets, followed by the centromere of the recipient chromosome. Thus, strain *FC(IV:XV:V)CEN4* bears an FC in which chromosome IV is the recipient, and chromosomes XV and V are the donors.

The model predicts two major changes in the FC strains. First, large (> 300 nm) displacements of donor chromosomes away from the SPB and slight (10–20 nm) displacement of recipient chromosomes toward the SPB (Figure 4 for IV:XII fusions, and Figure S4 for all FCs). Both of these displacements can be interpreted as a consequence of the deletion of centromeres in donor chromosomes. Indeed, centromere deletion removes the anchoring of donor chromosomes to the SPB, while also reducing chromosome density close to the SPB. Thus, abnormally large FCs will tend to occupy the space far from the SPB, whereas remaining centromeres will be allowed to occupy positions closer to the SPB. The combined action of these phenomena induces an effective pressure on the recipient chromosomes, which are pushed closer to the SPB compared to in the wild-type scenario (Figure S4).

Second, the model predicts displacement of loci in the fused chromosomes away from the nuclear periphery, as shown in Figure 5. To quantify this prediction, we computed the distance from the nuclear periphery of all 10-kb loci from the surface of the nuclear sphere for all chromosomes in all

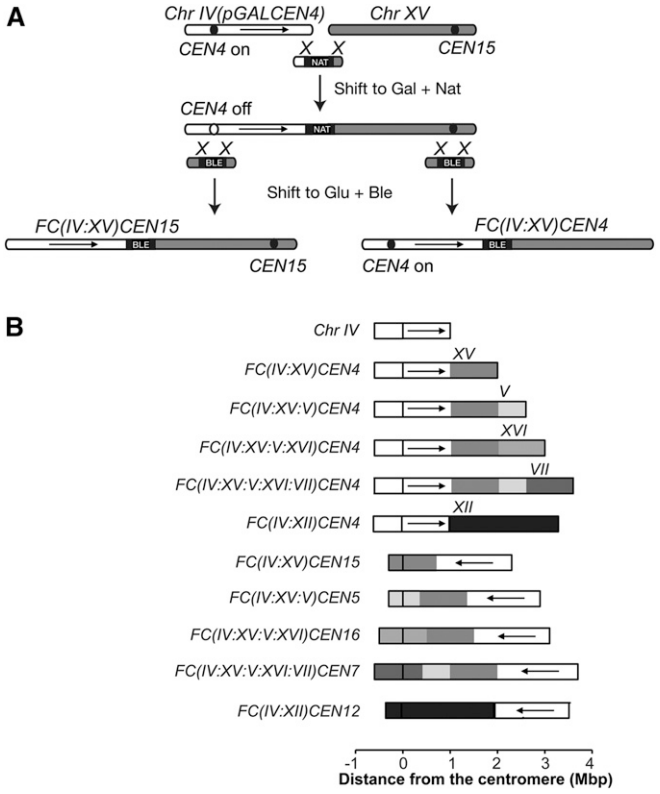

Figure 3 Generation of FC strains. (A) The generation of FCs [originally described in Neurohr *et al.* (2011) and Titos *et al.* (2014)] starts with the integration of *pGAL1* sequence upstream of the centromere to be inactivated. Next, the Chrs are fused by homologous recombination between a bridging PCR fragment and the telomeres of the Chrs. Finally, the deletion of one of two centromeres and the excision of the *pGAL1* sequence, as appropriate, generates the *FC* strain. Black circle is the centromere, black rectangle is the selection marker. (B) Schemes of all the *FC* strains used in this work. Chr IV is shown for comparison. Arrows indicate the relative orientation of this Chr in the fusions. Ble, bleomycin resistance cassette; Chr, chromosome; FC, fused chromosome; Gal, galactose; Glu, glucose; Nat, nourseothricin resistance cassette.

strains relative to wild-type. The model predicts that only loci on fused chromosomes are displaced away from the nuclear periphery, while the relative location of loci in nonfused chromosomes never varies by >50 nm (Figure 5A). Loci with the largest predicted displacement were located near telomeres (Figure 5, B–D) or centromeres (Figure 5E) before the fusion event. These displacements can be interpreted as a result of the deletion of centromeres and telomeres in fused chromosomes, as these elements provide anchoring to the SPB and the NE, respectively.

To validate predicted chromosome displacement in FC strains, we determined the distances of chromosome loci to each other, to the SPB, and to the nuclear periphery using fluorescence microscopy in wild-type and FC strains during G1. Loci in chromosome IV were visualized through Tet repressor fused to monomeric red fluorescent protein (TetR-mRFP) and Lac inhibitor fused to green fluorescent protein (LacI-GFP) reporters in cells bearing tetracycline and lactose operator arrays. These arrays were inserted, respectively, at the *TRP1* locus 10-kb away from *CEN4* in the right arm of chromosome IV and at the *LYS4* locus in the middle of the chromosome IV right arm, 470-kb away from *TRP1*. Spc42-GFP and Nup49-mCherry were used to label SPBs and the nuclear periphery, respectively. We first determined distances between these nuclear landmarks in wild-type and in the two FC strains *FC(IV:XII)CEN4* and *FC(IV:XII)CEN12* (see scheme in Figure 6A). We then compared these measured distances with model predictions. Measured and predicted distances were significantly correlated for all distances across the examined strains (Figure 6, B and C). Neither *TRP1* nor *LYS4* changed their distances from the nuclear periphery in either FC, consistent with model predictions. In contrast, the *CEN4*-associated *TRP1* locus was located in the vicinity of the SPB in wild-type and *FC(IV:XII)CEN4* nuclei, whereas the same locus was displaced away from the SPB in *FC(IV:XII)CEN12* (Figure 6C). This is consistent with the mitotic segregation timing (relative to spindle elongation) of these FCs (Neurohr *et al.* 2011; Titos *et al.* 2014) and with model predictions that donor chromosomes are displaced away from the SPB, as compared to the wild-type configuration. Furthermore, we observed that the distance between *TRP1* and *LYS4* was reduced in the *FC(IV:XII)CEN12* relative to wild-type and *FC(IV:XII)CEN4* cells, and that this was in agreement with the models (Figure 6C). Shortening of *TRP1-LYS4* distances was observed in all FC strains in which chromosome IV acted as a donor (Figure 6D), and again, this was in agreement with the models (Figure 6E). These observations suggest that displacement of a genomic region away from an active centromere and/or to a nuclear region away from the SPB leads to its increased compaction. This could be due to elimination of microtubule-dependent pulling forces on the neighboring kinetochore and/or to increased chromatin crowding in SPB-distal nuclear regions. Finally, FISH established that the *TEL4R*-proximal locus was closely associated with the nuclear periphery (labeled with DAPI) in wild-type cells, whereas the mean distance between *TEL4R* and the nuclear periphery was increased in both *FC(IV:XII)CEN4* and *FC(IV:XII)CEN12* fusions (Figure 6F). Because the *TEL4R* region is engaged in chromosome fusions in all FC strains (Figure 3B), this region is most likely displaced in these strains as well. This confirmed the model's prediction that subtelomeric loci engaged in a chromosome fusion event are displaced away from the periphery (Figure 5, B–D). Together, these results quantitatively confirm the model predictions that chromosome fusions lead to large changes in the subnuclear organization of chromosome regions relative to each other, to the SPBs, and to the nuclear periphery.

Chromosomal rearrangements reveal a correlation between increased expression and gene displacement from the nuclear periphery

To determine whether the genome reorganization caused by chromosome fusions led to changes in gene expression, we performed RNA-seq in the 10 FC strains (Figure 3), with four

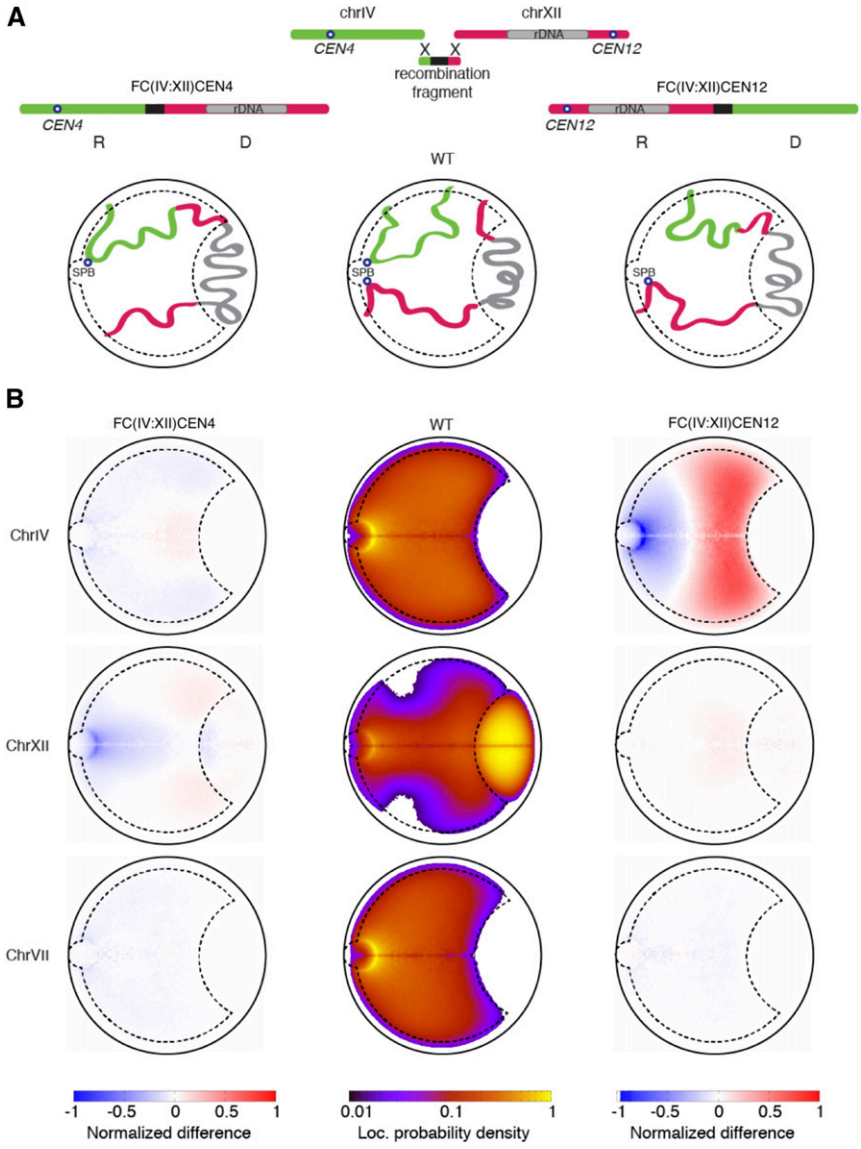

Figure 4 The donor Chrs are predicted to be strongly displaced in the nucleus. (A) Cartoon representations of WT, *FC(IV:XII)CEN4*, and *FC(IV:XII)CEN12* strains. "Donor" and "recipient" Chrs are labeled "D" and "R," respectively. (B) Predicted Chr loc. probability densities for Chrs IV, XII, and VII in the wild-type strain (central column), and the *FC* strains *FC(IV:XII)CEN4* (left column) and *FC(IV:XII)CEN12* (right column), shown normalized by the WT strain. The heatmaps show large differences in the positioning of the recipient and donor Chrs, and almost no difference in the nuclear organization of the largest nonfused one, Chr VII. Chr, chromosome; FC, fused chromosome; loc., location; rDNA, ribosomal RNA; WT, wild-type.

independent RNA-seq replicate experiments per strain. Consistent with all FC strains having wild-type growth rates (Neurohr *et al.* 2011; Titos *et al.* 2014), the presence of FCs did not correlate with strong changes in gene expression (Figure S5). This suggests that spatial chromosome displacements (such as changes in gene location relative to the SPB and to other chromosomes) do not strongly affect gene expression.

We then asked whether mild changes in expression correlated with changes in predicted gene position relative to the nuclear periphery. Gene expression analysis was performed with four biological replicates for wild-type, and three or four biological replicates for each of 10 FC genotypes, for a total of 42 RNA-seq experiments. To calculate differential expression we compared the median expression in the four replicates of wild-type to the median expression for all replicates of each FC strain. Thus, for each gene, we obtained 10 differential expression values. As each FC strain was also modeled separately, we generated a matched set of 10 predicted changes in location. Thus, each gene in each FC strain was a point defined by its measured change in expression and its predicted change in location. To obtain a more accurate value for expression in the absence of changes in nuclear location, for each gene we used the average expression level of that gene across all strains in which the percent peripheral was not predicted to increase or decrease by $>$ 1%. From this baseline expression value, we compared the fold change in expression for each strain with the predicted change in the frequency with which each gene was located in the nuclear periphery. Genes deleted during the fusion events were not considered. The results of this analysis show mild but statistically significant genome-wide expression changes for genes that change location relative to the nuclear periphery after chromosomal fusions (Figure 7, A and B). For example, the median gene with a predicted 25% decrease in association with the periphery due to chromosome fusion

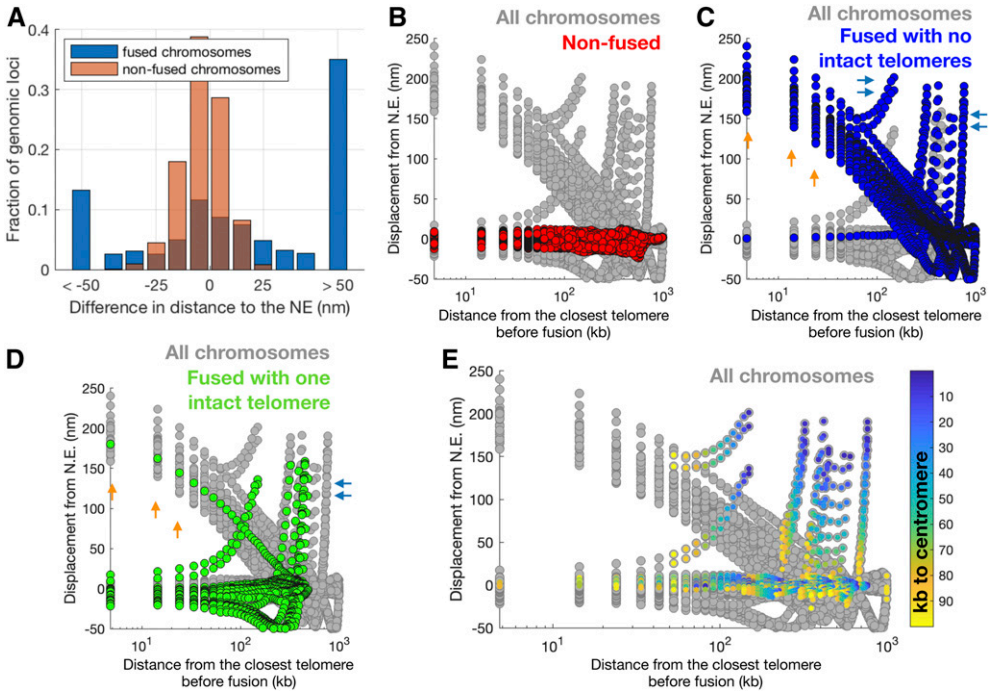

Figure 5 Loci predicted to be displaced away from the nuclear periphery are near centromeres and telomeres of fused chromosomes. (A) The predicted displacement with respect to the N.E. for loci of 10 kb in fused (blue) and nonfused (orange) chromosomes. Brown is the superposition of blue and orange. Only loci on fused chromosomes are displaced from the nuclear periphery. (B–E) The predicted displacement from the N.E. (*y*-axis) as a function of the distance from the telomere before chromosome fusion (*x*-axis). Each circle represents a 10-kb locus in the model. Models of all FC strains are included. In each panel, circles corresponding to a subset of chromosomes are colored, whereas the rest are gray. In (B–D), chromosomes are color-coded as "nonfused" (red), "fused with no intact telomeres" (blue), and "fused with one intact telomere" (green). For example, chromosome XV is fused with no intact telomeres in FC(IV:XV:V) strains, and fused with one intact telomere in FC(IV:XV) strains. (B) Loci in nonfused chromosomes are not displaced relatively to the N.E. (all values are near zero). (C) Loci in fused chromosomes that have both telomeres engaged in fusion events show two types of displacement. Most loci that are displaced away from the periphery are subtelomeric (orange arrows), indicating that subtelomeres that participate in fusions lose attachment to the nuclear periphery. However, some nonsubtelomeric loci are also displaced (blue arrows). (D) Loci in fused chromosomes that have only one telomere engaged in fusion events also show two types of displacement. Some subtelomeric loci are displaced from the periphery (presumably those that participate in a fusion event; orange arrows). Some nonsubtelomeric loci are also displaced (blue arrows). (E) Loci are colored not according to their location in fused or nonfused chromosomes, but according to their distance to a centromere before fusion. This shows that all noncentromeric loci that are displaced away from the periphery in (B–D) were pericentromeric before the fusion occurred. N.E., nuclear envelope.

exhibits a 25% increase in expression in FC strains (Figure 7B). While the effect on expression is weak, it is consistent across changes in localization and strains, and remains if we limit our analysis to genes not involved in the stress response, or to only highly expressed genes (Brauer *et al*. 2008; Gasch *et al*. 2000) (Figure S6). Importantly, the correlation between increased expression and predicted displacement from the nuclear periphery holds for both subtelomeric and nonsubtelomeric genes (Figure 7, C and D). Examples of correlated changes in expression and localization are shown for the *TEL4R*-proximal region, which is perinuclear in wild-type cells but is displaced away from the nuclear periphery in FC(IV:XII) (Figure 6F), and presumably in all other FC strains, as this region is always engaged in fusions (Figure 3). Most genes in this region show increased expression after predicted displacement toward the nuclear interior (Figure 7E). Of the almost 500 genes that were predicted to change their peripheral localization by >5%, 85 experienced changes in expression (Figure 7F, listed in Tables S3–S4).

The effects of nuclear location vs. centromere and telomere deletion

Increased expression could be caused by deletion of repressive elements in telomeres and centromeres during chromosome fusion, gene displacement away from the nuclear periphery, or from a combination of these two factors. As deletion of the centromere is highly correlated with changes in location, to determine if deletion of a centromere affects expression, we used ANOVA to determine if the distance to the centromere is predictive of changes in gene expression after first taking into account predicted changes in location and wild-type gene expression. We find that after taking into account the predicted change in location, the distance to the centromere (whether deleted or not) is not predictive of changes in expression (Figure 8). This suggests that spreading of a repressive signal in *cis* around centromeres is unlikely to measurably affect expression, and that distance to the nuclear periphery may be the dominant effect.

Deletion of telomeres may affect the expression of subtelomeric genes. To measure the effects of telomere deletion on gene expression, we used all FC strains and the subset of genes on a chromosome arm that underwent fusion and telomere loss, and predicted changes in expression from both distance to the deleted telomere and from the predicted frequency in the nuclear periphery. We then asked which is a better predictor of changes in gene expression. For the subset of genes on chromosome arms that underwent fusion, we took all genes X kb (+/− 10 kb) from the deleted telomere, and used a linear model to predict changes in expression from

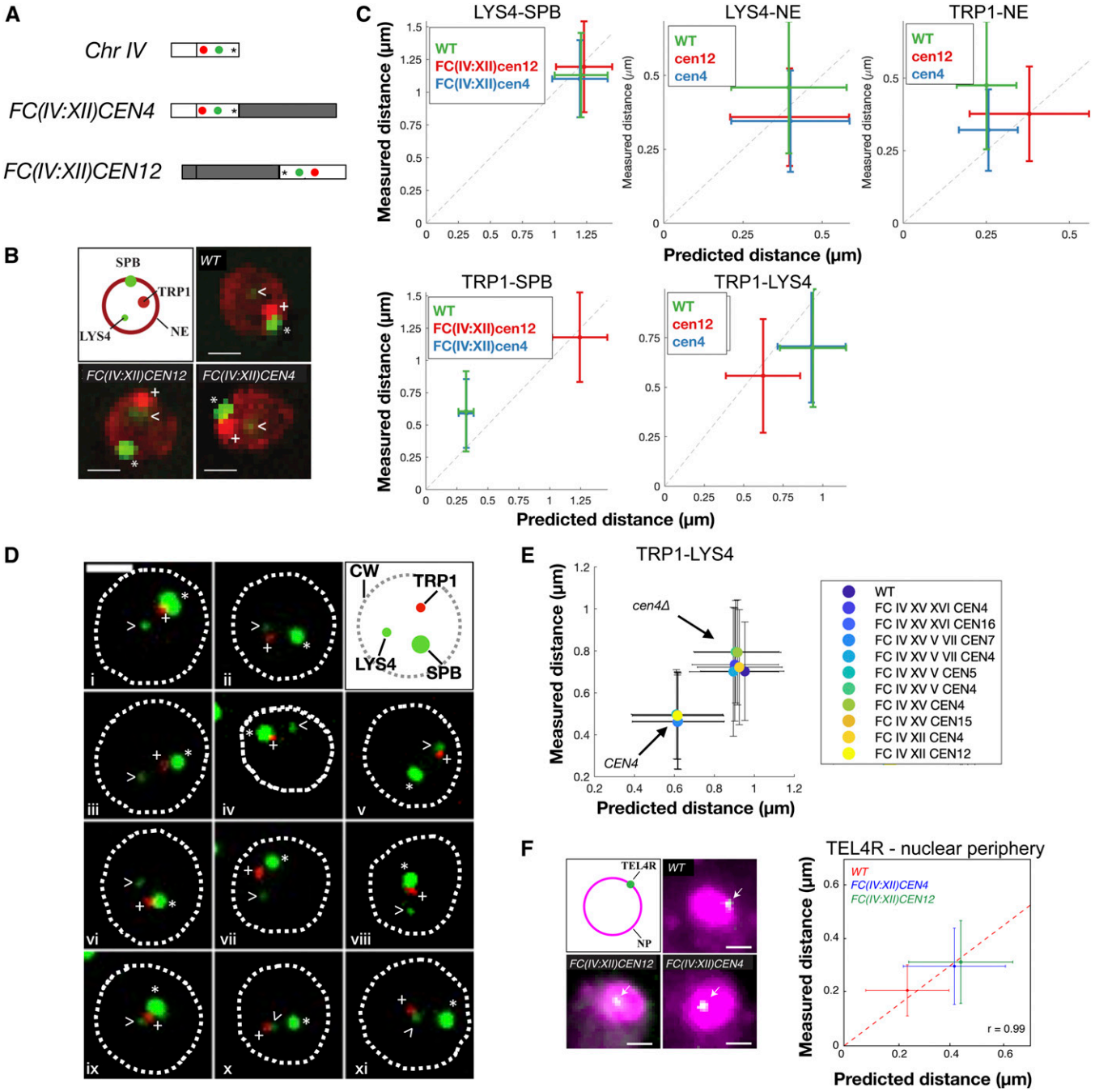

Figure 6 Validation of polymer models by live- and fixed-cell microscopy. (A) Position of *TRP1* (red), *LYS4* (green), and *TEL4R* (asterisk) on Chr IV and its indicated FC derivatives. (B) Live-cell microscopy of G1 cells of the indicated strains showing the localization of *TRP1* (red dot, marked with +), *LYS4* (faint green dot, arrowhead), the SPB (bright green dot, marked with an asterisk), and the nuclear periphery labeled with Nup49-mCherry (red). (C) Correlation of measured and predicted distances between the indicated nuclear loci, the SPB, and the nuclear periphery in the indicated strains. Graphs show the means and SDs for WT (151 cells), *FC(IV:XII)CEN4* (152 cells), and *FC(IV:XII)CEN12* (153 cells), and 10,000 independent simulations. (D) Live-cell microscopy of G1 cells of the indicated strains showing the localization of *TRP1*, *LYS4* and the SPB marked as in (B). Note that the NE is not labeled and the dotted line indicates the CW. Strains shown are: (i) *FC(IV-XII)CEN4*, (ii) *FC(IV-XII)CEN12*, (iii) *WT*, (iv) *FC(IV-XV)CEN4*, (v) *FC(IV-XV)CEN15*, (vi) *FC(IV-XV-V)CEN4*, (vii) *FC(IV-XV-XVI)CEN4*, (viii) *FC(IV-V-VII-XV)CEN4*, (ix) *FC(IV-XV-V)CEN5*, (x) *FC(IV-XV-XVI)CEN16*, and (xi) *FC(IV-V-VII-XV)CEN7*. Bar, 2 μm. (E) Correlation of measured and predicted distances between *TRP1* and *LYS4* in the indicated strains. Graphs show the means and SDs for simulations (10,000 iterations) and experimental data (>100 cells for each strain). Distances are shorter in strains in which Chr IV acts as a donor (*cen4Δ*) compared to Chrs in which it acts as a recipient of fusions (*CEN4*). (F) FISH of G1 cells of the indicated strains showing the localization of *TEL4R* (green dot, arrows) and the nuclear periphery labeled with DAPI (magenta). Graph shows the means and SDs from WT (95 cells), *FC(IV:XII)CEN4* (82 cells), and *FC(IV:XII)CEN12* (102 cells), and 10,000 independent simulations. Bar, 1 μm. Chr, chromosome; CW, cell wall; FC, fused chromosome; NE, nuclear envelope; SPB, spindle pole body; WT, wild type.

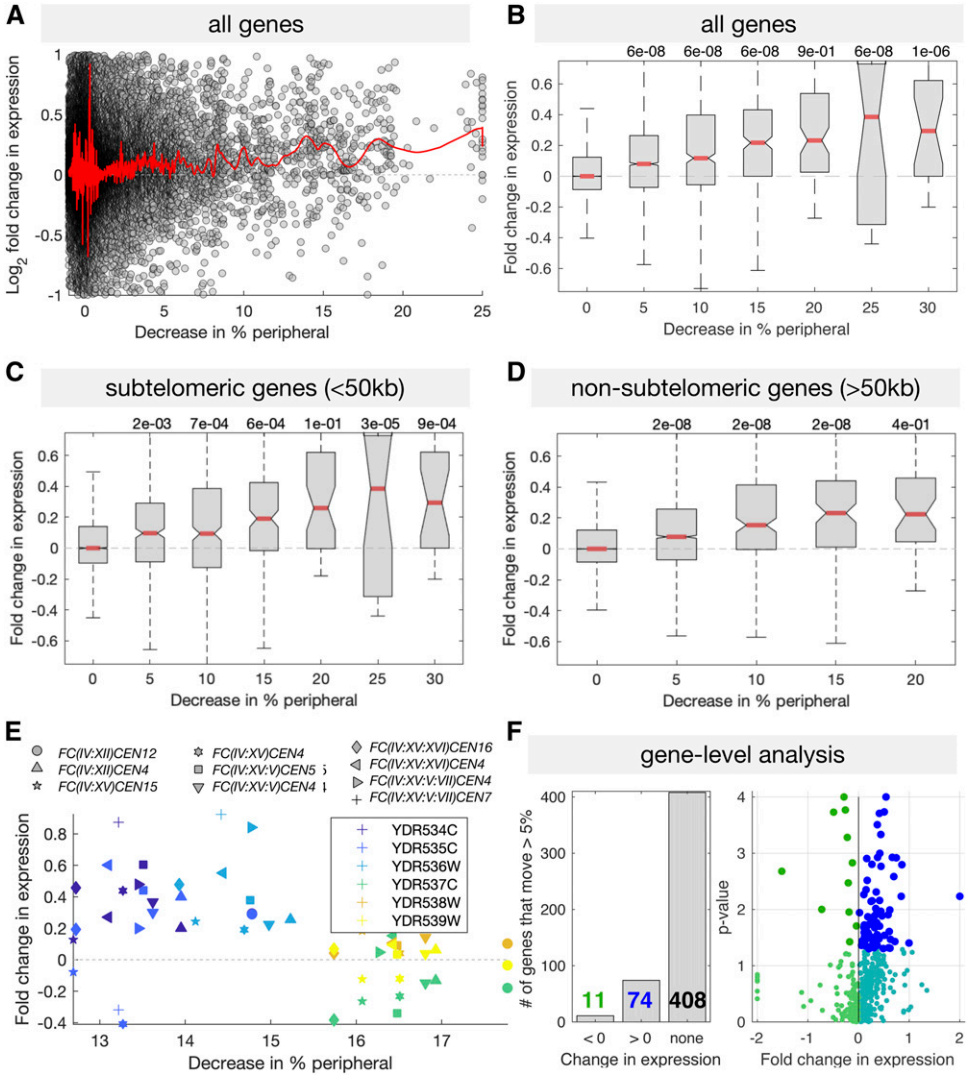

Figure 7 Gene displacement away from the nuclear periphery correlates with increased expression. (A) Shown for all genes and all strains are the fold changes in expression, and changes in the predicted localization to the nuclear periphery. Red line shows a LOESS fit with a window size of 100 genes (MATLAB smooth() with the "rloess" option). (B–D) The same data as in (A), with genes grouped by the predicted decrease in peripheral localization. (E) Measured expression and predicted change location for the six genes around TEL4R, which are shown to be displaced from the periphery in Figure 6F. Colors mark genes and symbols mark strains. This region is predicted to be in the periphery, has ~15% fewer nuclei, and all genes save YDR537C increase in expression. (F) The number of genes predicted to move >5% that exhibit significant (Student's *t*-test $P < 0.05$) changes in expression. (B–D) *P*-values are tests for difference in the mean between each group and the nondisplaced group, using Tukey's honestly significant difference criterion to correct for multiple hypothesis testing, using anova1() and multcompare() in MATLAB. LOESS, locally estimated scatterplot smoothing.

% peripheral or from distance to the deleted telomere for this set of genes, allowing us to correlate changes in expression with each feature. Thus, we obtained an r^2 for each, and the feature with the higher r^2 is the better predictor (Figure 9, A and C). Taking the log2(ratio) of the r^2 values, if the log2(ratio) is >0, then % peripheral is a better predictor. While both features are similarly predictive, increased expression correlates better with predicted frequency in the nuclear periphery for genes that are both close to the deleted telomere, as well as for genes further away (Figure 9, B and D). This suggests that these expression changes are not, or not entirely, due to distance from the deleted telomere, and that distance from the periphery plays a slightly more important role.

Discussion

Interphase yeast chromosomes are organized with centromeres clustering around the SPB, telomeres associating with the NE, and chromosome arms extending between these two anchoring points in a brush-like fashion. How this organization affects nuclear functions is not fully understood. Previous studies have reported altered expression of subtelomeric genes in mutants that disrupt heterochromatin formation or telomere clustering (Wyrick *et al.* 1999; Taddei *et al.* 2009). Importantly, these studies did not directly address the role of 3D chromosome organization, as the genetic perturbations used (depletion of histone H4, and mutations of the silencing factor *SIR3* and of the telomere tethering proteins *YKU70* and *ESC1*) affected multiple processes, including heterochromatin formation, genome-wide gene expression, and DNA repair.

In this study, we used tailored chromosome fusions (FC cells) to alter interphase nuclear organization in otherwise wild-type cells. Computational modeling validated with single-cell imaging revealed significant changes in nuclear organization after these chromosome fusion events. These changes included displacement of donor chromosomes away from the SPB after deletion of their centromeres and displacement of chromosome regions away from the nuclear periphery after

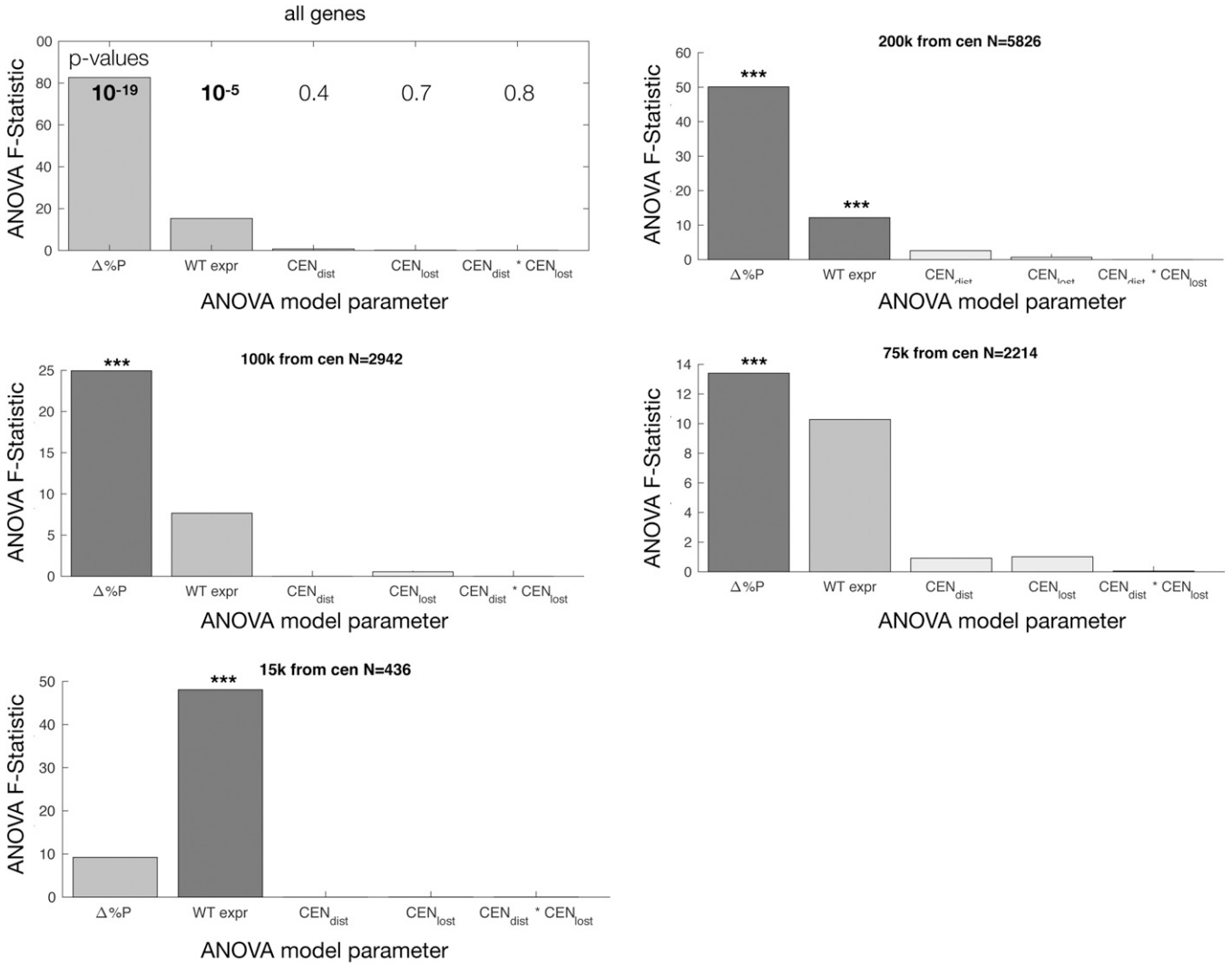

Figure 8 Deletion of the *CEN* element does not account for changes in the expression of nearby genes. ANOVA F-Statistic (the predictive power of each variable) for measured change in expression [log2(FC/WT)] for all genes, or only genes 200, 100, 75, or 15 kb from the centromere. Multivariate ANOVA shows that the only significant predictors of change in expression are the predicted change in localization relative to the nuclear periphery (Δ%P) and, to a lesser extent, the expression of that gene in WT cells (*** $P < 0.05$ after multiple hypothesis testing). In this ANOVA, terms are added sequentially, so the model is testing if WT_{expr} adds to the predictive power of a model that already includes Δ%P, then tests if adding CEN_{dist} further improves the model, and so on. CEN_{dist} tests if the distance to the centromere is correlated with changes in expression after taking into account all other features in the model (change in %peripheral, WT expression, etc). CEN_{lost} tests if deletion of a CEN element affects expression after taking into account all other features in the model (change in %peripheral, WT expression, etc). CEN_{dist}*CEN_{lost} (the last bar) is an interaction term testing if the distance to the centromere specifically matters for deleted centromeres. Cen, centromere; expr, expression; FC, fused chromosome; WT, wild-type.

deletion of neighboring telomeres. Furthermore, the distance between two chromosome loci in the arm of a donor chromosome was reduced upon fusion to a receiving chromosome, in both live cells and computational models. Notably, reduced distances between the same chromatin loci in FC strains were previously observed during anaphase chromosome segregation (Neurohr *et al.* 2011; Titos *et al.* 2014). This suggests that physical constraints acting on interphase chromatin of fused donor chromosomes can lead to their increased compaction, which is then maintained throughout the cell division cycle. This highlights the power of polymer-based modeling to reproduce nuclear organization features (Tjong *et al.* 2012; Wong *et al.* 2012) and further extends the applicability of these approaches to predict nuclear organization of yeast strains with chromosome fusions, based only on minimal imposed constraints.

Our analysis reveals that genome-wide gene expression levels remained generally unaffected by changes in chromosome organization. However, we also find that chromosome fusions result in consistent and reproducible increases in expression, with >100 genes exhibiting a mild but significant increase. This is consistent with normal growth of FC strains in rich media (Titos *et al.* 2014), and with recent reports that overall transcription is not affected by fusion of all yeast chromosomes into one or two mega-chromosomes (Luo *et al.* 2018; Shao *et al.* 2018). These two studies also

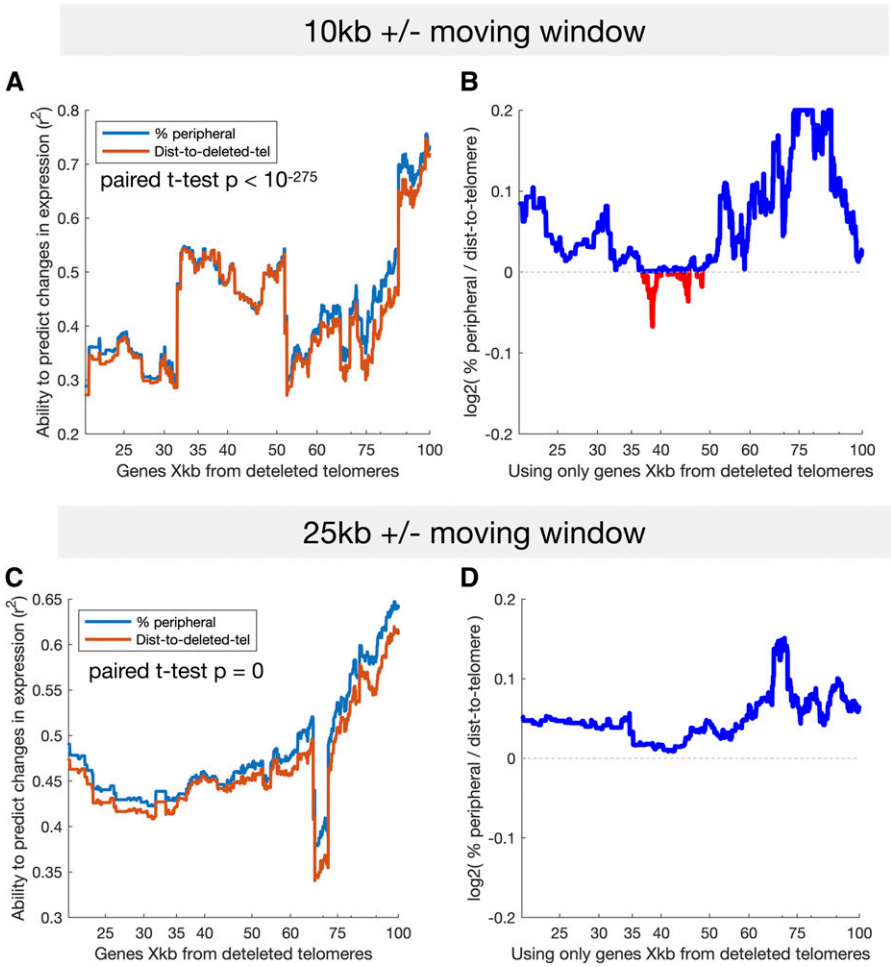

Figure 9 The predicted change in % peripheral is a better predictor of changes in gene expression than is the distance to the telomere. Using data from all FC strains, we selected the subset of genes on all chromosome arms that underwent fusion, and calculated the fold-change in expression (relative to wild-type), the change in % peripheral, and the distance to the former telomere. (A and C) The r^2 for predicting change in expression as a function of either % peripheral or distance to the telomere for all genes within a 20- (A) or 50-kb (B) moving window. This measures the correlation of each feature within each window. (B and D) Each point shows the fold difference between the ability of changes in % peripheral to predict expression and the ability of the log distance to the telomere to predict expression. Each value is the $\log2(r^2_{\%peripheral}/r^2_{dist\text{-}to\text{-}tel})$ for the set of genes that are in a 20- (B) or 50-kb (D) moving window centered X kb from the former telomere. Gene sets in which changes in % peripheral are better predictors of changes in expression ($\log2(r^2_{\%peripheral}/r^2_{dist\text{-}to\text{-}tel}) > 0$) are colored blue. dist-to-tel, distance to telomere; FC, fused chromosome.

reported derepression of subtelomeric genes near chromosome fusion sites, which was attributed to disruption of telomeric silencing. These studies used one to three RNA-seq biological replicates, whereas we used four biological replicates for wild-type, and three or four biological replicates for each of 10 FC genotypes, for a total of 42 experiments. Accurate quantification of expression changes of <50% requires >10 replicates (Schurch *et al.* 2016), potentially explaining why we identified a relatively higher number of genes with changes in expression of 10–20%. Because increased expression of these genes is correlated with both their 1D distance to the former telomere and their 3D distance to the periphery, both deletion of neighboring telomeres and spatial displacement away from the nuclear periphery may contribute to increased expression levels of subtelomeric genes. Our results suggest that, while deletion of telomere sequences may play a role, 3D distance to the periphery is likely a major factor affecting gene expression (Figure 9).

It is interesting to consider our results in the context of previous studies on the mechanisms of subtelomeric silencing in budding yeast. Transcription levels are known to decrease in proximity to telomeres [reviewed in Mondoux and Zakian (2006)]. Moreover, gene targeting to the nuclear periphery, either by integration of reporters in subtelomeric regions or by artificial anchoring to perinuclear proteins, leads to silencing that is dependent on perinuclear enrichment of SIR factors (Gottschling *et al.* 1990; Andrulis *et al.* 1998; Pryde and Louis 1999; Taddei *et al.* 2009). These observations led to the hypothesis that the NE is a transcriptionally repressive environment due to the local accumulation of repressive factors. However, a truncated telomere that does not localize to the nuclear periphery can still support silencing of a *URA3* reporter (Mondoux *et al.* 2007), and microarray analysis has shown that almost 80% of subtelomeric genes are still silenced after telomere detachment from the nuclear periphery in *esc1 yku70* mutants (Taddei *et al.* 2009). These findings raised the possibility that subtelomeric gene position and expression are independent of each other. In contrast, our results suggest that displacement from the nuclear periphery affects the expression levels of native subtelomeric genes, but that this effect is relatively mild, which may have escaped previous analysis using growth on selective media or microarrays. These findings support the hypothesis that regulation of perinuclear localization of subtelomeric genes (*e.g.*, by telomere detachment) may affect their expression in

response to environmental signals. Since chromosome detachment in the FC strains examined here caused relatively mild changes in expression, it remains unclear to what extent changes in position may contribute to the induction of subtelomeric gene expression in stress conditions.

Acknowledgments

We thank Guillaume Filion and all members of the Mendoza laboratory for comments, and the Centre for Genomic Regulation Genomics Unit for assistance with RNA-seq. This project was supported by European Research Council Starting grant 2010-St-20091118 and Spanish Ministry of Economy and Competitiveness grant BFU2012-37162 to M.M., and grant ANR-10-LABX-0030-INRT, which is a French State fund managed by the Agence Nationale de la Recherche under the frame Programme Investissements d'Avenir ANR-10-IDEX-0002-02 to the Institut de Génétique et de Biologie Moléculaire et Cellulaire. L.B.C. was supported by the Agència de Gestió d'Ajuts Universitaris i de Recerca (grant 2014 SGR 0974), and the Spanish Ministerio de Economía y Competitividad and the European Regional Development Fund (FEDER) (grant BFU2015-68351-P). M.A.M.-R. was supported by the European Union's Horizon 2020 research and innovation programme (grant agreement 676556) and the Spanish Ministry of Economy and Competitiveness (grant BFU2017-85926-P). We also acknowledge the support of the Spanish Ministry of Science and Innovation to the EMBL partnership, the 'Centro de Excelencia Severo Ochoa 2013-2017', SEV-2012-0208, the CERCA Programme/Generalitat de Catalunya, Spanish Ministry of Science and Innovation through the Instituto de Salud Carlos III, the Generalitat de Catalunya through Departament de Salut and Departament d'Empresa i Coneixement and the Co-financing by Spanish Ministry of Science and Innovation with funds from the European Regional Development Fund (ERDF) corresponding to the 2014-2020 Smart Growth Operating Program to the CRG. M.G.-A. is a recipient of a Postdoctoral Fellowship (APOSTD/2017/094) from the Generalitat Valenciana. The funders had no role in study design, data collection and analysis, the decision to publish, or preparation of the manuscript.

Literature Cited

Akhtar, A., and S. M. Gasser, 2007 The nuclear envelope and transcriptional control. Nat. Rev. Genet. 8: 507–517. https://doi.org/10.1038/nrg2122

Andrulis, E. D., A. M. Neiman, D. C. Zappulla, and R. Sternglanz, 1998 Perinuclear localization of chromatin facilitates transcriptional silencing. Nature 394: 592–595. https://doi.org/10.1038/29100

Boyle, S., S. Gilchrist, J. M. Bridger, N. L. Mahy, J. A. Ellis *et al.*, 2001 The spatial organization of human chromosomes within the nuclei of normal and emerin-mutant cells. Hum. Mol. Genet. 10: 211–219. https://doi.org/10.1093/hmg/10.3.211

Branco, M. R., and A. Pombo, 2006 Intermingling of chromosome territories in interphase suggests role in translocations and transcription-dependent associations. PLoS Biol. 4: e138. https://doi.org/10.1371/journal.pbio.0040138

Brauer, M. J., C. Huttenhower, E. M. Airoldi, R. Rosenstein, J. C. Matese *et al.*, 2008 Coordination of growth rate, cell cycle, stress response, and metabolic activity in yeast. Mol. Biol. Cell 19: 352–367. https://doi.org/10.1091/mbc.e07-08-0779

Brickner, J. H., and P. Walter, 2004 Gene recruitment of the activated INO1 locus to the nuclear membrane. PLoS Biol. 2: e342. https://doi.org/10.1371/journal.pbio.0020342

Bystricky, K., P. Heun, L. Gehlen, J. Langowski, and S. M. Gasser, 2004 Long-range compaction and flexibility of interphase chromatin in budding yeast analyzed by high-resolution imaging techniques. Proc. Natl. Acad. Sci. USA 101: 16495–16500. https://doi.org/10.1073/pnas.0402766101

Bystricky, K., T. Laroche, G. Van Houwe, M. Blaszczyk, and S. M. Gasser, 2005 Chromosome looping in yeast: telomere pairing and coordinated movement reflect anchoring efficiency and territorial organization. J. Cell Biol. 168: 375–387. https://doi.org/10.1083/jcb.200409091

Casolari, J. M., C. R. Brown, S. Komili, J. West, H. Hieronymus *et al.*, 2004 Genome-wide localization of the nuclear transport machinery couples transcriptional status and nuclear organization. Cell 117: 427–439. https://doi.org/10.1016/S0092-8674(04)00448-9

Casolari, J. M., C. R. Brown, D. A. Drubin, O. J. Rando, and P. A. Silver, 2005 Developmentally induced changes in transcriptional program alter spatial organization across chromosomes. Genes Dev. 19: 1188–1198. https://doi.org/10.1101/gad.1307205

Cremer, T., and C. Cremer, 2001 Chromosome territories, nuclear architecture and gene regulation in mammalian cells. Nat. Rev. Genet. 2: 292–301. https://doi.org/10.1038/35066075

Cremer, T., C. Cremer, T. Schneider, H. Baumann, L. Hens *et al.*, 1982 Analysis of chromosome positions in the interphase nucleus of Chinese hamster cells by laser-UV-microirradiation experiments. Hum. Genet. 62: 201–209. https://doi.org/10.1007/BF00333519

Croft, J. A., J. M. Bridger, S. Boyle, P. Perry, P. Teague *et al.*, 1999 Differences in the localization and morphology of chromosomes in the human nucleus. J. Cell Biol. 145: 1119–1131. https://doi.org/10.1083/jcb.145.6.1119

Cui, Y., and C. Bustamante, 2000 Pulling a single chromatin fiber reveals the forces that maintain its higher-order structure. Proc. Natl. Acad. Sci. USA 97: 127–132. https://doi.org/10.1073/pnas.97.1.127

Dekker, J., 2008 Mapping in vivo chromatin interactions in yeast suggests an extended chromatin fiber with regional variation in compaction. J. Biol. Chem. 283: 34532–34540. https://doi.org/10.1074/jbc.M806479200

Denker, A., and W. De Laat, 2016 The second decade of 3C technologies: detailed insights into nuclear organization. Genes Dev. 30: 1357–1382. https://doi.org/10.1101/gad.281964.116

Di Stefano, M., A. Rosa, V. Belcastro, D. di Bernardo, and C. Micheletti, 2013 Colocalization of coregulated genes: a steered molecular dynamics study of human chromosome 19. PLOS Comput. Biol. 9: e1003019. https://doi.org/10.1371/journal.pcbi.1003019

Di Stefano, M., J. Paulsen, T. G. Lien, E. Hovig, and C. Micheletti, 2016 Hi-C-constrained physical models of human chromosomes recover functionally-related properties of genome organization. Sci. Rep. 6: 35985. https://doi.org/10.1038/srep35985

Duan, Z., M. Andronescu, K. Schutz, S. McIlwain, Y. J. Kim *et al.*, 2010 A three-dimensional model of the yeast genome. Nature 465: 363–367. https://doi.org/10.1038/nature08973

Dultz, E., H. Tjong, E. Weider, M. Herzog, B. Young *et al.*, 2016 Global reorganization of budding yeast chromosome conformation in different physiological conditions. J. Cell Biol. 212: 321–334. https://doi.org/10.1083/jcb.201507069

Finlan, L. E., D. Sproul, I. Thomson, S. Boyle, E. Kerr *et al.*, 2008 Recruitment to the nuclear periphery can alter expression of genes in human cells. PLoS Genet. 4: e1000039. https://doi.org/10.1371/journal.pgen.1000039

Furlan-Magaril, M., C. Várnai, T. Nagano, and P. Fraser, 2015 3D genome architecture from populations to single cells. Curr. Opin. Genet. Dev. 31: 36–41. https://doi.org/10.1016/j.gde.2015.04.004

Gasch, A. P., P. T. Spellman, C. M. Kao, O. Carmel-Harel, M. B. Eisen *et al.*, 2000 Genomic expression programs in the response of yeast cells to environmental changes. Mol. Biol. Cell 11: 4241–4257. https://doi.org/10.1091/mbc.11.12.4241

Gibcus, J. H., and J. Dekker, 2013 The hierarchy of the 3D genome. Mol. Cell 49: 773–782. https://doi.org/10.1016/j.molcel.2013.02.011

Gotta, M., T. Laroche, and S. M. Gasser, 1999 Analysis of nuclear organization in Saccharomyces cerevisiae. Methods Enzymol. 304: 663–672. https://doi.org/10.1016/S0076-6879(99)04040-9

Gottschling, D. E., O. M. Aparicio, B. L. Billington, and V. A. Zakian, 1990 Position effect at S. cerevisiae telomeres: reversible repression of Pol II transcription. Cell 63: 751–762. https://doi.org/10.1016/0092-8674(90)90141-Z

Green, E. M., Y. Jiang, R. Joyner, and K. Weis, 2012 A negative feedback loop at the nuclear periphery regulates GAL gene expression. Mol. Biol. Cell 23: 1367–1375. https://doi.org/10.1091/mbc.e11-06-0547

Guelen, L., L. Pagie, E. Brasset, W. Meuleman, M. B. Faza *et al.*, 2008 Domain organization of human chromosomes revealed by mapping of nuclear lamina interactions. Nature 453: 948–951 [corrigenda: Nature 500: 242 (2013)]. https://doi.org/10.1038/nature06947

Haaf, T., and M. Schmid, 1991 Chromosome topology in mammalian interphase nuclei. Exp. Cell Res. 192: 325–332. https://doi.org/10.1016/0014-4827(91)90048-Y

Imakaev, M., G. Fudenberg, R. P. McCord, N. Naumova, A. Goloborodko *et al.*, 2012 Iterative correction of Hi-C data reveals hallmarks of chromosome organization. Nat. Methods 9: 999–1003. https://doi.org/10.1038/nmeth.2148

Jones, J. E., 1924 On the determination of molecular fields. II. From the equation of state of a gas. Proc. Royal Soc., Math. Phys. Eng. Sci. 106: 463–477. https://doi.org/10.1098/rspa.1924.0082

Kosak, S. T., J. A. Skok, K. L. Medina, R. Riblet, M. M. Le Beau *et al.*, 2002 Subnuclear compartmentalization of immunoglobulin loci during lymphocyte development. Science 296: 158–162. https://doi.org/10.1126/science.1068768

Kumar, A., P. Sharma, M. Gomar-Alba, Z. Shcheprova, A. Daulny *et al.*, 2018 Daughter-cell-specific modulation of nuclear pore complexes controls cell cycle entry during asymmetric division. Nat. Cell Biol. 20: 432–442. https://doi.org/10.1038/s41556-018-0056-9

Kumaran, R. I., and D. L. Spector, 2008 A genetic locus targeted to the nuclear periphery in living cells maintains its transcriptional competence. J. Cell Biol. 180: 51–65. https://doi.org/10.1083/jcb.200706060

Langowski, J., 2006 Polymer chain models of DNA and chromatin. Eur. Phys. J. E Soft Matter 19: 241–249. https://doi.org/10.1140/epje/i2005-10067-9

Lazar-Stefanita, L., V. F. Scolari, G. Mercy, H. Muller, T. M. Guérin *et al.*, 2017 Cohesins and condensins orchestrate the 4D dynamics of yeast chromosomes during the cell cycle. EMBO J. 36: 2684–2697. https://doi.org/10.15252/embj.201797342

Lemaître, C., and W. A. Bickmore, 2015 Chromatin at the nuclear periphery and the regulation of genome functions. Histochem. Cell Biol. 144: 111–122. https://doi.org/10.1007/s00418-015-1346-y

Lesne, A., J. Riposo, P. Roger, A. Cournac, and J. Mozziconacci, 2014 3D genome reconstruction from chromosomal contacts. Nat. Methods 11: 1141–1143. https://doi.org/10.1038/nmeth.3104

Luo, J., X. Sun, B. P. Cormack, and J. D. Boeke, 2018 Karyotype engineering by chromosome fusion leads to reproductive isolation in yeast. Nature 560: 392–396. https://doi.org/10.1038/s41586-018-0374-x

Markaki, Y., M. Gunkel, L. Schermelleh, S. Beichmanis, J. Neumann *et al.*, 2010 Functional nuclear organization of transcription and DNA replication: a topographical marriage between chromatin domains and the interchromatin compartment. Cold Spring Harb. Symp. Quant. Biol. 75: 475–492. https://doi.org/10.1101/sqb.2010.75.042

Menon, B. B., N. J. Sarma, S. Pasula, S. J. Deminoff, K. A. Willis *et al.*, 2005 Reverse recruitment: the Nup84 nuclear pore subcomplex mediates Rap1/Gcr1/Gcr2 transcriptional activation. Proc. Natl. Acad. Sci. USA 102: 5749–5754. https://doi.org/10.1073/pnas.0501768102

Mondoux, M. A., and V. A. Zakian, 2006 Telomere position effect: silencing near the end, pp. 261–316 in *Telomeres*, Ed. 2, edited by T. de Lange, V. Lundblad, and E. Blackburn. Cold Spring Harbor Laboratory Press, Cold Spring Harbor, NY.

Mondoux, M. A., J. G. Scaife, and V. A. Zakian, 2007 Differential nuclear localization does not determine the silencing status of Saccharomyces cerevisiae telomeres. Genetics 177: 2019–2029. https://doi.org/10.1534/genetics.107.079848

Neurohr, G., A. Naegeli, I. Titos, D. Theler, B. Greber *et al.*, 2011 A midzone-based ruler adjusts chromosome compaction to anaphase spindle length. Science 332: 465–468. https://doi.org/10.1126/science.1201578

O'Toole, E. T., M. Winey, and J. R. McIntosh, 1999 High-voltage electron tomography of spindle pole bodies and early mitotic spindles in the yeast Saccharomyces cerevisiae. Mol. Biol. Cell 10: 2017–2031. https://doi.org/10.1091/mbc.10.6.2017

Peric-Hupkes, D., W. Meuleman, L. Pagie, S. W. M. Bruggeman, I. Solovei *et al.*, 2010 Molecular maps of the reorganization of genome-nuclear lamina interactions during differentiation. Mol. Cell 38: 603–613. https://doi.org/10.1016/j.molcel.2010.03.016

Pickersgill, H., B. Kalverda, E. de Wit, W. Talhout, M. Fornerod *et al.*, 2006 Characterization of the Drosophila melanogaster genome at the nuclear lamina. Nat. Genet. 38: 1005–1014. https://doi.org/10.1038/ng1852

Plimpton, S., 1995 Fast parallel algorithms for short-range molecular dynamics. J. Comput. Phys. 117: 1–19. https://doi.org/10.1006/jcph.1995.1039

Pryde, F. E., and E. J. Louis, 1999 Limitations of silencing at native yeast telomeres. EMBO J. 18: 2538–2550. https://doi.org/10.1093/emboj/18.9.2538

Reddy, K. L., J. M. Zullo, E. Bertolino, and H. Singh, 2008 Transcriptional repression mediated by repositioning of genes to the nuclear lamina. Nature 452: 243–247. https://doi.org/10.1038/nature06727

Rosa, A., and R. Everaers, 2008 Structure and dynamics of interphase chromosomes. PLOS Comput. Biol. 4: e1000153. https://doi.org/10.1371/journal.pcbi.1000153

Schmid, M., G. Arib, C. Laemmli, J. Nishikawa, T. Durussel *et al.*, 2006 Nup-PI: the nucleopore-promoter interaction of genes in yeast. Mol. Cell 21: 379–391. https://doi.org/10.1016/j.molcel.2005.12.012

Schurch, N. J., P. Schofield, M. Gierliński, C. Cole, A. Sherstnev *et al.*, 2016 How many biological replicates are needed in an RNA-seq experiment and which differential expression tool should you use? RNA 22: 839–851. https://doi.org/10.1261/rna.053959.115

Serra, F., D. Baù, M. Goodstadt, D. Castillo, G. J. Filion *et al.*, 2017 Automatic analysis and 3D-modelling of Hi-C data using TADbit reveals structural features of the fly chromatin colors. PLOS Comput. Biol. 13: e1005665. https://doi.org/10.1371/journal.pcbi.1005665

Shao, Y., N. Lu, Z. Wu, C. Cai, S. Wang *et al.*, 2018 Creating a functional single-chromosome yeast. Nature 560: 331–335. https://doi.org/10.1038/s41586-018-0382-x

Taddei, A., and S. M. Gasser, 2012 Structure and function in the budding yeast nucleus. Genetics 192: 107–129. https://doi.org/10.1534/genetics.112.140608

Taddei, A., G. Van Houwe, F. Hediger, V. Kalck, F. Cubizolles *et al.*, 2006 Nuclear pore association confers optimal expression levels for an inducible yeast gene. Nature 441: 774–778. https://doi.org/10.1038/nature04845

Taddei, A., G. Van Houwe, S. Nagai, I. Erb, E. van Nimwegen *et al.*, 2009 The functional importance of telomere clustering: global changes in gene expression result from SIR factor dispersion. Genome Res. 19: 611–625. https://doi.org/10.1101/gr.083881.108

Taddei, A., H. Schober, and S. M. Gasser, 2010 The budding yeast nucleus. Cold Spring Harb. Perspect. Biol. 2: a000612. https://doi.org/10.1101/cshperspect.a000612

Therizols, P., T. Duong, B. Dujon, C. Zimmer, and E. Fabre, 2010 Chromosome arm length and nuclear constraints determine the dynamic relationship of yeast subtelomeres. Proc. Natl. Acad. Sci. USA 107: 2025–2030. https://doi.org/10.1073/pnas.0914187107

Titos, I., T. Ivanova, and M. Mendoza, 2014 Chromosome length and perinuclear attachment constrain resolution of DNA intertwines. J. Cell Biol. 206: 719–733. https://doi.org/10.1083/jcb.201404039

Tjong, H., K. Gong, L. Chen, and F. Alber, 2012 Physical tethering and volume exclusion determine higher-order genome organization in budding yeast. Genome Res. 22: 1295–1300. https://doi.org/10.1101/gr.129437.111

Vidal, E., F. le Dily, J. Quilez, R. Stadhouders, Y. Cuartero *et al.*, 2018 OneD: increasing reproducibility of Hi-C samples with abnormal karyotypes. Nucleic Acids Res. 46: e49. https://doi.org/10.1093/nar/gky064

Wong, H., H. Marie-Nelly, S. Herbert, P. Carrivain, H. Blanc *et al.*, 2012 A predictive computational model of the dynamic 3D interphase yeast nucleus. Curr. Biol. 22: 1881–1890. https://doi.org/10.1016/j.cub.2012.07.069

Wyrick, J. J., F. C. Holstege, E. G. Jennings, H. C. Causton, D. Shore *et al.*, 1999 Chromosomal landscape of nucleosome-dependent gene expression and silencing in yeast. Nature 402: 418–421. https://doi.org/10.1038/46567

Zimmer, C., and E. Fabre, 2011 Principles of chromosomal organization: lessons from yeast. J. Cell Biol. 192: 723–733. https://doi.org/10.1083/jcb.201010058

Zink, D., M. D. Amaral, A. Englmann, S. Lang, L. A. Clarke *et al.*, 2004 Transcription-dependent spatial arrangements of CFTR and adjacent genes in human cell nuclei. J. Cell Biol. 166: 815–825. https://doi.org/10.1083/jcb.200404107

Communicating editor: O. Cohen-Fix

7. Discussion

7.1. General conclusions on the paper

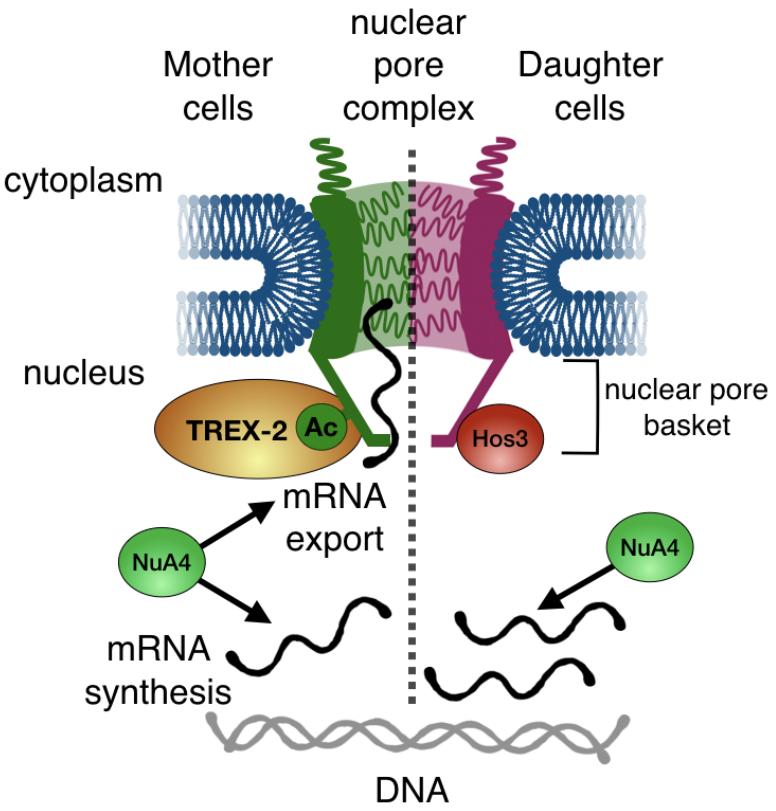

Figure 6 Esa1 coordinates mRNA synthesis and export during the G1/S transition through Nup60 acetylation *In mother cells, Esa1 promotes both mRNA synthesis and export. Mechanistically, mRNA export is promoted by the acetylation of Nup60, which increases the association between the mRNA export factor TREX-2 and the nuclear pore basket. In daughter cells, Hos3 deacetylates Nup60, which reduces TREX-2 association with the NPC, and thus mRNA export. Inhibition of Nup60 acetylation in daughter cells contributes to their longer G1 phase, possibly by delaying the export of mRNAs required for entry into the S phase such as CLN2, and inhibits the expression of the GAL1 gene in response to galactose.*

The results presented in the paper indicate that Esa1 lysine acetyltransferase (KAT) promotes G1/S transition termed Start in budding yeast. We show that the function of Esa1 is partially complemented by the acetyltransferase activity of Gcn5 which however plays a minor role. Esa1 and Gcn5 form parts of conserved NuA4 and SAGA complexes respectively, and together they are considered to be responsible for the majority of acetylation-driven transcriptional regulation in cells with partially shared

functions. SAGA and NuA4 are known to be recruited to activator-bound promoter regions through the interaction of a shared subunit Tra1 (Brown et al., 2001; Helmlinger & Tora, 2017) and to acetylate histone H3 and H4 N-terminal tails accordingly. This together with other functions of the complexes is thought to promote local chromatin remodeling and facilitate transcription, and we believe that our results indicate an important role of NuA4 and SAGA for transcriptional activation of hundreds of genes at G1/S transition.

However, both Esa1 and Gcn5 are known to target many non-histone proteins (Downey et al., 2015; Henriksen et al., 2012), and we find that the same protein complexes target nuclear pore complexes (NPC) to promote G1/S gene expression in a parallel pathway. We show that Esa1 and Gcn5 can acetylate Nup60 when overexpressed, and that acetylation of this nucleoporin promotes the export of *CLN2* mRNA encoding the periodically expressed G1 cyclin, one of the main drivers of G1/S transition. Nup60 acetylation contributes to the mRNA export mechanism utilized for many mRNAs since it partially compensates for the pronounced mRNA export defect observed in cells deficient in Esa1 function. Another indication of global mRNA export regulation by NPC acetylation is that Nup60 acetyl-mimic allele promotes *GAL1* promoter-driven expression, which is cell-cycle independent.

The most intriguing part of our findings is that Nup60 acetylation promotes mRNA export through increasing the interaction of TREX-2 complex (TRanscription and EXport complex 2) scaffold component Sac3 with the nuclear pore. TREX-2 at the nuclear periphery is known to promote mRNA export, yet we demonstrate its related role in G1/S cell cycle transition possibly linked with the export of *CLN2* and/or other mRNAs. The mechanism is inhibited in yeast daughter cells contributing to its longer G1 duration due to selective NPC deacetylation by the Hos3 enzyme localized specifically to the daughter nuclear pores in mitosis. Overall we have shown the predominant role of Esa1 in G1/S specific gene transcription and the existence of an Esa1-dependent pathway that regulates mRNA export through NPC acetylation in G1/S transition and beyond.

7.2. Role of lysine acetyltransferases in transcriptional regulation in G1/S

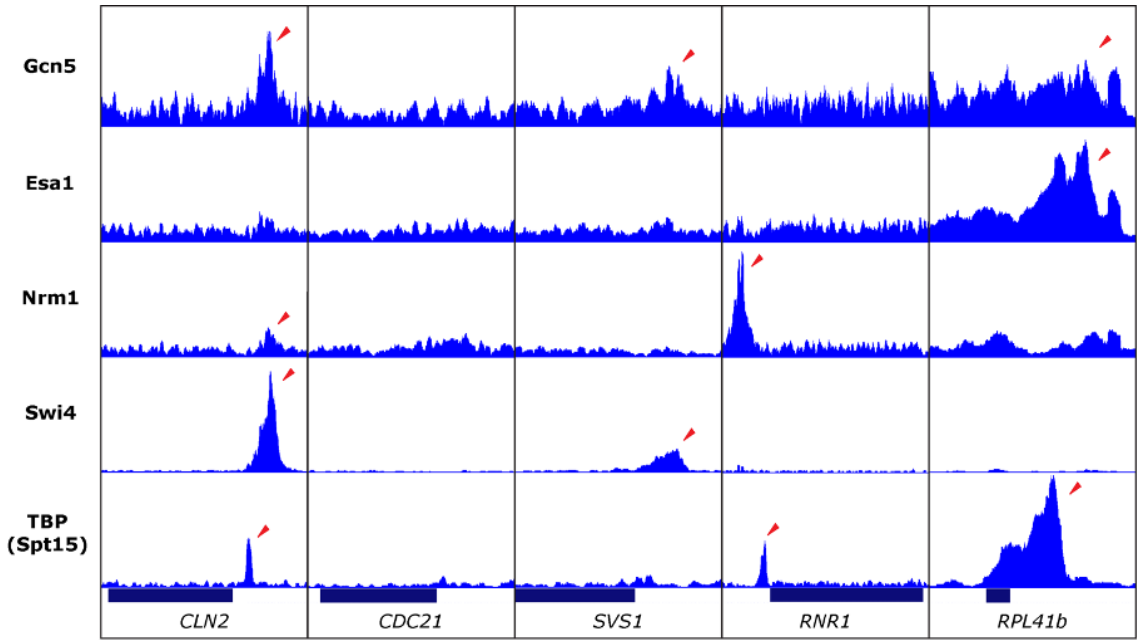

Figure 7 ChIP-seq profiles of the *S.cerevisiae* genes analyzed in (Gomar-Alba et al., 2022) **by RT-qPCR** *ChIP-seq profiles of diverse transcription factors (Nrm1, Swi4, and TBP) and gene expression co-activators (Gcn5 and Esa1) aligned against budding yeast genome for G1/S activated genes (CLN2, CDC21, SVS1, and RNR1) and their promoter regions and RPL41b gene implicated in ribosome biogenesis known to be regulated by Esa1/NuA4. Open reading frames are marked as blue bars at the bottom next to the gene names, red arrowheads indicate the protein binding peaks. Data is taken from a publicly available database located at yeastepigenome.org, track numbers: Gcn5 #11826, Esa1 #18477, Nrm1 #12878, Swi4 #12000, TBP/Spt15 #8599.*

The G1/S transition is happening in a switch-like and largely irreversible manner, bringing along the transcriptional induction of hundreds of genes. The coordinated gene expression is partially ensured by the dissociation of the Whi5 transcriptional repressor from the promoters and its export from the nucleus to the cytoplasm. *CLN2* is a gene that belongs to the regulon and, once expressed, Cln2 protein creates a crucial positive feedback loop increasing its own transcription and providing rapid activation of the rest of the regulon through targeting of Cdk1 to Whi5, causing whi5 phosphorylation and inactivation. Transcriptional induction is thus crucial for G1/S transition, and transcriptional activation is linked with the enrichment of lysine acetyltransferase complexes within the promoter regions and the coding sequences. These molecular machines are thought to facilitate transcription via histone tail acetylation, histone deubiquitination, recruitment of chromatin remodeling complexes, and contribution to pre-initiation complex formation.

Gcn5 acetyltransferase was found implicated in cell cycle progression through regulation of key molecules (e.g. cyclins and transcription factors) in chicken cell culture (Kikuchi et al., 2005) and later on it was shown to mildly affect the transcription of genes activated at Start in budding yeast. The minor effect of the *GCN5* deletion on the transcription with a significant concomitant decrease in Gcn5 histone targets (Kishkevich et al., 2019) indicated that, if histone acetylation is important for G1/S gene transcription then Gcn5 is not the main enzyme performing the task.

In our work, we have established an important role for Esa1 acetyltransferase in this process. Interestingly, if we compare the pattern of G1/S gene transcription (Figure 2 in the Gomar et al. 2022) with the association of the general transcription factor TBP (Spt15) in asynchronous cells (Figure 7), then we will see a clear correlation. The genes that have high levels of Spt15 bound in the promoter regions reach their maximal transcript levels upon Esa1 inactivation at the same time as the wild-type cells (*CLN2* and *RNR1*), whereas the peak of transcript abundance is shifted toward a later time point in the absence of Spt15 promoter enrichment (*CDC21* and *SVS1*). It could be hypothesized that Esa1 promotes timely expression at *CDC21* and *SVS1* promoters, possibly by contributing to the TFIID-dependent mode of TBP recruitment and pre-initiation complex formation. Both Esa1 and Gcn5 modulate the efficiency of transcription for all 4 genes evaluated, albeit to a different extent (Figure EV3 in the Gomar et al. 2022), likely by increasing promoter accessibility and RNA pol II association (Bruzzone et al., 2018; Imoberdorf et al., 2006). However, if Esa1 contributes to the expression as described above, it must be recruited to these genes, and since there is no prominent association of Esa1 with *CLN2*, *CDC21*, *SVS1,* or *RNR1* genes in asynchronous culture, it could be recruited dynamically at G1/S transition. This possibility remains to be explored in the future.

7.3. NPC acetylation in gene expression regulation

In our work we find that NPC acetylation promotes TREX-2 association with the nuclear periphery, which according to the known functions of TREX-2 could promote transcription and/or mRNA export of certain mRNAs. Cln2 protein accumulation is delayed in NuA4 deficient cells and this delay is rescued in cells expressing Nup60 allele mimicking its constitutive acetylation, however, no transcriptional advance for *CLN2* was found neither by regular RT-qPCR on total RNA nor by the analysis of nascent RNA production (my unpublished data), that allows to directly assess the synthesis rate and is

more sensitive (Wissink et al., 2019). However, we do demonstrate the role of Esa1 and NPC acetylation in promoting mRNA export.

At the end of anaphase, Hos3 deacetylase opposes Esa1 at the daughter nuclear baskets and deacetylates the NPC. We find that Esa1 and Nup60 acetylation contributes to faster G1/S transition, and Hos3 on the other hand delays G1/S transition specifically in daughter cells. While we directly show that *CLN2* mRNA export is impaired in Esa1-deficient cells, we also see the significant accumulation of polyadenylated RNA in the nuclei of Esa1-deficient cells and in cells with Hos3 constitutively localized to the nuclear periphery in mother and daughter cells (Hos3-NLS), suggesting a global mRNA export defect affecting multiple mRNAs. In wild-type cells, the association of Hos3 with the NE, corresponding to NPC deacetylation is quite transient and ends as cells exit mitosis. However, the low level of NPC acetylation assessed for Nup60 persists for 20-40 minutes after release from Cdc20-dependent anaphase arrest meaning that NPC is not reacetylated at least until late G1. Is mRNA export completely blocked during this time?

That seems unlikely, since the cells preferentially grow in the G1 phase, which presumably requires continuous export of many RNAs. It is therefore more plausible that the export of a subset of mRNAs including

1) the one(s) essential for cell cycle progression
2) the one(s) that are required in the following S
3) the one(s) that are undesired in the current G1

are affected by NPC acetylation. If that is the case, there must exist additional mechanisms that link the RNP structure and the probability to be exported depending on the NPC acetylation. In our work, we find that TREX-2 is less enriched in the nuclear periphery of daughter cells and that TREX-2 is increased at the periphery when the Nup60-KN allele mimicking constitutive acetylation of Nup60 is expressed. A recent study indicates that TREX-2 does not associate with some pores devoid of the Mlp1/2 components, termed “basketless”, present both in the nucleolus-associated and in other parts of the NE (Bensidoun et al., 2022). The decrease in TREX-2 in the nuclear periphery of the daughter cells that we observe could be therefore correlated with the increased number of basketless pores, which is an intriguing possibility we would like to verify.

If that is the case, what could be the consequences of the mRNA export for the daughters? The export of bigger transcripts and mRNAs containing longer polyA tail has been shown to preferentially occur through TREX-2-associated basket-containing pores (Bensidoun et al., 2022). Thus cell cycle-dependent regulation of polyA length coupled to

the regulation of the TREX-2 availability at the nuclear basket could present a mechanism of mRNA export regulation for a number of transcripts. One possible example is the case of histone mRNAs: for a long time it was known that their abundance peaks in the S phase and that they are barely detected in other cell cycle stages (Hereford et al., 1981), however, a more recent study uncovered an additional level of regulation for *HTB1* mRNA. Its polyA tails are longer in G1 and decrease their length roughly twofold as cells enter the S phase, which nicely correlates with *HTB1* mRNA being largely retained in the nucleus in G1. (Beggs et al., 2012) It may be proposed that certain mRNAs possessing longer polyA tails are selectively retained in the nucleus of G1 daughters due to a lower abundance of NPCs bound by TREX-2 and hence competent for export of such mRNAs.

Interestingly, *CLN2* was found within the limited group of mRNAs demonstrating a high population of oligoadenylated (3-5 adenosines) species (Tudek et al., 2021), which may indicate that *CLN2* is also regulated at the level of polyA length modulation. This is supported by the notion that overexpression of polyA-binding protein Pab1 suppresses the lethality of *bck swi6-ts* mutant cells, at the same time bringing *CLN2* mRNA levels almost to wild-type levels, which is coherent with the rescue of this mutant by ectopic G1 cyclin expression. However, in synchronized cells, the levels were not found to be increased (perhaps at G1/S, with compensation at other cell cycle stages - data was not shown), which could mean that it is not just the overall abundance, but the specific characteristics of the mRNA, such as polyA tail, could be modulated by Pab1 at G1/S. (Flick & Wittenberg, 2005)

Another link between mRNA metabolism of G1/S expressed genes and the NPC lies within the NPC association with the conserved Ccr4-Not complex: it modulates transcription initiation and elongation with the preference towards SAGA-controlled genes and contributes to mRNA degradation pathway (Azzouz et al., 2009; Cui et al., 2008), interacts with the Mlp1 of the nuclear basket (Kerr et al., 2011) and its RNA substrate recruiting subunit Not2 genetically interacts with Hos3 (Collins et al., 2007). The acute depletion of 2 of the Ccr4-Not components (Caf1 deadenylase and Not1 scaffold protein) leads to a major accumulation of mRNA in the cell and a delayed global downregulation of transcription; however, the decrease in transcription is significantly faster than the average for a number of G1- and S-specific genes. The authors hypothesize that the accumulation of these mRNAs (or of some related molecular player) signals back to inhibit transcription via the mechanisms that monitor cell size, nutrient availability, or to other cellular sensors. (Chappleboim et al., 2022) It could be proposed

that Ccr4-Not plays a role in the Hos3-dependent delay of daughter cells in the following way: Nup60 deacetylation leads to decreased number of Mlp1-containing NPCs and/or to decrease the association of Ccr4-Not with the nuclear periphery, thus causing the accumulation of mRNAs (or mRNA decay products) through the similar mechanism as upon Ccr4-Not depletion, resulting in the negative feedback signal to the transcription. This mechanism could be important for *CLN2* and/or other G1/S transition-regulating genes.

In order to directly show what kind of RNAs are affected by NPC acetylation, we would like to perform selective biotinylation of nuclearly retained RNAs with the following isolation of biotinylated RNAs and sequencing (Padrón et al., 2019). This could be done in cells synchronized in G1 to compare wild-type cells and the ones with *HOS3* deletion or otherwise to compare asynchronous cells with or without overexpression of Hos3-NLS. Such an experiment will give us a list of mRNAs that may contain candidate genes with a documented role in cell cycle progression regulation. Their retention in the wild type can be further verified by orthogonal methods (such as RNA FISH) and the functional significance of such retention can be assessed by a modification of the regulatory elements defining this retention.

So far in our work, we have been mostly focusing on the role of Nup60 acetylation in the function of the nuclear basket. Meanwhile, the nuclear basket seems to be the most prominently acetylated part of the NPC, its components being more reproducibly identified as acetylated and their acetylation being more conserved (see Supplementary tables 1 and 2). We would like to explore the consequences of acetylation for other basket nucleoporins. Nup2 mimicking constitutive acetylation, for example, could not rescue the G1/S transition delay of *esa1-ts* cells (my unpublished data). In our lab we want to make a comprehensive map of the nucleoporin acetylation sites in the wild-type cells and in the mutants of acetylation-modulating enzymes. To this end, Bogdan Cichocki works on the protocol to isolate all basket nucleoporins under denaturing conditions and to maximize the conservation of acetylation modifications for further detection by mass spectrometry.

7.4. How does Nup60 acetylation lead to Sac3 increased peripheral localization?

The answer to this question is yet hard to predict, partially because there is still not much known about the nuclear pore dynamical structural changes and the impact of post-translational modifications of its components on that. For example, there is a certain

incoherence between our results and the results reported in (Meinema et al., 2022) regarding the functional consequences of Nup60 acetylation on mRNA export. Nup60 acetylation in the NPCs adjacent to the nucleolus results in the loss of nuclear basket components (except Nup1) and the decreased association of mRNA export factors with the pores, including TREX-2 component Sac3. The fact that we observe the opposite effect while looking at the nuclear periphery as a whole, not focusing on the part next to the nucleolus, can be presumably explained by the compartment-specific effects of Nup60 acetylation on the NPC structure. Alternatively, it could be connected with changes in cell physiology of physiologically aged cells in (Meinema et al., 2022). At the same time it seems that in NPCs that are not associated with the nucleolus, the absence of Mlp1/2 in the presence of the rest of the basket nucleoporins is associated with decreased interaction with Sac3 (Bensidoun et al., 2022), indicating that Mlp1/2 plays a role in Sac3 driven mRNA export.

While Sac3 is known to interact with Nup1 (which likely binds the NPC independently of the rest of basket nucleoporins, at least in NPCs adjacent to the nucleolus), loss of either Nup1 or Nup60 causes an mRNA export defect (Fischer et al., 2002, 2004; Jani et al., 2014). Could it be that the Mlp1 component of the basket (whose binding depends on Nup60) promotes the interaction of Sac3 with Nup1 via the direct interaction of Mlp1 with the mRNP associated with Sac3? In this model, TREX-2 could establish interaction with Nup1 only upon mRNP passage through the channel, and this would be consistent with Nup60/NPC acetylation favoring the formation of Mlp1-containing baskets. The absence of Sac3 at the nuclear basket of Mlp1-devoid NPCs would be explained by TREX-2 preferential binding at Mlp1-positive baskets.

In order to verify this hypothesis I can do several simple experiments. First - I can check whether, indeed, Mlp1 association with the pore depends on NPC acetylation. For this, I will label Mlp1/2 in wild-type, *hos3,* and *nup60-KN* mutant cells, as well as in *esa1-ts* and *esa1-ts nup60-KN* cells, and examine the distribution/colocalization of Mlp1 with the central core nucleoporin such as Nup49 or Nup170. Next, I can check whether upon *MLP1* deletion Sac3 is localized to the nuclear periphery/co-immunoprecipitates with Nup1. Finally, I can check if upon global transcription shutdown, Sac3 relocalizes from the nuclear periphery.

The alternative explanations are multiple and none of them seems more plausible than the other. Nup60 acetylation could change the NPC structure in a different way than the one proposed above so that Nup1 has a higher probability of binding Sac3; Nup60 acetylation could either directly or indirectly affect Nup1 binding to the NPC and/or its

ability to bind Sac3; Nup60 upon acetylation could obtain the ability to bind Sac3 itself. To distinguish between these possibilities, it will be necessary to obtain structural information on the nuclear basket in different acetylation states.

One of the possible ways that Nup60 acetylation could influence the NPC structure is through modulation of Nup60 protein stability. Unpublished data from the lab (Merce Gomar) indicates that Nup60-KN demonstrates slightly but consistently elevated total protein levels as measured by western blot (data not shown); additionally, my data indicates that Nup60 levels in *gcn5* mutant cells and *esa1-ts* cells at restrictive temperature tend to be decreased compared to the wild type. If Nup60, one of the core nucleoporins of the basket, is degraded less upon acetylation, the basket may become more stable and this could influence Nup1 and its binding to Sac3. However, the cause and consequence, in this case, could be inverted, and a less stable basket may lead to higher levels of Nup60 degradation. To verify the first possibility we could first check whether upon protein synthesis shutdown Nup60 degrades faster than Nup60-KN and if yes, we could see if Sac3 association with the NPC is more stable in mutants of the protein degradation pathway.

7.5. "Meet me at the pore" or why genes go to the NPC

We have established that in the case of *CLN2* expression Nup60 acetylation plays a role in facilitating mRNA export but does not promote transcription. However, it remains to be answered what is the correlation between *CLN2* gene locus position within the nucleus and its mRNA export efficiency and/or its expression. Previous data from our lab indicates that the *CLN2* locus is located at the nuclear periphery in G1 and moves towards the nuclear interior in the S phase and that this does not depend on the positioning within the chromosome (Kumar et al., 2018). My preliminary data suggests that the moment of the switch between more constrained positioning at the nuclear periphery and the detachment, quantified relative to the moment of full Whi5 nuclear export, coincides with the moment when *CLN2* expression starts, according to the live *CLN2* mRNA measurements. This may suggest two non-mutually exclusive scenarios of *CLN2* regulation at the periphery:

1) *CLN2* locus binding to the nuclear periphery is inhibitory
2) *CLN2* locus needs to be at the nuclear periphery to be activated (i.e. it is "primed" for transcription)

The previously published work from our lab began to explore this question and *CLN2* locus was found to be repressed upon constitutive targeting to the integral

membrane protein Yif1, which localizes to the inner nuclear membrane. Initially, this was interpreted as evidence suggesting that *CLN2* is repressed at the NPC. However, Yif1 targeting may restrict *CLN2's* ability to interact with the NPC, which could be the opposite beneficial for gene induction, this is why we would like to modify this experiment and directly target the *CLN2* locus to the NPC.

Nevertheless, it is intriguing to speculate on the mechanism by which *CLN2* could be activated at the NPC. We show that Nup60 does not regulate transcription of *CLN2* but it promotes mRNA export, and the preliminary data from Max Ledoux Vanek is that in alpha-factor synchronized cells *HOS3* deletion does not promote transcription of *CLN2*. However, I would like to speculate on ways CLN2 could be activated not via NPC acetylation, and this kind of mechanism realized through Hos3 could be in place in asynchronous cells, but lost in cells that are under prolonged arrest with alpha-factor.

CLN2 expression is thought to be inhibited by the Whi5-dependent recruitment of the Rpd3(L) complex to the promoter region (Takahata et al., 2009). Rpd3 is a class I deacetylase, and its metazoan homologue HDAC1 is regulated by sumoylation, although the reported effects of the modification are conflicting with each other, ranging from sumoylation being required for transcriptional repression to no effect (Colombo et al., 2002; David et al., 2002). Even though the lysines modified in metazoans are absent in the budding yeast Rpd3 deacetylase, it could be that the overall mechanism of Rpd3(L) complex regulation by sumoylation is conserved. In particular, a sumoylated peptide belonging to Rpd3 was found in a mass spectrometry study looking for SUMO acceptor lysines (Esteras et al., 2017), while Sds3 and Rxt2 Rpd3(L) complex components are sumoylated under stress (Lewicki et al., 2015).

The desumoylation of Rpd3(L) complex by Mlp1-associated SUMO protease Ulp1 and its consequent inactivation leading to *CLN2* derepression could present part of the NPC-dependent mechanism of *CLN2* expression activation. Interestingly, it is the deletion of Ulp2 SUMO protease (which is localized to the nucleus), but not that of Ulp1, upon deletion leads to slow growth phenotype which is rescued by frequently occurring adaptive aneuploidy resulting in double the number of Chr I carrying *CLN3* and *CCR4* genes (S. J. Li & Hochstrasser, 2000). The alternative target for this kind of regulation at *CLN2* promoter is Tup1, a known transcription repressor that is thought to be removed from the promoter upon Ulp1-driven desumoylation (Jani et al., 2014; Texari et al., 2013).

While desumoylation of of Tup1, Rpd3(L), or some other factors localized next in the *CLN2* promoter region could contribute to its enhanced expression, the initial

binding to the Ulp1-containing NPC could depend on Sac3 (which is present at Mlp1-containing nuclear pores able to bind Ulp1). My preliminary data indicates that Nup60 acetylation mildly affects the delay between *CLN2* locus detachment from the nuclear periphery and complete Whi5 nuclear export: acetyl-mimic Nup60 leaves the nuclear periphery slightly earlier, and the opposite effect is observed for Nup60 allele mimicking constitutively deacetylation. Overall, sumoylation could be one of the directions to explore relative to the *CLN2* regulation at the nuclear pore.

The role of Nup60 acetylation and acetylation in general in the expression of *GAL* locus genes seems to be quite complex and requires careful exploration and interpretation in the future. For example, the unpublished observations from the lab (Maxime Ledoux Vanek) are that *GAL1* mRNA export is not promoted by Nup60-KN in *esa1-ts* cells, but the mRNA levels are increased, which would mean that acetylation of Nup60 has an effect in promoting transcription, but not export. However this observation seems to be limited, not just to the *esa1-ts* cells (we do not find a transcriptional effect for Nup60-KN in otherwise wild-type cells (Gomar-Alba et al., 2022)), but also to this specific background: the strains in this set of experiments have PP7 loops in *GAL1* mRNA, and the *GAL1* RNA levels are much lower than in the wild type cells. This could affect the results since the increase in *GAL1* transcript levels by Nup60-KN mutation is not reproduced in the strains with wild type *GAL1* gene. It is therefore important to use smFISH to verify the conclusions done with the PP7 strain.

Finally, our unpublished data indicate that, unlike *nup60-KN* mutation, *HOS3* deletion increases the mRNA levels of *GAL* locus genes compared to the wild type. This strengthens the suggestion that we make based on *GAL1/10::sfGFP* induction in (Gomar-Alba et al., 2022) that Nup60 is not the only target of Hos3 that acts in promoting *GAL* locus expression, which implies that other targets of Hos3, maybe within the nuclear pore, among histones or other proteins, upon deacetylation decrease the transcription of *GAL* locus.

The option that we never explored is that Hos3 regulates the *GAL* genes indirectly. It is interesting to note that though our RNA-seq data suggests that Nup60-KN has minimal effects on steady state RNA levels in regular culture conditions (YP, glucose 2%), the few genes that we find to be significantly differentially expressed between the wild type and *nup60-KN* strains are predominantly lowly expressed stress response genes, located next to the telomeres or centromeres of different chromosomes. These genes are located not too far from the pore in unperturbed cells due to the yeast chromatin organization principles that include anchoring of both telomeres and centromeres to the

nuclear periphery (Goh & Kilmartin, 1993; Gotta et al., 1996). When the cells sense the lack of glucose in the media and adapt to a new carbon source, genes upstream of *GAL* locus are activated, and some of them may be regulated by NPC acetylation and/or by Hos3. For example, the *GAL3* gene, which is induced by galactose and potentiates the expression of genes from the *GAL* locus (Lavy et al., 2012; Platt & Reece, 1998), is located right next to the centromere. It would be therefore interesting to check if *GAL3* expression is changed in *hos3* mutant cells. Another alternative to explore is whether the nuclear import of Gal3 or the Gal3-Gal80 protein complex (Peng Gang & Hopper James E., 2000) depends on NPC acetylation.

7.6. Correlations with other studies

In this section I will draw the parallels between our study and two other ones. I have already briefly discussed the conclusions of (Bensidoun et al. 2022) and I will refer to this study. I will briefly summarize another study by (Meinema et al. 2022), and then discuss matters that arise from our two studies.

Meinema *et al*. showed that in NPCs bound to extrachromosomal DNA circles, SAGA mutations, and acetylation-defective Nup60 mutants cause displacement of Nup60, Nup2, and Mlp1 (but not Nup1), and a number of cytoplasmic nucleoporins from NPCs of the NPC cap - the nuclear envelope structure associated with the DNA circles. Strikingly, the expression of the non-acetylatable mutant Nup60K467R restores not only its own binding to the NPCs, but also the binding of the cytoplasmic nucleoporins is recovered. This points towards a major remodeling of NPCs loaded with DNA circles, driven presumably just by Nup60 acetylation. Of note, Mlp1 is not restored as the component of the basket in the mutant Nup60K467R, which indicates that Mlp1 displacement from the DNA circle-associated NPCs is caused by additional mechanisms besides acetylation of Nup60. In addition, Nup60K467R mutant strain displayed a slightly but significantly increased longevity, which may stem from cells retaining part of their nuclear basket and cytoplasmic complexes which are otherwise lost in aged cells. Another finding is that DNA circle-bound NPCs remodeled by SAGA-driven acetylation of Nup60 are devoid of mRNA export and surveillance factors (including Sac3, Ulp1, Mex67, Mtr2, Dbp5, Yra1, and Nab2). On the contrary, most protein import and export factors were unaffected by DNA circle binding, and protein import and retention of proteins was not affected in aged cells containing many DNA circle-bound NPCs. (Meinema et al., 2022)

One could say that the fact that our conclusion that acetylation of Nup60 improves mRNA export contradicts the conclusions of Meinema *et al*, since they find that acetylation of Nup60 by SAGA decreases the association of mRNA export factors with the NPCs. However, there are two things that one should keep in mind. The first one is that the conditions in which we observe budding yeasts are quite different - we are looking at young daughter/mother cells, while in (Meinema et al. 2022) the authors are looking at cells with excessive amounts of DNA circles or old cells with increasing amounts of ERCs - thèse conditions could impact the effect of Nup60 acetylation on mRNA export.

The second point is that, while peripheral and certain basket nucleoporins as well a number of mRNA export factors are recovered in non-acetylatable Nup60K467R mutant, we do not know whether Sac3 localization is restored, while we definitely know that Mlp1 localization is not recovered at the NPC cap. If Sac3, the same as Mlp1, does not go back to the nuclear pore, this would be consistent with the publication of (Bensidoun et al. 2022) that claims that the pores that do not bind Mlp1 also lack Sac3. This would also be consistent with our results: non-acetalatable Nup60 could make the NPC less efficient in binding Sac3, than the acetylated one.

However, some questions would still be remaining. For example, is the acetylation of Nup60 sufficient to explain its dissociation from the NPC? Our results that acetyl-mimic Nup60K467N localizes to the NPC in amounts equal to the wild type indicate that there may be additional determinants of NPC integrity that are acting together with Nup60 acetylation in order to detach basket and cytoplasmic NPC components from the pore and to inhibit mRNA export in NPCs that bind the DNA circles. Another question is - why Mlp1 is not coming back to the NPC cap in the Nup60K467R mutant? My hypothesis would be that there is/are other modification(s) in the NPC components that lead to the NPC remodeling, in addition to Nup60 acetylation. In order to learn what they could be, profound studies of the NPC modifications are required, for example in the system used in (Meinema et al. 2022) in order to monitor changes in protein modifications.

One can think of at least two approaches. The first one is a candidate search. I would base the search on the nucleoporins that are facing the nucleoplasmic surface of the NPC, likely the central core ones, but also Nup1, which is the only basket one that remains; I would also include the non-nucleoporin components of the INM. The other approach is to go for NPC purification and further comparison between cells with

centromeric plasmids VS cells with excised centromere (making it DNA circles, see (Meinema et al. 2022) methods).

Additionally, there is a non-mentioned possibility, that it is not proteins that are modified, but the lipids (since both Nup60 and Nup1 have amphipathic helices interacting with the NE, this could be important). I have not found indications that DNA circles (or a naturally occurring form of circles, ERCs) are associated with the NE of some specific lipid mixture, however, this cannot be excluded.

7.7. Conservation in metazoans

Given that the NPC components, the lysine acetyltransferase complex NuA4, and the mRNA export machinery are largely conserved from budding yeast to metazoans, we are particularly interested in whether the role of NuA4 in NPC acetylation and mRNA can be demonstrated in mammals. Many individual features comprising the mechanism that we observe in budding yeasts are conserved. As in yeast, the TREX-2 complex is associated with the nuclear pore basket in human cells (Umlauf et al., 2013) and promotes the export of a subset of mRNAs together with the basket component TPR (Aksenova et al., 2020; Wickramasinghe et al., 2010, 2014). Furthermore, human nucleoporins are acetylated, including TPR and the Nup60 homologue Nup153 (see Supplementary table 2), and TPR physically interacts with Tip60/KAT5, the mammalian homologue of Esa1 (P. B. Chen et al., 2013); however, the physiological relevance of these modifications and interactions has not been determined.

The unpublished results from our lab (Faezeh Forouzan Far) indicate that indeed Tip60 (Esa1 homologue) plays a role in one of the stages preceding the mRNA exit to the cytoplasm since polyadenylated RNA accumulates in nuclear speckles upon Tip60 depletion in mouse embryonic stem cells (mES cells). Interestingly, even though nuclear speckles have been identified as splicing sites, they have been shown to incorporate naturally intronless mRNAs and promote their export competence (K. Wang et al., 2018). Since most budding yeast mRNAs are intronless, one could speculate that NuA4 may play a conserved role in promoting mRNA export for intronless genes.

It may very well be that Tip60/NuA4 promotes mRNA export already at the transcription site by co-transcriptional recruitment of factors necessary for further efficient export. The alternative hypothesis is that NuA4 functions within the speckles to promote the formation of export-competent mRNPs. Such a mechanism could be imagined since Esa1/Tip60 were reported to form discrete nuclear bodies in budding yeast and mammalian cells (Bakshi et al., 2017; Galarneau et al., 2000; Wee et al., 2014).

The simple candidate protein to be recruited by Tip60 would be TPR itself - like many other metazoan nucleoporins it can be found in the nucleoplasm (Zimowska et al., 1997) and it is specifically required for nuclear export of short mRNAs/lncRNAs containing few to one single exon (E. S. Lee et al., 2020).

Testing these possibilities, and identifying the still unexplored molecular mechanisms by which other KATs (such as SAGA) could regulate mRNA export in mammalian cells (e.g. by acetylation of non-histone proteins such as nucleoporins) remain a key subject for future studies.

Supplementary tables

Supplementary table 1

S.cerevisiae nucleoporins and their mapped acetylation sites

Nucleoporin	*Acetylated lysine (K) position*
Nup1	**675**(Henriksen et al. 2012; Downey et al. 2015), 568(Henriksen et al. 2012)
Nup2	{**262, 272**} our unpublished data & (Henriksen et al. 2012; Downey et al. 2015), **228**(Downey et al. 2015; Henriksen et al. 2012), {51, 57, 136, 280, 327, 378, 383, 409, 489, 509} (Henriksen et al. 2012)
Nup60	**467**(Henriksen et al. 2012; Downey et al. 2015), **57** our unpublished data x3 & (Henriksen et al. 2012), {29, 358, 363, 425}(Henriksen et al. 2012), {254} our unpublished data
Nup53	7(Downey et al. 2015), 223(Henriksen et al. 2012), 415(Downey et al. 2015)
Nup159	{840, 902, 1019}(Downey et al. 2015)
Nup100	714(Downey et al. 2015)
Mlp1	146(Henriksen et al. 2012), 1716(Downey et al. 2015)
Nup49	{371, 382}(Henriksen et al. 2012)
Nup57	382(Henriksen et al. 2012)
Nsp1	308(Henriksen et al. 2012)
Nup170	106(Henriksen et al. 2012)
Nup188	1638 (our unpublished data)
Nup145	**779** (our unpublished data x2)

In bold are lysine acetylation sites detected in >2 studies

Supplementary table 2

Mammalian nucleoporins and their mapped acetylation sites

Nucleoporin	*Acetylated lysine (K) position*
Nup50	**83**$_{a,b(Choudhary\ et\ al.\ 2009;\ Lundby\ et\ al.\ 2012;\ Beli\ et\ al.\ 2012;\ Weinert\ et\ al.\ 2013)}$, **127**$_{a,b,c(Lundby\ et\ al.\ 2012;\ Sol\ et\ al.\ 2012;\ Weinert\ et\ al.\ 2013)}$, {**59,275***}$_{a,b,c(Lundby\ et\ al.\ 2012;\ Yue\ Chen\ et\ al.\ 2012;\ Weinert\ et\ al.\ 2013)}$, 173$_{a,c(Yue\ Chen\ et\ al.\ 2012;\ Weinert\ et\ al.\ 2013)}$, 8$_{b,c(Lundby\ et\ al.\ 2012;\ Yue\ Chen\ et\ al.\ 2012)}$, 459$_{b(Lundby\ et\ al.\ 2012)}$, {192,311,320}$_{a(Weinert\ et\ al.\ 2013)}$, 257$_{c(Yue\ Chen\ et\ al.\ 2012)}$
Nup153	{**384,954**}$_{a,b(Choudhary\ et\ al.\ 2009;\ Beli\ et\ al.\ 2012;\ Lundby\ et\ al.\ 2012;\ Weinert\ et\ al.\ 2013)}$, **718**$_{a,b(Choudhary\ et\ al.\ 2009;\ Lundby\ et\ al.\ 2012;\ Weinert\ et\ al.\ 2013)}$, 1120$_{a(Choudhary\ et\ al.\ 2009)}$, 460$_{a(Weinert\ et\ al.\ 2013)}$, 597$_{c(Yue\ Chen\ et\ al.\ 2012)}$, {16,28,195,372,411,447,705,1072,1141,1150}$_{b(Lundby\ et\ al.\ 2012)}$
Tpr	**755***$_{a,b,c(Choudhary\ et\ al.\ 2009;\ Beli\ et\ al.\ 2012;\ Sol\ et\ al.\ 2012;\ Lundby\ et\ al.\ 2012;\ Yue\ Chen\ et\ al.\ 2012;\ Weinert\ et\ al.\ 2013)}$, **748**$_{a,b,c(Beli\ et\ al.\ 2012;\ Sol\ et\ al.\ 2012;\ Lundby\ et\ al.\ 2012;\ Yue\ Chen\ et\ al.\ 2012;\ Weinert\ et\ al.\ 2013)}$, **713***$_{a,b,c(Beli\ et\ al.\ 2012;\ Sol\ et\ al.\ 2012;\ Lundby\ et\ al.\ 2012;\ Weinert\ et\ al.\ 2013)}$, **723**$_{a,b,c(Beli\ et\ al.\ 2012;\ Yue\ Chen\ et\ al.\ 2012;\ Lundby\ et\ al.\ 2012)}$, **312**$_{a,b,c(Lundby\ et\ al.\ 2012;\ Sol\ et\ al.\ 2012;\ Beli\ et\ al.\ 2012)}$, {**252*,449**}$_{a,b,c(Yue\ Chen\ et\ al.\ 2012;\ Lundby\ et\ al.\ 2012;\ Weinert\ et\ al.\ 2013)}$, **1670**$_{a,b,c(Lundby\ et\ al.\ 2012;\ Sol\ et\ al.\ 2012;\ Weinert\ et\ al.\ 2013)}$, {531,1501}$_{b,c(Sol\ et\ al.\ 2012;\ Lundby\ et\ al.\ 2012)}$ {925,1571}$_{a(Weinert\ et\ al.\ 2013)}$, 1202$_{c(Sol\ et\ al.\ 2012)}$, 1760$_{c(Yue\ Chen\ et\ al.\ 2012)}$, {16,261,346,349,352,365,391,418,475,478,495,844,854,855,896, 1380,1428}$_{b(Lundby\ et\ al.\ 2012)}$
Nup214	143$_{a(Choudhary\ et\ al.\ 2009;\ Weinert\ et\ al.\ 2013)}$, 226$_{a,b(Lundby\ et\ al.\ 2012;\ Weinert\ et\ al.\ 2013)}$, 680$_{a(Weinert\ et\ al.\ 2013)}$
Nup188	38$_{a,b(Choudhary\ et\ al.\ 2009;\ Lundby\ et\ al.\ 2012)}$
Pom121	{714,717}$_{a(Choudhary\ et\ al.\ 2009)}$
Nup107	423$_{c(Yue\ Chen\ et\ al.\ 2012)}$, 699$_{b(Lundby\ et\ al.\ 2012)}$
Nup88	590$_{b(Lundby\ et\ al.\ 2012)}$
Nup155	998$_{b(Lundby\ et\ al.\ 2012)}$
RAE1	131$_{a(Weinert\ et\ al.\ 2013)}$
Nup93	103$_{a,c(Sol\ et\ al.\ 2012;\ Weinert\ et\ al.\ 2013)}$
Nup205	41$_{a(Choudhary\ et\ al.\ 2009;\ Beli\ et\ al.\ 2012)}$, 44$_{a(Choudhary\ et\ al.\ 2009)}$
Nup98	193$_{c(Yue\ Chen\ et\ al.\ 2012)}$, 586$_{a(Choudhary\ et\ al.\ 2009)}$
Nup160	574$_{c(Yue\ Chen\ et\ al.\ 2012)}$
Nup133	**786**$_{b,c(Yue\ Chen\ et\ al.\ 2012;\ Lundby\ et\ al.\ 2012;\ Sol\ et\ al.\ 2012)}$, 758$_{a(Weinert\ et\ al.\ 2013)}$, 823$_{b(Lundby\ et\ al.\ 2012)}$

a: *Homo sapiens*, b: *Rattus norwegicus*, c: *Mus musculus*

In bold are lysine acetylation sites detected in >2 studies; in case of incomplete homology causing different site numbers between species sites are numbered according

to *H.sapiens* sequence; * corresponds to amino acid conservation in budding yeast

Table of references

Adam, M., F. Robert, M. Larochelle, and L. Gaudreau. 2001. "H2A.Z Is Required for Global Chromatin Integrity and for Recruitment of RNA Polymerase II under Specific Conditions." *Molecular and Cellular Biology* 21 (18): 6270–79.

Adams, Rebecca L., Laura J. Terry, and Susan R. Wente. 2015. "A Novel Saccharomyces Cerevisiae FG Nucleoporin Mutant Collection for Use in Nuclear Pore Complex Functional Experiments." *G3* 6 (1): 51–58.

Adamus, Klaudia, Cyril Reboul, Jarrod Voss, Cheng Huang, Ralf B. Schittenhelm, Sarah N. Le, Andrew M. Ellisdon, Hans Elmlund, Marion Boudes, and Dominika Elmlund. 2021. "SAGA and SAGA-like SLIK Transcriptional Coactivators Are Structurally and Biochemically Equivalent." *The Journal of Biological Chemistry* 296 (January): 100671.

Ainger, K., D. Avossa, A. S. Diana, C. Barry, E. Barbarese, and J. H. Carson. 1997. "Transport and Localization Elements in Myelin Basic Protein mRNA." *The Journal of Cell Biology* 138 (5): 1077–87.

Aksenova, Vasilisa, Alexandra Smith, Hangnoh Lee, Prasanna Bhat, Caroline Esnault, Shane Chen, James Iben, et al. 2020. "Nucleoporin TPR Is an Integral Component of the TREX-2 mRNA Export Pathway." *Nature Communications*. https://doi.org/10.1038/s41467-020-18266-2.

Albaugh, Brittany N., Erin M. Kolonko, and John M. Denu. 2010. "Kinetic Mechanism of the Rtt109-Vps75 Histone Acetyltransferase-Chaperone Complex." *Biochemistry* 49 (30): 6375–85.

Alcázar-Román, Abel R., Elizabeth J. Tran, Shuangli Guo, and Susan R. Wente. 2006. "Inositol Hexakisphosphate and Gle1 Activate the DEAD-Box Protein Dbp5 for Nuclear mRNA Export." *Nature Cell Biology* 8 (7): 711–16.

Allard, S., R. T. Utley, J. Savard, A. Clarke, P. Grant, C. J. Brandl, L. Pillus, J. L. Workman, and J. Côté. 1999. "NuA4, an Essential Transcription Adaptor/histone H4 Acetyltransferase Complex Containing Esa1p and the ATM-Related Cofactor Tra1p." *The EMBO Journal* 18 (18): 5108–19.

Allegretti, Matteo, Christian E. Zimmerli, Vasileios Rantos, Florian Wilfling, Paolo Ronchi, Herman K. H. Fung, Chia-Wei Lee, et al. 2020. "In-Cell Architecture of the Nuclear Pore and Snapshots of Its Turnover." *Nature* 586 (7831): 796–800.

Allfrey, V. G., R. Faulkner, and A. E. Mirsky. 1964. "ACETYLATION AND METHYLATION OF HISTONES AND THEIR POSSIBLE ROLE IN THE REGULATION OF RNA SYNTHESIS." *Proceedings of the National Academy of Sciences of the United States of America* 51 (May): 786–94.

Allfrey, V. G., V. C. Littau, and A. E. Mirsky. 1963. "ON THE ROLE OF HISTONES IN REGULATING RIBONUCLEIC ACID SYNTHESIS IN THE CELL NUCLEUS*." *Proceedings of the National Academy of Sciences* 49 (3): 414–21.

Altaf, Mohammed, Andréanne Auger, Julie Monnet-Saksouk, Joëlle Brodeur, Sandra Piquet, Myriam

Cramet, Nathalie Bouchard, et al. 2010. “NuA4-Dependent Acetylation of Nucleosomal Histones H4 and H2A Directly Stimulates Incorporation of H2A.Z by the SWR1 Complex*.” *The Journal of Biological Chemistry* 285 (21): 15966–77.

Amon, A. 1997. “Regulation of B-Type Cyclin Proteolysis by Cdc28-Associated Kinases in Budding Yeast.” *The EMBO Journal* 16 (10): 2693–2702.

Anderson, J. T., S. M. Wilson, K. V. Datar, and M. S. Swanson. 1993. “NAB2: A Yeast Nuclear Polyadenylated RNA-Binding Protein Essential for Cell Viability.” *Molecular and Cellular Biology* 13 (5): 2730–41.

Andrews, B. J., and I. Herskowitz. 1989. “The Yeast SWI4 Protein Contains a Motif Present in Developmental Regulators and Is Part of a Complex Involved in Cell-Cycle-Dependent Transcription.” *Nature* 342 (6251): 830–33.

Angus-Hill, M. L., R. N. Dutnall, S. T. Tafrov, R. Sternglanz, and V. Ramakrishnan. 1999. “Crystal Structure of the Histone Acetyltransferase Hpa2: A Tetrameric Member of the Gcn5-Related N-Acetyltransferase Superfamily.” *Journal of Molecular Biology* 294 (5): 1311–25.

Arnone, James T., Alison D. Walters, and Orna Cohen-Fix. 2013. “The Dynamic Nature of the Nuclear Envelope: Lessons from Closed Mitosis.” *Nucleus* 4 (4): 261–66.

Ashkenazy-Titelman, Asaf, Mohammad Khaled Atrash, Alon Boocholez, Noa Kinor, and Yaron Shav-Tal. 2022. “RNA Export through the Nuclear Pore Complex Is Directional.” *Nature Communications* 13 (1): 5881.

Azzouz, Nowel, Olesya O. Panasenko, Cécile Deluen, Julien Hsieh, Grégory Theiler, and Martine A. Collart. 2009. “Specific Roles for the Ccr4-Not Complex Subunits in Expression of the Genome.” *RNA* 15 (3): 377–83.

Babiarz, Joshua E., Jeffrey E. Halley, and Jasper Rine. 2006. “Telomeric Heterochromatin Boundaries Require NuA4-Dependent Acetylation of Histone Variant H2A.Z in Saccharomyces Cerevisiae.” *Genes & Development* 20 (6): 700–710.

Bagchi, Dia N., Anna M. Battenhouse, Daechan Park, and Vishwanath R. Iyer. 2020. “The Histone Variant H2A.Z in Yeast Is Almost Exclusively Incorporated into the +1 Nucleosome in the Direction of Transcription.” *Nucleic Acids Research* 48 (1): 157–70.

Bakshi, Karishma, B. Ranjitha, Shraddha Dubey, Jaisri Jagannadham, Bharti Jaiswal, and Ashish Gupta. 2017. “Novel Complex of HAT Protein TIP60 and Nuclear Receptor PXR Promotes Cell Migration and Adhesion.” *Scientific Reports* 7 (1): 3635.

Bannister, A. J., and E. A. Miska. 2000. “Regulation of Gene Expression by Transcription Factor Acetylation.” *Cellular and Molecular Life Sciences: CMLS* 57 (8-9): 1184–92.

Baptista, Tiago, Sebastian Grünberg, Nadège Minoungou, Maria J. E. Koster, H. T. Marc Timmers, Steve Hahn, Didier Devys, and László Tora. 2018. “SAGA Is a General Cofactor for RNA Polymerase II Transcription.” *Molecular Cell* 70 (6): 1163–64.

Barber, Felix, Ariel Amir, and Andrew W. Murray. 2020. “Cell-Size Regulation in Budding Yeast Does Not

Depend on Linear Accumulation of Whi5." *Proceedings of the National Academy of Sciences of the United States of America* 117 (25): 14243–50.

Batisse, Julien, Claire Batisse, Aidan Budd, Bettina Böttcher, and Ed Hurt. 2009. "Purification of Nuclear poly(A)-Binding Protein Nab2 Reveals Association with the Yeast Transcriptome and a Messenger Ribonucleoprotein Core Structure." *The Journal of Biological Chemistry* 284 (50): 34911–17.

Bayliss, R., T. Littlewood, and M. Stewart. 2000. "Structural Basis for the Interaction between FxFG Nucleoporin Repeats and Importin-Beta in Nuclear Trafficking." *Cell* 102 (1): 99–108.

Bean, James M., Eric D. Siggia, and Frederick R. Cross. 2005. "High Functional Overlap between MluI Cell-Cycle Box Binding Factor and Swi4/6 Cell-Cycle Box Binding Factor in the G1/S Transcriptional Program in Saccharomyces Cerevisiae." *Genetics* 171 (1): 49–61.

Beggs, Suzanne, Tharappel C. James, and Ursula Bond. 2012. "The PolyA Tail Length of Yeast Histone mRNAs Varies during the Cell Cycle and Is Influenced by Sen1p and Rrp6p." *Nucleic Acids Research* 40 (6): 2700–2711.

Beli, Petra, Natalia Lukashchuk, Sebastian A. Wagner, Brian T. Weinert, Jesper V. Olsen, Linda Baskcomb, Matthias Mann, Stephen P. Jackson, and Chunaram Choudhary. 2012. "Proteomic Investigations Reveal a Role for RNA Processing Factor THRAP3 in the DNA Damage Response." *Molecular Cell* 46 (2): 212–25.

Bensidoun, Pierre, Taylor Reiter, Ben Montpetit, Daniel Zenklusen, and Marlene Oeffinger. 2022. "Nuclear mRNA Metabolism Drives Selective Basket Assembly on a Subset of Nuclear Pore Complexes in Budding Yeast." *Molecular Cell*, October. https://doi.org/10.1016/j.molcel.2022.09.019.

Berger, S. L., B. Piña, N. Silverman, G. A. Marcus, J. Agapite, J. L. Regier, S. J. Triezenberg, and L. Guarente. 1992. "Genetic Isolation of ADA2: A Potential Transcriptional Adaptor Required for Function of Certain Acidic Activation Domains." *Cell* 70 (2): 251–65.

Berndsen, Christopher E., Toshiaki Tsubota, Scott E. Lindner, Susan Lee, James M. Holton, Paul D. Kaufman, James L. Keck, and John M. Denu. 2008. "Molecular Functions of the Histone Acetyltransferase Chaperone Complex Rtt109-Vps75." *Nature Structural & Molecular Biology* 15 (9): 948–56.

Bernstein, B. E., J. K. Tong, and S. L. Schreiber. 2000. "Genomewide Studies of Histone Deacetylase Function in Yeast." *Proceedings of the National Academy of Sciences of the United States of America* 97 (25): 13708–13.

Bertoli, Cosetta, Jan M. Skotheim, and Robertus A. M. de Bruin. 2013. "Control of Cell Cycle Transcription during G1 and S Phases." *Nature Reviews. Molecular Cell Biology* 14 (8): 518–28.

Bhagwat, Madhura, Shreya Nagar, Pritpal Kaur, Riddhi Mehta, Ivana Vancurova, and Ales Vancura. 2021. "Replication Stress Inhibits Synthesis of Histone mRNAs in Yeast by Removing Spt10p and Spt21p from the Histone Promoters." *The Journal of Biological Chemistry* 297 (5): 101246.

Bieluszewski, Tomasz, Weronika Sura, Wojciech Dziegielewski, Anna Bieluszewska, Catherine Lachance, Michał Kabza, Maja Szymanska-Lejman, et al. 2022. "NuA4 and H2A.Z Control Environmental

Responses and Autotrophic Growth in Arabidopsis." *Nature Communications* 13 (1): 277.

Bird, Alexander W., David Y. Yu, Marilyn G. Pray-Grant, Qifeng Qiu, Kirsty E. Harmon, Paul C. Megee, Patrick A. Grant, M. Mitchell Smith, and Michael F. Christman. 2002. "Acetylation of Histone H4 by Esa1 Is Required for DNA Double-Strand Break Repair." *Nature* 419 (6905): 411–15.

Björk, Glenn R., Bo Huang, Olof P. Persson, and Anders S. Byström. 2007. "A Conserved Modified Wobble Nucleoside (mcm5s2U) in Lysyl-tRNA Is Required for Viability in Yeast." *RNA* 13 (8): 1245–55.

Blobel, G. 1985. "Gene Gating: A Hypothesis." *Proceedings of the National Academy of Sciences of the United States of America* 82 (24): 8527–29.

Borah, Sapan, David J. Thaller, Zhanna Hakhverdyan, Elisa C. Rodriguez, Anthony W. Isenhour, Michael P. Rout, Megan C. King, and C. Patrick Lusk. 2021. "Heh2/Man1 May Be an Evolutionarily Conserved Sensor of NPC Assembly State." *Molecular Biology of the Cell* 32 (15): 1359–73.

Brickner, Donna Garvey, Ivelisse Cajigas, Yvonne Fondufe-Mittendorf, Sara Ahmed, Pei-Chih Lee, Jonathan Widom, and Jason H. Brickner. 2007. "H2A.Z-Mediated Localization of Genes at the Nuclear Periphery Confers Epigenetic Memory of Previous Transcriptional State." *PLoS Biology* 5 (4): e81.

Brown, C. E., L. Howe, K. Sousa, S. C. Alley, M. J. Carrozza, S. Tan, and J. L. Workman. 2001. "Recruitment of HAT Complexes by Direct Activator Interactions with the ATM-Related Tra1 Subunit." *Science* 292 (5525): 2333–37.

Brownell, J. E., and C. D. Allis. 1995. "An Activity Gel Assay Detects a Single, Catalytically Active Histone Acetyltransferase Subunit in Tetrahymena Macronuclei." *Proceedings of the National Academy of Sciences of the United States of America* 92 (14): 6364–68.

Brownell, J. E., J. Zhou, T. Ranalli, R. Kobayashi, D. G. Edmondson, S. Y. Roth, and C. D. Allis. 1996. "Tetrahymena Histone Acetyltransferase A: A Homolog to Yeast Gcn5p Linking Histone Acetylation to Gene Activation." *Cell* 84 (6): 843–51.

Bruin, Robertus A. M. de, Tatyana I. Kalashnikova, Charly Chahwan, W. Hayes McDonald, James Wohlschlegel, John Yates 3rd, Paul Russell, and Curt Wittenberg. 2006. "Constraining G1-Specific Transcription to Late G1 Phase: The MBF-Associated Corepressor Nrm1 Acts via Negative Feedback." *Molecular Cell* 23 (4): 483–96.

Bruin, Robertus A. M. de, W. Hayes McDonald, Tatyana I. Kalashnikova, John Yates 3rd, and Curt Wittenberg. 2004. "Cln3 Activates G1-Specific Transcription via Phosphorylation of the SBF Bound Repressor Whi5." *Cell* 117 (7): 887–98.

Bruzzone, Maria Jessica, Sebastian Grünberg, Slawomir Kubik, Gabriel E. Zentner, and David Shore. 2018. "Distinct Patterns of Histone Acetyltransferase and Mediator Deployment at Yeast Protein-Coding Genes." *Genes & Development* 32 (17-18): 1252–65.

Buratowski, S., S. Hahn, L. Guarente, and P. A. Sharp. 1989. "Five Intermediate Complexes in Transcription Initiation by RNA Polymerase II." *Cell* 56 (4): 549–61.

Burgess, Rebecca J., Hui Zhou, Junhong Han, and Zhiguo Zhang. 2010. “A Role for Gcn5 in Replication-Coupled Nucleosome Assembly.” *Molecular Cell* 37 (4): 469–80.

Cabal, Ghislain G., Auguste Genovesio, Susana Rodriguez-Navarro, Christophe Zimmer, Olivier Gadal, Annick Lesne, Henri Buc, et al. 2006. “SAGA Interacting Factors Confine Sub-Diffusion of Transcribed Genes to the Nuclear Envelope.” *Nature* 441 (7094): 770–73.

Cai, Ling, Benjamin M. Sutter, Bing Li, and Benjamin P. Tu. 2011. “Acetyl-CoA Induces Cell Growth and Proliferation by Promoting the Acetylation of Histones at Growth Genes.” *Molecular Cell* 42 (4): 426–37.

Cai, Ying, and Bruce Futcher. 2013. “Effects of the Yeast RNA-Binding Protein Whi3 on the Half-Life and Abundance of CLN3 mRNA and Other Targets.” *PloS One* 8 (12): e84630.

Callan, H. G., and S. G. Tomlin. 1950. “Experimental Studies on Amphibian Oocyte Nuclei. I. Investigation of the Structure of the Nuclear Membrane by Means of the Electron Microscope.” *Proceedings of the Royal Society of London. Series B, Containing Papers of a Biological Character. Royal Society* 137 (888): 367–78.

Carmen, A. A., P. R. Griffin, J. R. Calaycay, S. E. Rundlett, Y. Suka, and M. Grunstein. 1999. “Yeast HOS3 Forms a Novel Trichostatin A-Insensitive Homodimer with Intrinsic Histone Deacetylase Activity.” *Proceedings of the National Academy of Sciences of the United States of America* 96 (22): 12356–61.

Celic, Ivana, Hiroshi Masumoto, Wendell P. Griffith, Pamela Meluh, Robert J. Cotter, Jef D. Boeke, and Alain Verreault. 2006. “The Sirtuins hst3 and Hst4p Preserve Genome Integrity by Controlling Histone h3 Lysine 56 Deacetylation.” *Current Biology: CB* 16 (13): 1280–89.

Chang, Jennifer S., and Fred Winston. 2011. “Spt10 and Spt21 Are Required for Transcriptional Silencing in Saccharomyces Cerevisiae.” *Eukaryotic Cell* 10 (1): 118–29.

Chang, Ya-Lan, Shun-Fu Tseng, Yu-Ching Huang, Zih-Jie Shen, Pang-Hung Hsu, Meng-Hsun Hsieh, Chia-Wei Yang, et al. 2017. “Yeast Cip1 Is Activated by Environmental Stress to Inhibit Cdk1-G1 Cyclins via Mcm1 and Msn2/4.” *Nature Communications* 8 (1): 56.

Chappleboim, Alon, Daphna Joseph-Strauss, Omer Gershon, and Nir Friedman. 2022. “Transcription Feedback Dynamics in the Wake of Cytoplasmic mRNA Degradation Shutdown.” *Nucleic Acids Research* 50 (10): 5864–80.

Chen, Hua, Ling Zhang, Qikai Wang, Chenxi He, Lauren Frances Dender, and Feng Gong. 2021. “A Role for Gcn5 in Heterochromatin Structure, Gene Silencing and NER at the HML Locus in Budding Yeast.” *bioRxiv*. https://doi.org/10.1101/2021.02.28.433071.

Chen, Poshen B., Jui-Hung Hung, Taylor L. Hickman, Andrew H. Coles, James F. Carey, Zhiping Weng, Feixia Chu, and Thomas G. Fazzio. 2013. “Hdac6 Regulates Tip60-p400 Function in Stem Cells.” *eLife* 2 (December): e01557.

Chen, Xiao-Fen, Lynn Lehmann, Justin J. Lin, Ajay Vashisht, Ryan Schmidt, Roberto Ferrari, Chengyang Huang, et al. 2012. “Mediator and SAGA Have Distinct Roles in Pol II Preinitiation Complex Assembly and Function.” *Cell Reports* 2 (5): 1061–67.

Chen, Yue, Wenhui Zhao, Jeong Soo Yang, Zhongyi Cheng, Hao Luo, Zhike Lu, Minjia Tan, Wei Gu, and Yingming Zhao. 2012. "Quantitative Acetylome Analysis Reveals the Roles of SIRT1 in Regulating Diverse Substrates and Cellular Pathways." *Molecular & Cellular Proteomics: MCP* 11 (10): 1048–62.

Chen, Yuping, Gang Zhao, Jakub Zahumensky, Sangeet Honey, and Bruce Futcher. 2020. "Differential Scaling of Gene Expression with Cell Size May Explain Size Control in Budding Yeast." *Molecular Cell* 78 (2): 359–70.e6.

Chinenov, Yurii. 2002. "A Second Catalytic Domain in the Elp3 Histone Acetyltransferases: A Candidate for Histone Demethylase Activity?" *Trends in Biochemical Sciences* 27 (3): 115–17.

Choudhary, Chunaram, Chanchal Kumar, Florian Gnad, Michael L. Nielsen, Michael Rehman, Tobias C. Walther, Jesper V. Olsen, and Matthias Mann. 2009. "Lysine Acetylation Targets Protein Complexes and Co-Regulates Major Cellular Functions." *Science* 325 (5942): 834–40.

Chu, Daniel B., Tatiana Gromova, Trent A. C. Newman, and Sean M. Burgess. 2017. "The Nucleoporin Nup2 Contains a Meiotic-Autonomous Region That Promotes the Dynamic Chromosome Events of Meiosis." *Genetics* 206 (3): 1319–37.

Cibulka, Jakub, Fabio Bisaccia, Katarina Radisavljević, Ricardo M. Gudino Carrillo, and Alwin Köhler. 2022. "Assembly Principle of a Membrane-Anchored Nuclear Pore Basket Scaffold." *Science Advances* 8 (6): eabl6863.

Clarke, A. S., J. E. Lowell, S. J. Jacobson, and L. Pillus. 1999. "Esa1p Is an Essential Histone Acetyltransferase Required for Cell Cycle Progression." *Molecular and Cellular Biology* 19 (4): 2515–26.

Collins, Sean R., Kyle M. Miller, Nancy L. Maas, Assen Roguev, Jeffrey Fillingham, Clement S. Chu, Maya Schuldiner, et al. 2007. "Functional Dissection of Protein Complexes Involved in Yeast Chromosome Biology Using a Genetic Interaction Map." *Nature* 446 (7137): 806–10.

Colombi, Paolo, Brant M. Webster, Florian Fröhlich, and C. Patrick Lusk. 2013. "The Transmission of Nuclear Pore Complexes to Daughter Cells Requires a Cytoplasmic Pool of Nsp1." *The Journal of Cell Biology* 203 (2): 215–32.

Colombo, Riccardo, Roberto Boggio, Christian Seiser, Giulio F. Draetta, and Susanna Chiocca. 2002. "The Adenovirus Protein Gam1 Interferes with Sumoylation of Histone Deacetylase 1." *EMBO Reports* 3 (11): 1062–68.

Corden, J. L. 1990. "Tails of RNA Polymerase II." *Trends in Biochemical Sciences* 15 (10): 383–87.

Cosma, M. P., T. Tanaka, and K. Nasmyth. 1999. "Ordered Recruitment of Transcription and Chromatin Remodeling Factors to a Cell Cycle- and Developmentally Regulated Promoter." *Cell* 97 (3): 299–311.

Costanzo, Michael, Joy L. Nishikawa, Xiaojing Tang, Jonathan S. Millman, Oliver Schub, Kevin Breitkreuz, Danielle Dewar, Ivan Rupes, Brenda Andrews, and Mike Tyers. 2004. "CDK Activity Antagonizes Whi5, an Inhibitor of G1/S Transcription in Yeast." *Cell* 117 (7): 899–913.

Cross, F. R. 1988. “DAF1, a Mutant Gene Affecting Size Control, Pheromone Arrest, and Cell Cycle Kinetics of Saccharomyces Cerevisiae.” *Molecular and Cellular Biology* 8 (11): 4675–84.

Cui, Yajun, Deepti B. Ramnarain, Yueh-Chin Chiang, Liang-Hao Ding, Jeffrey S. McMahon, and Clyde L. Denis. 2008. “Genome Wide Expression Analysis of the CCR4-NOT Complex Indicates That It Consists of Three Modules with the NOT Module Controlling SAGA-Responsive Genes.” *Molecular Genetics and Genomics: MGG* 279 (4): 323–37.

Dai, Junbiao, Edel M. Hyland, Daniel S. Yuan, Hailiang Huang, Joel S. Bader, and Jef D. Boeke. 2008. “Probing Nucleosome Function: A Highly Versatile Library of Synthetic Histone H3 and H4 Mutants.” *Cell* 134 (6): 1066–78.

D’Angelo, Maximiliano A., Daniel J. Anderson, Erin Richard, and Martin W. Hetzer. 2006. “Nuclear Pores Form de Novo from Both Sides of the Nuclear Envelope.” *Science* 312 (5772): 440–43.

Daniel, Jeremy A., Michael S. Torok, Zu-Wen Sun, David Schieltz, C. David Allis, John R. Yates, and Patrick A. Grant. 2004. “Deubiquitination of Histone H2B by a Yeast Acetyltransferase Complex Regulates Transcription *.” *The Journal of Biological Chemistry* 279 (3): 1867–71.

Danin-Kreiselman, Michal, Chrissie Young Lee, and Guillaume Chanfreau. 2003. “RNAse III-Mediated Degradation of Unspliced Pre-mRNAs and Lariat Introns.” *Molecular Cell* 11 (5): 1279–89.

D’Arcy, Sheena, and Karolin Luger. 2011. “Understanding Histone Acetyltransferase Rtt109 Structure and Function: How Many Chaperones Does It Take?” *Current Opinion in Structural Biology* 21 (6): 728–34.

David, Gregory, Mychell A. Neptune, and Ronald A. DePinho. 2002. “SUMO-1 Modification of Histone Deacetylase 1 (HDAC1) Modulates Its Biological Activities.” *The Journal of Biological Chemistry* 277 (26): 23658–63.

Dawson, T. Renee, Michelle D. Lazarus, Martin W. Hetzer, and Susan R. Wente. 2009. “ER Membrane–bending Proteins Are Necessary for de Novo Nuclear Pore Formation.” *The Journal of Cell Biology* 184 (5): 659–75.

De Bondt, H. L., J. Rosenblatt, J. Jancarik, H. D. Jones, D. O. Morgan, and S. H. Kim. 1993. “Crystal Structure of Cyclin-Dependent Kinase 2.” *Nature* 363 (6430): 595–602.

Derrer, Carina Patrizia, Roberta Mancini, Pascal Vallotton, Sébastien Huet, Karsten Weis, and Elisa Dultz. 2019. “The RNA Export Factor Mex67 Functions as a Mobile Nucleoporin.” *The Journal of Cell Biology* 218 (12): 3967–76.

Dhillon, Namrita, Masaya Oki, Shawn J. Szyjka, Oscar M. Aparicio, and Rohinton T. Kamakaka. 2006. “H2A.Z Functions to Regulate Progression through the Cell Cycle.” *Molecular and Cellular Biology* 26 (2): 489–501.

Dilworth, David J., Alan J. Tackett, Richard S. Rogers, Eugene C. Yi, Rowan H. Christmas, Jennifer J. Smith, Andrew F. Siegel, Brian T. Chait, Richard W. Wozniak, and John D. Aitchison. 2005. “The Mobile Nucleoporin Nup2p and Chromatin-Bound Prp20p Function in Endogenous NPC-Mediated Transcriptional Control.” *The Journal of Cell Biology* 171 (6): 955–65.

Dilworth, D. J., A. Suprapto, J. C. Padovan, B. T. Chait, R. W. Wozniak, M. P. Rout, and J. D. Aitchison. 2001. “Nup2p Dynamically Associates with the Distal Regions of the Yeast Nuclear Pore Complex.” *The Journal of Cell Biology* 153 (7): 1465–78.

Dokudovskaya, Svetlana, Francois Waharte, Avner Schlessinger, Ursula Pieper, Damien P. Devos, Ileana M. Cristea, Rosemary Williams, et al. 2011. “A Conserved Coatomer-Related Complex Containing Sec13 and Seh1 Dynamically Associates with the Vacuole in Saccharomyces Cerevisiae.” *Molecular & Cellular Proteomics: MCP* 10 (6): M110.006478.

Donczew, Rafal, Linda Warfield, Derek Pacheco, Ariel Erijman, and Steven Hahn. 2020. “Two Roles for the Yeast Transcription Coactivator SAGA and a Set of Genes Redundantly Regulated by TFIID and SAGA.” *eLife* 9 (January). https://doi.org/10.7554/eLife.50109.

Dorsey, Savanna, Sylvain Tollis, Jing Cheng, Labe Black, Stephen Notley, Mike Tyers, and Catherine A. Royer. 2018. “G1/S Transcription Factor Copy Number Is a Growth-Dependent Determinant of Cell Cycle Commitment in Yeast.” *Cell Systems* 6 (5): 539–54.e11.

Downey, Michael, Jeffrey R. Johnson, Norman E. Davey, Billy W. Newton, Tasha L. Johnson, Shastyn Galaang, Charles A. Seller, Nevan Krogan, and David P. Toczyski. 2015. “Acetylome Profiling Reveals Overlap in the Regulation of Diverse Processes by Sirtuins, gcn5, and esa1.” *Molecular & Cellular Proteomics: MCP* 14 (1): 162–76.

Downey, Michael, Britta Knight, Ajay A. Vashisht, Charles A. Seller, James A. Wohlschlegel, David Shore, and David P. Toczyski. 2013. “Gcn5 and Sirtuins Regulate Acetylation of the Ribosomal Protein Transcription Factor Ifh1.” *Current Biology: CB* 23 (17): 1638–48.

Doyon, Yannick, and Jacques Côté. 2004. “The Highly Conserved and Multifunctional NuA4 HAT Complex.” *Current Opinion in Genetics & Development* 14 (2): 147–54.

Dultz, Elisa, Matthias Wojtynek, Ohad Medalia, and Evgeny Onischenko. 2022. “The Nuclear Pore Complex: Birth, Life, and Death of a Cellular Behemoth.” *Cells* 11 (9). https://doi.org/10.3390/cells11091456.

Durant, Melissa, and B. Franklin Pugh. 2006. “Genome-Wide Relationships between TAF1 and Histone Acetyltransferases in Saccharomyces Cerevisiae.” *Molecular and Cellular Biology* 26 (7): 2791–2802.

Eberharter, A., D. E. Sterner, D. Schieltz, A. Hassan, J. R. Yates 3rd, S. L. Berger, and J. L. Workman. 1999. “The ADA Complex Is a Distinct Histone Acetyltransferase Complex in Saccharomyces Cerevisiae.” *Molecular and Cellular Biology* 19 (10): 6621–31.

Ehrenhofer-Murray, A. E., D. H. Rivier, and J. Rine. 1997. “The Role of Sas2, an Acetyltransferase Homologue of Saccharomyces Cerevisiae, in Silencing and ORC Function.” *Genetics* 145 (4): 923–34.

Esteras, Miguel, I-Chun Liu, Ambrosius P. Snijders, Adam Jarmuz, and Luis Aragon. 2017. “Identification of SUMO Conjugation Sites in the Budding Yeast Proteome.” *Microbial Cell Factories* 4 (10): 331–41.

Falcón, Alaric A., Shaoping Chen, Michael S. Wood, and John P. Aris. 2010. “Acetyl-Coenzyme A

Synthetase 2 Is a Nuclear Protein Required for Replicative Longevity in Saccharomyces Cerevisiae." *Molecular and Cellular Biochemistry* 333 (1-2): 99–108.

Fasken, Milo B., Murray Stewart, and Anita H. Corbett. 2008. "Functional Significance of the Interaction between the mRNA-Binding Protein, Nab2, and the Nuclear Pore-Associated Protein, Mlp1, in mRNA Export." *The Journal of Biological Chemistry* 283 (40): 27130–43.

Ferrezuelo, Francisco, Martí Aldea, and Bruce Futcher. 2009. "Bck2 Is a Phase-Independent Activator of Cell Cycle-Regulated Genes in Yeast." *Cell Cycle* 8 (2): 239–52.

Fillingham, Jeffrey, Judith Recht, Andrea C. Silva, Bernhard Suter, Andrew Emili, Igor Stagljar, Nevan J. Krogan, C. David Allis, Michael-Christopher Keogh, and Jack F. Greenblatt. 2008. "Chaperone Control of the Activity and Specificity of the Histone H3 Acetyltransferase Rtt109." *Molecular and Cellular Biology* 28 (13): 4342–53.

Fischer, Tamás, Susana Rodríguez-Navarro, Gislene Pereira, Attila Rácz, Elmar Schiebel, and Ed Hurt. 2004. "Yeast Centrin Cdc31 Is Linked to the Nuclear mRNA Export Machinery." *Nature Cell Biology* 6 (9): 840–48.

Fischer, Tamás, Katja Sträßer, Attila Rácz, Susana Rodriguez-Navarro, Marisa Oppizzi, Petra Ihrig, Johannes Lechner, and Ed Hurt. 2002. "The mRNA Export Machinery Requires the Novel Sac3p–Thp1p Complex to Dock at the Nucleoplasmic Entrance of the Nuclear Pores." *The EMBO Journal* 21 (21): 5843–52.

Fiserova, Jindriska, Matthew Spink, Shane A. Richards, Christopher Saunter, and Martin W. Goldberg. 2014. "Entry into the Nuclear Pore Complex Is Controlled by a Cytoplasmic Exclusion Zone Containing Dynamic GLFG-Repeat Nucleoporin Domains." *Journal of Cell Science* 127 (Pt 1): 124–36.

Flick, Karin, and Curt Wittenberg. 2005. "Multiple Pathways for Suppression of Mutants Affecting G1-Specific Transcription in Saccharomyces Cerevisiae." *Genetics* 169 (1): 37–49.

Folz, Hanne, Carlos A. Niño, Surayya Taranum, Stefanie Caesar, Lorenz Latta, François Waharte, Jean Salamero, Gabriel Schlenstedt, and Catherine Dargemont. 2019. "SUMOylation of the Nuclear Pore Complex Basket Is Involved in Sensing Cellular Stresses." *Journal of Cell Science* 132 (7). https://doi.org/10.1242/jcs.224279.

Frey, Steffen, and Dirk Görlich. 2007. "A Saturated FG-Repeat Hydrogel Can Reproduce the Permeability Properties of Nuclear Pore Complexes." *Cell* 130 (3): 512–23.

Friis, R. Magnus N., Bob P. Wu, Stacey N. Reinke, Darren J. Hockman, Brian D. Sykes, and Michael C. Schultz. 2009. "A Glycolytic Burst Drives Glucose Induction of Global Histone Acetylation by picNuA4 and SAGA." *Nucleic Acids Research* 37 (12): 3969–80.

Frolov, Maxim V., and Nicholas J. Dyson. 2004. "Molecular Mechanisms of E2F-Dependent Activation and pRB-Mediated Repression." *Journal of Cell Science* 117 (Pt 11): 2173–81.

Füßl, Magdalena, Ines Lassowskat, Guillaume Née, Minna M. Koskela, Annika Brünje, Priyadarshini Tilak, Jonas Giese, et al. 2018. "Beyond Histones: New Substrate Proteins of Lysine Deacetylases in Arabidopsis Nuclei." *Frontiers in Plant Science* 9 (April): 461.

Galarneau, L., A. Nourani, A. A. Boudreault, Y. Zhang, L. Héliot, S. Allard, J. Savard, W. S. Lane, D. J. Stillman, and J. Côté. 2000. "Multiple Links between the NuA4 Histone Acetyltransferase Complex and Epigenetic Control of Transcription." *Molecular Cell* 5 (6): 927–37.

Galy, Vincent, Olivier Gadal, Micheline Fromont-Racine, Alper Romano, Alain Jacquier, and Ulf Nehrbass. 2004. "Nuclear Retention of Unspliced mRNAs in Yeast Is Mediated by Perinuclear Mlp1." *Cell* 116 (1): 63–73.

Galy, V., J. C. Olivo-Marin, H. Scherthan, V. Doye, N. Rascalou, and U. Nehrbass. 2000. "Nuclear Pore Complexes in the Organization of Silent Telomeric Chromatin." *Nature* 403 (6765): 108–12.

Garí, E., T. Volpe, H. Wang, C. Gallego, B. Futcher, and M. Aldea. 2001. "Whi3 Binds the mRNA of the G1 Cyclin CLN3 to Modulate Cell Fate in Budding Yeast." *Genes & Development* 15 (21): 2803–8.

Gatfield, David, and Elisa Izaurralde. 2002. "REF1/Aly and the Additional Exon Junction Complex Proteins Are Dispensable for Nuclear mRNA Export." *The Journal of Cell Biology* 159 (4): 579–88.

Georgakopoulos, T., and G. Thireos. 1992. "Two Distinct Yeast Transcriptional Activators Require the Function of the GCN5 Protein to Promote Normal Levels of Transcription." *The EMBO Journal* 11 (11): 4145–52.

Ghosh, Suman, Jennifer M. Gardner, Christine J. Smoyer, Jennifer M. Friederichs, Jay R. Unruh, Brian D. Slaughter, Richard Alexander, et al. 2012. "Acetylation of the SUN Protein Mps3 by Eco1 Regulates Its Function in Nuclear Organization." *Molecular Biology of the Cell* 23 (13): 2546–59.

Giaimo, Benedetto Daniele, Francesca Ferrante, Andreas Herchenröther, Sandra B. Hake, and Tilman Borggrefe. 2019. "The Histone Variant H2A.Z in Gene Regulation." *Epigenetics & Chromatin* 12 (1): 37.

Gibbs, Eric B., Tatiana N. Laremore, Grace A. Usher, Bede Portz, Erik C. Cook, and Scott A. Showalter. 2017. "Substrate Specificity of the Kinase P-TEFb towards the RNA Polymerase II C-Terminal Domain." *Biophysical Journal* 113 (9): 1909–11.

Gilchrist, Daniel, Brook Mykytka, and Michael Rexach. 2002. "Accelerating the Rate of Disassembly of Karyopherin.cargo Complexes." *The Journal of Biological Chemistry* 277 (20): 18161–72.

Gilmore, Joshua M., Mihaela E. Sardiu, Swaminathan Venkatesh, Brent Stutzman, Allison Peak, Chris W. Seidel, Jerry L. Workman, Laurence Florens, and Michael P. Washburn. 2012. "Characterization of a Highly Conserved Histone Related Protein, Ydl156w, and Its Functional Associations Using Quantitative Proteomic Analyses." *Molecular & Cellular Proteomics: MCP* 11 (4): M111.011544.

Ginsburg, Daniel S., Chhabi K. Govind, and Alan G. Hinnebusch. 2009. "NuA4 Lysine Acetyltransferase Esa1 Is Targeted to Coding Regions and Stimulates Transcription Elongation with Gcn5." *Molecular and Cellular Biology* 29 (24): 6473–87.

Glozak, Michele A., Nilanjan Sengupta, Xiaohong Zhang, and Edward Seto. 2005. "Acetylation and Deacetylation of Non-Histone Proteins." *Gene* 363 (December): 15–23.

Goh, P. Y., and J. V. Kilmartin. 1993. “NDC10: A Gene Involved in Chromosome Segregation in Saccharomyces Cerevisiae.” *The Journal of Cell Biology* 121 (3): 503–12.

Gomar-Alba, Mercè, Vasilisa Pozharskaia, Bogdan Cichocki, Celia Schaal, Arun Kumar, Basile Jacquel, Gilles Charvin, J. Carlos Igual, and Manuel Mendoza. 2022. “Nuclear Pore Complex Acetylation Regulates mRNA Export and Cell Cycle Commitment in Budding Yeast.” *The EMBO Journal* 41 (15): e110271.

Gotta, M., T. Laroche, A. Formenton, L. Maillet, H. Scherthan, and S. M. Gasser. 1996. “The Clustering of Telomeres and Colocalization with Rap1, Sir3, and Sir4 Proteins in Wild-Type Saccharomyces Cerevisiae.” *The Journal of Cell Biology* 134 (6): 1349–63.

Govind, Chhabi K., Fan Zhang, Hongfang Qiu, Kimberly Hofmeyer, and Alan G. Hinnebusch. 2007. “Gcn5 Promotes Acetylation, Eviction, and Methylation of Nucleosomes in Transcribed Coding Regions.” *Molecular Cell* 25 (1): 31–42.

Grant, P. A., L. Duggan, J. Côté, S. M. Roberts, J. E. Brownell, R. Candau, R. Ohba, et al. 1997. “Yeast Gcn5 Functions in Two Multisubunit Complexes to Acetylate Nucleosomal Histones: Characterization of an Ada Complex and the SAGA (Spt/Ada) Complex.” *Genes & Development* 11 (13): 1640–50.

Grant, P. A., A. Eberharter, S. John, R. G. Cook, B. M. Turner, and J. L. Workman. 1999. “Expanded Lysine Acetylation Specificity of Gcn5 in Native Complexes.” *The Journal of Biological Chemistry* 274 (9): 5895–5900.

Green, Deanna M., Christie P. Johnson, Henry Hagan, and Anita H. Corbett. 2003. “The C-Terminal Domain of Myosin-like Protein 1 (Mlp1p) Is a Docking Site for Heterogeneous Nuclear Ribonucleoproteins That Are Required for mRNA Export.” *Proceedings of the National Academy of Sciences of the United States of America* 100 (3): 1010–15.

Griffis, Eric R., Nihal Altan, Jennifer Lippincott-Schwartz, and Maureen A. Powers. 2002. “Nup98 Is a Mobile Nucleoporin with Transcription-Dependent Dynamics.” *Molecular Biology of the Cell* 13 (4): 1282–97.

Gruenbaum, Yosef, and Roland Foisner. 2015. “Lamins: Nuclear Intermediate Filament Proteins with Fundamental Functions in Nuclear Mechanics and Genome Regulation.” *Annual Review of Biochemistry* 84 (February): 131–64.

Grund, Stefanie E., Tamás Fischer, Ghislain G. Cabal, Oreto Antúnez, José E. Pérez-Ortín, and Ed Hurt. 2008. “The Inner Nuclear Membrane Protein Src1 Associates with Subtelomeric Genes and Alters Their Regulated Gene Expression.” *The Journal of Cell Biology* 182 (5): 897–910.

Gurskiy, Dmitriy, Anastasija Orlova, Nadezhda Vorobyeva, Elena Nabirochkina, Alexey Krasnov, Yulii Shidlovskii, Sofia Georgieva, and Daria Kopytova. 2012. “The DUBm Subunit Sgf11 Is Required for mRNA Export and Interacts with Cbp80 in Drosophila.” *Nucleic Acids Research* 40 (21): 10689–700.

Hakhverdyan, Zhanna, Kelly R. Molloy, Sarah Keegan, Thurston Herricks, Dante M. Lepore, Mary Munson, Roman I. Subbotin, et al. 2021. “Dissecting the Structural Dynamics of the Nuclear Pore

Complex." *Molecular Cell* 81 (1): 153–65.e7.

Hall, D. D., D. D. Markwardt, F. Parviz, and W. Heideman. 1998. "Regulation of the Cln3-Cdc28 Kinase by cAMP in Saccharomyces Cerevisiae." *The EMBO Journal* 17 (15): 4370–78.

Hampoelz, Bernhard, Amparo Andres-Pons, Panagiotis Kastritis, and Martin Beck. 2019. "Structure and Assembly of the Nuclear Pore Complex." *Annual Review of Biophysics* 48 (May): 515–36.

Han, Qiuju, Jun Lu, Jizhou Duan, Dongmei Su, Xiaozhe Hou, Fen Li, Xiuli Wang, and Baiqu Huang. 2008. "Gcn5- and Elp3-Induced Histone H3 Acetylation Regulates hsp70 Gene Transcription in Yeast." *Biochemical Journal* 409 (3): 779–88.

Harris, J. Ieuan. 1959. "Structure of a Melanocyte-Stimulating Hormone from the Human Pituitary Gland." *Nature* 184 (4681): 167–69.

Hartl, Markus, Magdalena Füßl, Paul J. Boersema, Jan-Oliver Jost, Katharina Kramer, Ahmet Bakirbas, Julia Sindlinger, et al. 2017. "Lysine Acetylome Profiling Uncovers Novel Histone Deacetylase Substrate Proteins in Arabidopsis." *Molecular Systems Biology* 13 (10): 949.

Hassan, Ahmed H., Salma Awad, Zeina Al-Natour, Samah Othman, Farah Mustafa, and Tahir A. Rizvi. 2007. "Selective Recognition of Acetylated Histones by Bromodomains in Transcriptional Co-Activators." *Biochemical Journal* 402 (1): 125–33.

Hebbes, T. R., A. W. Thorne, and C. Crane-Robinson. 1988. "A Direct Link between Core Histone Acetylation and Transcriptionally Active Chromatin." *The EMBO Journal* 7 (5): 1395–1402.

Hediger, Florence, Karine Dubrana, and Susan M. Gasser. 2002. "Myosin-like Proteins 1 and 2 Are Not Required for Silencing or Telomere Anchoring, but Act in the Tel1 Pathway of Telomere Length Control." *Journal of Structural Biology* 140 (1-3): 79–91.

Heidinger-Pauli, Jill M., Elçin Unal, and Douglas Koshland. 2009. "Distinct Targets of the Eco1 Acetyltransferase Modulate Cohesion in S Phase and in Response to DNA Damage." *Molecular Cell* 34 (3): 311–21.

Helmlinger, Dominique, Gábor Papai, Didier Devys, and László Tora. 2021. "What Do the Structures of GCN5-Containing Complexes Teach Us about Their Function?" *Biochimica et Biophysica Acta, Gene Regulatory Mechanisms* 1864 (2): 194614.

Helmlinger, Dominique, and László Tora. 2017. "Sharing the SAGA." *Trends in Biochemical Sciences* 42 (11): 850–61.

Henriksen, Peter, Sebastian A. Wagner, Brian T. Weinert, Satyan Sharma, Giedre Bacinskaja, Michael Rehman, André H. Juffer, Tobias C. Walther, Michael Lisby, and Chunaram Choudhary. 2012. "Proteome-Wide Analysis of Lysine Acetylation Suggests Its Broad Regulatory Scope in Saccharomyces Cerevisiae." *Molecular & Cellular Proteomics: MCP* 11 (11): 1510–22.

Hentze, Matthias W., Alfredo Castello, Thomas Schwarzl, and Thomas Preiss. 2018. "A Brave New World of RNA-Binding Proteins." *Nature Reviews. Molecular Cell Biology* 19 (5): 327–41.

Hereford, L. M., M. A. Osley, T. R. Ludwig 2nd, and C. S. McLaughlin. 1981. "Cell-Cycle Regulation of

Yeast Histone mRNA." *Cell* 24 (2): 367–75.

Hess, David, Bingsheng Liu, Nadia R. Roan, Rolf Sternglanz, and Fred Winston. 2004. "Spt10-Dependent Transcriptional Activation in Saccharomyces Cerevisiae Requires Both the Spt10 Acetyltransferase Domain and Spt21." *Molecular and Cellular Biology* 24 (1): 135–43.

Hess, David, and Fred Winston. 2005. "Evidence That Spt10 and Spt21 of Saccharomyces Cerevisiae Play Distinct Roles in Vivo and Functionally Interact with MCB-Binding Factor, SCB-Binding Factor and Snf1." *Genetics* 170 (1): 87–94.

Hieronymus, Haley, and Pamela A. Silver. 2003. "Genome-Wide Analysis of RNA-Protein Interactions Illustrates Specificity of the mRNA Export Machinery." *Nature Genetics* 33 (2): 155–61.

Hilleren, P., T. McCarthy, M. Rosbash, R. Parker, and T. H. Jensen. 2001. "Quality Control of mRNA 3'-End Processing Is Linked to the Nuclear Exosome." *Nature* 413 (6855): 538–42.

Hilleren, P., and R. Parker. 2001. "Defects in the mRNA Export Factors Rat7p, Gle1p, Mex67p, and Rat8p Cause Hyperadenylation during 3'-End Formation of Nascent Transcripts." *RNA* 7 (5): 753–64.

Hodge, Christine A., Vineet Choudhary, Michael J. Wolyniak, John J. Scarcelli, Roger Schneiter, and Charles N. Cole. 2010. "Integral Membrane Proteins Brr6 and Apq12 Link Assembly of the Nuclear Pore Complex to Lipid Homeostasis in the Endoplasmic Reticulum." *Journal of Cell Science* 123 (Pt 1): 141–51.

Hodge, Christine A., Elizabeth J. Tran, Kristen N. Noble, Abel R. Alcazar-Roman, Rakefet Ben-Yishay, John J. Scarcelli, Andrew W. Folkmann, Yaron Shav-Tal, Susan R. Wente, and Charles N. Cole. 2011. "The Dbp5 Cycle at the Nuclear Pore Complex during mRNA Export I: dbp5 Mutants with Defects in RNA Binding and ATP Hydrolysis Define Key Steps for Nup159 and Gle1." *Genes & Development* 25 (10): 1052–64.

Holzer, Guillaume, Paola De Magistris, Cathrin Gramminger, Ruchika Sachdev, Adriana Magalska, Allana Schooley, Anja Scheufen, et al. 2021. "The Nucleoporin Nup50 Activates the Ran Guanine Nucleotide Exchange Factor RCC1 to Promote NPC Assembly at the End of Mitosis." *The EMBO Journal* 40 (23): e108788.

Hoppe, Georg J., Jason C. Tanny, Adam D. Rudner, Scott A. Gerber, Sherwin Danaie, Steven P. Gygi, and Danesh Moazed. 2002. "Steps in Assembly of Silent Chromatin in Yeast: Sir3-Independent Binding of a Sir2/Sir4 Complex to Silencers and Role for Sir2-Dependent Deacetylation." *Molecular and Cellular Biology* 22 (12): 4167–80.

Horiuchi, J., N. Silverman, B. Piña, G. A. Marcus, and L. Guarente. 1997. "ADA1, a Novel Component of the ADA/GCN5 Complex, Has Broader Effects than GCN5, ADA2, or ADA3." *Molecular and Cellular Biology* 17 (6): 3220–28.

Howe, L., D. Auston, P. Grant, S. John, R. G. Cook, J. L. Workman, and L. Pillus. 2001. "Histone H3 Specific Acetyltransferases Are Essential for Cell Cycle Progression." *Genes & Development* 15 (23): 3144–54.

Huang, Dongqing, Supipi Kaluarachchi, Dewald van Dyk, Helena Friesen, Richelle Sopko, Wei Ye, Nazareth Bastajian, et al. 2009. "Dual Regulation by Pairs of Cyclin-Dependent Protein Kinases

and Histone Deacetylases Controls G1 Transcription in Budding Yeast." *PLoS Biology* 7 (9): e1000188.

Huang, J. N., I. Park, E. Ellingson, L. E. Littlepage, and D. Pellman. 2001. "Activity of the APC(Cdh1) Form of the Anaphase-Promoting Complex Persists until S Phase and Prevents the Premature Expression of Cdc20p." *The Journal of Cell Biology* 154 (1): 85–94.

Huisinga, Kathryn L., and B. Franklin Pugh. 2004. "A Genome-Wide Housekeeping Role for TFIID and a Highly Regulated Stress-Related Role for SAGA in Saccharomyces Cerevisiae." *Molecular Cell* 13 (4): 573–85.

Huo, Shuaidong, Shubin Jin, Xiaowei Ma, Xiangdong Xue, Keni Yang, Anil Kumar, Paul C. Wang, Jinchao Zhang, Zhongbo Hu, and Xing-Jie Liang. 2014. "Ultrasmall Gold Nanoparticles as Carriers for Nucleus-Based Gene Therapy due to Size-Dependent Nuclear Entry." *ACS Nano* 8 (6): 5852–62.

Hurt, E., K. Strässer, A. Segref, S. Bailer, N. Schlaich, C. Presutti, D. Tollervey, and R. Jansen. 2000. "Mex67p Mediates Nuclear Export of a Variety of RNA Polymerase II Transcripts." *The Journal of Biological Chemistry* 275 (12): 8361–68.

Ibarra, Arkaitz, and Martin W. Hetzer. 2015. "Nuclear Pore Proteins and the Control of Genome Functions." *Genes & Development* 29 (4): 337–49.

Iglesias, Nahid, Evelina Tutucci, Carole Gwizdek, Patrizia Vinciguerra, Elodie Von Dach, Anita H. Corbett, Catherine Dargemont, and Françoise Stutz. 2010. "Ubiquitin-Mediated mRNP Dynamics and Surveillance prior to Budding Yeast mRNA Export." *Genes & Development* 24 (17): 1927–38.

Imoberdorf, Rachel Maria, Irini Topalidou, and Michel Strubin. 2006. "A Role for gcn5-Mediated Global Histone Acetylation in Transcriptional Regulation." *Molecular and Cellular Biology* 26 (5): 1610–16.

Irvali, Deniz, Fabian P. Schlottmann, Prathibha Muralidhara, Iliya Nadelson, N. Ezgi Wood, Andreas Doncic, and Jennifer C. Ewald. 2021. "When Yeast Cells Change Their Mind: Cell Cycle 'Start' Is Reversible under Starvation." *bioRxiv*. https://doi.org/10.1101/2021.10.31.466668.

Ito-Harashima, Sayoko, Kazushige Kuroha, Tsuyako Tatematsu, and Toshifumi Inada. 2007. "Translation of the poly(A) Tail Plays Crucial Roles in Nonstop mRNA Surveillance via Translation Repression and Protein Destabilization by Proteasome in Yeast." *Genes & Development* 21 (5): 519–24.

Ivanov, Dmitri, Alexander Schleiffer, Frank Eisenhaber, Karl Mechtler, Christian H. Haering, and Kim Nasmyth. 2002. "Eco1 Is a Novel Acetyltransferase That Can Acetylate Proteins Involved in Cohesion." *Current Biology: CB* 12 (4): 323–28.

Iyer, V. R., C. E. Horak, C. S. Scafe, D. Botstein, M. Snyder, and P. O. Brown. 2001. "Genomic Binding Sites of the Yeast Cell-Cycle Transcription Factors SBF and MBF." *Nature* 409 (6819): 533–38.

Izawa, Shingo, Reiko Takemura, and Yoshiharu Inoue. 2004. "Gle2p Is Essential to Induce Adaptation of the Export of Bulk poly(A)+ mRNA to Heat Shock in Saccharomyces Cerevisiae." *The Journal of Biological Chemistry* 279 (34): 35469–78.

Jackson, V., A. Shires, N. Tanphaichitr, and R. Chalkley. 1976. “Modifications to Histones Immediately after Synthesis.” *Journal of Molecular Biology* 104 (2): 471–83.

Jani, Divyang, Eugene Valkov, and Murray Stewart. 2014. “Structural Basis for Binding the TREX2 Complex to Nuclear Pores, GAL1 Localisation and mRNA Export.” *Nucleic Acids Research* 42 (10): 6686–97.

Jaspersen, Sue L., and Suman Ghosh. 2012. “Nuclear Envelope Insertion of Spindle Pole Bodies and Nuclear Pore Complexes.” *Nucleus* 3 (3): 226–36.

Jeronimo, Célia, and François Robert. 2014. “Kin28 Regulates the Transient Association of Mediator with Core Promoters.” *Nature Structural & Molecular Biology* 21 (5): 449–55.

Jiang, Shuangying, Yan Liu, Caiyue Xu, Yun Wang, Jianhui Gong, Yue Shen, Qingyu Wu, Jef D. Boeke, and Junbiao Dai. 2017. “Dissecting Nucleosome Function with a Comprehensive Histone H2A and H2B Mutant Library.” *G3* 7 (12): 3857–66.

John, S., L. Howe, S. T. Tafrov, P. A. Grant, R. Sternglanz, and J. L. Workman. 2000. “The Something about Silencing Protein, Sas3, Is the Catalytic Subunit of NuA3, a yTAF(II)30-Containing HAT Complex That Interacts with the Spt16 Subunit of the Yeast CP (Cdc68/Pob3)-FACT Complex.” *Genes & Development* 14 (10): 1196–1208.

Johnson, Sara Ann, Gabrielle Cubberley, and David L. Bentley. 2009. “Cotranscriptional Recruitment of the mRNA Export Factor Yra1 by Direct Interaction with the 3’ End Processing Factor Pcf11.” *Molecular Cell* 33 (2): 215–26.

Johnsson, Anna, Mickaël Durand-Dubief, Yongtao Xue-Franzén, Michelle Rönnerblad, Karl Ekwall, and Anthony Wright. 2009. “HAT-HDAC Interplay Modulates Global Histone H3K14 Acetylation in Gene-Coding Regions during Stress.” *EMBO Reports* 10 (9): 1009–14.

Johnston, G. C., J. R. Pringle, and L. H. Hartwell. 1977. “Coordination of Growth with Cell Division in the Yeast Saccharomyces Cerevisiae.” *Experimental Cell Research* 105 (1): 79–98.

Kaluarachchi Duffy, Supipi, Supipi Kaluarachchi Duffy, Helena Friesen, Anastasia Baryshnikova, Jean-Philippe Lambert, Yolanda T. Chong, Daniel Figeys, and Brenda Andrews. 2012. “Exploring the Yeast Acetylome Using Functional Genomics.” *Cell*. https://doi.org/10.1016/j.cell.2012.02.064.

Kaneb, Hannah M., Andrew W. Folkmann, Véronique V. Belzil, Li-En Jao, Claire S. Leblond, Simon L. Girard, Hussein Daoud, et al. 2015. “Deleterious Mutations in the Essential mRNA Metabolism Factor, hGle1, in Amyotrophic Lateral Sclerosis.” *Human Molecular Genetics* 24 (5): 1363–73.

Kapinos, Larisa E., Rafael L. Schoch, Raphael S. Wagner, Kai D. Schleicher, and Roderick Y. H. Lim. 2014. “Karyopherin-Centric Control of Nuclear Pores Based on Molecular Occupancy and Kinetic Analysis of Multivalent Binding with FG Nucleoporins.” *Biophysical Journal* 106 (8): 1751–62.

Katan-Khaykovich, Yael, and Kevin Struhl. 2002. “Dynamics of Global Histone Acetylation and Deacetylation in Vivo: Rapid Restoration of Normal Histone Acetylation Status upon Removal of Activators and Repressors.” *Genes & Development* 16 (6): 743–52.

Kawashima, Tadashi, Matteo Pellegrini, and Guillaume F. Chanfreau. 2009. “Nonsense-Mediated mRNA Decay Mutes the Splicing Defects of Spliceosome Component Mutations.” *RNA* 15 (12): 2236–47.

Kehat, Izhak, Federica Accornero, Bruce J. Aronow, and Jeffery D. Molkentin. 2011. “Modulation of Chromatin Position and Gene Expression by HDAC4 Interaction with Nucleoporins.” *Journal of Cell Biology*. https://doi.org/10.1083/jcb.201101046.

Kelly, T. J., S. Qin, D. E. Gottschling, and M. R. Parthun. 2000. “Type B Histone Acetyltransferase Hat1p Participates in Telomeric Silencing.” *Molecular and Cellular Biology* 20 (19): 7051–58.

Kenna, M. A., J. G. Petranka, J. L. Reilly, and L. I. Davis. 1996. “Yeast N1e3p/Nup170p Is Required for Normal Stoichiometry of FG Nucleoporins within the Nuclear Pore Complex.” *Molecular and Cellular Biology* 16 (5): 2025–36.

Kerr, Shana C., Nowel Azzouz, Stephen M. Fuchs, Martine A. Collart, Brian D. Strahl, Anita H. Corbett, and R. Nicholas Laribee. 2011. “The Ccr4-Not Complex Interacts with the mRNA Export Machinery.” *PloS One* 6 (3): e18302.

Kikuchi, Hidehiko, Yasunari Takami, and Tatsuo Nakayama. 2005. “GCN5: A Supervisor in All-Inclusive Control of Vertebrate Cell Cycle Progression through Transcription Regulation of Various Cell Cycle-Related Genes.” *Gene* 347 (1): 83–97.

Kim, Jeong-Hoon, Anita Saraf, Laurence Florens, Michael Washburn, and Jerry L. Workman. 2010. “Gcn5 Regulates the Dissociation of SWI/SNF from Chromatin by Acetylation of Swi2/Snf2.” *Genes & Development* 24 (24): 2766–71.

Kim, Seung Joong, Javier Fernandez-Martinez, Ilona Nudelman, Yi Shi, Wenzhu Zhang, Barak Raveh, Thurston Herricks, et al. 2018. “Integrative Structure and Functional Anatomy of a Nuclear Pore Complex.” *Nature* 555 (7697): 475–82.

Kim, Yeonjung, and David J. Clark. 2002. “SWI/SNF-Dependent Long-Range Remodeling of Yeast *HIS3* Chromatin.” *Proceedings of the National Academy of Sciences of the United States of America* 99 (24): 15381–86.

King, Grant A., Rahel Wettstein, Joseph M. Varberg, Keerthana Chetlapalli, Madison E. Walsh, Ludovic Gillet, Claudia Hernández-Armenta, et al. 2022. “Meiotic Nuclear Pore Complex Remodeling Provides Key Insights into Nuclear Basket Organization.” *bioRxiv*. https://doi.org/10.1101/2022.04.14.488376.

Kishkevich, A., S. L. Cooke, M. R. A. Harris, and R. A. M. de Bruin. 2019. “Gcn5 and Rpd3 Have a Limited Role in the Regulation of Cell Cycle Transcripts during the G1 and S Phases in Saccharomyces Cerevisiae.” *Scientific Reports* 9 (1): 10686.

Kleff, S., E. D. Andrulis, C. W. Anderson, and R. Sternglanz. 1995. “Identification of a Gene Encoding a Yeast Histone H4 Acetyltransferase.” *The Journal of Biological Chemistry* 270 (42): 24674–77.

Klöckner, Christoph, Maren Schneider, Sheila Lutz, Divyang Jani, Dieter Kressler, Murray Stewart, Ed Hurt, and Alwin Köhler. 2009. “Mutational Uncoupling of the Role of Sus1 in Nuclear Pore Complex Targeting of an mRNA Export Complex and Histone H2B Deubiquitination.” *The*

Journal of Biological Chemistry 284 (18): 12049–56.

Knockenhauer, Kevin E., and Thomas U. Schwartz. 2016. "The Nuclear Pore Complex as a Flexible and Dynamic Gate." *Cell* 164 (6): 1162–71.

Koch, C., A. Schleiffer, G. Ammerer, and K. Nasmyth. 1996. "Switching Transcription on and off during the Yeast Cell Cycle: Cln/Cdc28 Kinases Activate Bound Transcription Factor SBF (Swi4/Swi6) at Start, Whereas Clb/Cdc28 Kinases Displace It from the Promoter in G2." *Genes & Development* 10 (2): 129–41.

Köhler, Alwin, Pau Pascual-García, Ana Llopis, Meritxell Zapater, Francesc Posas, Ed Hurt, and Susana Rodríguez-Navarro. 2006. "The mRNA Export Factor Sus1 Is Involved in Spt/Ada/Gcn5 Acetyltransferase-Mediated H2B Deubiquitinylation through Its Interaction with Ubp8 and Sgf11." *Molecular Biology of the Cell* 17 (10): 4228–36.

Kõivomägi, Mardo, Matthew P. Swaffer, Jonathan J. Turner, Georgi Marinov, and Jan M. Skotheim. 2021. "G1 cyclin–Cdk Promotes Cell Cycle Entry through Localized Phosphorylation of RNA Polymerase II." *Science* 374 (6565): 347–51.

Kõivomägi, Mardo, Ervin Valk, Rainis Venta, Anna Iofik, Martin Lepiku, Eva Rose M. Balog, Seth M. Rubin, David O. Morgan, and Mart Loog. 2011. "Cascades of Multisite Phosphorylation Control Sic1 Destruction at the Onset of S Phase." *Nature* 480 (7375): 128–31.

Komachi, Kelly, and Sean M. Burgess. 2022. "The Nup2 Meiotic-Autonomous Region Relieves Inhibition of Nup60 to Promote Progression of Meiosis and Sporulation in Saccharomyces Cerevisiae." *Genetics* 221 (1). https://doi.org/10.1093/genetics/iyac045.

Komarnitsky, P., E. J. Cho, and S. Buratowski. 2000. "Different Phosphorylated Forms of RNA Polymerase II and Associated mRNA Processing Factors during Transcription." *Genes & Development* 14 (19): 2452–60.

Koyama, Hirofumi, Masayuki Itoh, Kohji Miyahara, and Eiko Tsuchiya. 2002. "Abundance of the RSC Nucleosome-Remodeling Complex Is Important for the Cells to Tolerate DNA Damage in Saccharomyces Cerevisiae." *FEBS Letters* 531 (2): 215–21.

Kralt, Annemarie, Matthias Wojtynek, Jonas S. Fischer, Arantxa Agote-Aran, Roberta Mancini, Elisa Dultz, Elad Noor, et al. 2022. "An Amphipathic Helix in Brl1 Is Required for Membrane Fusion during Nuclear Pore Complex Biogenesis in S. Cerevisiae." *bioRxiv*. https://doi.org/10.1101/2022.03.04.483005.

Kristjuhan, Arnold, and Jesper Q. Svejstrup. 2004. "Evidence for Distinct Mechanisms Facilitating Transcript Elongation through Chromatin in Vivo." *The EMBO Journal* 23 (21): 4243–52.

Kristjuhan, Arnold, Jane Walker, Noriyuki Suka, Michael Grunstein, Douglas Roberts, Bradley R. Cairns, and Jesper Q. Svejstrup. 2002. "Transcriptional Inhibition of Genes with Severe Histone h3 Hypoacetylation in the Coding Region." *Molecular Cell* 10 (4): 925–33.

Kristjuhan, Arnold, Birgitte O. Wittschieben, Jane Walker, Douglas Roberts, Bradley R. Cairns, and Jesper Q. Svejstrup. 2003. "Spreading of Sir3 Protein in Cells with Severe Histone H3 Hypoacetylation." *Proceedings of the National Academy of Sciences of the United States of America* 100 (13):

7551–56.

Kumar, Arun, Priyanka Sharma, Mercè Gomar-Alba, Zhanna Shcheprova, Anne Daulny, Trinidad Sanmartín, Irene Matucci, Charlotta Funaya, Miguel Beato, and Manuel Mendoza. 2018. "Daughter-Cell-Specific Modulation of Nuclear Pore Complexes Controls Cell Cycle Entry during Asymmetric Division." *Nature Cell Biology* 20 (4): 432–42.

Kuo, M. H., J. E. Brownell, R. E. Sobel, T. A. Ranalli, R. G. Cook, D. G. Edmondson, S. Y. Roth, and C. D. Allis. 1996. "Transcription-Linked Acetylation by Gcn5p of Histones H3 and H4 at Specific Lysines." *Nature* 383 (6597): 269–72.

Kuo, M. H., J. Zhou, P. Jambeck, M. E. Churchill, and C. D. Allis. 1998. "Histone Acetyltransferase Activity of Yeast Gcn5p Is Required for the Activation of Target Genes in Vivo." *Genes & Development* 12 (5): 627–39.

Kurdistani, Siavash K., and Michael Grunstein. 2003. "Histone Acetylation and Deacetylation in Yeast." *Nature Reviews. Molecular Cell Biology* 4 (4): 276–84.

Kurischko, Cornelia, Venkata K. Kuravi, Christopher J. Herbert, and Francis C. Luca. 2011. "Nucleocytoplasmic Shuttling of Ssd1 Defines the Destiny of Its Bound mRNAs." *Molecular Microbiology* 81 (3): 831–49.

Kurshakova, Maria M., Alexey N. Krasnov, Daria V. Kopytova, Yulii V. Shidlovskii, Julia V. Nikolenko, Elena N. Nabirochkina, Danièle Spehner, Patrick Schultz, Làszlò Tora, and Sofia G. Georgieva. 2007. "SAGA and a Novel Drosophila Export Complex Anchor Efficient Transcription and mRNA Export to NPC." *The EMBO Journal* 26 (24): 4956–65.

Lange, A., and A. H. Corbett. 2013. "Nuclear Pores and Nuclear Import/Export." In *Encyclopedia of Biological Chemistry (Second Edition)*, edited by William J. Lennarz and M. Daniel Lane, 318–23. Waltham: Academic Press.

Lanker, S., M. H. Valdivieso, and C. Wittenberg. 1996. "Rapid Degradation of the G1 Cyclin Cln2 Induced by CDK-Dependent Phosphorylation." *Science* 271 (5255): 1597–1601.

Lau, Corine K., Thomas H. Giddings Jr, and Mark Winey. 2004. "A Novel Allele of Saccharomyces Cerevisiae NDC1 Reveals a Potential Role for the Spindle Pole Body Component Ndc1p in Nuclear Pore Assembly." *Eukaryotic Cell* 3 (2): 447–58.

Lautier, Ophélie, Arianna Penzo, Jérôme O. Rouvière, Guillaume Chevreux, Louis Collet, Isabelle Loïodice, Angela Taddei, Frédéric Devaux, Martine A. Collart, and Benoit Palancade. 2021. "Co-Translational Assembly and Localized Translation of Nucleoporins in Nuclear Pore Complex Biogenesis." *Molecular Cell* 81 (11): 2417–27.e5.

Lavy, Tali, P. Rajesh Kumar, Hongzhen He, and Leemor Joshua-Tor. 2012. "The Gal3p Transducer of the GAL Regulon Interacts with the Gal80p Repressor in Its Ligand-Induced Closed Conformation." *Genes & Development* 26 (3): 294–303.

Law, Michael J., Michael J. Mallory, Roland L. Dunbrack Jr, and Randy Strich. 2014. "Acetylation of the Transcriptional Repressor Ume6p Allows Efficient Promoter Release and Timely Induction of the Meiotic Transient Transcription Program in Yeast." *Molecular and Cellular Biology* 34 (4):

631–42.

Lee, Eliza S., Eric J. Wolf, Sean S. J. Ihn, Harrison W. Smith, Andrew Emili, and Alexander F. Palazzo. 2020. “TPR Is Required for the Efficient Nuclear Export of mRNAs and lncRNAs from Short and Intron-Poor Genes.” *Nucleic Acids Research* 48 (20): 11645–63.

Lee, Kenneth K., and Jerry L. Workman. 2007. “Histone Acetyltransferase Complexes: One Size Doesn’t Fit All.” *Nature Reviews. Molecular Cell Biology* 8 (4): 284–95.

Lee, T. I., and R. A. Young. 2000. “Transcription of Eukaryotic Protein-Coding Genes.” *Annual Review of Genetics* 34: 77–137.

Lei, Elissa P., and Pamela A. Silver. 2002. “Intron Status and 3’-End Formation Control Cotranscriptional Export of mRNA.” *Genes & Development* 16 (21): 2761–66.

Lei, E. P., H. Krebber, and P. A. Silver. 2001. “Messenger RNAs Are Recruited for Nuclear Export during Transcription.” *Genes & Development* 15 (14): 1771–82.

Lemieux, Karine, Marc Larochelle, and Luc Gaudreau. 2008. “Variant Histone H2A.Z, but Not the HMG Proteins Nhp6a/b, Is Essential for the Recruitment of Swi/Snf, Mediator, and SAGA to the Yeast GAL1 UAS(G).” *Biochemical and Biophysical Research Communications* 369 (4): 1103–7.

Lewicki, Megan C., Tharan Srikumar, Erica Johnson, and Brian Raught. 2015. “The S. Cerevisiae SUMO Stress Response Is a Conjugation-Deconjugation Cycle That Targets the Transcription Machinery.” *Journal of Proteomics* 118 (April): 39–48.

Lewis, J. D., D. Görlich, and I. W. Mattaj. 1996. “A Yeast Cap Binding Protein Complex (yCBC) Acts at an Early Step in Pre-mRNA Splicing.” *Nucleic Acids Research* 24 (17): 3332–36.

Liao, X., and R. A. Butow. 1993. “RTG1 and RTG2: Two Yeast Genes Required for a Novel Path of Communication from Mitochondria to the Nucleus.” *Cell* 72 (1): 61–71.

Li, Christina, Alexander Goryaynov, and Weidong Yang. 2016. “The Selective Permeability Barrier in the Nuclear Pore Complex.” *Nucleus* 7 (5): 430–46.

Lim, Roderick Y. H., Birthe Fahrenkrog, Joachim Köser, Kyrill Schwarz-Herion, Jie Deng, and Ueli Aebi. 2007. “Nanomechanical Basis of Selective Gating by the Nuclear Pore Complex.” *Science* 318 (5850): 640–43.

Lindsay, Mark E., Kendra Plafker, Alicia E. Smith, Bruce E. Clurman, and Ian G. Macara. 2002. “Npap60/Nup50 Is a Tri-Stable Switch That Stimulates Importin-Alpha:beta-Mediated Nuclear Protein Import.” *Cell* 110 (3): 349–60.

Ling, X., T. A. Harkness, M. C. Schultz, G. Fisher-Adams, and M. Grunstein. 1996. “Yeast Histone H3 and H4 Amino Termini Are Important for Nucleosome Assembly in Vivo and in Vitro: Redundant and Position-Independent Functions in Assembly but Not in Gene Regulation.” *Genes & Development* 10 (6): 686–99.

Lin, Yu-Yi, Jin-Ying Lu, Junmei Zhang, Wendy Walter, Weiwei Dang, Jun Wan, Sheng-Ce Tao, et al. 2009. “Protein Acetylation Microarray Reveals That NuA4 Controls Key Metabolic Target Regulating

Gluconeogenesis." *Cell* 136 (6): 1073–84.

Li, Pan, Xueqin Liu, Zhimin Hao, Yanrong Jia, Xiangdong Zhao, Debao Xie, Jingao Dong, and Fanli Zeng. 2020. "Dual Repressive Function by Cip1, a Budding Yeast Analog of p21, in Cell-Cycle START Regulation." *Frontiers in Microbiology* 11 (July): 1623.

Li, Qing, Hui Zhou, Hugo Wurtele, Brian Davies, Bruce Horazdovsky, Alain Verreault, and Zhiguo Zhang. 2008. "Acetylation of Histone H3 Lysine 56 Regulates Replication-Coupled Nucleosome Assembly." *Cell* 134 (2): 244–55.

Li, S. J., and M. Hochstrasser. 2000. "The Yeast ULP2 (SMT4) Gene Encodes a Novel Protease Specific for the Ubiquitin-like Smt3 Protein." *Molecular and Cellular Biology* 20 (7): 2367–77.

Li, Tianlu, Nikki De Clercq, Daniel A. Medina, Elena Garre, Per Sunnerhagen, José E. Pérez-Ortín, and Paula Alepuz. 2016. "The mRNA Cap-Binding Protein Cbc1 Is Required for High and Timely Expression of Genes by Promoting the Accumulation of Gene-Specific Activators at Promoters." *Biochimica et Biophysica Acta* 1859 (2): 405–19.

Litsios, Athanasios, Pooja Goswami, Hanna M. Terpstra, Carleton Coffin, Luc-Alban Vuillemenot, Mattia Rovetta, Ghada Ghazal, et al. 2022. "The Timing of Start Is Determined Primarily by Increased Synthesis of the Cln3 Activator rather than Dilution of the Whi5 Inhibitor." *Molecular Biology of the Cell*.

Litsios, Athanasios, Daphne H. E. W. Huberts, Hanna M. Terpstra, Paolo Guerra, Alexander Schmidt, Katarzyna Buczak, Alexandros Papagiannakis, et al. 2019. "Differential Scaling between G1 Protein Production and Cell Size Dynamics Promotes Commitment to the Cell Division Cycle in Budding Yeast." *Nature Cell Biology* 21 (11): 1382–92.

Li, Xinjian, Gabor Egervari, Yugang Wang, Shelley L. Berger, and Zhimin Lu. 2018. "Regulation of Chromatin and Gene Expression by Metabolic Enzymes and Metabolites." *Nature Reviews. Molecular Cell Biology* 19 (9): 563–78.

Li, Yichen, Vasilisa Aksenova, Mark Tingey, Jingjie Yu, Ping Ma, Alexei Arnaoutov, Shane Chen, Mary Dasso, and Weidong Yang. 2021. "Distinct Roles of Nuclear Basket Proteins in Directing the Passage of mRNA through the Nuclear Pore." *Proceedings of the National Academy of Sciences of the United States of America* 118 (37). https://doi.org/10.1073/pnas.2015621118.

Logie, C., C. Tse, J. C. Hansen, and C. L. Peterson. 1999. "The Core Histone N-Terminal Domains Are Required for Multiple Rounds of Catalytic Chromatin Remodeling by the SWI/SNF and RSC Complexes." *Biochemistry* 38 (8): 2514–22.

Longman, Dasa, Iain L. Johnstone, and Javier F. Cáceres. 2003. "The Ref/Aly Proteins Are Dispensable for mRNA Export and Development in Caenorhabditis Elegans." *RNA* 9 (7): 881–91.

Lundby, Alicia, Kasper Lage, Brian T. Weinert, Dorte B. Bekker-Jensen, Anna Secher, Tine Skovgaard, Christian D. Kelstrup, et al. 2012. "Proteomic Analysis of Lysine Acetylation Sites in Rat Tissues Reveals Organ Specificity and Subcellular Patterns." *Cell Reports* 2 (2): 419–31.

Lund, Mette K., and Christine Guthrie. 2005. "The DEAD-Box Protein Dbp5p Is Required to Dissociate Mex67p from Exported mRNPs at the Nuclear Rim." *Molecular Cell* 20 (4): 645–51.

Luo, Kunheng, Miguel A. Vega-Palas, and Michael Grunstein. 2002. “Rap1–Sir4 Binding Independent of Other Sir, yKu, or Histone Interactions Initiates the Assembly of Telomeric Heterochromatin in Yeast.” *Genes & Development* 16 (12): 1528–39.

Lu, Phoebe Y. T., Alyssa C. Kirlin, Maria J. Aristizabal, Hilary T. Brewis, Nancy Lévesque, Dheva T. Setiaputra, Nikita Avvakumov, et al. 2022. “A Balancing Act: Interactions within NuA4/TIP60 Regulate picNuA4 Function in Saccharomyces Cerevisiae and Humans.” *Genetics*, September. https://doi.org/10.1093/genetics/iyac136.

Madrid, Alexis S., Joel Mancuso, W. Zacheus Cande, and Karsten Weis. 2006. “The Role of the Integral Membrane Nucleoporins Ndc1p and Pom152p in Nuclear Pore Complex Assembly and Function.” *The Journal of Cell Biology* 173 (3): 361–71.

Makhnevych, Taras, C. Patrick Lusk, Andrea M. Anderson, John D. Aitchison, and Richard W. Wozniak. 2003. “Cell Cycle Regulated Transport Controlled by Alterations in the Nuclear Pore Complex.” *Cell* 115 (7): 813–23.

Makio, Tadashi, Diego L. Lapetina, and Richard W. Wozniak. 2013. “Inheritance of Yeast Nuclear Pore Complexes Requires the Nsp1p Subcomplex.” *The Journal of Cell Biology* 203 (2): 187–96.

Malumbres, Marcos. 2014. “Cyclin-Dependent Kinases.” *Genome Biology* 15 (6): 122.

Mandart, E., and R. Parker. 1995. “Effects of Mutations in the Saccharomyces Cerevisiae RNA14, RNA15, and PAP1 Genes on Polyadenylation in Vivo.” *Molecular and Cellular Biology* 15 (12): 6979–86.

Mann, Matthias, and Ole N. Jensen. 2003. “Proteomic Analysis of Post-Translational Modifications.” *Nature Biotechnology* 21 (3): 255–61.

Mao, X., B. Schwer, and S. Shuman. 1995. “Yeast mRNA Cap Methyltransferase Is a 50-Kilodalton Protein Encoded by an Essential Gene.” *Molecular and Cellular Biology* 15 (8): 4167–74.

Marcus, G. A., N. Silverman, S. L. Berger, J. Horiuchi, and L. Guarente. 1994. “Functional Similarity and Physical Association between GCN5 and ADA2: Putative Transcriptional Adaptors.” *The EMBO Journal* 13 (20): 4807–15.

Marino, Giada, Ulrich Eckhard, and Christopher M. Overall. 2015. “Protein Termini and Their Modifications Revealed by Positional Proteomics.” *ACS Chemical Biology* 10 (8): 1754–64.

Martin, Benjamin J. E., Julie Brind’Amour, Anastasia Kuzmin, Kristoffer N. Jensen, Zhen Cheng Liu, Matthew Lorincz, and Leann J. Howe. 2021. “Transcription Shapes Genome-Wide Histone Acetylation Patterns.” *Nature Communications* 12 (1): 210.

Martínez-Balbás, M. A., U. M. Bauer, S. J. Nielsen, A. Brehm, and T. Kouzarides. 2000. “Regulation of E2F1 Activity by Acetylation.” *The EMBO Journal* 19 (4): 662–71.

Martinez, Juan S., Dah-Eun Jeong, Eunyoung Choi, Brian M. Billings, and Mark C. Hall. 2006. “Acm1 Is a Negative Regulator of the CDH1-Dependent Anaphase-Promoting Complex/cyclosome in Budding Yeast.” *Molecular and Cellular Biology* 26 (24): 9162–76.

Masuda, A., M. Oyamada, T. Nagaoka, N. Tateishi, and T. Takamatsu. 1998. “Regulation of

Cytosol-Nucleus pH Gradients by K+/H+ Exchange Mechanism in the Nuclear Envelope of Neonatal Rat Astrocytes." *Brain Research* 807 (1-2): 70–77.

McIntosh, E. M., T. Atkinson, R. K. Storms, and M. Smith. 1991. "Characterization of a Short, Cis-Acting DNA Sequence Which Conveys Cell Cycle Stage-Dependent Transcription in Saccharomyces Cerevisiae." *Molecular and Cellular Biology* 11 (1): 329–37.

McMahon, S. B., H. A. Van Buskirk, K. A. Dugan, T. D. Copeland, and M. D. Cole. 1998. "The Novel ATM-Related Protein TRRAP Is an Essential Cofactor for the c-Myc and E2F Oncoproteins." *Cell* 94 (3): 363–74.

Megee, P. C., B. A. Morgan, and M. M. Smith. 1995. "Histone H4 and the Maintenance of Genome Integrity." *Genes & Development* 9 (14): 1716–27.

Meinema, Anne C., Anna Marzelliusardottir, Mihailo Mirkovic, Théo Aspert, Sung Sik Lee, Gilles Charvin, and Yves Barral. 2022. "DNA Circles Promote Yeast Ageing in Part through Stimulating the Reorganization of Nuclear Pore Complexes." *eLife* 11 (April). https://doi.org/10.7554/eLife.71196.

Mekhail, Karim, Jan Seebacher, Steven P. Gygi, and Danesh Moazed. 2008. "Role for Perinuclear Chromosome Tethering in Maintenance of Genome Stability." *Nature* 456 (7222): 667–70.

Meseroll, Rebecca A., and Orna Cohen-Fix. 2016. "The Malleable Nature of the Budding Yeast Nuclear Envelope: Flares, Fusion, and Fenestrations." *Journal of Cellular Physiology* 231 (11): 2353–60.

Mészáros, Noémi, Jakub Cibulka, Maria Jose Mendiburo, Anete Romanauska, Maren Schneider, and Alwin Köhler. 2015. "Nuclear Pore Basket Proteins Are Tethered to the Nuclear Envelope and Can Regulate Membrane Curvature." *Developmental Cell* 33 (3): 285–98.

Metkar, Mihir, Hakan Ozadam, Bryan R. Lajoie, Maxim Imakaev, Leonid A. Mirny, Job Dekker, and Melissa J. Moore. 2018. "Higher-Order Organization Principles of Pre-Translational mRNPs." *Molecular Cell* 72 (4): 715–26.e3.

Mi, Lan, Alexander Goryaynov, Andre Lindquist, Michael Rexach, and Weidong Yang. 2015. "Quantifying Nucleoporin Stoichiometry inside Single Nuclear Pore Complexes in Vivo." *Scientific Reports* 5 (March): 9372.

Misra, Ashish, and Michael R. Green. 2016. "From Polyadenylation to Splicing: Dual Role for mRNA 3' End Formation Factors." *RNA Biology* 13 (3): 259–64.

Moazed, D. 2001. "Enzymatic Activities of Sir2 and Chromatin Silencing." *Current Opinion in Cell Biology* 13 (2): 232–38.

Morgan, B. A., B. A. Mittman, and M. M. Smith. 1991. "The Highly Conserved N-Terminal Domains of Histones H3 and H4 Are Required for Normal Cell Cycle Progression." *Molecular and Cellular Biology* 11 (8): 4111–20.

Morgan, D. O. 1997. "Cyclin-Dependent Kinases: Engines, Clocks, and Microprocessors." *Annual Review of Cell and Developmental Biology* 13: 261–91.

Morgan, Jeffrey T., Gerald R. Fink, and David P. Bartel. 2019. “Excised Linear Introns Regulate Growth in Yeast.” *Nature* 565 (7741): 606–11.

Nanni, Simona, Agnese Re, Cristian Ripoli, Aoife Gowran, Patrizia Nigro, Domenico D’Amario, Antonio Amodeo, et al. 2016. “The Nuclear Pore Protein Nup153 Associates with Chromatin and Regulates Cardiac Gene Expression in Dystrophic Mdx Hearts.” *Cardiovascular Research* 112 (2): 555–67.

Narita, Kozo, and Junko Ishii. 1962. “N-Terminal Sequence in Ovalbumin.” *Journal of Biochemistry* 52 (5): 367–73.

Narita, Takeo, Brian T. Weinert, and Chunaram Choudhary. 2019. “Functions and Mechanisms of Non-Histone Protein Acetylation.” *Nature Reviews Molecular Cell Biology*. https://doi.org/10.1038/s41580-018-0081-3.

Nash, R., G. Tokiwa, S. Anand, K. Erickson, and A. B. Futcher. 1988. “The WHI1+ Gene of Saccharomyces Cerevisiae Tethers Cell Division to Cell Size and Is a Cyclin Homolog.” *The EMBO Journal* 7 (13): 4335–46.

Natsoulis, G., C. Dollard, F. Winston, and J. D. Boeke. 1991. “The Products of the SPT10 and SPT21 Genes of Saccharomyces Cerevisiae Increase the Amplitude of Transcriptional Regulation at a Large Number of Unlinked Loci.” *The New Biologist* 3 (12): 1249–59.

Neuwald, A. F., and D. Landsman. 1997. “GCN5-Related Histone N-Acetyltransferases Belong to a Diverse Superfamily That Includes the Yeast SPT10 Protein.” *Trends in Biochemical Sciences* 22 (5): 154–55.

Niepel, Mario, Kelly R. Molloy, Rosemary Williams, Julia C. Farr, Anne C. Meinema, Nicholas Vecchietti, Ileana M. Cristea, Brian T. Chait, Michael P. Rout, and Caterina Strambio-De-Castillia. 2013. “The Nuclear Basket Proteins Mlp1p and Mlp2p Are Part of a Dynamic Interactome Including Esc1p and the Proteasome.” *Molecular Biology of the Cell* 24 (24): 3920–38.

Niepel, Mario, Caterina Strambio-de-Castillia, Joseph Fasolo, Brian T. Chait, and Michael P. Rout. 2005. “The Nuclear Pore Complex–associated Protein, Mlp2p, Binds to the Yeast Spindle Pole Body and Promotes Its Efficient Assembly.” *The Journal of Cell Biology* 170 (2): 225–35.

Ni, Julie Z., Leslie Grate, John Paul Donohue, Christine Preston, Naomi Nobida, Georgeann O’Brien, Lily Shiue, Tyson A. Clark, John E. Blume, and Manuel Ares Jr. 2007. “Ultraconserved Elements Are Associated with Homeostatic Control of Splicing Regulators by Alternative Splicing and Nonsense-Mediated Decay.” *Genes & Development* 21 (6): 708–18.

Niño, Carlos A., David Guet, Alexandre Gay, Sergine Brutus, Frédéric Jourquin, Shweta Mendiratta, Jean Salamero, Vincent Géli, and Catherine Dargemont. 2016. “Posttranslational Marks Control Architectural and Functional Plasticity of the Nuclear Pore Complex Basket.” *The Journal of Cell Biology* 212 (2): 167–80.

Noguchi, Chiaki, Tanu Singh, Melissa A. Ziegler, Jasmine D. Peake, Lyne Khair, Ana Aza, Toru M. Nakamura, and Eishi Noguchi. 2019. “The NuA4 Acetyltransferase and Histone H4 Acetylation Promote Replication Recovery after Topoisomerase I-Poisoning.” *Epigenetics & Chromatin* 12

(1): 24.

Nourani, Amine, Rhea T. Utley, Stéphane Allard, and Jacques Côté. 2004. “Recruitment of the NuA4 Complex Poises the PHO5 Promoter for Chromatin Remodeling and Activation.” *The EMBO Journal* 23 (13): 2597–2607.

Nousiainen, Heidi O., Marjo Kestilä, Niklas Pakkasjärvi, Heli Honkala, Satu Kuure, Jonna Tallila, Katri Vuopala, Jaakko Ignatius, Riitta Herva, and Leena Peltonen. 2008. “Mutations in mRNA Export Mediator GLE1 Result in a Fetal Motoneuron Disease.” *Nature Genetics* 40 (2): 155–57.

Occhipinti, Laura, Yiming Chang, Martin Altvater, Anna M. Menet, Stefan Kemmler, and Vikram G. Panse. 2013. “Non-FG Mediated Transport of the Large Pre-Ribosomal Subunit through the Nuclear Pore Complex by the mRNA Export Factor Gle2.” *Nucleic Acids Research* 41 (17): 8266–79.

Oeffinger, Marlene, and Daniel Zenklusen. 2012. “To the Pore and through the Pore: A Story of mRNA Export Kinetics.” *Biochimica et Biophysica Acta* 1819 (6): 494–506.

Ohyama, Yoshifumi, Koji Kasahara, and Tetsuro Kokubo. 2010. “Saccharomyces Cerevisiae Ssd1p Promotes CLN2 Expression by Binding to the 5’-Untranslated Region of CLN2 mRNA.” *Genes to Cells: Devoted to Molecular & Cellular Mechanisms* 15 (12): 1169–88.

Ondracka, Andrej, Jonathan A. Robbins, and Frederick R. Cross. 2016. “An APC/C-Cdh1 Biosensor Reveals the Dynamics of Cdh1 Inactivation at the G1/S Transition.” *PloS One* 11 (7): e0159166.

Onischenko, Evgeny, Elad Noor, Jonas S. Fischer, Ludovic Gillet, Matthias Wojtynek, Pascal Vallotton, and Karsten Weis. 2020. “Maturation Kinetics of a Multiprotein Complex Revealed by Metabolic Labeling.” *Cell* 183 (7): 1785–1800.e26.

Onischenko, Evgeny, Jeffrey H. Tang, Kasper R. Andersen, Kevin E. Knockenhauer, Pascal Vallotton, Carina P. Derrer, Annemarie Kralt, et al. 2017. “Natively Unfolded FG Repeats Stabilize the Structure of the Nuclear Pore Complex.” *Cell* 171 (4): 904–17.e19.

Ostapenko, Denis, Janet L. Burton, Ruiwen Wang, and Mark J. Solomon. 2008. “Pseudosubstrate Inhibition of the Anaphase-Promoting Complex by Acm1: Regulation by Proteolysis and Cdc28 Phosphorylation.” *Molecular and Cellular Biology* 28 (15): 4653–64.

Ostapenko, Denis, and Mark J. Solomon. 2011. “Anaphase Promoting Complex-Dependent Degradation of Transcriptional Repressors Nrm1 and Yhp1 in Saccharomyces Cerevisiae.” *Molecular Biology of the Cell* 22 (13): 2175–84.

Otsuka, Shotaro, Khanh Huy Bui, Martin Schorb, M. Julius Hossain, Antonio Z. Politi, Birgit Koch, Mikhail Eltsov, Martin Beck, and Jan Ellenberg. 2016. “Nuclear Pore Assembly Proceeds by an inside-out Extrusion of the Nuclear Envelope.” *eLife* 5 (September). https://doi.org/10.7554/eLife.19071.

Padrón, Alejandro, Shintaro Iwasaki, and Nicholas T. Ingolia. 2019. “Proximity RNA Labeling by APEX-Seq Reveals the Organization of Translation Initiation Complexes and Repressive RNA Granules.” *Molecular Cell* 75 (4): 875–87.e5.

Paik, W. K., D. Pearson, H. W. Lee, and S. Kim. 1970. “Nonenzymatic Acetylation of Histones with Acetyl-CoA.” *Biochimica et Biophysica Acta* 213 (2): 513–22.

Palancade, Benoit, Xianpeng Liu, Maria Garcia-Rubio, Andrès Aguilera, Xiaolan Zhao, and Valérie Doye. 2007. “Nucleoporins Prevent DNA Damage Accumulation by Modulating Ulp1-Dependent Sumoylation Processes.” *Molecular Biology of the Cell* 18 (8): 2912–23.

Papai, Gabor, Alexandre Frechard, Olga Kolesnikova, Corinne Crucifix, Patrick Schultz, and Adam Ben-Shem. 2020. “Structure of SAGA and Mechanism of TBP Deposition on Gene Promoters.” *Nature* 577 (7792): 711–16.

Parker, Roy. 2012. “RNA Degradation in Saccharomyces Cerevisae.” *Genetics* 191 (3): 671–702.

Parthun, M. R., J. Widom, and D. E. Gottschling. 1996. “The Major Cytoplasmic Histone Acetyltransferase in Yeast: Links to Chromatin Replication and Histone Metabolism.” *Cell* 87 (1): 85–94.

Peng Gang, and Hopper James E. 2000. “Evidence for Gal3p’s Cytoplasmic Location and Gal80p's Dual Cytoplasmic-Nuclear Location Implicates New Mechanisms for Controlling Gal4p Activity inSaccharomyces Cerevisiae.” *Molecular and Cellular Biology* 20 (14): 5140–48.

Pérez, Alexis P., Marta H. Artés, David F. Moreno, Josep Clotet, and Martí Aldea. 2022. “Mad3 Modulates the G_1 Cdk and Acts as a Timer in the Start Network.” *Science Advances* 8 (18): eabm4086.

Peters, Reiner. 2005. “Translocation through the Nuclear Pore Complex: Selectivity and Speed by Reduction-of-Dimensionality.” *Traffic* 6 (5): 421–27.

Petrenko, Natalia, Yi Jin, Liguo Dong, Koon Ho Wong, and Kevin Struhl. 2019. “Requirements for RNA Polymerase II Preinitiation Complex Formation in Vivo.” *eLife* 8 (January): e43654.

Petrenko, Natalia, Yi Jin, Koon Ho Wong, and Kevin Struhl. 2017. “Evidence That Mediator Is Essential for Pol II Transcription, but Is Not a Required Component of the Preinitiation Complex in Vivo.” *eLife* 6 (July): e28447.

Phillips, D. M. 1963. “The Presence of Acetyl Groups of Histones.” *Biochemical Journal* 87 (May): 258–63.

Platt, A., and R. J. Reece. 1998. “The Yeast Galactose Genetic Switch Is Mediated by the Formation of a Gal4p-Gal80p-Gal3p Complex.” *The EMBO Journal* 17 (14): 4086–91.

Polevoda, Bogdan, and Fred Sherman. 2002. “The Diversity of Acetylated Proteins.” *Genome Biology* 3 (5): reviews0006.

Polevoda, B., and F. Sherman. 2000. “Nalpha -Terminal Acetylation of Eukaryotic Proteins.” *The Journal of Biological Chemistry* 275 (47): 36479–82.

Pollard, K. J., and C. L. Peterson. 1997. “Role for ADA/GCN5 Products in Antagonizing Chromatin-Mediated Transcriptional Repression.” *Molecular and Cellular Biology* 17 (11): 6212–22.

Polymenis, M., and E. V. Schmidt. 1997. “Coupling of Cell Division to Cell Growth by Translational Control of the G1 Cyclin CLN3 in Yeast.” *Genes & Development* 11 (19): 2522–31.

Poveda, Ana, Mercè Pamblanco, Stefan Tafrov, Vicente Tordera, Rolf Sternglanz, and Ramon Sendra. 2004. “Hif1 Is a Component of Yeast Histone Acetyltransferase B, a Complex Mainly Localized in the Nucleus.” *The Journal of Biological Chemistry* 279 (16): 16033–43.

Powrie, Erin A., Daniel Zenklusen, and Robert H. Singer. 2011. “A Nucleoporin, Nup60p, Affects the Nuclear and Cytoplasmic Localization of ASH1 mRNA in S. Cerevisiae.” *RNA* 17 (1): 134–44.

Pray-Grant, Marilyn G., David Schieltz, Stacey J. McMahon, Jennifer M. Wood, Erin L. Kennedy, Richard G. Cook, Jerry L. Workman, John R. Yates 3rd, and Patrick A. Grant. 2002. “The Novel SLIK Histone Acetyltransferase Complex Functions in the Yeast Retrograde Response Pathway.” *Molecular and Cellular Biology* 22 (24): 8774–86.

Pritchard, C. E., M. Fornerod, L. H. Kasper, and J. M. van Deursen. 1999. “RAE1 Is a Shuttling mRNA Export Factor That Binds to a GLEBS-like NUP98 Motif at the Nuclear Pore Complex through Multiple Domains.” *The Journal of Cell Biology* 145 (2): 237–54.

Pyhtila, Brook, and Michael Rexach. 2003. “A Gradient of Affinity for the Karyopherin Kap95p along the Yeast Nuclear Pore Complex.” *The Journal of Biological Chemistry* 278 (43): 42699–709.

Qin, Song, and Mark R. Parthun. 2006. “Recruitment of the Type B Histone Acetyltransferase Hat1p to Chromatin Is Linked to DNA Double-Strand Breaks.” *Molecular and Cellular Biology* 26 (9): 3649–58.

Quilis, Inma, and J. Carlos Igual. 2017. “A Comparative Study of the Degradation of Yeast Cyclins Cln1 and Cln2.” *FEBS Open Bio* 7 (1): 74–87.

Qu, Yimiao, Jun Jiang, Xiang Liu, Ping Wei, Xiaojing Yang, and Chao Tang. 2019. “Cell Cycle Inhibitor Whi5 Records Environmental Information to Coordinate Growth and Division in Yeast.” *Cell Reports* 29 (4): 987–94.e5.

Rabut, Gwénaël, Valérie Doye, and Jan Ellenberg. 2004. “Mapping the Dynamic Organization of the Nuclear Pore Complex inside Single Living Cells.” *Nature Cell Biology* 6 (11): 1114–21.

Raices, Marcela, and Maximiliano A. D’Angelo. 2022. “Structure, Maintenance, and Regulation of Nuclear Pore Complexes: The Gatekeepers of the Eukaryotic Genome.” *Cold Spring Harbor Perspectives in Biology* 14 (3). https://doi.org/10.1101/cshperspect.a040691.

Rajoo, Sasikumar, Pascal Vallotton, Evgeny Onischenko, and Karsten Weis. 2017. “Stoichiometry and Compositional Plasticity of the Yeast Nuclear Pore Complex Revealed by Quantitative Fluorescence Microscopy.” *bioRxiv*. bioRxiv. https://doi.org/10.1101/215376.

Ramachandran, L. K., and K. Narita. 1958. “Reactions Involving the Amide and Carboxyl Groups of Tobacco Mosaic Virus (TMV) Protein.” *Biochimica et Biophysica Acta* 30 (3): 616–24.

Ree, Rasmus, Sylvia Varland, and Thomas Arnesen. 2018. “Spotlight on Protein N-Terminal Acetylation.” *Experimental & Molecular Medicine* 50 (7): 1–13.

Reeves, Wendy M., and Steven Hahn. 2005. “Targets of the Gal4 Transcription Activator in Functional Transcription Complexes.” *Molecular and Cellular Biology* 25 (20): 9092–9102.

Reifsnyder, C., J. Lowell, A. Clarke, and L. Pillus. 1996. “Yeast SAS Silencing Genes and Human Genes Associated with AML and HIV-1 Tat Interactions Are Homologous with Acetyltransferases.” *Nature Genetics* 14 (1): 42–49.

Ricci, Andrea R., Julie Genereaux, and Christopher J. Brandl. 2002. “Components of the SAGA Histone Acetyltransferase Complex Are Required for Repressed Transcription of ARG1 in Rich Medium.” *Molecular and Cellular Biology* 22 (12): 4033–42.

Richardson, H. E., C. Wittenberg, F. Cross, and S. I. Reed. 1989. “An Essential G1 Function for Cyclin-like Proteins in Yeast.” *Cell* 59 (6): 1127–33.

Robinson, Philip J., Michael J. Trnka, David A. Bushnell, Ralph E. Davis, Pierre-Jean Mattei, Alma L. Burlingame, and Roger D. Kornberg. 2016. “Structure of a Complete Mediator-RNA Polymerase II Pre-Initiation Complex.” *Cell* 166 (6): 1411–22.e16.

Robyr, Daniel, Yuko Suka, Ioannis Xenarios, Siavash K. Kurdistani, Amy Wang, Noriyuki Suka, and Michael Grunstein. 2002. “Microarray Deacetylation Maps Determine Genome-Wide Functions for Yeast Histone Deacetylases.” *Cell* 109 (4): 437–46.

Rollins, Meaghen, Sylvain Huard, Alan Morettin, Jennifer Takuski, Trang Thuy Pham, Morgan D. Fullerton, Jocelyn Côté, and Kristin Baetz. 2017. “Lysine Acetyltransferase NuA4 and Acetyl-CoA Regulate Glucose-Deprived Stress Granule Formation in Saccharomyces Cerevisiae.” *PLoS Genetics* 13 (2): e1006626.

Rossi, Matthew J., Prashant K. Kuntala, William K. M. Lai, Naomi Yamada, Nitika Badjatia, Chitvan Mittal, Guray Kuzu, et al. 2021. “A High-Resolution Protein Architecture of the Budding Yeast Genome.” *Nature* 592 (7853): 309–14.

Rothballer, Andrea, and Ulrike Kutay. 2013. “Poring over Pores: Nuclear Pore Complex Insertion into the Nuclear Envelope.” *Trends in Biochemical Sciences* 38 (6): 292–301.

Rougemaille, Mathieu, Rajani Kanth Gudipati, Jens Raabjerg Olesen, Rune Thomsen, Bertrand Seraphin, Domenico Libri, and Torben Heick Jensen. 2007. “Dissecting Mechanisms of Nuclear mRNA Surveillance in THO/sub2 Complex Mutants.” *The EMBO Journal* 26 (9): 2317–26.

Rout, M. P., J. D. Aitchison, A. Suprapto, K. Hjertaas, Y. Zhao, and B. T. Chait. 2000. “The Yeast Nuclear Pore Complex: Composition, Architecture, and Transport Mechanism.” *The Journal of Cell Biology* 148 (4): 635–51.

Rout, M. P., and S. R. Wente. 1994. “Pores for Thought: Nuclear Pore Complex Proteins.” *Trends in Cell Biology* 4 (10): 357–65.

Rundlett, S. E., A. A. Carmen, R. Kobayashi, S. Bavykin, B. M. Turner, and M. Grunstein. 1996. “HDA1 and RPD3 Are Members of Distinct Yeast Histone Deacetylase Complexes That Regulate Silencing and Transcription.” *Proceedings of the National Academy of Sciences of the United States of America* 93 (25): 14503–8.

Rusché, Laura N., Ann L. Kirchmaier, and Jasper Rine. 2002. “Ordered Nucleation and Spreading of Silenced Chromatin inSaccharomyces Cerevisiae.” *Molecular Biology of the Cell* 13 (7): 2207–22.

Rüthnick, Diana, Annett Neuner, Franziska Dietrich, Daniel Kirrmaier, Ulrike Engel, Michael Knop, and Elmar Schiebel. 2017. “Characterization of Spindle Pole Body Duplication Reveals a Regulatory Role for Nuclear Pore Complexes.” *The Journal of Cell Biology* 216 (8): 2425–42.

Ryan, Kathryn J., J. Michael McCaffery, and Susan R. Wente. 2003. “The Ran GTPase Cycle Is Required for Yeast Nuclear Pore Complex Assembly.” *The Journal of Cell Biology*. https://doi.org/10.1083/jcb.200209116.

Sabò, Arianna, Marina Lusic, Anna Cereseto, and Mauro Giacca. 2008. “Acetylation of Conserved Lysines in the Catalytic Core of Cyclin-Dependent Kinase 9 Inhibits Kinase Activity and Regulates Transcription.” *Molecular and Cellular Biology* 28 (7): 2201–12.

Sachs, A. 1990. “The Role of poly(A) in the Translation and Stability of mRNA.” *Current Opinion in Cell Biology* 2 (6): 1092–98.

Saik, Natasha O., Nogi Park, Christopher Ptak, Neil Adames, John D. Aitchison, and Richard W. Wozniak. 2020. “Recruitment of an Activated Gene to the Yeast Nuclear Pore Complex Requires Sumoylation.” *Frontiers in Genetics* 11 (March): 174.

Sampath, Vinaya, Bingsheng Liu, Stefan Tafrov, Madhusudhan Srinivasan, Robert Rieger, Emily I. Chen, and Rolf Sternglanz. 2013. “Biochemical Characterization of Hpa2 and Hpa3, Two Small Closely Related Acetyltransferases from Saccharomyces Cerevisiae.” *The Journal of Biological Chemistry* 288 (30): 21506–13.

Sanders, Steven L., Jennifer Jennings, Adrian Canutescu, Andrew J. Link, and P. Anthony Weil. 2002. “Proteomics of the Eukaryotic Transcription Machinery: Identification of Proteins Associated with Components of Yeast TFIID by Multidimensional Mass Spectrometry.” *Molecular and Cellular Biology* 22 (13): 4723–38.

Sayani, Shakir, Michael Janis, Chrissie Young Lee, Isabelle Toesca, and Guillaume F. Chanfreau. 2008. “Widespread Impact of Nonsense-Mediated mRNA Decay on the Yeast Intronome.” *Molecular Cell* 31 (3): 360–70.

Scarcelli, John J., Christine A. Hodge, and Charles N. Cole. 2007. “The Yeast Integral Membrane Protein Apq12 Potentially Links Membrane Dynamics to Assembly of Nuclear Pore Complexes.” *The Journal of Cell Biology* 178 (5): 799–812.

Schaffrath, Raffael, and Sebastian A. Leidel. 2017. “Wobble Uridine Modifications-a Reason to Live, a Reason to Die?!” *RNA Biology* 14 (9): 1209–22.

Schlaich, N. L., and E. C. Hurt. 1995. “Analysis of Nucleocytoplasmic Transport and Nuclear Envelope Structure in Yeast Disrupted for the Gene Encoding the Nuclear Pore Protein Nup1p.” *European Journal of Cell Biology* 67 (1): 8–14.

Schlissel, Gavin, Marek K. Krzyzanowski, Fabrice Caudron, Yves Barral, and Jasper Rine. 2017. “Aggregation of the Whi3 Protein, Not Loss of Heterochromatin, Causes Sterility in Old Yeast Cells.” *Science* 355 (6330): 1184–87.

Schmidt, Oliver, and David Teis. 2012. “The ESCRT Machinery.” *Current Biology: CB* 22 (4): R116–20.

Schmoller, Kurt M., Michael C. Lanz, Jacob Kim, Mardo Koivomagi, Yimiao Qu, Chao Tang, Igor V. Kukhtevich, et al. 2022. “Whi5 Is Diluted and Protein Synthesis Does Not Dramatically Increase in Pre-Start G1.” *Molecular Biology of the Cell* 33 (5): lt1.

Schmoller, Kurt M., J. J. Turner, M. Kõivomägi, and Jan M. Skotheim. 2015. “Dilution of the Cell Cycle Inhibitor Whi5 Controls Budding-Yeast Cell Size.” *Nature* 526 (7572): 268–72.

Schneider, B. L., Q. H. Yang, and A. B. Futcher. 1996. “Linkage of Replication to Start by the Cdk Inhibitor Sic1.” *Science* 272 (5261): 560–62.

Schneider, Jessica, Pratibha Bajwa, Farley C. Johnson, Sukesh R. Bhaumik, and Ali Shilatifard. 2006. “Rtt109 Is Required for Proper H3K56 Acetylation: A Chromatin Mark Associated with the Elongating RNA Polymerase II.” *The Journal of Biological Chemistry* 281 (49): 37270–74.

Schwob, E., T. Böhm, M. D. Mendenhall, and K. Nasmyth. 1994. “The B-Type Cyclin Kinase Inhibitor p40SIC1 Controls the G1 to S Transition in S. Cerevisiae.” *Cell* 79 (2): 233–44.

Schwob, E., and K. Nasmyth. 1993. “CLB5 and CLB6, a New Pair of B Cyclins Involved in DNA Replication in Saccharomyces Cerevisiae.” *Genes & Development* 7 (7A): 1160–75.

Sealy, L., and R. Chalkley. 1978. “DNA Associated with Hyperacetylated Histone Is Preferentially Digested by DNase I.” *Nucleic Acids Research* 5 (6): 1863–76.

Seidel, Maximilian, Anja Becker, Filipa Pereira, Jonathan J. M. Landry, Nayara Trevisan Doimo de Azevedo, Claudia M. Fusco, Eva Kaindl, et al. 2022. “Co-Translational Assembly Orchestrates Competing Biogenesis Pathways.” *Nature Communications* 13 (1): 1224.

Seksek, O., and J. Bolard. 1996. “Nuclear pH Gradient in Mammalian Cells Revealed by Laser Microspectrofluorimetry.” *Journal of Cell Science* 109 (Pt 1) (January): 257–62.

Selvadurai, Kiruthika, Pei Wang, Joseph Seimetz, and Raven H. Huang. 2014. “Archaeal Elp3 Catalyzes tRNA Wobble Uridine Modification at C5 via a Radical Mechanism.” *Nature Chemical Biology* 10 (10): 810–12.

Sharma, Deepak, Leah L. Zagore, Matthew M. Brister, Xuan Ye, Carlos E. Crespo-Hernández, Donny D. Licatalosi, and Eckhard Jankowsky. 2021. “The Kinetic Landscape of an RNA-Binding Protein in Cells.” *Nature* 591 (7848): 152–56.

Shcheprova, Zhanna, Sandro Baldi, Stephanie Buvelot Frei, Gaston Gonnet, and Yves Barral. 2008. “A Mechanism for Asymmetric Segregation of Age during Yeast Budding.” *Nature* 454 (7205): 728–34.

Shen, Chang-Hui, Benoit P. Leblanc, Carolyn Neal, Ramin Akhavan, and David J. Clark. 2002. “Targeted Histone Acetylation at the Yeast CUP1 Promoter Requires the Transcriptional Activator, the TATA Boxes, and the Putative Histone Acetylase Encoded by SPT10.” *Molecular and Cellular Biology* 22 (18): 6406–16.

Shen, E. C., T. Stage-Zimmermann, P. Chui, and P. A. Silver. 2000. “7The Yeast mRNA-Binding Protein Npl3p Interacts with the Cap-Binding Complex.” *The Journal of Biological Chemistry* 275 (31): 23718–24.

Shia, Wei-Jong, Bing Li, and Jerry L. Workman. 2006. “SAS-Mediated Acetylation of Histone H4 Lys 16 Is Required for H2A.Z Incorporation at Subtelomeric Regions in Saccharomyces Cerevisiae.” *Genes & Development* 20 (18): 2507–12.

Shia, Wei-Jong, Shigehiro Osada, Laurence Florens, Selene K. Swanson, Michael P. Washburn, and Jerry L. Workman. 2005. “Characterization of the Yeast Trimeric-SAS Acetyltransferase Complex.” *The Journal of Biological Chemistry* 280 (12): 11987–94.

Shibagaki, Y., N. Itoh, H. Yamada, S. Nagata, and K. Mizumoto. 1992. “mRNA Capping Enzyme. Isolation and Characterization of the Gene Encoding mRNA Guanylytransferase Subunit from Saccharomyces Cerevisiae.” *The Journal of Biological Chemistry* 267 (14): 9521–28.

Shi, Di, Shuaijun Zhao, Mei-Qing Zuo, Jingjing Zhang, Wenya Hou, Meng-Qiu Dong, Qinhong Cao, and Huiqiang Lou. 2020. “The Acetyltransferase Eco1 Elicits Cohesin Dimerization during S Phase.” *The Journal of Biological Chemistry* 295 (22): 7554–65.

Shi, Lei, and Benjamin P. Tu. 2013. “Acetyl-CoA Induces Transcription of the Key G1 Cyclin *CLN3* to Promote Entry into the Cell Division Cycle in *Saccharomyces Cerevisiae*.” *Proceedings of the National Academy of Sciences* 110 (18): 7318–23.

Shukla, Abhijit, Pratibha Bajwa, and Sukesh R. Bhaumik. 2006. “SAGA-Associated Sgf73p Facilitates Formation of the Preinitiation Complex Assembly at the Promoters Either in a HAT-Dependent or Independent Manner in Vivo.” *Nucleic Acids Research* 34 (21): 6225–32.

Skoglund, U., K. Andersson, B. Björkroth, M. M. Lamb, and B. Daneholt. 1983. “Visualization of the Formation and Transport of a Specific hnRNP Particle.” *Cell* 34 (3): 847–55.

Skotheim, Jan M., Stefano Di Talia, Eric D. Siggia, and Frederick R. Cross. 2008. “Positive Feedback of G1 Cyclins Ensures Coherent Cell Cycle Entry.” *Nature* 454 (7202): 291–96.

Smith, E. R., A. Eisen, W. Gu, M. Sattah, A. Pannuti, J. Zhou, R. G. Cook, J. C. Lucchesi, and C. D. Allis. 1998. “ESA1 Is a Histone Acetyltransferase That Is Essential for Growth in Yeast.” *Proceedings of the National Academy of Sciences of the United States of America* 95 (7): 3561–65.

Soifer, Ilya, and Naama Barkai. 2014. “Systematic Identification of Cell Size Regulators in Budding Yeast.” *Molecular Systems Biology* 10 (November): 761.

Sol, Eri Maria, Sebastian A. Wagner, Brian T. Weinert, Amit Kumar, Hyun-Seok Kim, Chu-Xia Deng, and Chunaram Choudhary. 2012. “Proteomic Investigations of Lysine Acetylation Identify Diverse Substrates of Mitochondrial Deacetylase sirt3.” *PloS One* 7 (12): e50545.

Sood, Varun, and Jason H. Brickner. 2014. “Nuclear Pore Interactions with the Genome.” *Current Opinion in Genetics & Development* 25 (April): 43–49.

Soucek, Sharon, Yi Zeng, Deepti L. Bellur, Megan Bergkessel, Kevin J. Morris, Qiudong Deng, Duc Duong, et al. 2016. “The Evolutionarily-Conserved Polyadenosine RNA Binding Protein, Nab2, Cooperates with Splicing Machinery to Regulate the Fate of Pre-mRNA.” *Molecular and Cellular Biology* 36 (21): 2697–2714.

Stedman, Edgar, and Ellen Stedman. 1951. “The Basic Proteins of Cell Nuclei.” *Philosophical*

Transactions of the Royal Society of London. Series B, Biological Sciences 235 (630): 565–95.

Sterner, David E., and Shelley L. Berger. 2000. "Acetylation of Histones and Transcription-Related Factors." *Microbiology and Molecular Biology Reviews*. https://doi.org/10.1128/mmbr.64.2.435-459.2000.

Sterner, D. E., P. A. Grant, S. M. Roberts, L. J. Duggan, R. Belotserkovskaya, L. A. Pacella, F. Winston, J. L. Workman, and S. L. Berger. 1999. "Functional Organization of the Yeast SAGA Complex: Distinct Components Involved in Structural Integrity, Nucleosome Acetylation, and TATA-Binding Protein Interaction." *Molecular and Cellular Biology* 19 (1): 86–98.

Stevens, Scott W., and John Abelson. 2002. "Yeast Pre-mRNA Splicing: Methods, Mechanisms, and Machinery." In *Methods in Enzymology*, 351:200–220. Academic Press.

Stewart, Murray. 2007. "Molecular Mechanism of the Nuclear Protein Import Cycle." *Nature Reviews. Molecular Cell Biology* 8 (3): 195–208.

Stewart, Murray. 2019. "Polyadenylation and Nuclear Export of mRNAs." *The Journal of Biological Chemistry* 294 (9): 2977–87.

Strambio-de-Castillia, C., G. Blobel, and M. P. Rout. 1999. "Proteins Connecting the Nuclear Pore Complex with the Nuclear Interior." *The Journal of Cell Biology* 144 (5): 839–55.

Strässer, K., J. Bassler, and E. Hurt. 2000. "Binding of the Mex67p/Mtr2p Heterodimer to FXFG, GLFG, and FG Repeat Nucleoporins Is Essential for Nuclear mRNA Export." *The Journal of Cell Biology* 150 (4): 695–706.

Strässer, K., and E. Hurt. 2000. "Yra1p, a Conserved Nuclear RNA-Binding Protein, Interacts Directly with Mex67p and Is Required for mRNA Export." *The EMBO Journal* 19 (3): 410–20.

Sung, Min-Kyung, Gyubum Lim, Dae-Gwan Yi, Yeon Ji Chang, Eun Bin Yang, Kiyoung Lee, and Won-Ki Huh. 2013. "Genome-Wide Bimolecular Fluorescence Complementation Analysis of SUMO Interactome in Yeast." *Genome Research* 23 (4): 736–46.

Sutendra, Gopinath, Adam Kinnaird, Peter Dromparis, Roxane Paulin, Trevor H. Stenson, Alois Haromy, Kyoko Hashimoto, Nancy Zhang, Eric Flaim, and Evangelos D. Michelakis. 2014. "A Nuclear Pyruvate Dehydrogenase Complex Is Important for the Generation of Acetyl-CoA and Histone Acetylation." *Cell* 158 (1): 84–97.

Takahashi, Hidekazu, J. Michael McCaffery, Rafael A. Irizarry, and Jef D. Boeke. 2006. "Nucleocytosolic Acetyl-Coenzyme a Synthetase Is Required for Histone Acetylation and Global Transcription." *Molecular Cell* 23 (2): 207–17.

Takahata, Shinya, Yaxin Yu, and David J. Stillman. 2009. "The E2F Functional Analogue SBF Recruits the Rpd3(L) HDAC, via Whi5 and Stb1, and the FACT Chromatin Reorganizer, to Yeast G1 Cyclin Promoters." *The EMBO Journal* 28 (21): 3378–89.

Takechi, S., and T. Nakayama. 1999. "Sas3 Is a Histone Acetyltransferase and Requires a Zinc Finger Motif." *Biochemical and Biophysical Research Communications* 266 (2): 405–10.

Tanner, K. G., M. R. Langer, Y. Kim, and J. M. Denu. 2000. “Kinetic Mechanism of the Histone Acetyltransferase GCN5 from Yeast.” *The Journal of Biological Chemistry* 275 (29): 22048–55.

Taunton, J., C. A. Hassig, and S. L. Schreiber. 1996. “A Mammalian Histone Deacetylase Related to the Yeast Transcriptional Regulator Rpd3p.” *Science* 272 (5260): 408–11.

Terry, Laura J., and Susan R. Wente. 2007. “Nuclear mRNA Export Requires Specific FG Nucleoporins for Translocation through the Nuclear Pore Complex.” *The Journal of Cell Biology* 178 (7): 1121–32.

Teufel, Lotte, Katja Tummler, Max Flöttmann, Andreas Herrmann, Naama Barkai, and Edda Klipp. 2019. “A Transcriptome-Wide Analysis Deciphers Distinct Roles of G1 Cyclins in Temporal Organization of the Yeast Cell Cycle.” *Scientific Reports* 9 (1): 3343.

Texari, Lorane, Guennaëlle Dieppois, Patrizia Vinciguerra, Mariana Pardo Contreras, Anna Groner, Audrey Letourneau, and Françoise Stutz. 2013. “The Nuclear Pore Regulates GAL1 Gene Transcription by Controlling the Localization of the SUMO Protease Ulp1.” *Molecular Cell* 51 (6): 807–18.

Thomsen, Rune, Domenico Libri, Jocelyne Boulay, Michael Rosbash, and Torben Heick Jensen. 2003. “Localization of Nuclear Retained mRNAs in Saccharomyces Cerevisiae.” *RNA* 9 (9): 1049–57.

Timney, Benjamin L., Barak Raveh, Roxana Mironska, Jill M. Trivedi, Seung Joong Kim, Daniel Russel, Susan R. Wente, Andrej Sali, and Michael P. Rout. 2016. “Simple Rules for Passive Diffusion through the Nuclear Pore Complex.” *The Journal of Cell Biology* 215 (1): 57–76.

Titani, K., K. Narita, and K. Okunuki. 1962. “N-Terminal Sequence in Beef- and Horse-Heart Cytochrome c.” *Journal of Biochemistry* 51 (May): 350–58.

Tran, Elizabeth J., Yingna Zhou, Anita H. Corbett, and Susan R. Wente. 2007. “The DEAD-Box Protein Dbp5 Controls mRNA Export by Triggering Specific RNA:protein Remodeling Events.” *Molecular Cell* 28 (5): 850–59.

Tsubota, Toshiaki, Christopher E. Berndsen, Judith A. Erkmann, Corey L. Smith, Lanhao Yang, Michael A. Freitas, John M. Denu, and Paul D. Kaufman. 2007. “Histone H3-K56 Acetylation Is Catalyzed by Histone Chaperone-Dependent Complexes.” *Molecular Cell* 25 (5): 703–12.

Tsukamoto, T., Y. Shibagaki, S. Imajoh-Ohmi, T. Murakoshi, M. Suzuki, A. Nakamura, H. Gotoh, and K. Mizumoto. 1997. “Isolation and Characterization of the Yeast mRNA Capping Enzyme Beta Subunit Gene Encoding RNA 5’-Triphosphatase, Which Is Essential for Cell Viability.” *Biochemical and Biophysical Research Communications* 239 (1): 116–22.

Tu, Benjamin P., Andrzej Kudlicki, Maga Rowicka, and Steven L. McKnight. 2005. “Logic of the Yeast Metabolic Cycle: Temporal Compartmentalization of Cellular Processes.” *Science* 310 (5751): 1152–58.

Tudek, Agnieszka, Paweł S. Krawczyk, Seweryn Mroczek, Rafał Tomecki, Matti Turtola, Katarzyna Matylla-Kulińska, Torben Heick Jensen, and Andrzej Dziembowski. 2021. “Global View on the Metabolism of RNA poly(A) Tails in Yeast Saccharomyces Cerevisiae.” *Nature Communications* 12 (1): 4951.

Umlauf, David, Jacques Bonnet, François Waharte, Marjorie Fournier, Matthieu Stierle, Benoit Fischer,

Laurent Brino, Didier Devys, and László Tora. 2013. “The Human TREX-2 Complex Is Stably Associated with the Nuclear Pore Basket.” *Journal of Cell Science* 126 (Pt 12): 2656–67.

Uprety, Bhawana, Rwik Sen, and Sukesh R. Bhaumik. 2015. “Eaf1p Is Required for Recruitment of NuA4 in Targeting TFIID to the Promoters of the Ribosomal Protein Genes for Transcriptional Initiation In Vivo.” *Molecular and Cellular Biology* 35 (17): 2947–64.

VanDemark, Andrew P., Margaret M. Kasten, Elliott Ferris, Annie Heroux, Christopher P. Hill, and Bradley R. Cairns. 2007. “Autoregulation of the rsc4 Tandem Bromodomain by gcn5 Acetylation.” *Molecular Cell* 27 (5): 817–28.

Varberg, Joseph M., Jay R. Unruh, Andrew J. Bestul, Azqa A. Khan, and Sue L. Jaspersen. 2022. “Quantitative Analysis of Nuclear Pore Complex Organization in Schizosaccharomyces Pombe.” *Life Science Alliance* 5 (7). https://doi.org/10.26508/lsa.202201423.

Vargas, Diana Y., Arjun Raj, Salvatore A. E. Marras, Fred Russell Kramer, and Sanjay Tyagi. 2005. “Mechanism of mRNA Transport in the Nucleus.” *Proceedings of the National Academy of Sciences of the United States of America* 102 (47): 17008–13.

Vergés, Emili, Neus Colomina, Eloi Garí, Carme Gallego, and Martí Aldea. 2007. “Cyclin Cln3 Is Retained at the ER and Released by the J Chaperone Ydj1 in Late G1 to Trigger Cell Cycle Entry.” *Molecular Cell* 26 (5): 649–62.

Verma, R., R. S. Annan, M. J. Huddleston, S. A. Carr, G. Reynard, and R. J. Deshaies. 1997. “Phosphorylation of Sic1p by G1 Cdk Required for Its Degradation and Entry into S Phase.” *Science* 278 (5337): 455–60.

Vicente-Muñoz, Sara, Paco Romero, Lorena Magraner-Pardo, Celia P. Martinez-Jimenez, Vicente Tordera, and Mercè Pamblanco. 2014. “Comprehensive Analysis of Interacting Proteins and Genome-Wide Location Studies of the Sas3-Dependent NuA3 Histone Acetyltransferase Complex.” *FEBS Open Bio* 4 (November): 996–1006.

Vinciguerra, Patrizia, Nahid Iglesias, Jurgi Camblong, Daniel Zenklusen, and Françoise Stutz. 2005. “Perinuclear Mlp Proteins Downregulate Gene Expression in Response to a Defect in mRNA Export.” *The EMBO Journal* 24 (4): 813–23.

Wagner, Michelle V., Marcus B. Smolka, Rob A. M. de Bruin, Huilin Zhou, Curt Wittenberg, and Steven F. Dowdy. 2009. “Whi5 Regulation by Site Specific CDK-Phosphorylation in Saccharomyces Cerevisiae.” *PloS One* 4 (1): e4300.

Wang, Amy, Siavash K. Kurdistani, and Michael Grunstein. 2002. “Requirement of Hos2 Histone Deacetylase for Gene Activity in Yeast.” *Science* 298 (5597): 1412–14.

Wang, Ke, Lantian Wang, Jianshu Wang, Suli Chen, Min Shi, and Hong Cheng. 2018. “Intronless mRNAs Transit through Nuclear Speckles to Gain Export Competence.” *The Journal of Cell Biology* 217 (11): 3912–29.

Wang, L., L. Liu, and S. L. Berger. 1998. “Critical Residues for Histone Acetylation by Gcn5, Functioning in Ada and SAGA Complexes, Are Also Required for Transcriptional Function in Vivo.” *Genes & Development* 12 (5): 640–53.

Warfield, Linda, Srinivas Ramachandran, Tiago Baptista, Didier Devys, Laszlo Tora, and Steven Hahn. 2017. “Transcription of Nearly All Yeast RNA Polymerase II-Transcribed Genes Is Dependent on Transcription Factor TFIID.” *Molecular Cell* 68 (1): 118–29.e5.

Watanabe, Shinya, Marta Radman-Livaja, Oliver J. Rando, and Craig L. Peterson. 2013. “A Histone Acetylation Switch Regulates H2A.Z Deposition by the SWR-C Remodeling Enzyme.” *Science* 340 (6129): 195–99.

Waterborg, Jakob H. 2000. “Steady-State Levels of Histone Acetylation in Saccharomyces Cerevisiae *.” *The Journal of Biological Chemistry* 275 (17): 13007–11.

Webster, Brant M., Paolo Colombi, Jens Jäger, and C. Patrick Lusk. 2014. “Surveillance of Nuclear Pore Complex Assembly by ESCRT-III/Vps4.” *Cell* 159 (2): 388–401.

Wee, Caroline L., Shaun Teo, Nicodemus E. Oey, Graham D. Wright, Hendrika M. A. VanDongen, and Antonius M. J. VanDongen. 2014. “Nuclear Arc Interacts with the Histone Acetyltransferase Tip60 to Modify H4K12 Acetylation(1,2,3).” *eNeuro* 1 (1). https://doi.org/10.1523/ENEURO.0019-14.2014.

Weinert, Brian T., Vytautas Iesmantavicius, Tarek Moustafa, Christian Schölz, Sebastian A. Wagner, Christoph Magnes, Rudolf Zechner, and Chunaram Choudhary. 2014. “Acetylation Dynamics and Stoichiometry in Saccharomyces Cerevisiae.” *Molecular Systems Biology* 10 (January): 716.

Weinert, Brian T., Christian Schölz, Sebastian A. Wagner, Vytautas Iesmantavicius, Dan Su, Jeremy A. Daniel, and Chunaram Choudhary. 2013. “Lysine Succinylation Is a Frequently Occurring Modification in Prokaryotes and Eukaryotes and Extensively Overlaps with Acetylation.” *Cell Reports* 4 (4): 842–51.

Weinert, Brian T., Sebastian A. Wagner, Heiko Horn, Peter Henriksen, Wenshe R. Liu, Jesper V. Olsen, Lars J. Jensen, and Chunaram Choudhary. 2011. “Proteome-Wide Mapping of the Drosophila Acetylome Demonstrates a High Degree of Conservation of Lysine Acetylation.” *Science Signaling* 4 (183): ra48.

Weirich, Christine S., Jan P. Erzberger, Jeffrey S. Flick, James M. Berger, Jeremy Thorner, and Karsten Weis. 2006. “Activation of the DExD/H-Box Protein Dbp5 by the Nuclear-Pore Protein Gle1 and Its Coactivator InsP6 Is Required for mRNA Export.” *Nature Cell Biology* 8 (7): 668–76.

Wente, Susan R., and Michael P. Rout. 2010. “The Nuclear Pore Complex and Nuclear Transport.” *Cold Spring Harbor Perspectives in Biology* 2 (10): a000562.

Wickramasinghe, Vihandha O., Robert Andrews, Peter Ellis, Cordelia Langford, John B. Gurdon, Murray Stewart, Ashok R. Venkitaraman, and Ronald A. Laskey. 2014. “Selective Nuclear Export of Specific Classes of mRNA from Mammalian Nuclei Is Promoted by GANP.” *Nucleic Acids Research* 42 (8): 5059–71.

Wickramasinghe, Vihandha O., Paul I. A. McMurtrie, Anthony D. Mills, Yoshinori Takei, Sue Penrhyn-Lowe, Yoko Amagase, Sarah Main, Jackie Marr, Murray Stewart, and Ronald A. Laskey. 2010. “mRNA Export from Mammalian Cell Nuclei Is Dependent on GANP.” *Current Biology: CB* 20 (1): 25–31.

Wijnen, H., and B. Futcher. 1999. “Genetic Analysis of the Shared Role of CLN3 and BCK2 at the G(1)-S Transition in Saccharomyces Cerevisiae.” *Genetics* 153 (3): 1131–43.

Winey, M., D. Yarar, T. H. Giddings Jr, and D. N. Mastronarde. 1997. “Nuclear Pore Complex Number and Distribution throughout the Saccharomyces Cerevisiae Cell Cycle by Three-Dimensional Reconstruction from Electron Micrographs of Nuclear Envelopes.” *Molecular Biology of the Cell* 8 (11): 2119–32.

Winkler, G. Sebastiaan, Arnold Kristjuhan, Hediye Erdjument-Bromage, Paul Tempst, and Jesper Q. Svejstrup. 2002. “Elongator Is a Histone H3 and H4 Acetyltransferase Important for Normal Histone Acetylation Levels in Vivo.” *Proceedings of the National Academy of Sciences of the United States of America* 99 (6): 3517–22.

Wissink, Erin M., Anniina Vihervaara, Nathaniel D. Tippens, and John T. Lis. 2019. “Nascent RNA Analyses: Tracking Transcription and Its Regulation.” *Nature Reviews. Genetics* 20 (12): 705–23.

Wittenberg, C., K. Sugimoto, and S. I. Reed. 1990. “G1-Specific Cyclins of S. Cerevisiae: Cell Cycle Periodicity, Regulation by Mating Pheromone, and Association with the p34CDC28 Protein Kinase.” *Cell* 62 (2): 225–37.

Wittschieben, B. O., J. Fellows, W. Du, D. J. Stillman, and J. Q. Svejstrup. 2000. “Overlapping Roles for the Histone Acetyltransferase Activities of SAGA and Elongator in Vivo.” *The EMBO Journal* 19 (12): 3060–68.

Wong, Chi-Ming, Hongfang Qiu, Cuihua Hu, Jinsheng Dong, and Alan G. Hinnebusch. 2007. “Yeast Cap Binding Complex Impedes Recruitment of Cleavage Factor IA to Weak Termination Sites.” *Molecular and Cellular Biology* 27 (18): 6520–31.

Wong, Xianrong, Ashley J. Melendez-Perez, and Karen L. Reddy. 2022. “The Nuclear Lamina.” *Cold Spring Harbor Perspectives in Biology* 14 (2). https://doi.org/10.1101/cshperspect.a040113.

Wu, Wei-Hua, Samar Alami, Edward Luk, Chwen-Huey Wu, Subhojit Sen, Gaku Mizuguchi, Debbie Wei, and Carl Wu. 2005. “Swc2 Is a Widely Conserved H2AZ-Binding Module Essential for ATP-Dependent Histone Exchange.” *Nature Structural & Molecular Biology* 12 (12): 1064–71.

Xu, Feng, Kangling Zhang, and Michael Grunstein. 2005. “Acetylation in Histone H3 Globular Domain Regulates Gene Expression in Yeast.” *Cell* 121 (3): 375–85.

Yamada, Justin, Joshua L. Phillips, Samir Patel, Gabriel Goldfien, Alison Calestagne-Morelli, Hans Huang, Ryan Reza, et al. 2010. “A Bimodal Distribution of Two Distinct Categories of Intrinsically Disordered Structures with Separate Functions in FG Nucleoporins*.” *Molecular & Cellular Proteomics: MCP* 9 (10): 2205–24.

Yang, Jiahui H., and Catherine H. Freudenreich. 2010. “The Rtt109 Histone Acetyltransferase Facilitates Error-Free Replication to Prevent CAG/CTG Repeat Contractions.” *DNA Repair* 9 (4): 414–20.

Yow, Geok-Yong, Takuma Uo, Tohru Yoshimura, and Nobuyoshi Esaki. 2006. “Physiological Role of D-Amino Acid-N-Acetyltransferase of Saccharomyces Cerevisiae: Detoxification of D-Amino Acids.” *Archives of Microbiology* 185 (1): 39–46.

Zencir, Sevil, Daniel Dilg, David Shore, and Benjamin Albert. 2022. “Pitfalls in Using Phenanthroline to Study the Causal Relationship between Promoter Nucleosome Acetylation and Transcription.” *Nature Communications* 13 (1): 1–4.

Zhang, Jinglan, Xiaomin Shi, Yehua Li, Beom-Jun Kim, Junling Jia, Zhiwei Huang, Tao Yang, et al. 2008. “Acetylation of Smc3 by Eco1 Is Required for S Phase Sister Chromatid Cohesion in Both Human and Yeast.” *Molecular Cell* 31 (1): 143–51.

Zhang, Wanlu, Azqa Khan, Jlenia Vitale, Annett Neuner, Kerstin Rink, Christian Lüchtenborg, Britta Brügger, Thomas H. Söllner, and Elmar Schiebel. 2021. “A Short Perinuclear Amphipathic α-Helix in Apq12 Promotes Nuclear Pore Complex Biogenesis.” *Open Biology* 11 (11): 210250.

Zhao, Xiaolan, Chia-Yung Wu, and Günter Blobel. 2004. “Mlp-Dependent Anchorage and Stabilization of a Desumoylating Enzyme Is Required to Prevent Clonal Lethality.” *The Journal of Cell Biology* 167 (4): 605–11.

Zhukovsky, Mikhail A., Angela Filograna, Alberto Luini, Daniela Corda, and Carmen Valente. 2019. “Phosphatidic Acid in Membrane Rearrangements.” *FEBS Letters* 593 (17): 2428–51.

Zimowska, G., J. P. Aris, and M. R. Paddy. 1997. “A Drosophila Tpr Protein Homolog Is Localized Both in the Extrachromosomal Channel Network and to Nuclear Pore Complexes.” *Journal of Cell Science* 110 (Pt 8) (April): 927–44.

Zou, Yanfei, and Xin Bi. 2008. “Positive Roles of SAS2 in DNA Replication and Transcriptional Silencing in Yeast.” *Nucleic Acids Research* 36 (16): 5189–5200.

Université de Strasbourg

Vasilisa POZHARSKAIA

Contrôle de l'expression génétique et du cycle cellulaire par modulation des complexes des pores nucléaires

École doctorale Sciences de la vie et de la santé | ED 414
Université de Strasbourg

Résumé

Les complexes des pores nucléaires (NPC) assurent la communication entre le noyau et le cytoplasme et régulent ainsi l'expression génétique en interagissant avec les facteurs de transcription et d'exportation de l'ARNm. Les lysine acétyltransférases (KAT) favorisent la transcription par l'acétylation de protéines associées à la chromatine. Nous avons découvert que Esa1 (la sous-unité KAT du complexe NuA4 chez la levure) acétyle également Nup60 (un composant nucléoplasmique du pore nucléaire) et promeut ainsi l'exportation de l'ARNm. L'acétylation de Nup60 recrute le facteur d'exportation d'ARNm Sac3 (la sous-unité échafaud du complexe de Transcription et d'Exportation 2 (TREX-2)) vers l'unité nucléoplasmique du NPC. L'exportation nucléaire des ARNm médiée par Esa1 favorise en conséquent l'étape du passage de la phase G1 à la phase S. Chez les cellules filles en G1, cette étape est inhibée par la désacétylase Hos3 afin d'empêcher l'initiation prématurée d'un nouveau cycle cellulaire. Ce mécanisme ne se limite pas qu'aux gènes de progression dans le cycle cellulaire, mais inhibe également l'expression du gène GAL1 (qui lui est régulé par les nutriments) spécifiquement chez les cellules filles. Globalement, ces résultats révèlent par quels mécanismes l'acétylation peut contribuer à la plasticité fonctionnelle des NPCs chez les cellules mères et filles. De plus, notre travail démontre une double régulation de l'expression des gènes par le complexe NuA4, au niveau de la transcription et au stade de l'exportation de l'ARNm en modifiant le domaine nucléoplasmique des pores nucléaires.

Mots clés : complexe du pore nucléaire, Nup60, expression génétique, exportation de l'ARNm, acétylation, transition G1/S

Résumé en anglais

Nuclear pore complexes (NPCs) mediate communication between the nucleus and the cytoplasm, and regulate gene expression by interacting with transcription and mRNA export factors. Lysine acetyltransferases (KATs) promote transcription through acetylation of chromatin-associated proteins. We find that Esa1, the KAT subunit of the yeast NuA4 complex, also acetylates the nuclear pore basket component Nup60 to promote mRNA export. Acetylation of Nup60 recruits the mRNA export factor Sac3, the scaffolding subunit of the Transcription and Export 2 (TREX-2) complex, to the nuclear basket. The Esa1-mediated nuclear export of mRNAs in turn promotes entry into S phase, which is inhibited by the Hos3 deacetylase in G1 daughter cells to restrain their premature commitment to a new cell division cycle. This mechanism is not only limited to G1/S-expressed genes but also inhibits the expression of the nutrient-regulated *GAL1* gene specifically in daughter cells. Overall, these results reveal how acetylation can contribute to the functional plasticity of NPCs in mother and daughter yeast cells. In addition, our work demonstrates dual gene expression regulation by the evolutionarily conserved NuA4 complex, at the level of transcription and at the stage of mRNA export by modifying the nucleoplasmic entrance to nuclear pores.

Keywords : nuclear pore complex, Nup60, gene expression, mRNA export, acetylation, G1/S transition